THE UNIVERSITY
of EDINBURGH

Neuropathology and Molecular Biology of Iatrogenic Creutzfeldt-Jakob Disease in UK Human Growth Hormone Recipients

James Wilson Ironside

Doctor of Medicine

The University of Edinburgh

2016

Abstract of Thesis

Creutzfeldt-Jakob disease (CJD) is the commonest form of human prion disease and occurs in sporadic, genetic and acquired forms. The causative agents (prions) appear to be composed entirely of a modified host protein, the prion protein, which undergoes misfolding to a disease-associated isoform closely associated with infectivity that is resistant to conventional methods of decontamination. Prions can be transmitted from one individual to another by medical and surgical procedures, resulting in iatrogenic CJD (iCJD). The commonest cause of iCJD is the inoculation of cadaveric pituitary-derived human growth hormone (hGH) to treat growth hormone deficiency in children; this form of treatment was abandoned in 1985 after the first UK case of iCJD in a hGH recipient was identified. Seventy-eight cases of iCJD have since occurred in the UK cohort of 1849 hGH recipients, including a case in 2016.

This thesis describes a comprehensive tissue-based and molecular genetic analysis of the largest series (35 cases) of UK hGH-iCJD cases reported to date, including *in vitro* kinetic molecular modelling of genotypic factors influencing prion transmission. The results show that the polymorphism at codon 129 of the prion protein gene strongly influences the disease incubation period in hGH-iCJD (from 7.8-32.3 years in this series) and interacts with the infectious prion strain to govern the molecular and pathological characteristics of iCJD. The findings are consistent with the hypothesis that the UK hGH-iCJD epidemic resulted from transmission of the V2 human prion strain, which is found in the second most common form of sporadic CJD.

The investigation also found accumulation of the amyloid beta (Aβ) protein associated with Alzheimer's disease (AD) in the brains and cerebral blood vessels in 18/35 hGH-iCJD patients and 5/12 control patients who had been treated with hGH, but died from causes other than iCJD. In contrast, Aβ accumulation was markedly less prevalent in age-matched patients who died from sporadic CJD (1/15 cases) and variant CJD (2/33 cases). These results are consistent with the hypothesis that Aβ, which can accumulate in the pituitary gland, was present in the inoculated hGH preparations and seeded into the brains of around 50% of all hGH recipients, producing AD-like neuropathology and cerebral amyloid angiopathy (CAA). This provides further evidence of the prion-like properties of Aβ and gives insight into the potential for possible transmission of AD/CAA. It is uncertain whether any Aβ seeding within the brains of surviving patients in the UK hGH recipient cohort will ultimately result in clinical AD; however, the CAA in these patients may be complicated by intracerebral haemorrhage resulting from rupture of the blood vessels damaged by Aβ accumulation within their walls.

Lay Summary

Creutzfeldt-Jakob disease (CJD) is a rare fatal neurological disease that can occur by chance, or within a family, or be acquired by accidental transmission from one individual to another. The transmissible agents in CJD are known as prions, which are composed of an abnormal form of the human prion protein that has undergone a change in its shape and become infectious. Prions are very resistant to standard cleaning and decontamination processes. Accidental transmission of CJD can occur after certain medical or surgical procedures. The commonest procedure resulting in accidental transmission of CJD is treatment with injections of human growth hormone (GH) obtained from the pituitary gland (at the base of the brain) obtained from deceased individuals at autopsy. This hormone was used to treat children with short stature who were deficient in growth hormone, starting in the 1960s. In 1985, a case of acquired CJD was identified in a UK patient who had been treated with GH, after which this form of treatment was stopped. However, cases of acquired CJD continue to occur in the group of 1849 UK patients treated with GH, most recently in 2016, indicating that incubation periods for this disease can be very long indeed.

This project investigates a group of 35 UK patients with acquired CJD following GH treatment. We have performed genetic studies, showing that the incubation period for acquired CJD is strongly influenced by a variable part of the gene that produces the prion protein. This gene also interacts with the prions causing acquired CJD and influences the patterns of brain damage that occur in these patients. We have conducted experiments to study how these genetic influences work, which suggest that a particular strain of prions (known as the V2 strain) is likely to have caused the acquired CJD in this group of patients.

We also investigated another protein, amyloid beta (Aβ), which accumulates in the brain in a commoner fatal neurological disease, Alzheimer's disease (AD). Aβ can also accumulate in the pituitary gland, and could have been present in the GH preparations used to treat the groups of patients in our study. We observed Aβ accumulation in the brain and in blood vessels around the brain in around half of all the patients we examined with acquired CJD, and also in around half of a smaller group of patients who were treated with GH, but died from causes other than CJD. These findings suggest that Aβ from the GH injections can spread in the body and "seed" in the brain and its blood vessels. We are not sure if this means that any of the surviving group of UK GH recipients might develop AD in the future. However, they might be at increased risk of a haemorrhage in the brain from blood vessels that are prone to rupture due to the accumulation of Aβ in the vessel wall.

Declaration

I declare that the thesis has been composed by myself and that the work has not be submitted for any other degree or professional qualification. I confirm that the work submitted is my own, except where work which has formed part of jointly-authored publications has been included. My contribution and those of the other authors to this work have been explicitly indicated below. I confirm that appropriate credit has been given within this thesis where reference has been made to the work of others.

I conceived the project, planned the investigative strategy, undertook the neuropathological investigations and analysed all the results in this thesis. I undertook the neuropathological analysis and contributed to writing the publication "UK iatrogenic Creutzfeldt-Jakob disease: investigating human prion transmission across genotypic barriers using human tissue-based and molecular approaches" included in Appendix 15 to this thesis. I obtained permission from Taylor and Francis Press to use illustrations from my co-authored Chapter 18 "Prion Diseases" in Greenfield's Neuropathology 9e, Vol. 2, pp1016-1086, CRC Press, 2015: Figures 18.1, 18.3 18.16, 18.25, 18.26, 18.27, 18.47, 18.49 and 18.50 in this thesis.

Dr Mark Head planned and managed the biochemical investigations in this thesis and in "UK iatrogenic Creutzfeldt-Jakob disease: investigating human prion transmission across genotypic barriers using human tissue-based and molecular approaches", to which he also contributed to writing.

Dr Diane Ritchie performed independent neuropathological analysis, PET blot analysis, double immunohistochemistry and managed the database for the results included in this thesis. Dr Ritchie also provided the Western blot and independent

neuropathological analyses described in this thesis and in "UK iatrogenic Creutzfeldt-Jakob disease: investigating human prion transmission across genotypic barriers using human tissue-based and molecular approaches".

Dr Marcelo Barria performed the PMCA analysis, Dr Alexander Peden performed the RT-QuIC analysis and NaPTA Western blots, and Ms Helen Yull performed the *PRNP* codon 129 analysis and some biochemical investigations in this thesis and in "UK iatrogenic Creutzfeldt-Jakob disease: investigating human prion transmission across genotypic barriers using human tissue-based and molecular approaches". Dr Head, Dr Ritchie, Dr Peden, Dr Barria and Ms Yull also contributed to the Figures in this thesis and in "UK iatrogenic Creutzfeldt-Jakob disease: investigating human prion transmission across genotypic barriers using human tissue-based and molecular approaches".

Dr Anna Molesworth and Catriona Graham provided statistical advice for this thesis.

Mrs Linda McCardle (now retired) and Ms Suzanne Lowrie managed the Neuropathology Laboratory in NCJDRSU, planned the neuropathological laboratory work and aided data retrieval. Mrs Margaret LeGrice and Ms Kimberley Burns performed all the neuropathological techniques described in this thesis.

Dr Peter Adlard (Institute of Child Health) provided the clinical data on hGH recipients. Professor Patrick Chinnery and Dr Michael Keogh (University of Cambridge) provided the genomic data and *APOE* data. Dr Tara Spires-Jones and Ms Rosemary Jackson (University of Edinburgh) also provided *APOE* data. Professor Stuart Pickering-Brown (University of Manchester) provided the *C9ORF72* data.

James Wilson Ironside

Acknowledgements

The work in this thesis would not have been possible without the collaboration of my colleagues in the National CJD Research & Surveillance Unit (NCJDRSU).

In particular, I wish to acknowledge and thank Dr Mark Head, with whom I have worked for over 18 years; I could not have undertaken or completed this work without Mark's considerable insight into human prion diseases, his expertise in prion protein biochemistry and his enthusiasm and support for this project.

I also wish to acknowledge Dr Diane Ritchie, who has supported me throughout this work by independently reviewing the neuropathological findings, performing a range of laboratory techniques and managing a very complex database. Our frequent discussions on the results of this work, particularly the microscopy, have contributed greatly to the analysis and presentation of the results and conclusions of this study.

I am most grateful to the other NCJDRSU scientists who contributed to this project: Dr Alexander Peden for NaPTA western blotting and RT-QuIC technology; Dr Marcelo Barria for PMCA technology; Ms Helen Yull for prion protein biochemistry and *PRNP* codon 129 analysis

My special thanks go to the Neuropathology Laboratory staff: Mrs Linda McCardle (now retired), Ms Suzanne Lowrie, Mrs Margaret LeGrice and Ms Kimberley Burns, some of whom I have worked with for over 20 years. Their organisational skills, laboratory expertise, high standards of work and willingness to undertake the voluminous quantity of tissue processing, microtomy and staining required for this project have been critical to this project's successful conclusion.

I wish to thank other NCJDRSU staff: Professor Robert G Will, who established the NCJDRSU in 1990, Professor Richard Knight for being my Supervisor, Dr Anna Molesworth for statistical advice, Ms Jan Mackenzie for clinical data and analysis, and Dr Matthew Bishop for genetics methodology. I am indebted to Professor Colin Smith for his neuropathological expertise and invaluable comments on the thesis. In Edinburgh University, I thank Catriona Graham for statistical advice, Dr Tara Spires-Jones and Ms Rosemary Jackson for *APOE* analysis, and Dr Abigail Diack and Professor Jean Manson for providing Tg mouse brain tissue. I thank Professor Patrick Chinnery and Dr Michael Keogh (University of Cambridge) for genomics and *APOE* analysis, Professor Stuart Pickering-Brown (University of Manchester) for *C9ORF72* analysis and Dr Peter Adlard, Institute of Child Health London, for helpful discussion and providing data from the UK Registry of hGH recipients.

This work could not have taken place without the generosity of the relatives of the deceased in giving consent for research use of the autopsy tissues studied in this thesis. I thank the UK Neuropathologists and their staff for supporting the work of the NCJDRSU and wish to acknowledge the support of the Department of Health and the Scottish Government, who have funded NCJDRSU for over 25 years.

Finally, and most importantly, I wish to thank my family and friends for persuading me that undertaking the work for this thesis in my seventh decade of life was neither an act of folly nor an impossibility, and for encouraging me in this endeavour. Their unflinching support was essential throughout all the stages of work on this thesis, for which I am deeply and gratefully indebted.

James Wilson Ironside

List of Figures

List of Tables

List of Abbreviations

A	adenine
Aβ	amyloid beta
ABC	Scores for Alzheimer pathology (A=Thal phase for amyloid beta deposits; B=Braak stage for neurofibrillary pathology; C=CERAD score for neuritic plaques)
AC	anterior commissure
AD	Alzheimer's disease
AG	adrenal gland
AP	appendix
apoE	apolipoprotein E
APOE	apolipoprotein E gene
APP	amyloid precursor protein gene
BA	Brodmann area
BM	bone marrow
bp	base pair
BSE	bovine spongiform encephalopathy
C	cytosine
CAA	cerebral amyloid angiopathy
Cb	cerebellum
CbC	cerebellar cortex
CD68	cluster of differentiation 68
CERAD	Consortium to Establish a Registry for Alzheimer's Disease
CHMP2B	charged multivesicular protein 2B gene
CJD	Creutzfeldt-Jakob disease
CNS	central nervous system
CP	craniopharyngioma
CSF	cerebrospinal fluid
CSFIR	colony stimulating factor-I receptor gene
CV	Cresyl violet stain
C9ORF72	chromosome 9 open reading frame 72 gene
dH_2O	distilled water

List of Abbreviations (continued)

DHSS	Department of Health and Social Security
DMV	dorsal motor nucleus of the vagus nerve
DNA	deoxyribonucleic acid
DOB	date of birth
DOD	date of death
DR	dorsal root ganglion
DU	duodenum
DWI	diffusion-weighted imaging
ε	allelle of apolipoprotein gene; ε2, ε3 or ε4
EC	entorhinal cortex
EEG	electroencephalography
f	female
FA	formic acid
FC	frontal cortex
fCJD	familial Creutzfeldt-Jakob disease
FFI	fatal familial insomnia
FLAIR	fluid-attenuated inversion recovery
FLD	frontotemporal lobar degeneration
FUS	fused in sarcoma gene
g	gramme
g	gravitational force unit
G	guanine
GFAP	glial fibrillary acidic protein
GRB	progranulin gene
GSS	Gerstmann-Sträussler-Scheinker syndrome
h	hour
hDM	human dura mater
HE	heart
H&E	haematoxylin and eosin stain
hGH	human growth hormone
HuMM	transgenic mouse expressing human *PRNP* codon 129 MM

List of Abbreviations (continued)

HuMV	transgenic mouse expressing human *PRNP* codon 129 MV
HuVV	transgenic mouse expressing human *PRNP* codon 129 VV
HWP-hGH	human growth hormone produced by the Hartree modification of the Wilhelmi protocol
i	intermediate PrP^{res} isoform
iCJD	iatrogenic Creutzfeldt-Jakob disease
IGHD	idiopathic growth hormone deficiency
IHC	immunohistochemistry
IMS	industrial methylated spirits
IPHP	idiopathic panhypopituitarism
$iPrP^{C}$	insoluble aggregated PrP species
ITM2B	integral membrane protein 2 gene
K	kuru plaques
KI	kidney
kDa	kilodalton
l	litre
LBD	Lewy body disease
LBs	Lewy bodies
LC	locus ceruleus
LFB	luxol fast blue stain
LI	large intestine
LN	lymph node
LU	lung
LV	liver
m	male
M	methionine
M1	prion strain responsible for sCJD MM1/MV1 subtypes
MAPT	tau gene
Mb	millions of base pairs
mg	milligrammes
min	minutes

List of Abbreviations (continued)

ml	millilitre
mmol	millimole
MND	motor neurone disease
mo	month
mol	mole
MRC	Medical Research Council
MRI	magnetic resonance imaging
MU	muscle
MV2C	MV2 subtype of sCJD with cortical confluent spongiform change
MV2K	MV2 subtype of sCJD with kuru-type plaques and cortical confluent spongiform change
MV2K+C	MV2 subtype of sCJD with kuru-type plaques and cortical
mw	microwave
μg	microgramme
μl	microlitre
μm	micrometre
n	number
nm	nanometre
N/A	not available
NaPTA	sodium phosphotungstic acid
NCJDRSU	National Creutzfeldt-Jakob disease Research & Surveillance Unit
NFT	neurofibrillary tangles
ng	nanogram
NOTCH3	notch3 gene
NP	neuritic plaque
NspI	DNA restriction enzyme cloned in *Escherichia coli* from source Nostoc Sp. C (recognises 5'RCATGY:3'YGTACR)
OC	occipital cortex
PA	pancreas
PAS	periodic acid/Schiff stain
PBS	phosphate-buffered saline

List of Abbreviations (continued)

PC	parietal cortex
PCR	polymerase chain reaction
PD	Parkinson's disease
PET	positron emission tomography
PET blot	paraffin-embedded tissue blot
PHF	paired helical filaments
PI	pituitary
PK	proteinase K
PMCA	protein misfolding cyclical amplification
pmol	picomole
PN	peripheral nerve
pop	population
Prnp	prion protein gene in non-human mammals
PRNP	human prion protein gene.
PrP^{C}	cellular prion protein
PrP^{res}	protease-resistant core of PrP^{Sc} visualised on Western blots
PrP^{Sc}	disease-associated isoform of the cellular prion protein
PSEN1	presenilin 1 gene
PSEN2	presenilin 2 gene
QuIC	quaking-induced conversion
recPrP	recombinant prion protein
RNA	ribonucleic acid
rpm	revolutions per minute
RSS	Russell-Silver syndrome
RT-QuIC	real-time quaking-induced conversion
SC	spinal cord
sCJD	sporadic Creutzfeldt-Jakob disease
sd	standard deviation
SDS-PAGE	sodium dodecyl sulphate polyacrylamide gel electrophoresis
sec	second
senPrP	protease-sensitive intermediate form of PrP^{Sc}

List of Abbreviations (continued)

SERPINI1	neuroserpin gene
SG	salivary gland
SI	small intestine
SN	substantia nigra
SP	spleen
SQSTM1	sequestosome TM1 gene
SY	sympathetic chain
T	thymine
TARDBP	transactive response DNA binding protein-43 gene
TC	temporal cortex
TDP-43	Transactive response DNA binding protein - 43
Tg	transgenic
TG	trigeminal ganglion
Th	thalamus
ThT	thioflavin T
TO	tonsil
TREM2	triggering receptor on myeloid cells 2 gene
TSEs	transmissible spongiform encephalopathies
TY	thyroid gland
TYROBP	tyrosine kinase binding protein gene
UK	United Kingdom
USA	United States of America
UTR	untranslated end
UV	ultraviolet
v	volt
V	valine
V2	prion strain responsible for sCJD VV2 and MV2 subtypes
vCJD	variant Creutzfeldt-Jakob disease
VCP	valosin-containing protein gene
VPSPr	variably protease-sensitive prionopathy
WB	Western blot

List of Abbreviations (continued)

w/v	weight to volume ratio
y	years
+	positive
-	negative

Neuropathology and Molecular Biology of Iatrogenic Creutzfeldt-Jakob Disease in UK Human Growth Hormone Recipients

1. Introduction

1.1. Introduction to prion diseases

Prion diseases (also known as the transmissible spongiform encephalopathies or TSEs) are a group of fatal neurodegenerative disorders that affect both animals and humans and are associated with spongiform degeneration of the grey matter of the central nervous system (CNS) (Table 1.1). The CNS is the target system for prion diseases, within which high levels of infectivity (over 10^8 intracerebral Ld_{50}/g) are reached during the clinical disease (Robinson *et al*., 1990). Unlike commoner human neurodegenerative disorders such as Alzheimer's disease (AD) and Parkinson's disease (PD), human prion diseases are transmissible between individuals, with incubation periods measuring up to several decades (Ironside, 1998). The naturally occurring animal prion diseases are similarly transmissible; one of these diseases, bovine spongiform encephalopathy (BSE), has not only transmitted to a wide range of animal species (Table 1.1), but has also spread as a zoonotic infection to humans, resulting in variant Creutzfeldt-Jakob disease (vCJD) (Will *et al*., 1996).

1.1.1. A brief history of prions

Scrapie is the archetypal prion disease, described in the 18th century (Brown & Bradley 1998), but not demonstrated to be transmissible until 1936 (Cuillé & Chelle, 1936). Cuillé & Chelle assumed that some type of virus was the most likely causative agent and the term "slow virus infection" was proposed by Sigurdsson in 1954 because of the prolonged incubation periods associated with scrapie transmission (Sigurdsson, 1954). This assumption was challenged by subsequent studies of the scrapie agent,

Table 1.1.

Classification of human and animal prion diseases

Human prion diseases	
Idiopathic	Sporadic Creutzfeldt-Jakob disease
	Sporadic fatal insomnia
	Variably protease-sensitive prionopathy
Genetic	Familial Creutzfeldt-Jakob disease
	Gerstmann-Sträussler-Scheinker syndrome
	Fatal familial insomnia
	Prion protein cerebral amyloid angiopathy
Acquired	
Human origin:	Kuru
	Iatrogenic Creutzfeldt-Jakob disease
Bovine origin:	Variant Creutzfeldt-Jakob disease
Animal prion diseases	
Acquired	Scrapie (sheep, goats, mouflon) – classical and atypical forms (e.g. Nor 98)
	Chronic wasting disease (white-tailed deer, mule deer, elk, caribou, moose)
	Transmissible mink encephalopathy
	Bovine spongiform encephalopathy (domestic cattle) – classical and atypical forms
	Novel prion diseases related to bovine spongiform encephalopathy occur as :
	(a) Feline spongiform encephalopathy in domestic cats and Asian golden cat, cheetah, lion, ocelot, puma, tiger
	(b) exotic ungulate encephalopathy in zoo animals (American bison, Ankole cow, Arabian oryx, eland, gemsbok, greater kudu, nyala, scimitar-horned oryx)

which was found to be of remarkably small size and resistant to conventional methods of pathogen inactivation, including high temperatures, treatment with nucleases and ionising radiation (reviewed in Alper *et al*., 1978). Furthermore, no virus particles or nucleic acids were identified and no evidence of a host immune response to the scrapie agent could be found. These results led to the suggestions that the scrapie agent did not depend upon nucleic acid for replication (Alper *et al*., 1967) and that the agent might be composed only of protein (Griffith, 1967), which were received with considerable scepticism.

Subsequent work on rodent-passaged scrapie brain homogenates identified a glycoprotein that was the main constituent of the most highly infective brain homogenate fractions and accumulated in the brains of infected animals, sometimes forming amyloid structures (Prusiner *et al.*, 1978). Prusiner published the prion hypothesis in 1982: the term prion (from *pro*teinaceous *in*fectious particle) was proposed to distinguish the infectious scrapie pathogen from viruses or viroids (Prusiner, 1982). Prions were defined as "small proteinaceous infectious particles that resist inactivation by procedures which modify nucleic acids". The gene encoding the prion protein was identified in 1985 (Oechs *et al*., 1985), and its product, the cellular prion protein (PrP^{C}) was found to have the same amino acid sequence as the disease-associated prion protein (PrP^{Sc}), but with a different structure and physicochemical properties (see below) (Borchelt *et al*., 1990; Caughey & Raymond, 1991) (Figure 1.1).

Since the publication of this initially controversial hypothesis, a substantial body of experimental evidence has been published to support the prion hypothesis, although

contrary (but increasingly solitary) views persist (Botsios & Manuelidis, 2016). In particular, a range of novel synthetic prion strains has been generated from misfolded recombinant prion protein *in vitro*, some with high titres of infectivity that cause disease in wild-type mice (Legname *et al*., 2004; Kim *et al*., 2010; Makarava *et al*., 2010). Another approach to the de novo *in vitro* generation of prion strains has employed protein misfolding cyclical amplification (PMCA) methodology (see below), in which manipulation of the conditions under which the reaction occurs can influence the biological properties of the prion strains generated (Castilla *et al*., 2005; Barria *et al*., 2009).

1.2. Prion biology

1.2.1. PrP^C

The normal (cellular) form of the prion protein, PrP^C, has a three-exon structure in most species and is encoded by a single copy gene. The human prion protein gene (*PRNP*) is located on human chromosome 20p12-pterminus (Sparkes *et al*., 1986), with the final exon encoding the entire open reading frame of PrP^C. However, although *PRNP* contains a large exon 2-like sequence, the second exon is not spliced into the final mRNA sequence (unlike most other species apart from hamsters) (Lee *et al*., 1998). The other exons contain untranslated sequences including the promoter and termination sites, and intron 1 has been identified as essential for full promoter activity (Mahal *et al*., 2001). *PRNP* is developmentally regulated (Mobley *et al.*, 1988), with expression increasing to a steady level in the CNS from 10–20 days post conception in the hamster embryo (McKinley *et al*., 1987) and 13.5 days post conception in the mouse (Manson *et al*., 1992). More recently, PrP^C has been shown *in vitro* to control

the differentiation of human embryonic stem cells towards neurone-, oligodendrocyte-, and astrocyte-committed lineages and is therefore likely to be involved in the differentiation of uncommitted neural progenitor cells in the developing CNS (Lee & Baskakov, 2014).

PrP^C is highly conserved in many species and is expressed at highest levels in the CNS by neurones (enriched at synapses), with lower levels of expression in astrocytes and in a wide range of non-CNS tissues including skeletal muscle, heart, lung and platelets (Herms *et al*., 1999). It is a copper-binding glycoprotein that is bound to the outer leaflet of the cell membrane by a glycosylphosphatidylinositol (GPI) anchor in lipid raft microdomains (Harris *et al*., 2004) (Figure 1.1). Nascent PrP^C is 253 amino acids in length, with an unstructured N-terminal region and a structured C-terminal domain consisting of 3 α helices, a small β sheet region and a signal sequence for the attachment of the GP anchor (Alfonso *et al*., 2007; Linden *et al*., 2008) (Figure 1.1). PrP^C undergoes a number of post-translational modifications, which are initiated by the removal of the N- and C-terminal signal peptides and importation into the endoplasmic reticulum, followed by the attachment of the GPI anchor, attachment of 2 N-linked glycans and the formation of a disulphide bond between Cys178 and Cys213 (Mangé *et al*., 2004; Hooper, 2005) (Figure 1.2).

A complete loss of PrP^C function in prion protein gene "knock-out" transgenic animals does not adversely affect the lifespan and reproductive capacity of such animals, although a range of other minor phenotypic features have been reported that vary according to the transgenic model studied (reviewed in del Rio & Gavin, 2016). PrP

null mice are resistant to prion infection (even following intracerebral inoculation), emphasising the importance of the conversion of PrP^{C} to nascent PrP^{Sc} in the disease process; PrP^{Sc} when introduced into the CNS by inoculation is not neurotoxic in the absence of PrP^{C} (Brandner *et al*., 1996a, 1996b). PrP null mice and cell lines have also been explored closely for evidence of the function of PrP^{C}, sometimes with variable and apparently contradictory findings depending on the model system used (reviewed in Sakudo & Onodera 2015; del Rio & Gavin, 2016)

The function of PrP^{C} is still incompletely understood; in addition to its metal binding properties (Brown *et al*., 1997), a range of proposed CNS functions include cell signalling, neuronal growth and differentiation, synaptic plasticity and neuroprotection, particularly against oxidative stress (reviewed in Linden *et al*., 2008; Biasini *et al*., 2012; Atkinson *et al*., 2016). In peripheral nerves, PrP^{C} promotes myelin homeostasis through flexible tail-mediated Gpr126 agonism (Küffer *et al*., 2016). In other tissues, proposed roles for PrP^{C} include roles in the development, activation and proliferation of T lymphocytes, and in modulating macrophage phagocytosis (Mattei *et al*., 2004; de Almeida *et al*., 2005). Potential roles in cancer development, progression and multi-drug resistance have also been proposed (Zhao *et al*., 2002: Antonagopoulou *et al*., 2008, 2010) and apparently conflicting roles in both the removal of Aβ from the brain and transduction of the toxic actions of Aβ in AD are currently under investigation (Kudo *et al*., 2012; Jarosz-Griffiths *et al*., 2016).

Figure 1.1
Structure of PrP^{C} and PrP^{Sc} (with permission from Taylor and Francis, UK)

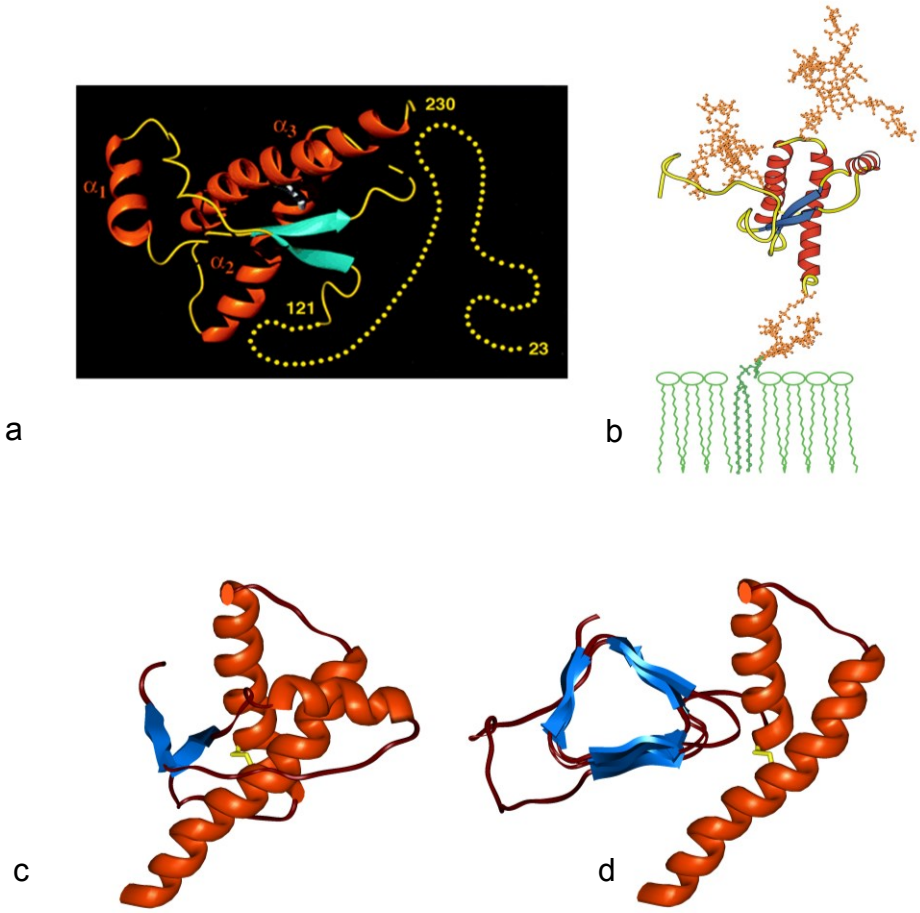

Cartoon of the 3-dimensional structure of human PrP^{C} (residues 23-230). The α helices are red, the β strands are cyan and the flexibly disordered C terminal region is represented by yellow dots (b) Schematic of PrP^{C} (residues 93-31) in its glycosylated form attached to the cell membrane by a glycosylphosphatidylinositol (GPI) anchor. The α helices are red, the short anti-parallel β sheet region is blue. The glycans and the carbohydrate component of the GPI anchor are orange. The lipid component of the GPI anchor and the cell membrane are green. (c) The structure of PrP^{C} contains mostly α helical structures (3 red ribbons) and a small portion of β sheet (blue arrows). The increase in a sheet (blue arrows) on conversion to PrP^{Sc} is depicted in (d). This theoretical structure shows the C-terminal α-helices to be preserved and (as in PrP^{C}) are linked by a disulphide bridge (yellow), but with more extensive β-sheet structures wound into what has been termed as a β-helix.

Abbreviations: PrP^{C}: cellular prion protein; PrP^{Sc}: disease-associated prion protein.
(a) Courtesy of Professor Kurt Wuthrich, Zurich, Switzerland; (b) Courtesy of Dr Mark Wormald and Professors Pauline Rudd and Raymond Dwek, Oxford, UK; (c ,d) Courtesy of Professor Fred Cohen, San Francisco, USA.

1.2.2. PrP^{Sc}

The human prion diseases (Table 1.1) are all characterised by the deposition of disease-associated PrP^{Sc} in the brain. The structure of PrP^{Sc} is markedly different from that of PrP^{C} and is closely associated with prion infectivity, but PrP^{Sc} has the same amino acid sequence and undergoes the same post-translational modifications as PrP^{C} (reviewed in Silva *et al*., 2015). PrP^{C} is readily soluble in non-denaturing detergent solutions and sensitive to digestion by proteinase K (PK) (Prusiner, 1998a). In contrast, PrP^{Sc} has an increased β-pleated sheet content, decreased solubility and increased protease-resistance compared with PrP^{C}, probably as a result of refolding of the central and N-terminal regions of the protein and self-aggregation (Figure 1.1). PrP^{Sc} and PrP^{C} are conformational isoforms (Figure 1.1); denaturation of PrP^{Sc} results in loss of its associated infectivity (Colby & Prusiner, 2011b).

The *de novo* formation of PrP^{Sc} is central to the pathogenesis of prion disease. This results from the conversion of PrP^{C} to PrP^{Sc}, which is thought to involve other co-factors (e.g. a hypothesised "protein X") (Telling *et al*., 1995); polyanions (RNA and glycosaminoglycans) and lipids have been implicated as likely cofactors (reviewed in Gill *et al*., 2010). Although the site of this conversion process is not fully established, PrP^{C} molecules on the cell surface of scrapie-infected cells may re-enter the cells through cholesterol-rich caveolae domains (Taraboulos *et al*., 1995). GPI-anchored PrP^{C} can then be converted into PrP^{Sc} by a templating process in which PrP^{C} refolds into a structure with an increased β-sheet content without further cleavage or alterations in glycosylation (Peters *et al*., 2003) (Figure 1.1).

Despite intensive investigation, the structure of PrP^{Sc} is still uncertain; it is difficult to obtain in large quantities, insoluble in non-denaturing detergents and has not been crystallised. Limited proteolysis by PK has therefore been used to explore the structure of PrP^{Sc}, which has also been examined by cryo-electron microscopy, X-ray diffraction, mass spectrometry and epitope analysis using panels of anti-PrP antibodies (reviewed in Silva *et al*., 2015). Recent molecular modelling studies have suggested that each PrP^{Sc} monomer is likely to be stacked as a 4-rung β solenoid, with areas of high resistance to PK in the β strands, with areas of higher PK sensitivity in turns and loops (Vazquez-Fernandez *et al*., 2012). In this model, the upper and lower β solenoids could template an unfolded PrP^{C} molecule, creating additional β solenoid rungs that can also participate in the process of templating (Silva *et al*., 2015). The process of PrP^{C} conversion is likely to include an intermediate stage in which the partially refolded molecule still retains PK sensitivity (Daude *et al*., 1997). The presence of such molecules (designated $senPrP^{Sc}$) in human prion diseases has been investigated by conformation-dependent immunoassay studies on brain biopsy samples (Safar *et al*., 2005).

Partially refolded PrP can form soluble, low molecular weight oligomers that are partially resistant to PK, neurotoxic *in vitro* on primary cultures of neurons and *in vivo* after subcortical stereotaxic injection into the brain (Silveira *et al*., 2005; Simoneau *et al*., 2007). Antibody rescue studies have shown that exposure of the hydrophobic stretch of PrP at the oligomeric surface is necessary for toxicity (Simoneau *et al*., 2007). Monomeric PrP^{Sc} was not toxic under these conditions and insoluble, fibrillar forms of PrP^{Sc} exhibited no toxicity *in vitro* and were less toxic than their oligomeric

counterparts *in vivo*. These findings suggest that oligomeric species of PrP^{Sc} are the most toxic forms of the molecule (Aguzzi & Falsig, 2012), as appears to be the case for other amyloidogenic proteins in neurodegenerative diseases, e.g. Aβ in AD (Salahuddin *et al*., 2016). Our understanding of the complex processes resulting in neuronal neurotoxicity in prion diseases is incomplete. Suggested mechanisms included early impairment of the ubiquitin-proteasome system (McKinnon *et al*., 2016), activation of complex cell stress pathways involving the endoplasmic reticulum, NAD^+ depletion and the RESET pathway (Zhou *et al*., 2015; Mays & Soto, 2016), altered mitochondrial function, protein synthesis machinery and purine metabolism (Ansoleaga *et al*., 2016), or sustained translational repression by elF2α-P (Moreno *et al*., 2012).

However, the classical neuropathological changes prion diseases (spongiform change, neuronal loss, gliosis and amyloid plaques) may develop in the CNS in some animal models in the apparent absence of detectable PrP^{Sc} (Lasmezas *et al*., 1997), although these models have not been fully explored for the presence of $senPrP^{Sc}$. Conversely, small amounts of insoluble aggregated PrP species (designated $iPrP^{C}$) can be detected in human brains without either clinical or neuropathological evidence of a prion disease (Yuan *et al*., 2006). This finding is of uncertain significance; a role for $iPrP^{C}$ in binding to Aβ species has been suggested, potentially increasing Aβ toxicity at neuronal synapses in aging and in AD (Xiao *et al*., 2012).

1.2.3. Prion strains

Serial passage of sheep scrapie in mice by intracerebral inoculation has identified

distinct strains of the transmissible agent on the basis of individual biological properties that become stable on serial passage (Bruce *et al*., 1993). These properties include the disease incubation period and neuropathological phenotype, particularly the distribution and severity of spongiform change in the brain (Bruce, 2003). In the absence of any nucleic acid associated with the transmissible agent, these variations in strain properties have been accounted for by conformational variability in PrP^{Sc} that is self-propagating (Prusiner, 1998a). This concept was reinforced by the discovery of distinct strains ("hyper" and "drowsy") of transmissible mink encephalopathy that are associated with different isoforms of PrP^{Sc} (Bessen & Marsh, 1994). More recent structural studies of synthetic prion strains derived from recombinant mouse prion protein also support this concept (Colby and Prusiner, 2011a).

The mouse prion protein gene (*Prnp*) (first identified as the *sinc* (scrapie incubation) gene) also exerts an effect on disease incubation period and phenotype (Moore *et al*., 1998). The primary transmission of sheep or bovine prions to mice is often inefficient, with only a proportion of the inoculated animals succumbing to disease with variable and sometimes protracted incubation periods, a phenomenon often referred to as the "species barrier" (Bruce *et al*., 1994). Serial passage in mice results in shortening and stabilisation of both the incubation period and the disease phenotype (Bessen and Marsh, 1994; Beringue *et al*., 2008). The underlying basis of the species barrier is not fully understood, but appears to be influenced by the degree of structural similarity between the prion proteins of the two species involved and the *Prnp* sequence similarities between these species (reviewed in Caughey, 2003; Beringue *et al*., 2008). The concept of prion strains has also been investigated in human prion diseases. The

prion strain causing vCJD appears distinct from those causing sporadic Creutzfeldt-Jakob disease (sCJD), and closely resembles the BSE strain, providing evidence that vCJD results from human exposure to BSE (Bruce *et al*., 1997, Scott *et al*., 1999). However, the number of strains occurring in sCJD and other human prion diseases is still a subject of debate (see below).

Conformational differences in the PrP^{Sc} in different prion strains can be assessed indirectly by examining the size of the core fragment of PrP^{Sc} after proteolytic degradation (PrP^{res}) using Western blotting (Parchi *et al*., 1996). Two major conformational variants of PrP^{res} occur in human prion diseases, which in the most commonly used nomenclature are termed type 1 and type 2 (Parchi *et al*., 1996) (Figure 1.2). Type 1 PrP^{res} is a core fragment with an N-terminus at glycine 82 with a molecular weight of around 21kDa. Type 2 PrP^{res} is more extensively digested, resulting in a core fragment with an N-terminus at serine 97 and a molecular weight of around 19kDa (Parchi *et al*., 2000). Western blots also demonstrate the proportion
of the three possible glycoforms of PrP (di-, mono, and non-glycosylated); the suffix A is used when the mono- or unglycosylated bands of PrP^{res} predominate and the suffix B is used when the diglycosylated band predominates (Parchi *et al*., 1997). The PrP^{res} type nomenclature employed throughout this thesis is that used by Parchi *et al*. and the vast majority of workers in this field (reviewed in Gambetti *et al*., 2003). Typical examples of the PrP^{res} isoforms found on Western blot (WB) examination of the brain in human prion diseases are shown in diagrammatic and pictorial form in Figure 1.2.

Figure 1.2.

Molecular typing of abnormal prion protein found in the brain in different forms of human prion disease

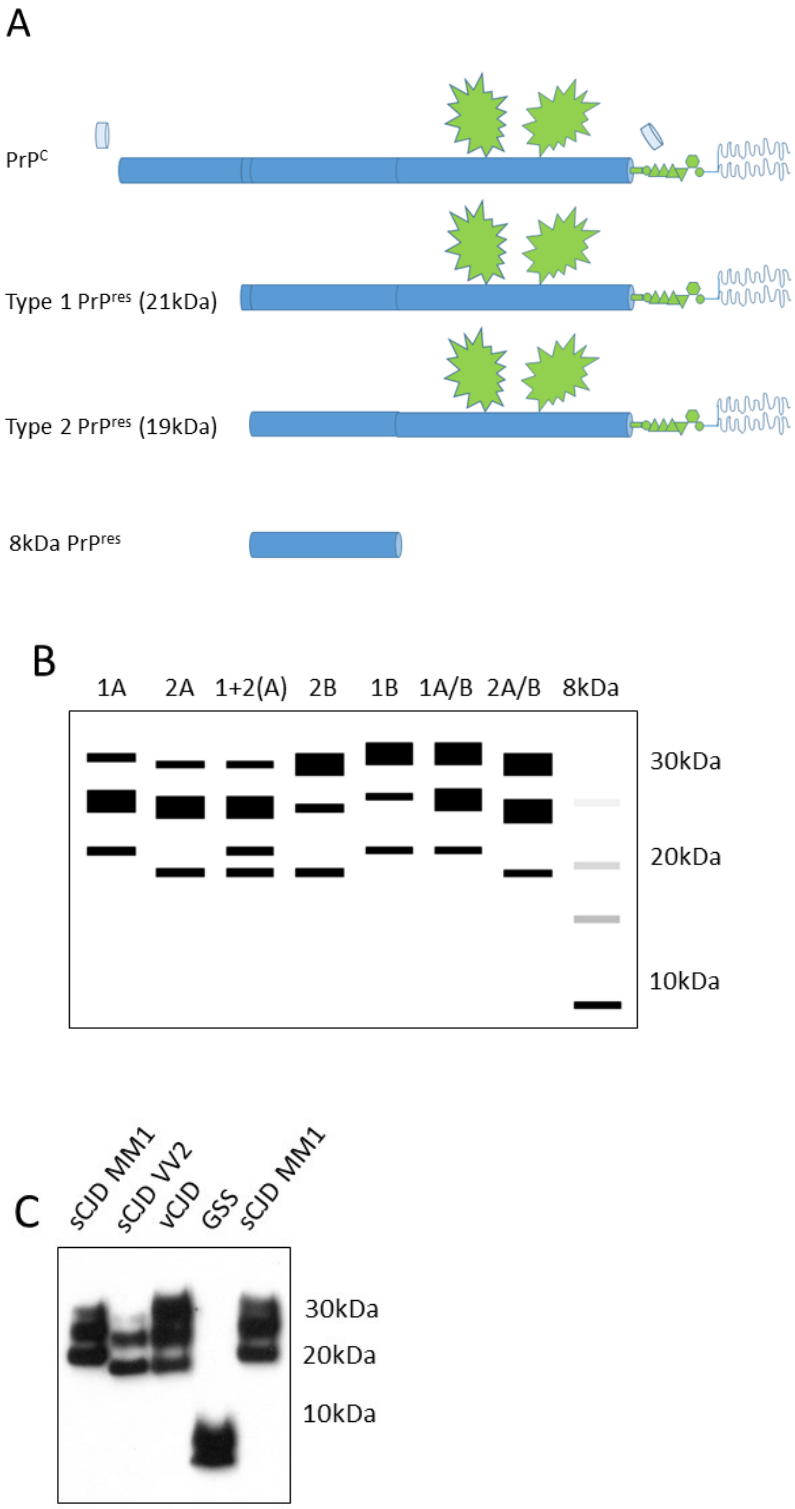

Courtesy of Dr Mark W Head, Edinburgh, UK.

Legend to Figure 1.2.

(A) Diagram showing the normal cellular prion protein (PrP^{C}) and the protease resistant fragments of the disease-associated isoform (PrP^{res}). The polypeptide backbone is shown as a blue cylinder and the two N-linked glycans and the glycosylphosphatidylinositol (GPI) anchor are shown in green, with the lipid component of the GPI anchor shown as blue lines. The N-terminal endoplasmic reticulum signal sequence and the C-terminal GPI anchor sequence are shown cleaved as light blue short cylinders. The diagram shows the protease resistant core fragments of the prion protein (PrP^{res}) remaining after digestion with proteinase K. Three major PrP^{res} fragments occur that differ in the extent of N-terminal digestion and whether or not C-terminal digestions occurs. The 21kDa type 1 and 19kDa type 2 forms contain the two N-linked glycosylation sites, whereas the 8kDa PrP^{res} fragment does not. (B) The combination of PrP^{res} fragment sizes (type 1, type 2 and 8kDa) and the variable occupancy of two potential glycosylation sites produce distinct banding patters when protease digested human prion disease brain homogenates are analysed by Western blotting using antibodies such as 3F4 that bind to the central region of the prion protein. The glycoform pattern is designated A when the middle (monoglycosylated) band predominates, B when the top (diglycosylated) band predominates and A/B when the mono- and di-glycosylated bands predominate at the expense of the bottom (non-glycosylated) band. Types 1A, 2A, 1+2(A) are characteristic of sCJD and iCJD. Type 2B is associated with vCJD. Types 1B, 1A/B and 2A/B are often found in genetic CJD, GSS and FFI. The 8kDa pattern is characteristic of some cases of GSS and of VPSPr. The faint ladder of bands that sometimes accompanies the 8kDa band in VPSPr is shown in grey. (C) shows an example of a Western blot analysis of post-mortem brain samples from individuals with sCJD of two distinct subtypes (sCJD MM1 and sCJD VV2), vCJD and GSS. The approximate positions of molecular mass markers are indicated in (B) and (C) in kilodaltons.

Abbreviations: CJD: Creutzfeldt-Jakob disease; FFI: fatal familial insomnia; GSS: Gerstmann-Sträussler-Scheinker syndrome; i: iatrogenic; M: methionine; s:sporadic; v: variant; V: valine; VPSPr: variably protease-sensitive prionopathy

1.2.4. Prion genetics

Studies of scrapie in sheep have identified three polymorphisms in the sheep *Prnp* gene (codon 136 A/V, codon 154 R/H and codon 171 Q/R) that have a major influence on both the disease incubation period and phenotype (Gonzalez *et al*, 2002; Baylis & Goldmann, 2004). The five major alleles VRQ, ARQ, ARH, AHQ and ARR show variable sensitivity to different scrapie strains; the ARR allele confers the greatest resistance to classical scrapie (Hunter *et al*., 1997). Several polymorphisms have also been identified in *PRNP*, of which the methionine (M) / valine (V) polymorphism at codon 129 (Figure 1.3) has a powerful effect on the clinicopathological phenotype in idiopathic, genetic and acquired diseases and the incubation period in acquired human prion diseases (Parchi *et al*., 1996, 1999; Collinge *et al*., 2006). Genetic human prion diseases - familial Creutzfeldt-Jakob disease (fCJD), Gerstmann-Sträussler-Scheinker syndrome (GSS), fatal familial insomnia (FFI) and prion protein cerebral amyloid angiopathy - are all associated with missense, insertion, deletion or amber mutations in the open reading frame of *PRNP*, of which over 50 have been identified (reviewed in Schmitz *et al*., 2016) (Figure 1.3).

1.3. *In vitro* models of prion disease

Early experimental work on scrapie in the 20th century was greatly facilitated by the transmission of the scrapie agent to mice by Chandler in 1961 (Chandler, 1961) allowing small animals rather than sheep or goats to be used as disease models and promoting the intensive studies of the scrapie agent from the 1960s onwards. Despite this, researchers still had to work on animal models with lengthy incubation periods

Figure 1.3.

Diagrammatic representation of the human prion protein gene open reading frame (codons 1-235) with the structural landmarks of the encoded prion protein marked (with permission from Taylor and Francis, UK)

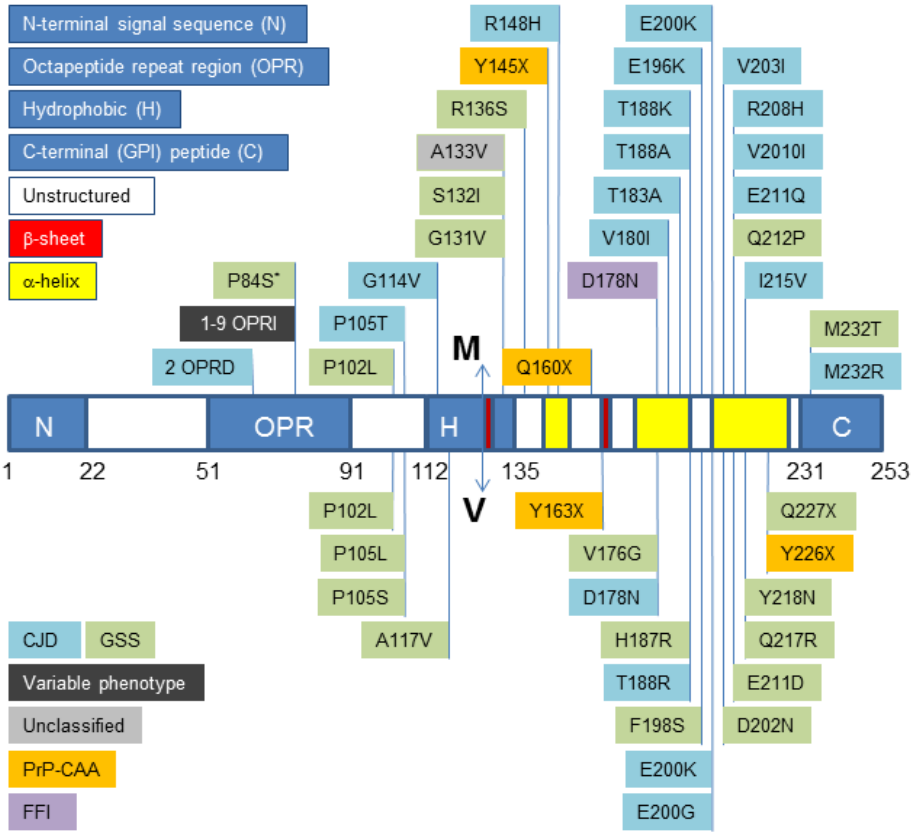

The positions of pathogenic mutations are superimposed using codon number and single letter amino acid codes. The mutations are colour coded with respect to the disease phenotype and are place above or below the schematic to indicate the haplotype with respect to the codon 129 polymorphism of the mutated allele. The position of the codon 129 polymorphism (methionine (M)/valine(V)) is also indicated. An asterix (*) indicates a currently unknown haplotype.

Abbreviations: CJD: Creutzfeldt-Jakob disease; CAA: cerebral amyloid angiopathy; FFI: fatal familial insomnia; GSS: Gerstmann-Sträussler-Scheinker syndrome; PrP: prion protein.

and logistical and financial limits to the numbers used for experimental study. A suitable cell culture system to support the replication of the scrapie agent and to study its cell biology was therefore sought. This proved difficult as different sources and strains of scrapie and other prion diseases appeared to have their own unique requirements *in vitro*. Consequently, most cell culture work on scrapie has been performed with a mouse neuroblastoma cell line that can infected with scrapie (Butler *et al*., 1988) and has been used in a wide range of applications including the study of PrP^{Sc} conversion, subcellular localisation, pathophysiology and species barrier determinants (Solassol *et al*., 2003). More recently, other cell lines that support scrapie replication have been developed, and advances in molecular genetics have contributed to the increasing range of cell lines now available for work with animal prions and synthetic prions (Solassol *et al*., 2003; Klohn *et al*., 2003; van der Merwe *et al*., 2015). However, there remains a lack of cell culture systems suitable for research on human prions. Self-renewing populations of human embryonic stem cells were challenged with sCJD, vCJD and BSE and rapidly took up PrP^{Sc}. However, when the infectious source was removed, the intracellular levels of PrP^{Sc} fell rapidly (Krejciova *et al*., 2011). This work has been invaluable in helping determine how exogenous prions are dealt with by cultured cells, but the challenge of developing a cell line that can be infected with (and hopefully cured of) human prions still remains.

In contrast, cell free *in vitro* conversion systems have more recently been developed to model PrP^{C} conversion and other aspects of prion biology, to study transmission barriers and allow the sensitive detection of PrP^{Sc}. Work in this field began in the 1990s with the *in vitro* conversion assay, where samples of tissue (usually brain tissue)

containing PrP^{Sc} were incubated with a substrate containing radiolabelled PrP^{C} (Kocisko *et al*., 1994; Raymond, *et al*., 1997). This approach has now been refined by the addition of a shaking step during the incubation process of the PrP^{Sc} seed with a substrate, now termed quaking induced conversion (QuIC) (Orru *et al*., 2009). A recent development of this technique is to incorporate thioflavin T (ThT) into the reaction, which binds to the amyloid structures generated by the PrP conversion process, causing a change in the ThT fluorescence emission spectrum that can be measured in real time (RT-QuIC) (Atarashi *et al.*, 2011) (Figure 1.4A). RT-QuIC allows the rapid and sensitive detection of PrP^{Sc} generated from a variety of recombinant PrP substrates, including truncated PrP substrates (Zanusso *et al*., 2016). This technique is now being applied in clinical diagnosis, particularly in the detection of PrP^{Sc} in CSF samples from sCJD patients with very high sensitivity and specificity (McGuire *et al*., 2016).

Another cell free *in vitro* conversion assay to be developed recently is the protein misfolding cyclical amplification (PMCA) assay (Saborio *et al*., 2001). This also uses PrP^{Sc} seeds and PrP^{C} substrates (e.g. normal brain homogenates or recombinant PrP) in sequential rounds of incubation and sonication to promote PrP^{C} conversion to PrP^{Sc}, which is then detected by Western blotting at the end of the reaction as PrP^{res} (Castilla *et al*., 2006) (Figure 1.4B). The ability to undertake numerous sequential rounds of PMCA conversion allows the amplification and ultrasensitive detection of PrP^{Sc} in tissues, fluids and the environment (reviewed in Saa & Cervenakova, 2014). PMCA can also be used to investigate the conversion potential of various combinations of substrates and seeds, e.g. vCJD and sCJD seeds with human PrP^{C} substrates of

Figure 1.4.

Schematic representation of real-time quaking-induced conversion (RT-QuIC) and protein misfolding cyclic amplification (PMCA)

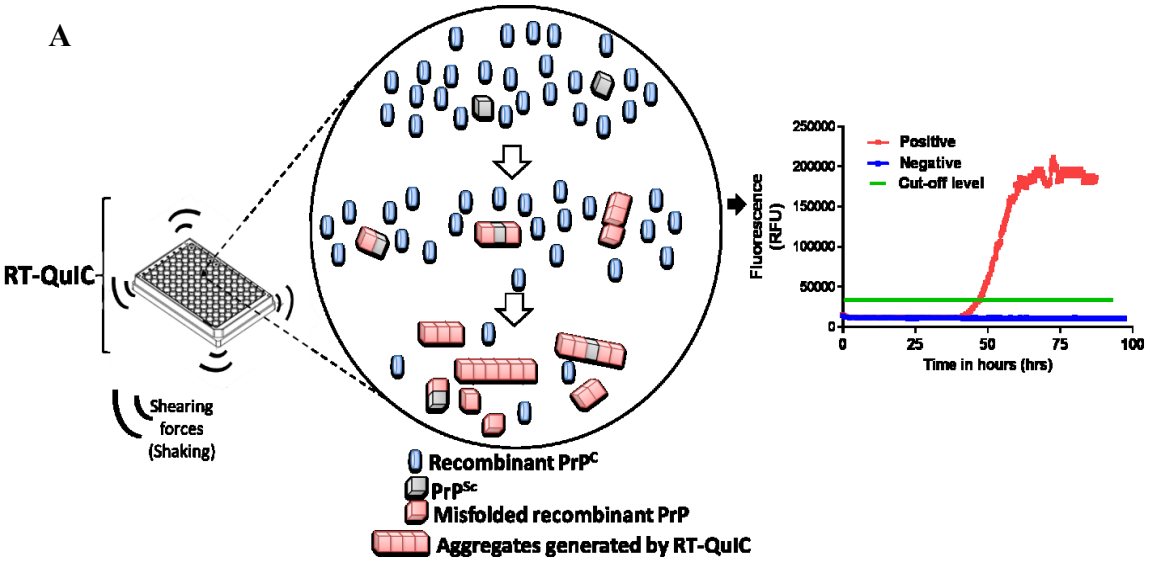

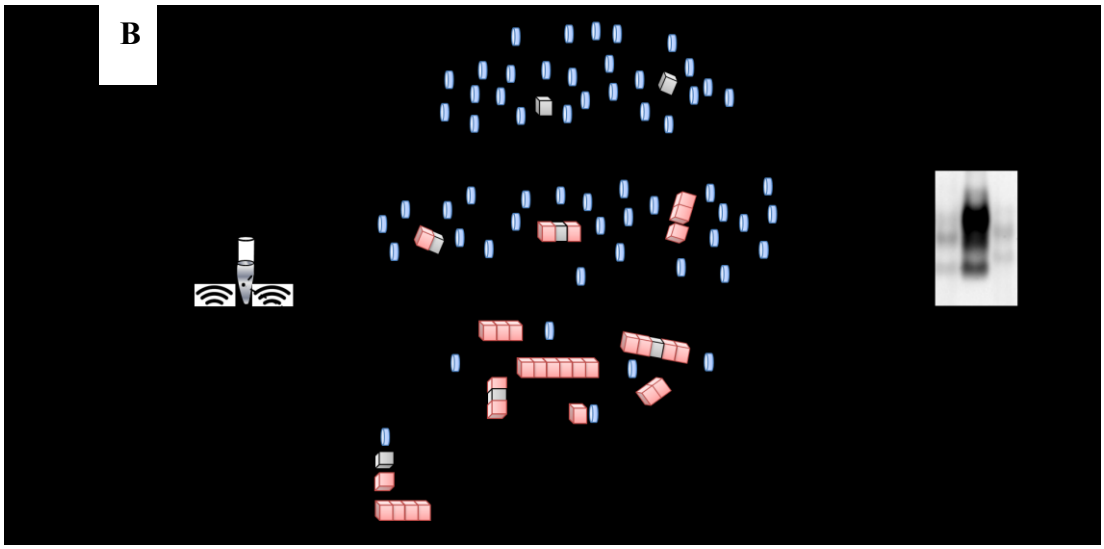

B

Courtesy of Dr A Peden and Dr M Barria, Edinburgh, UK.

Legend to Figure 1.4.

A: In RT-QuIC**,** a large excess of recombinant PrP^{C} substrate is incubated with minimal quantities of PrP^{Sc} seed in the presence of Thioflavin T (ThT), followed by cycles of incubation and shaking. PrP^{C} in the substrate is converted into PrP^{Sc} in β-sheet structures that grow, converting and incorporating further PrP^{C} molecules. Each cycle of shaking and incubation (represented by arrows) breaks the nascent PrP^{Sc} aggregates, creating further seeds for PrP^{C} conversion. Aggregate formation is monitored over time by plotting the increasing ThT fluorescence (when ThT binds β-sheet structures) as a graph.

B: PMCA is comparable to RT-QuIC, except that mammalian brain PrP^{C} is used a substrate and sonication is used to disrupt the nascent PrP^{Sc} aggregates. At the end of PMCA, the PrP^{Sc} generated in the amplification reaction is detected by western blotting as PrP^{res}. Densitometry is used to assess the PrP^{res} level in the amplified sample in comparison with the PrP^{res} level in the non-amplified seed.

Abbreviations: PMCA: protein misfolding cyclical amplification; PrP^{C}: cellular prion protein; PrP^{res}: protease-resistant prion protein; PrP^{Sc}: disease-associated prion protein; RT-QuIC: real-time quaking-induced conversion.

differing *PRNP* codon 129 genotypes (Jones *et al*., 2011) and cross-species PMCA to explore the zoonotic potential of different animal PrP^{Sc} seeds for differing human PrP^{C} substrates (Barria *et al*., 2014). This method also has diagnostic applications, such as the detection of PrP^{Sc} in the urine and blood of patients with vCJD (Moda *et al*., 2014; Lacroux *et al*., 2014). The PMCA technique also amplifies infectivity in the seed for the reaction, thus supporting the prion hypothesis (reviewed in Morales *et al*, 2012). The exploration of factors influencing PrP^{C} conversion indicates that currently unknown components present in normal brain homogenates have a positive influence, but polyanions (including short RNA sequences) also promote conversion (Deleault *et al*., 2003, 2007). Finally, repeated PMCA cycles in the absence of a PrP^{Sc} seed can result in the *de novo* generation of PrP^{Sc} and infectivity by apparently chance misfolding of the PrP substrate (Castilla *et al*., 2005; Barria *et al*., 2009). Modification of these PMCA reactions using defined substrate components (a "recipe for prions") can influence the strain characteristics of the resulting prions, providing further evidence in support of the prion hypothesis (Lee & Caughey, 2007; Deleault *et al*., 2007; Abid *et al*., 2010).

1.4. Human prion diseases

1.4.1. Introduction

The expanding spectrum of human prion diseases includes idiopathic (sporadic), genetic (inherited) and acquired (infectious) disorders (Table 1.1). Human prion diseases are characterised clinically by progressive multifocal neurological signs and symptoms, including rapidly progressive cognitive decline with dementia, visual abnormalities, movement disorders, myoclonus and ataxia. The duration of the clinical

illness is variable, but ranges from a few months in sCJD to several years in some genetic prion disease. Prion diseases have characteristic neuropathological features that include spongiform change in the grey matter with variable neuronal loss, reactive gliosis and the accumulation of PrP^{Sc} in the brain, sometimes in the form of amyloid plaques. PrP^{Sc} can be detected biochemically in the CNS by WB examination (Figure 1.2) and by other tissue-based investigations, including immunohistochemistry (IHC) and paraffin-embedded tissue (PET) blots (Ritchie *et al*., 2004).

Neuropathological examination of the CNS is essential for a "definite" diagnosis of a human prion disease according to internationally accepted diagnostic criteria (see Tables 1.4, 1.5, 1.7 and 1.9 below). This is usually confined to autopsy brain examination, since brain biopsy in patients with prion diseases often results in subsequent clinical deterioration and the neurosurgical instruments coming into contact with the prion-infected brain have to be destroyed to prevent the risk of subsequent iatrogenic transmission (Advisory Committee on Dangerous Pathogens: www.gov.uk/ government/ uploads/ system/uploads/attachment_data /file/ 427854/ Infection _ control v3.0.pdf). Brain biopsy is therefore usually confined to patients in whom the possibility of an alternative treatable condition exists, e.g. cerebral vasculitis.

1.4.2. Historical background

In the 1920s, Hans Creutzfeldt and Alfons Jakob separately reported 5 cases of an unusual fatal neurological disorder of unknown aetiology (Creutzfeldt, 1920; Jakob, 1921a, 1921b, 1923). The term "Creutzfeldt-Jakob disease" (CJD) was introduced in

1922 (Spielmeyer, 1922) and was subsequently used to describe a range of neurological conditions, including the "amyotrophic form of CJD", many of which are now considered not to be human prion diseases (Masters & Gajdusek, 1982). Subsequent neuropathological review of Creutzfeldt's original case indicated that it is unlikely to be an example of a human prion disease, likewise for 3/5 of Jakob's cases reported in 1921 and 1923 (Masters & Gajdusek, 1982). The term originally used by Jakob was 'spastic pseudosclerosis', since it clinically resembled some cases of multiple sclerosis, but had "remarkable anatomical findings" (Jakob, 1921a, 1921b, 1923). Jakob experimentally inoculated rabbits in an attempt to demonstrate an infectious origin for CJD, which was unsuccessful; rabbits are now known to be relatively resistant to prion diseases (Collinge, 2005). Consequently, an infectious aetiology was not considered likely, particularly since there was no neuropathological evidence of an inflammatory reaction in the brain or other features indicating infection by any of the then known CNS pathogens. In the following years many different aetiologies were proposed for CJD, including neurodegenerative, vascular and metabolic disorders (Nevin *et al*., 1960). Familial forms of 'spastic pseudosclerosis' were identified as early as 1924 (Kirschbaum, 1924) and GSS was reported in 1936 as an inherited spinocerebellar ataxia with distinctive neuropathological features that did not appear to be related to CJD (Gerstmann *et al*., 1936).

In the late 1950s, Gajdusek and Zigas reported an acute progressive degenerative CNS disorder that was endemic in a remote tribe in the Highlands of New Guinea, known as "kuru" in the native population (Gajdusek & Zigas, 1957, 1959). The aetiology of kuru was unknown; however, a detailed study of a series of kuru brains suggested that

there were similarities to the neuropathology of sCJD, which was not known at that time to be a transmissible disease (Klatzo *et al*, 1959). In the same year, on the basis of his observation that the neuropathology of kuru in humans resembled that of scrapie in sheep, Hadlow proposed an infectious aetiology for kuru (Hadlow, 1959). This led to the experimental transmission of kuru to chimpanzees in 1965 (Gajdusek *et al*., 1966), followed by similar transmissions of sCJD and later GSS to chimpanzees (Gibbs *et al*., 1968; Masters *et al*., 1981).

The genetic basis of GSS was reported in 1989, when a *PRNP* P102L mutation was identified in two affected kindreds (Hsiao *et al*., 1989); in the same year, a 144 bp insertional mutation in *PRNP* was identified in a UK kindred with familial CJD (Owen *et al*., 1989). Since then, many pathogenic mutations, non-pathogenic mutations and polymorphisms in *PRNP* have also been identified, including the polymorphisms at codon 129 (Table 1.2) and codon 219 that predispose to certain forms of human prion disease (Schmitz *et al*., 2016) (Figure 1.3). A human source of acquired CJD was reported in 1974, when iatrogenic transmission of CJD was identified in a corneal graft recipient (Duffy *et al*., 1974). Early epidemiological surveillance studies of sCJD in the UK attempted to identify possible sources of acquired infection and identified a series of 3 cases associated with transmission via neurosurgery (Will & Matthews, 1982). The first cases of iatrogenic CJD in human growth hormone recipients were reported in 1985 from both the United States of America (USA) and the United Kingdom (UK) (Koch *et al*., 1985; Gibbs *et al*., 1985; Powell-Jackson *et al*., 1985).
The genetic basis of fatal familial insomnia (a familial disease described over centuries in Italy with no similarities to CJD or GSS) was finally revealed when the D178N

mutation at codon 178 in *PRNP* with methionine at codon 129 was identified in 1992 (Medori *et al*., 1992). The underlying genetic mutation in the family described by Kirschbaum in 1924 was identified in 1994 as the D178N mutation with valine at codon 129 (Brown *et al*., 1994). Variant CJD was identified in the UK in 1996 and attributed to oral infection from BSE in the foodchain (Will *et al*., 1996). The latest member of the ever-expanding group of human prion diseases, variably protease-resistant prionopathy, was reported in the USA in 2008 (Gambetti *et al*., 2008).

1.5. Overview of human prion diseases

The subject of this thesis, iatrogenic CJD in human growth hormone recipients in the UK, has a likely origin from sCJD and can be compared with other acquired human prion diseases in the UK, including iatrogenic CJD acquired from human dura mater grafts and variant CJD. Accordingly, these forms of human prion disease will be the main subjects of this section, but the other forms of human prion disease are included more briefly for the sake of completeness. Animal prion diseases are discussed only in terms of their known relationships to human prion diseases.

1.5.1. Sporadic CJD

1.5.1.1. *Epidemiology*

Sporadic CJD accounts for around 85% of all human prion diseases. It is a rare disorder with a worldwide incidence of around 1-2 cases per million per annum in most national surveys (Ladogana *et al*., 2005). No good evidence exists to indicate an environmental source of infection (Cousens *et al*., 1997) and detailed case-control studies have failed to demonstrate any other significant risk factors (Linsell *et al*., 2004; de Pedro Cuesta

et al., 2012). A history of surgery has been identified as a possible risk factor in some, but not all studies (Ward *et al*., 2002, de Pedro Cuesta *et al*., 2011). No occupational risk factors have been identified, including in medical or paramedical staff (Alcalde-Cabero e*t al*., 2012). No definitive evidence exists to suggest that sCJD is transmissible via blood transfusion (Dorsey *et al*., 2009; Puopolo *et al.*, 2011). However, recent experimental transmission studies in transgenic mice overexpressing human prion protein with codon 129 MM has detected infectivity in plasma from a small series of sCJD patients (Douet *et al*., 2014). Sporadic CJD has been transmitted by contaminated neurosurgical instruments, intracerebral electrodes and inoculated tissue extracts, grafts and implants, resulting in iatrogenic CJD (see below). Since there is no persuasive evidence to indicate that sCJD is an acquired disease, it has been proposed that sCJD results either from the random conversion of PrP^{C} to PrP^{Sc} in the CNS, or a somatic pathogenic mutation in *PRNP*, resulting in the self-replication and accumulation of PrP^{Sc} in the CNS and leading to neuronal dysfunction, the onset of clinical signs and symptoms and ultimately death (Prusiner, 1998b).

1.5.1.2. *Subgroups of sporadic CJD*

Studies of large cohorts of sCJD cases have identified some key factors influencing the disease phenotype, which helps explain the variable clinical presentations and disease course. Sporadic CJD can be divided into subgroups that are defined by the *PRNP* codon 129 polymorphism that encodes either methionine (M) or valine (V) (Table 1.2). The three possible genetic subgroups (MM, MV, VV) can be subdivided according to the PrP^{res} isoform detected by WB analysis of brain tissue homogenates in each case: type 1 or type 2. This gives 6 possible subgroups - MM1, MM2, MV1,

MV2, VV1 and VV2; the MM1 and MV1 subtypes have a common phenotype (MM1/MV1) and the MM2 subtype is divided into the cortical and thalamic variants, with markedly different clinical features and neuropathology (Parchi *et al*., 1999). Table 1.3 summarizes the predominant clinical and neuropathological features of these sCJD subtypes. The MM2 thalamic subtype of sCJD is increasingly being referred to as sporadic fatal insomnia because of its clinical and neuropathological similarities to fatal familial insomnia (see below), in the absence of the *PRNP* haplotype associated with this genetic prion disease (Mastrianni *et al*., 1999). Not all cases of sCJD cases exhibit the characteristic features summarized in Table 1.3 and atypical cases are increasingly being recognised in terms of both their clinical and neuropathological features (Ironside *et al*., 2005).

Table 1.2.

PRNP codon 129 polymorphisms in the normal population and in prion diseases

	***PRNP* codon 129 polymorphisms (%)**		
	MM	**MV**	**VV**
Normal population[1]	39	50	11
Sporadic CJD[2]	60	20	20
Variant CJD[3]	99	1	-

[1]Data pooled from five studies (http://www.cjd.ed.ac.uk/documents/report23.pdf).

[2]UK deaths from sporadic CJD 1996-2014 for whom genetic data are available (n=856) (http://www.cjd.ed.ac.uk/documents/report23.pdf).

[3]National CJD Research & Surveillance Unit 2016 (http://www.cjd.ed.ac.uk/documents/worldfigs.pdf).

Abbreviations: CJD: Creutzfeldt-Jakob disease; M: methionine; *PRNP*: prion protein gene; v: valine.

Table 1.3.

Major subtypes of sporadic CJD classified by *PRNP* codon 129 genotype and PrP^{res} isoform (data from the UK National Creutzfeldt-Jakob Disease Research & Surveillance Unit)

*sCJD SUBTYPE	FREQUENCY (%)	MEDIAN AGE AT ONSET (y)	MEDIAN DURATION OF ILLNESS (m)	DISTRIBUTION OF VACUOLATION	PrP DEPOSITION PATTERN
MM1	57	66	3	Cerebral cortex (occipital)	Synaptic Perineuronal
MM2	7	52	17	Cerebral cortex Entorhinal cortex	Perivacuolar
VV1	2	53	10	Cerebral cortex (temporal) Entorhinal cortex Striatum	Synaptic
VV2	14	66	6	Cerebellum Striatum Thalamus Hippocampus	Perineuronal (linear) Synaptic Plaque-like
MV1	6	73	5	Cerebral cortex (occipital) Cerebellum	Synaptic Perineuronal
MV2	14	65	11	Cerebral cortex Striatum Thalamus Hippocampus	Kuru plaques Synaptic

* Cases with mixed PrP^{res} subtypes are not included

Abbreviations: CJD: Creutzfeldt-Jakob disease; M: methionine: PrP: prion protein; PrP^{res}: protease-resistant prion protein; V: valine.

1.5.1.3. *Clinical features*

Sporadic CJD occurs as a progressive neurological disorder affecting predominantly elderly patients, with an average age of around 65 years and an equal sex distribution. However, a wide age range can be affected, including rare cases in teenagers.

Patients present most commonly with rapidly progressive dementia, ataxia, visual abnormalities and myoclonus (Head *et al*., 2015). Early diagnosis is challenging as patients may present with isolated abnormalities such as cerebellar ataxia (particularly in the VV2 subtype) or cortical visual impairment (particularly in the MM1 subtype). Most patients with sCJD die within 4 months after the onset of neurological abnormalities, but there is a wide variation in the duration of illness, with some patients surviving for more than 2 years (particularly the MM2 subtype).

The clinical diagnosis of sCJD and other human prion diseases is aided by specialised investigations, including electroencephalography (EEG), magnetic resonance imaging (MRI) of the brain and examination of the cerebrospinal fluid (CSF), which are all included in internationally accepted criteria for the clinical diagnosis of sCJD (Table 1.4). Periodic triphasic EEG complexes are diagnostic of sCJD and occur commonly in the MM1/ MV1 subgroup, but do not occur in all other subgroups (Zerr *et al*., 2000). MRI shows increased signal in the caudate nucleus, putamen, and/or cerebral cortex (cortical "ribboning") on diffusion-weighted imaging in up to 80% of cases (Meissner *et al*., 2009a). A positive CSF assay for 14-3-3 protein is not specific for sCJD per se, as this investigation can be positive in other conditions associated with rapid neuronal death, eg stroke or herpes simplex encephalitis, but is useful when other conditions potentially causing elevated CSF levels of 14-3-3 are excluded (Green *et al*., 2007).

RT-QuIC amplification of PrP^{Sc} in the CSF has a remarkably high sensitivity and specificity for sCJD and is now included in the diagnostic criteria (McGuire *et al*., 2016). Olfactory mucosa biopsy combined with RT-QuIC amplification of PrP^{Sc} also has potential as a highly sensitive and specific diagnostic test (Zanusso *et al*., 2016).

Table 1.4.

Diagnostic criteria for sporadic Creutzfeldt-Jakob disease.
(http://www.cjd.ed.ac.uk/documents/criteria.pdf)

1. Sporadic CJD (from 1 January 2017)

1.1 **DEFINITE:**
Neuropathologically/ immunocytochemically confirmed

1.2 **PROBABLE:**

I	Rapidly progressive dementia
II	A Myoclonus B Visual or cerebellar problems C Pyramidal or extrapyramidal features D Akinetic mutism
III	Typical EEG (generalised periodic complexes)
IV	High signal in caudate/putamen on MRI brain scan or at least 2 cortical regions (temporal, parietal occipital) either on DWI or FLAIR

1.2.1 I + 2 of II + III, OR

1.2.2 I + 2 of II + IV, OR

1.2.3 Possible + positive 14-3-3, OR

1.2.4 Progressive neurological syndrome and positive RT-QuIC in CSF or other tissues

1.3 **POSSIBLE:** I + two of II + duration < 2 years

Abbreviations: CJD: Creutzfeldt-Jakob disease; EEG: electroencephalogram; MRI: magnetic resonance imaging

1.5.1.4. *Neuropathology*

Macroscopic examination of the brain in sCJD usually shows only age-related changes, often with sparing of the hippocampus. Cerebellar atrophy, most evident in the superior vermis, is present in some cases of sCJD, particularly the VV2 subtype. Cerebral and cerebellar atrophy may occur in cases with a long duration of illness; severe cerebral atrophy is accompanied by secondary degeneration of the cerebral white matter, referred to as panencephalopathic CJD (Jansen *et al*., 2009).

The microscopic neuropathology of sCJD is characterised by spongiform change, reactive gliosis involving microglia and astrocytes, and the accumulation of PrP^{Sc} , with amyloid plaque formation in the form of the kuru-type plaques that are characteristic of the MV2 subtype (Head *et al*., 2015). These features vary in their distribution and severity within a single brain, but characteristic readily identifiable pathological features have been described for each of the different sCJD subtypes (Parchi *et al*., 2012). Spongiform change comprises collections of rounded vacuoles in the grey matter of the brain. In the microvacuolar spongiform change found in the MM1/MV1 subtypes, the vacuoles vary from 2–20 μm in diameter. Larger vacuoles occur in the confluent spongiform change in the cerebral cortex in the in the MM2 and MV2 sCJD subtypes (Parchi *et al*., 1999). Status spongiosis in the cerebral cortex occurs when there is severe neuronal loss and gliosis, collapse of the cortical cytoarchitecture and numerous large, coarse vacuoles are present. Although status spongiosis can occur in other disorders e.g. frontotemporal lobar degeneration and severe hypoxic brain damage, it is characteristic of panencephalopathic sCJD. Ultrastructural studies of sCJD have revealed tubulovesicular structures within

neurones, the origin of which is uncertain (Liberski *et al*., 1992). Although also present in many other forms of human prion disease, these structures do not label with antibodies to PrP (Liberski *et al*., 2005).

PrP^{Sc} aggregates in various patterns in the grey matter in sCJD, including granular/synaptic deposits in the MM1/MV1 subtypes, perivacuolar accumulation in the MM2 cortical subtype, perineuronal and plaque-like accumulations in the VV2 subtype, and kuru-type amyloid plaques in the MV2 subtype (Parchi *et al*., 1999). PrP^{Sc} may also be detected in extraneural tissues in sCJD, including the peripheral nervous system, pituitary gland and (rarely) in the spleen (Glatzel *et al*., 2003; Head *et al*., 2004b; Peden *et al*., 2006, 2007). The characteristic histological and immunohistochemical features of the six sCJD subtypes are illustrated in Figure 1.5.

1.5.1.5. *Molecular biology*

Western blot examination of different brain regions in sCJD has revealed that different PrP^{res} types can occur in different brain regions. In some cases, the co-occurrence of PrP^{res} types 1 and 2 has been identified in the same brain region (Head & Ironside, 2012). These abnormalities appear to occur in approximately 30% of sCJD cases, resulting in a review of the classification system described above (Parchi *et al*., 2009); these abnormalities may provide further explanation for phenotypic variability in sCJD. It has been proposed that the different PrP^{res} isoforms in CJD may also be linked to different causative prion strains, a concept referred to as "molecular strain typing" (Parchi *et al*., 1999; Haik *et al*., 2011).

Figure 1.5.

Characteristic histological and immunohistochemical features of sCJD subtypes. (with permission from Taylor and Francis, UK)

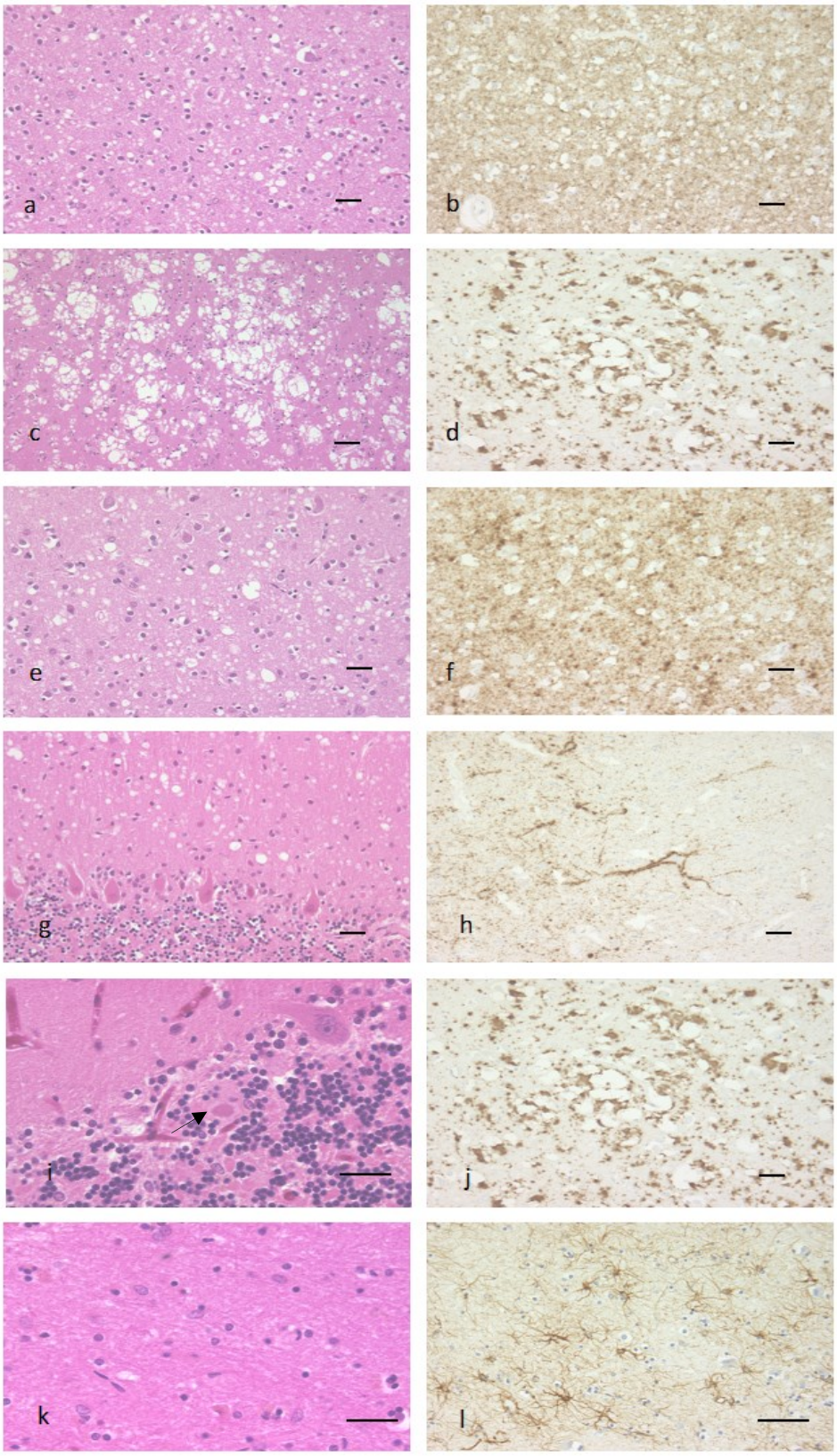

Legend to Figure 1.5.

The MM1/MV1 subtype of sCJD shows widespread microvacuolar change in the frontal cortex (a) with a predominantly granular/synaptic pattern of PrP accumulation (b).

The MM2C subtype of sCJD shows widespread confluent spongiform change in the temporal cortex (c), with intense perivacuolar immunoreactivity for PrP (d).

The VV1 subtype of sCJD shows widespread microvacuolar spongiform change in the temporal cortex (e), and synaptic and focal perineuronal positivity for PrP on immunohistochemistry (f).

The VV2 subtype of sCJD shows widespread vacuolation, neuronal loss and gliosis in the cerebellum (g), and a perineuronal and synaptic pattern of PrP immunoreactivity in the parietal cortex (h).

The MV2 subtype of sCJD is characterised by kuru-type amyloid plaques in the cerebellum (arrow) (i), with both plaque and plaque-like immunoreactivity for PrP (j).

Sporadic fatal insomnia (sCJD MM2T subtype) shows severe neuronal loss and gliosis in the anterior and medial thalamic nuclei, with little spongiform change (k). Thalamic gliosis is demonstrated by immunohistochemistry for glial fibrillary acidic protein (l).

(Sections a, c, e, g, i and k are stained with haematoxylin and eosin and sections b, d, f, h, j, and l are stained by immunohistochemistry for PrP using the KG9 antibody.)
Scale bar=250μm

Abbreviations: M: methionine; sCJD: sporadic Creutzfeldt-Jakob disease; PrP: prion protein; V: valine.

Experimental transmission studies have been performed to identify and characterise the strains of prions that cause sCJD (Bishop *et al*., 2010; Parchi *et al*., 2010; Gambetti *et al*., 2011; Moda *et al*., 2012). Overall, the results indicate that more than a single strain is responsible for this disorder, but there appears to be no direct correlation between the prion strains identified and the sCJD subtypes described in Table 1.3. Most researchers agree that at least five different prion strains can be identified in the different sCJD subtypes; these are provisionally designated the M1, M2C, M2T, V1 and V2 strains (Haik *et al.*, 2011). The M1 strain has been isolated from sCJDMM1 and MV1 cases, the M2C strain from sCJDMM2 cortical cases and the M2T strain from sCJDMM2 thalamic cases; the V1 strain has been isolated in sCDVV1 cases only, but the V2 strain has been isolated from both sCJDVV2 and sCJDMV2 cases. Further work in characterising sCJD strains is in progress, using both experimental transmission studies and in vitro conversion/seeding studies, making it is highly likely that any further information on this topic will reveal increasing complexity (Chapuis *et al*., 2016).

1.5.2. Variably protease-sensitive prionopathy

Variably protease-sensitive prionopathy (VPSPr) was first described in the USA in 2008 as a novel idopathic human prion disease with unique biochemical findings in the brain (Gambetti *et al*., 2008). Similar cases were subsequently identified in Europe (Head *et al*., 2013). No predisposing environmental cause for VPSPr has been reported and no mutations in the *PRNP* coding sequence have been identified to date. VPSPr occurs most commonly in the *PRNP* codon 129 VV genotype, followed by the MV and MM genotypes, in contrast to sCJD (Zou *et al*., 2010). As for sCJD, most VPSPr

patients are in the seventh decade or older, but the clinical history is lengthy (usually over 2 years) and includes movement disorders, extrapyramidal signs, cerebellar ataxia, and cognitive impairment. Rapidly progressive dementia is uncommon (Zou *et al*., 2010). No clinical diagnostic criteria for VPSPr have yet been defined; consequently, the precise incidence of this disorder is unknown. However, a retrospective review in the UK indicated that although it is underascertained, it appears to be much rarer than sCJD (Head *et al*., 2013).

Microscopy of the brain shows irregular collections of vacuoles of intermediate size in the cerebral cortex, basal ganglia, thalamus, and cerebellar cortex (Gambetti *et al*., 2008). The most striking neuropathological feature is the presence of microplaques, often arranged in a "target" pattern in the cerebellar molecular layer, particularly in the *PRNP* codon 129 VV genotype (Zou *et al*., 2010). Microplaques may also be found in the thalamus, basal ganglia, hippocampus, and cerebral cortex, hippocampus, basal ganglia and thalamus, and are periodic acid/Schiff-(PAS) positive with intense labeling on immunohistochemistry for prion protein. Differential labelling of microplaques with panels of different anti-PrP antibodies is another characteristic feature of VPSPr (Head *et al*., 2013), which can readily be identified from the VV2 and MV2 subtypes of sCJD (Parchi *et al*., 1999). The *PRNP* codon 129 genotype modifies the neuropathological phenotype of VPSPr, with larger plaques appearing in the MM genotype (Zou *et al*., 2010).

VPSPr was so named because of the presence of PrP^{Sc} in the brain that is poorly resistant to PK digestion, yielding a characteristic 8-kDa N- and C-terminally truncated

band in Western blots (Figure 1.2). These are often accompanied by a faint "ladder" of bands extending into the 18–30 kDa range (Fig. 6) (Gambetti *et al*., 2008). Some recent cases of VPSPr have also contained a sCJD-like type 2A isoform in the cerebellum, suggesting a possible molecular overlap with sCJD (Head *et al*., 2013). Recent experimental transmission studies have shown that VPSPr is poorly transmissible to transgenic mice, with transmission characteristics markedly different from those of sCJD (Diack *et al*., 2014; Notari *et al*., 2014).

1.5.3. Genetic prion diseases

Genetic forms of human prion disease are thought to account for around 10-15% of all cases of human prion disease (Ladogana *et al*., 2005). They are inherited as autosomal dominant disorders, usually with almost complete penetrance and a markedly variable age at onset (Kong *et al*., 2004). A clear-cut family history of a neurological disorder is not always obtained (possibly due to spontaneous *PRNP* mutations), favouring the collective term of genetic prion disease to an alternative of familial prion disease (Kovacs *et al*., 2005). Historical clinical classification into different forms - familial Creutzfeldt-Jakob disease (fCJD), fatal familial insomnia (FFI) and GSS - is now accompanied by *PRNP* sequence analysis, which has found over 50 distinct point, amber, insertional and deletion mutations associated with disease (Schmitz *et al*., 2016) (Figure 1.3). The internationally agreed diagnostic criteria for genetic prion diseases are summarised in Table 1.5. Phenotypic variation occurs within kindreds carrying an identical *PRNP* mutation; the polymorphic codons at 129 and 219 on both the mutant and non-mutated *PRNP* alleles are major influences in determining phenotypic variation in many forms of genetic prion diseases (Head *et al*., 2015).

Many, but not all, familial prion diseases have been transmitted experimentally; some of those transmitted more recently have used a transgenic mouse with a corresponding *PRNP* mutation to achieve transmission, since earlier attempts to transmit the disease to wild-type mice were unsuccessful (reviewed in Head *et al*., 2015).

1.5.3.1. *Principal disease subtypes*

Familial CJD is the commonest form of genetic prion disease and closely resembles sCJD in its clinical and neuropathological features, occasionally being identified only after *PRNP* sequencing in cases of apparently sporadic CJD, with no relevant family history. The *PRNP* mutation associated with most cases of familial CJD is E200K, which has been identified in many countries across the world, but numerous other *PRNP* mutations have been identified in association with this disorder (Head *et al*., 2015) (Figure 1.3).

GSS was first identified as a progressive spinocerebellar syndrome accompanied by other neurological features including pyramidal signs and progressive cognitive decline, which does not always result in dementia (Gerstmann *et al*., 1936). GSS patients in the past have been diagnosed with other inherited disorders, e.g. spinocerebellar ataxia, particularly if *PRNP* gene sequencing is not performed or neuropathological examination of the CNS is not carried out (Head *et al*., 2015). The P102L mutation was the first *PRNP* mutation to be identified in GSS (Hsiao *et al*., 1989); an ever- increasing number of point mutations associated with GSS have since been identified (Figure 1.3). The neuropathology of GSS is characterised by the multicentric PrP-amyloid plaques in the cerebellar cortex and occasionally in other grey matter regions (Ghetti *et al*., 1996). Spongiform change is often absent, or

Table 1.5.

Diagnostic criteria for genetic prion diseases.
(http://www.cjd.ed.ac.uk/documents/criteria.pdf)

3.1 **DEFINITE**

3.1.1 Definite TSE + definite or probable TSE in 1st degree relative

3.1.2 Definite TSE with a pathogenic *PRNP* mutation (see box)

(TSE: transmissible spongiform encephalopathy; *PRNP*: prion protein gene)

3.2 **PROBABLE**

3.2.1 Progressive neuropsychiatric disorder + definite or probable TSE in 1st degree relative

3.2.2 Progressive neuropsychiatric disorder + pathogenic *PRNP* mutation (see box)

- **PRNP MUTATIONS ASSOCIATED WITH GSS NEUROPATHOLOGICAL PHENOTYPE**
  P102L, P105L, A117V, G131V, F198S, D202N, Q212P, Q217R, M232T, 192 bpi
- **PRNP MUTATIONS ASSOCIATED WITH CJD NEUROPATHOLOGICAL PHENOTYPE**
  D178N-129V, V180I, V180I+M232R, T183A, T188A, E196K, E200K, V203I, R208H, V210I, E211Q, M232R, 96 bpi, 120 bpi, 144 bpi, 168 bpi, 48 bp*del*
- **PRNP MUTATIONS ASSOCIATED WITH FFI NEUROPATHOLOGICAL PHENOTYPE**
  D178N-129M
- **PRNP MUTATION ASSOCIATED WITH VASCULAR PrP AMYLOID**
  Y145s
- **PRNP MUTATIONS ASSOCIATED WITH PROVEN BUT UNCLASSIFIED PRION DISEASE**
  H187R, 216 bpi,
- **MUTATIONS ASSOCIATED WITH NEURO-PSYCHIATRIC DISORDER BUT NOT PROVEN PRION DISEASE**
  I138M, G142S, Q160S, T188K, M232R, 24 bpi, 48 bpi, 48 bpi + nucleotide substitution in other octapeptides
- **PRNP MUTATIONS WITHOUT CLINICAL AND NEUROPATHOLOGICAL DATA**
  T188R, P238S
- **PRNP POLYMORPHISMS WITH ESTABLISHED INFLUENCE ON PHENOTYPE**
  M129V
- **PRNP POLYMORPHISMS WITH SUGGESTED INFLUENCE ON PHENOTYPE**
  N171S, E219K, 24 bp deletion
- **PRNP POLYMORPHISMS WITHOUT ESTABLISHED INFLUENCE ON PHENOTYPE**
  P68P, A117A, G124G, V161V, N173N, H177H, T188T, D202D, Q212Q, R228R, S230S

variable in its severity and distribution. Some *PRNP* mutations, e.g. F198S, are associated with widespread neurofibrillary tangles in the cerebral cortex in addition to multicentric amyloid plaques (Ghetti *et al*., 1995). The presence of widespread amyloid plaques in GSS is frequently accompanied by a 8kDa PrP^{res} band on Western blot examination of unfixed brain tissue (Piccardo *et al*., 1998).

FFI is characterised clinically by sleep disturbance, dysautonomia, cognitive impairment and variable pyramidal signs (Medori *et al*., 1992). Neuropathological examination shows severe thalamic gliosis with marked neuronal loss, particularly in the anterior thalamic nuclei. The inferior olivary nuclei, the cerebral and cerebellar cortex exhibit more variable neuronal loss and gliosis. Spongiform change and PrP^{Sc} deposition in the brain are absent in most brain regions (including the thalamus), but may occasionally be found in the entorhinal cortex (Parchi *et al*., 1998). FFI is associated with the *PRNP* D178N-129M haplotype (Medori *et al*., 1992). The *PRNP* D178N mutation also occurs in some patients with familial CJD; however, these cases are associated with a D178N-129V haplotype (Goldfarb *et al*., 1992). Phenotypic variability in FFI is influenced by the *PRNP* codon 129 genotype on the wild-type allele (Harder *et al*., 1999).

Some of the rarer forms of genetic prion diseases, particularly those caused by caused by *PRNP* insertional mutations, have in the past been misdiagnosed clinically as other neurodegenerative disorders, including AD and Huntington's disease (Harder *et al*., 1999; Mead *et al*., 2006). It is therefore likely that the frequency of these and other rarer forms of genetic prion disease is underestimated. However, a recent large-scale

genetic study has found that apparently pathogenic mutations in *PRNP* are at least 30 times more common than expected in the general population on the basis of genetic prion disease prevalence (Minikel *et al*., 2016). Although this finding may be attributable to some benign genetic variants mistakenly being assigned as pathogenic, other variants have genuine effects on disease susceptibility, but confer lifetime risks ranging from <0.1 to ~100%. This study also found that truncating variants in *PRNP* have position-dependent effects, with true loss-of-function alleles found in healthy older individuals.

1.5.4. Kuru

Kuru was first reported in the 1950s as a common neurological disorder affecting particularly women and children in the isolated Fore tribe in the Eastern Highlands of Papua New Guinea (Gajdusek & Vigas, 1957, 1959). The main clinical features were a progressive ataxic syndrome with dysarthria, dysphagia, tremor, pyramidal and extrapyramidal motor dysfunction. Emotional lability occurred in the final stages of the illness, but cognitive decline and dementia were rare. The neuropathology was characterized by spongiform change in the grey matter of the CNS and the presence of large numbers rounded amyloid deposits with a solid core and radiating fibrils in the cerebellar cortex, referred to as "kuru plaques" (Klatzo *et al*., 1959).

A number of causes for cause of kuru were suggested, including genetic, endocrine, nutritional and toxic causes, until the neuropathological changes were proposed to resemble those of scrapie, a disorder that was not apparently transmissible to human and had hitherto been largely ignored by medical science (Hadlow, 1959). This

observation led to the intracerebral inoculation of kuru to chimpanzees, which were kept under long term surveillance. In 1965, three of these animals developed a kuru-like illness 18-21 months after inoculation, proving that kuru was a transmissible spongiform encephalopathy of humans (Gajdusek *et al*., 1966).

Kuru occurred as an epidemic within the Fore tribe, transmitted by ritualistic endocannibalism of deceased tribe members, during which the brain was handled or consumed mainly by women and children (reviewed in Liberski *et al*., 2012). The youngest recorded patient was 5 years old, while in the 1950s the mean age at death in the tribe was 49 years. After this ritual was discouraged in the tribe, the age at death of kuru patient increased. The final patients dying in the early 21st century were over 60 years old, with incubation periods of over 40 years (Collinge *et al*., 2006). Kuru is now extinct; it had affected all *PRNP* codon 129 genotypes in the tribe; heterozygotes appear to have had significantly longer incubation periods than homozygotes, particularly the methionine homozygotes (Collinge *et al*., 2006). Genetic analysis of kuru patients and the New Guinea population has identified a novel *PRNP* polymorphism (G12V) that was found exclusively in inhabitants of the region in which kuru was prevalent. It was present in half of the otherwise susceptible women from the region of highest kuru exposure and appears to represent an acquired resistance factor selected during the kuru epidemic (Mead *et al*., 2009). Kuru may have originated from the chance consumption of a tribe member who had died with sCJD; this possibility is supported by transmission studies of a few recent kuru cases, which found transmission characteristics similar to sporadic CJD, but different from variant CJD (Wadsworth *et al*., 2008).

Recent neuropathological re-examination of kuru brains confirms the earlier observations of a similarity to sCJD and demonstrates widespread accumulation of PrP^{Sc}, particularly in the form of kuru plaques (McLean *et al*., 1998). The neuropathological features appear to be influenced by the *PRNP* codon 129 genotype, with kuru-type plaques generally associated with the MV genotype. No evidence of PrP^{Sc} accumulation in lymphoid tissues was noted in a recent kuru case, in which the PrP^{res} isoform in the brain resembled that of the type 2 isoform found in sCJD (Brandner *et al*., 2008).

1.5.5. Variant CJD

1.5.5.1. *Variant CJD and BSE*

Variant CJD was identified in 1996 as a new form of human prion disease in the UK that might have resulted from human exposure to BSE by the consumption of contaminated meat products (Will *et al*., 1996). BSE occurred as an epizootic in the UK, with the first cases were reported in 1987 (Wells *et al*., 1987). However, it is highly likely that cattle were affected for several years prior to this date: 1980 is a generally accepted date for the beginning of the BSE epizootic, but BSE may have occurred before this estimated date of onset (Wells & Wilesmith, 1995).

BSE appears to have been transmitted by the feeding of contaminated meat and bone meal animal feed produced from cattle carcasses to dairy cattle, which after death were then rendered and recycled for the production of meat and bone meal animal feed (Wells & Wilesmith, 1995). The origin of BSE remains unknown; possible sources of infection include scrapie from sheep that were also recycled for animal feed, a sporadic

case of BSE, or a mutation in the cattle *Prnp* gene resulting in a BSE-like illness in one or more cattle (Richt & Hall, 2008). BSE also spread to some other species fed with the same product, including exotic ungulates and domestic cats (Table 1.1) – interestingly, the case in a UK zoo nyala was identified in 1986 before the first cases of BSE in cattle were reported (Kirkwood & Cunningham, 1994). BSE also infected wild cats in UK zoos that were fed with contaminated cattle carcasses (Table 1.1). Although over 180,000 clinical cases of BSE were identified in the UK, the number of asymptomatic infected animals entering the human food chain is likely to have been much higher, possibly as many as 3 million up to 1996, when the reinforced animal feed ban to abolish the feeding of ruminant-derived proteins to cattle was introduced in the UK (Smith & Bradley 2003). The BSE epizootic reached its peak in 1992, since when it has declined markedly due to the effects of the 1996 reinforced animal feed ban, although isolated cases were still detected up to 2015, almost 20 years after the ban (Department of the Environment, Food and Rural Affairs, 2016).

Transmission studies in wild-type and transgenic mice (Bruce *et al*., 1997; Scott *et al*., 1999) have provided evidence that the transmissible agent in vCJD (but not sCJD) has similar strain characteristics to the BSE agent. vCJD most likely results from dietary consumption of high-titre BSE-infected tissues in the food chain (Ward *et al*., 2006). Concerns that there might be a large epidemic of vCJD in the UK have not yet materialised, since the numbers of new vCJD cases peaked in 2000 and have subsequently declined. Humans are likely to have a high species barrier to BSE and the infectious oral dose for transmission of BSE to humans also appears to be high (Lasmezas *et al*., 2005; Bishop *et al*., 2006). These factors are likely to have helped

restrict the UK vCJD epidemic to 175 primary cases to date. Three additional secondary vCJD cases have occurred in the UK as a likely consequence of transmission via transfusion of packed red blood cells from UK vCJD-infected donors (reviewed in Urwin *et al*., 2016) (Figure 1.6).

1.5.5.2. *Genetics*

All tested definite and probable UK cases of vCJD up to 2015 belong to the *PRNP* codon 129 MM subgroup, but a definite case in 2016 was identified in a *PRNP* codon 129 MV patient (Table 1.2; Figure 1.6). This recent case raises the possibility of a further cases in this genotype, which is the commonest in the UK.

The incubation period for vCJD is unknown, but a mean value of 16 years has been estimated (Valleron *et al*., 2001). The full extent of the vCJD epidemic cannot yet be determined, particularly because of the possibility of further cases in *PRNP* codon 129 heterozygotes, which may have a more prolonged incubation period than the codon 129 MM cases (Garske & Ghani, 2010). Smaller numbers of vCJD cases have been identified in other countries (Table 1.6), either as a result of local exposure to BSE-contaminated meat products, or to exposure during a period of residence in the United Kingdom during 1980–1996, when dietary BSE exposure was likely. The number of new cases of vCJD in these countries has also declined, although a further case was reported in Italy in 2016.

Figure 1.6.

Annual deaths from variant CJD in the United Kingdom.

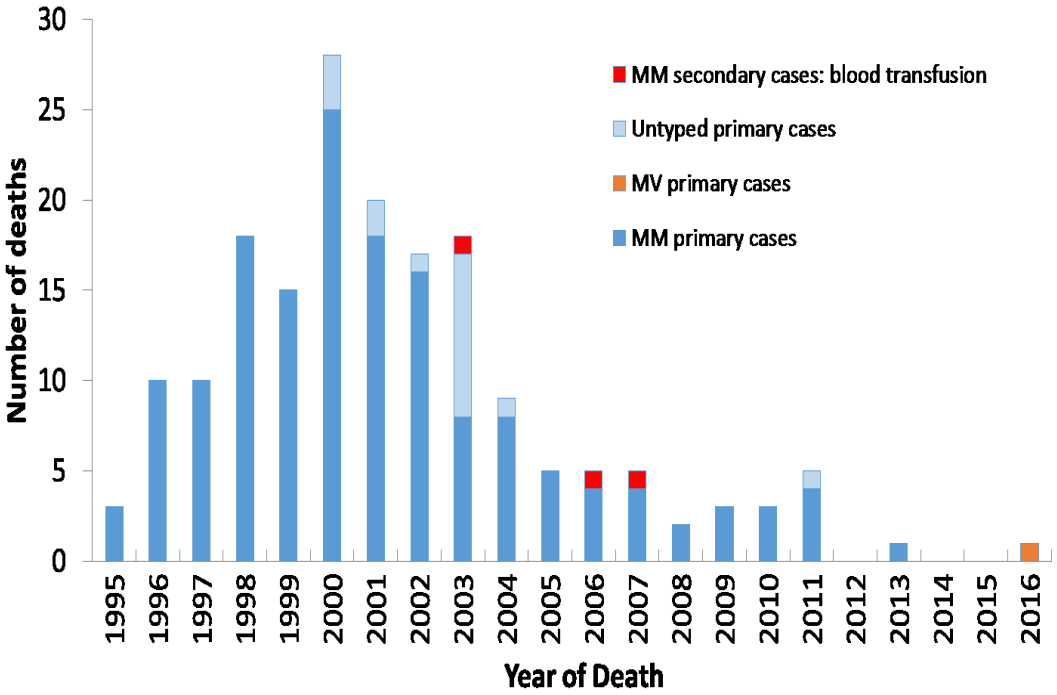

Numbers of variant CJD cases in the UK grouped by the year of death and the numbers of deaths per year. *PRNP* codon 129 genotype data is provided where known (unknown cases are indicated as untyped) and the three secondary variant CJD cases occurring as a result of infection via transfusion of packed red blood cells are also indicated.

Abbreviations: CJD: Creutzfeldt-Jakob disease. M: methionine; *PRNP*: prion protein gene; V: valine

Courtesy of Ms Jan Mackenzie, Edinburgh, UK.

Table 1.6.

Worldwide cases of variant CJD (http://www.cjd.ed.ac.uk/documents/worldfigs.pdf)

COUNTRY	TOTAL NUMBER OF PRIMARY CASES (NUMBER ALIVE)	TOTAL NUMBER OF SECONDARY CASES: BLOOD TRANSFUSION (NUMBER ALIVE)	RESIDENCE IN UK > 6 MONTHS DURING PERIOD 1980-1996
UK	175 (0)	3 (0)	178§
France	27 (0)	-	1
Republic of Ireland	4 (0)	-	2
Italy	3 (0)	-	0
USA	4† (0)	-	2
Canada	2 (0)	-	1
Saudi Arabia	1 (0)	-	0
Japan	1* (0)	-	0
Netherlands	3 (0)	-	0
Portugal	2 (0)	-	0
Spain	5 (0)	-	0
Taiwan	1 (0)	-	1

† The third US patient with variant CJD was born and raised in Saudi Arabia and has lived permanently in the United States since late 2005. According to the US case-report, the patient was most likely infected as a child when living in Saudi Arabia.
The completed investigation of the fourth US patient did not support the patient's having had extended travel to European countries, including the United Kingdom or travel to Saudi Arabia. It confirmed that the case was in a United States of America citizen born outside the Americas and indicated that his infection occurred before he moved to the United States; the patient had resided in Kuwait, Russia and Lebanon. (http://wwwnc.cdc.gov/eid/article/21/5/pdfs/14-2017.pdf)

* The case from Japan had resided in the UK for 24 days in the period 1980-1996.
§ Case 178 from the UK was heterozygous (methionine/valine) at codon 129 of the *PRNP* gene

Abbreviations: CJD: Creutzfeldt-Jakob disease; *PRNP*: prion protein gene.

1.5.5.3. *Clinical features*

Variant CJD affects young patients with a mean age at death of 30 years and a median duration of illness of 14 months (Heath *et al*., 2011). The youngest case had an onset at 11 years and was reported from Portugal (Barbot *et al*., 2010). The age distribution may be attributable to age-related differences in dietary BSE exposure (Cooper & Bird 2002), or age-related disease susceptibility (Boelle *et al*., 2004). The presenting symptoms are nonspecific and usually psychiatric (anxiety, depression, personality change), often with painful sensory symptoms, for a mean of 6 months before the emergence of neurological signs and symptoms, including progressive ataxia, visual problems, cognitive decline and involuntary movements, including myoclonus, dystonia and chorea (Zeidler *et al*., 1997a, 1997b) (Table 1.7). The terminal stages are characterised by akinetic mutism, similar to sCJD. Death is usually due to intercurrent infection. Six UK vCJD cases over the age of 55 years have been identified, of which only two were diagnosed in life, reinforcing the need for autopsy to provide a definitive diagnosis and for effective disease surveillance (el Tawil *et al*., 2015). Further similar cases can be predicted on the basis of epidemiological data and disease modelling (Valleron *et al*., 2001), implying that the full extent of the vCJD epidemic cannot yet be established. The internationally agreed diagnostic criteria for vCJD are summarised in Table 1.7.

The EEG usually appears normal in vCJD; the periodic triphasic complexes characteristic of sCJD have only rarely been reported in the terminal stages of vCJD (Binelli *et al*., 2006; Yamada, 2006). CSF analysis of 14-3-3 is positive in around 50% of vCJD cases (Green *et al*., 2001), while the RT-QuiC test for PrP^{Sc} in CSF has been

Table 1.7.
Diagnostic criteria for variant Creutzfeldt-Jakob disease
(http://www.cjd.ed.ac.uk/documents/criteria.pdf)

4.1 **DEFINITE**

1A **and** neuropathological confirmation of variant Creutzfeldt-Jakob disease[e].

4.2 **PROBABLE**

4.2.1 I **and** 4/5 of II **and** IIIA **and** IIIB

4.2.2 I **and** IV A[d]

4.3 **POSSIBLE**

I **and** 4/5 of II **and** III A

I A Progressive neuropsychiatric disorder
B Duration of illness > 6 months
C Routine investigations do not suggest an alternative diagnosis
D No history of potential iatrogenic exposure
E No evidence of a familial form of prion disease

II A Early psychiatric symptoms[a]
B Persistent painful sensory symptoms[b]
C Ataxia
D Myoclonus or chorea or dystonia
E Dementia

III A Electroencephalogram does not show the typical appearance of sporadic CJD[c] in the early stages of illness
B Bilateral pulvinar high signal on brain magnetic resonance imaging

IV A Positive tonsil biopsy[d]

---

a depression, anxiety, apathy, withdrawal, delusions.
b this includes both frank pain and/or dysaesthesia.
c the typical appearance of the electroencephalogram in sporadic CJD consists of generalised triphasic periodic complexes at approximately one per second. These may occasionally be seen in the late stages of variant CJD.
d tonsil biopsy is **not** recommended routinely, nor in cases with electroencephalogram appearances typical of sporadic CJD, but may be useful in suspect cases in which the clinical features are compatible with variant CJD and magnetic resonance imaging does not show bilateral pulvinar high signal.
e spongiform change and extensive prion protein deposition with florid plaques throughout the cerebrum and cerebellum.

Abbreviation: CJD: Creutzfeldt-Jakob disease.

negative to date. MRI scans show high signal in the posterior thalamus (the so-called "pulvinar sign") and in the periaqueductal region of the midbrain on fluid-attenuated inversion recovery (FLAIR) and/or diffusion-weighted imaging (DWI) sequences in over 90% of vCJD cases in *PRNP* codon 129 MM patients (Collie *et al*., 2003) (Fig. 9). The recent *PRNP* codon 129 heterozygote vCJD patient case had similar clinical features to previous cases, but the MRI scan showed features more in keeping with sporadic CJD. Tonsil biopsy in vCJD patients can demonstrate abnormal prion protein accumulation in the lymphoid follicles on IHC and PrP^{res} on WB examination (Hill *et al*., 1999). However, this procedure is not without risk and is not recommended in patients who otherwise satisfy the clinical diagnostic criteria for vCJD.

1.5.5.4. *Neuropathology*

In marked contrast to sCJD, the neuropathology of vCJD is stereotyped and characterised by the presence of large numbers of florid plaques in the cerebral cortex and cerebellar cortex, composed of a central eosinophilic amyloid core with radiating linear amyloid fibrils surrounded by a corona of spongiform change (Fig. 10) (Will *et al*., 1996). Spongiform change is present to a variable extent in the cerebral cortex and cerebellum, but is most marked in the caudate nucleus and putamen. The thalamus shows less spongiform change and amyloid plaque formation, but there is severe neuronal loss and gliosis in the posterior nuclei, particularly the pulvinar (Ironside *et al*., 2000). The distribution of these abnormalities corresponds to the abnormalities identified in this region of the brain on MRI (Collie *et al*., 2003). The brainstem and

spinal cord show no evidence of florid plaques and exhibit minimal spongiform change.

Immunohistochemistry for prion protein shows intense labeling of the florid plaques in the cerebral and cerebellar cortex, and also demonstrate small amorphous "feathery" deposits of abnormal PrP around small capillaries and neurones, along with numerous smaller cluster plaques that are not present on routine stains (Fig. 9) (Ironside *et al*., 2002). The characteristic histological and immunohistochemical features of vCJD are illustrated in Figure 1.7. The neuropathological features described above in large numbers of *PRN*P codon 129 MM patients were also present in the recently reported case of vCJD in a UK *PRNP* codon 129 MV patient (Professor S Brandner, personal communication, 2016).

1.5.5.5. *Peripheral pathogenesis*

Experimental oral transmission of scrapie and BSE to mice has established that the agent crosses the wall of the small intestine, most likely via M cells (Heppner *et al*., 2001; Donaldson *et al*., 2012) and replicates in the follicular dendritic cells in Peyer's patches. It can then spread to replicate in other lymphoid tissues, including
the spleen and lymph nodes, but can also spread retrogradely via the parasympathetic nerves in the gut via the vagus to the medulla (McBride *et al*., 2001). Centripetal spread from the spleen via the sympathetic nervous system to the spinal cord can also occur, followed by spread to the brain (Figure 1.8). Centrifugal spread from the CNS to sensory ganglia and muscles may also occur at a later stage in the disease (Beekes & McBride, 2007).

Figure 1.7.

Characteristic histological and immunohistochemical features of vCJD (with permission from Taylor and Francis, UK)

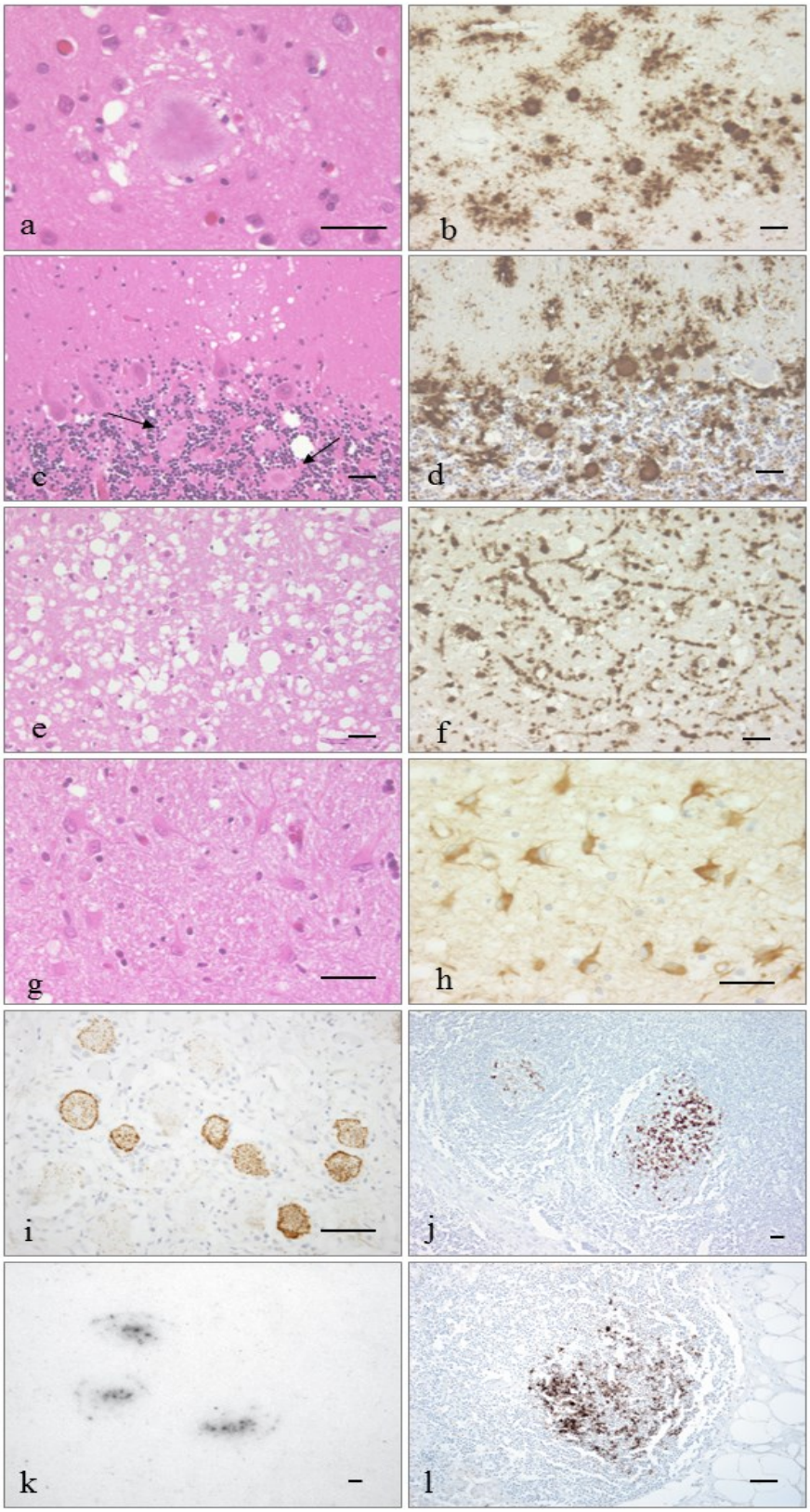

Legend to Figure 1.7.

Large rounded amyloid plaques are present in the frontal cortex in the form of florid plaques (a), and in the cerebellum as rounded plaques with little surrounding vacuolation in the granular layer (arrows) (c). Immunohistochemistry for PrP shows intense labelling of these large plaques, and also demonstrates multiple smaller cluster plaques in addition to amorphous and pericellular PrP deposits in the frontal cortex (b) and in the cerebellar cortex (d).

The caudate nucleus shows intense spongiform change, with little evidence of amyloid plaque formation (e). PrP accumulation in the caudate nucleus and other regions of the basal ganglia shows multiple small punctate deposits around neurones and also apparently around axons in a linear pattern (f).

The pulvinar in vCJD shows extensive neuronal loss and gliosis with patchy spongiform change and little evidence of amyloid plaque formation (g). The intense gliosis in the pulvinar is demonstrated on immunohistochemistry for glial fibrillary acidic protein (h).

Peripheral pathology in vCJD. Immunohistochemistry shows evidence of PrP accumulation in: dorsal root ganglion cells (i); germinal centres within the tonsil (j) follicular dendritic cells in small germinal centres in the spleen (PET blot) (k) a cervical lymph node in an asymptomatic patient who had received a blood transfusion from a donor who subsequently died from vCJD, providing evidence of asymptomatic infection at the time of death (l).

(Sections a, c, e, and g are stained with haematoxylin and eosin, and sections b, d, f, i, j, and l are stained by immunohistochemistry for PrP using the KG9 antibody. The 3F4 antibody was used in the PET blot in section k).

Scale bar=250 μm

Abbreviations: PET: paraffin-embedded tissue; PrP: prion protein; vCJD: variant Creutzfeldt-Jakob disease.

Figure 1.8.

Spread of the scrapie agent from the gut along two distinct neuroanatomical pathways to the CNS (with permission from Taylor and Francis, UK)

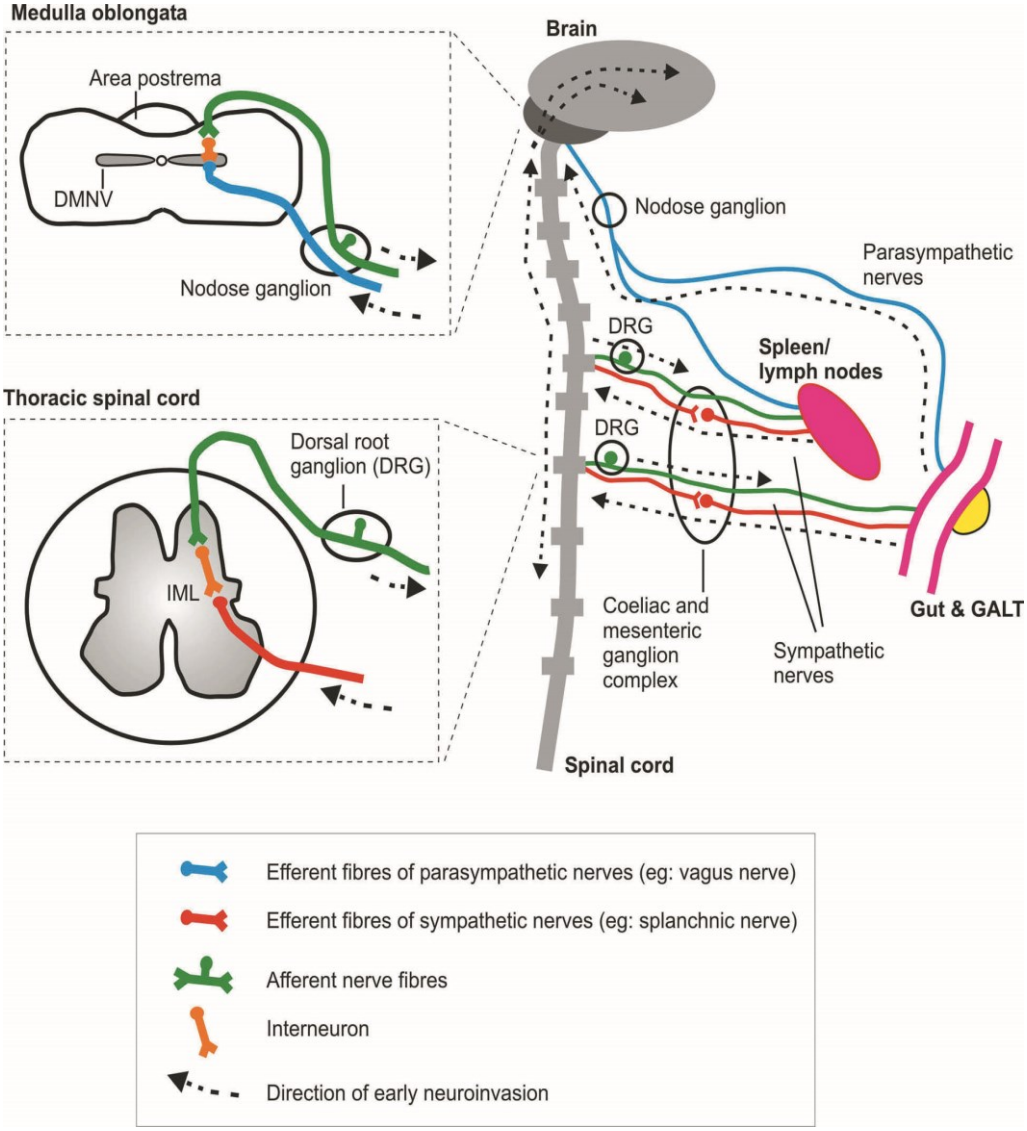

Following oral inoculation with scrapie, the agent crosses the gut mucosa and replicates in the gut-associated lymphoid tissues (GALT) and can then spread to other lymphoid organs, including the spleen. From the spleen, the agent can spread along sympathetic nerves from the splanchnic plexus to the intermediolateral (IML) column of the spinal cord and then to the brain. Direct spread from the gut to the CNS can also occur along parasympathetic fibres of the vagus nerve to the dorsal motor nucleus of the vagus (DMNV) within the medulla. (DRG: dorsal root ganglion)

Courtesy of Professor Neil Mabbott, Edinburgh, UK.

Variant CJD is also characterised by the accumulation of PrP^{Sc} in follicular dendritic cells within follicles in lymphoid tissues throughout the body that is readily detected by immunohistochemistry, PET blot, or WB analysis (Head *et al*., 2004a; Ritchie *et al*., 2004). This finding has enabled the use of tonsil biopsy as a diagnostic tool for vCJD (see above). PrP^{Sc} has also been detected by these techniques in peripheral autonomic ganglia in vCJD (Haik *et al*., 2003). In a vCJD case from the United States with a lengthy clinical history, PrP^{Sc} was detected in a wider range of tissues using a high sensitivity WB technique, including skeletal muscle and skin, following autopsy (Notari *et al*., 2010).

1.5.5.6. *Molecular biology*

WB analysis of the brain in vCJD shows a uniform single PrP^{res} type (type 2B) with predominance of the diglycosylated fragment, in contrast to sCJD and other forms of human prion diseases (Head & Ironside, 2012). A similar PrP^{res} isoform is present in lymphoid tissues in vCJD, including tonsil, thymus, spleen, lymph nodes, and gut-associated lymphoid tissues (Head *et al*., 2004b). The PrP^{res} isoform in vCJD is also similar to that found in the CNS in cattle and in other species infected with BSE, including antelopes and cats (Collinge *et al*., 1996), supporting the concept of molecular strain typing.

Significant levels of infectivity are present in lymphoid tissues in vCJD, although the levels are less than those in the CNS (Bruce *et al*., 2001). Concerns over possible infectivity also being present in blood led to the establishment of the UK Transfusion Medicine Epidemiology Review project, a lookback study that identified three patients

who died from vCJD after receiving non-leukodepleted packed red blood cell transfusions from asymptomatic donors who subsequently died from vCJD (reviewed in Urwin *et al*., 2016). The incubation period from transfusion to the onset of symptoms in recipients was 7–9 years and the period prior to clinical signs in the donors was 1–3 years. A further UK recipient of a similar transfusion died of an unrelated illness with no neurological signs or symptoms 5 years later. After autopsy, accumulation of PrP^{res} characteristic of vCJD was found by WB, IHC and PET blot in the spleen and a lymph node, indicating an asymptomatic vCJD infection (Peden *et al*., 2004), subsequently proven by experimental transmission (Bishop *et al*., 2013). This individual was a *PRNP* codon 129 heterozygote. A UK patient with haemophilia, but no neurological signs or symptoms suggestive of vCJD, was also found to have PrP^{res} characteristic of vCJD in an autopsy spleen sample, raising the possibility that UK plasma products may also transmit vCJD (Peden *et al*., 2010). The biological properties and the PrP^{res} isoform of the vCJD prion strain in brain tissue from these UK patients with secondary transfusion-related vCJD and in spleen tissue from the individual with an asymptomatic transfusion-acquired vCJD infection have not altered significantly in experimental transmission studies (Bishop *et al*., 2008), even following passage in the *PRNP* codon 129 heterozygous individual (Bishop *et al*., 2013). Transmission studies to transgenic mice overexpressing bovine prion protein have recently demonstrated infectivity in leucocytes, plasma and erythrocytes in vCJD patients (Douet *et al*., 2014).

1.5.5.7. *Prevalence of asymptomatic vCJD infection*

To date, 231 cases of vCJD have been identified worldwide, with 178 occurring in the UK (Table 1.6). There is ongoing concern about the possible numbers of UK residents with asymptomatic vCJD infection, given the wide exposure of the UK population to BSE via the food chain in the 1980s and 1990s, and concerns over the safety of blood transfusion in the UK still remain (House of Commons Science and Technology Committee, 2014). In the absence of a blood based screening test for vCJD (see below), several tissue-based studies using IHC to detect abnormal PrP accumulation in lymphoid tissues in appendix and tonsil specimens from UK patients have been undertaken to address these concerns, since abnormal prion protein can accumulate in the appendix before the onset of symptoms in vCJD (Hilton *et al*., 1998). Positive immunohistochemical labelling of follicular dendritic cells within lymphoid follicles is specific for vCJD (Hilton *et al*., 2004b). The patients in these large studies underwent surgery because of suspected appendicitis or tonsillitis, but were otherwise normal.

The first study (Appendix I) in 2004 found 3/12,674 positive specimens, giving an estimated prevalence of asymptomatic vCJD infection of 237 per million, or approximately 1 in 4000 in the UK, with a wide confidence interval (Hilton *et al*., 2004a). A subsequent study (Appendix II) examined 32,441 appendix samples from individuals born in birth cohorts from 1941–1960 and 1961–1985. 16 positive cases from both cohorts were identified, giving an estimated prevalence of asymptomatic vCJD infection in the UK of 493 per million, or approximately 1 in 2000, also with a wide confidence interval (Gill *et al*., 2013). This difference between the results of these

two studies is not statistically significant (Gill *et al*., 2013). Genetic analysis found 2 of the 3 positive cases in the first study to have the *PRNP* codon 129 VV genotype (Ironside *et al*., 2006), and the 16 positive cases in the 2013 study comprised 8 VV, 4 MV and 4 MM codon 129 genotypes (Gill *et al*., 2013). It therefore appears that all three *PRNP* codon 129 genotypes are susceptible to vCJD infection and may develop vCJD after an unknown and possibly lengthy incubation period. Preliminary results from the latest study (Appendix III) found 7/29516 appendix cases to be positive for prion protein (Public Health England, 2016). Of these, 2 were found in the 5,865 appendices removed between 1977-79 and 5 positives were identified in the 14,824 appendices removed between 2000-14 in patients born between 1996-2000, suggesting that dietary BSE exposure in the UK may have occurred over a wider time period than initially thought.

At present, several groups are working on a blood test for vCJD, some with encouraging progress. However, none of the methods currently under development has been used to detect asymptomatic vCJD infection in humans, although this can be achieved in some animal models (Saa *et al*., 2006; Edgeworth *et al*., 2011; Lacroux *et al*., 2014; Sawyer *et al*., 2015; Concha-Marambio *et al*., in press). Further progress is required to refine the most recent estimates for the prevalence of asymptomatic vCJD infection from tissue-based studies and a protocol for the evaluation of a test for its suitability in the diagnosis of vCJD has been proposed (Cooper *et al*., 2013). Blood tests for vCJD could also be used in the screening of blood donations or individuals prior to surgery in the UK; such uses will first require detailed ethical consideration (Turner, 2006).

1.5.6. Iatrogenic CJD

The first reported case of iatrogenic CJD (iCJD) was published in 1974 in a recipient of a corneal graft from a donor who had died from sCJD (Duffy *et al*., 1974). Since then hundreds of cases of iCJD have been identified in groups of patients exposed to human tissue grafts and implants, inoculated with tissue homogenates or operated on with instruments or electrodes previously used on the brains of patients with CJD, most likely sCJD (Table 1.8).

The largest groups of iCJD cases have occurred in patients inoculated with human growth hormone (hGH) or human pituitary gonadotrophins, and patients who received an implant of human dura mater (hDM) during neurosurgery. Over 200 cases have occurred worldwide in each of these groups, and their numbers are still increasing with time, with incubation periods of up to 40 years in some cases (Brown *et al*., 2012). There have also been a few cases of iCJD linked to contaminated neurosurgical instruments, intracerebral depth electrodes and corneal grafts (Table 1.8), but most of these causes are now historical. The internationally agreed diagnostic criteria for iCJD are summarised in Table 1.9.

1.5.6.1. *Epidemiology*

The incidence of hGH iCJD varies from country to country in general relation to the scale of the local hGH production process and the likelihood of prion contamination in the selection of autopsy cases for pituitary collection (Brown *et al*., 2012). The incidence of iCJD in human dura mater recipients reflects in general the frequency of use of Lyodura (a commercially processed lyophilised hDM product implicated in

Table 1.8.
Worldwide cases of iatrogenic CJD, modified from Brown *et al*., 2012

SOURCE OF INFECTION	TOTAL NUMBER OF CASES	COUNTRIES REPORTING CASES	INCUBATION PERIOD DETAILS	COMMENTS
Human Growth Hormone	239	Vast majority of cases in France, UK and USA.	5-42 years	Incubation Period uncertain- calculated from mid-point of hormone treatment. Risk period generally before mid 1980s.
Dura Mater Grafts	206	Over half the cases in Japan. Also in France, Germany, Spain, UK, Australia, Canada, Italy, USA.	1.3-30 years	Virtually all related to one commercial product (Lyodura) Risk period generally up to 1987.
Neurosurgical Instruments	4	UK and France	1-2.3 years	
Brain Depth Electrodes	2	Switzerland	1.3 & 1.7 years	
Corneal Transplants	2	USA, Germany	1.5 & 27 years	
Human Gonadotrophin Hormone	4	Australia	12-16 years	
Blood (variant CJD)	3*	UK	6.5-8.3 years	All from non-leucodepleted red cell concentrates
Blood Products	0**	-	-	

* An additional instance of subclinical vCJD infection in a *PRNP* codon 129 MV recipient (Peden *et al*., 2004).

** A report of probable subclinical vCJD infection in a *PRNP* codon 129 MV recipient of Factor VIII (Peden *et al*., 2010).

Abbreviations: CJD: Creutzfeldt-Jakob disease; UK: United Kingdom; USA: United States of America.

Table 1.9.

Diagnostic criteria for iatrogenic Creutzfeldt-Jakob disease
(http://www.cjd.ed.ac.uk/documents/criteria.pdf)

2.1 **DEFINITE**

Definite CJD with a recognised iatrogenic risk factor (see box)

2.2 **PROBABLE**

2.2.1 Progressive predominant cerebellar syndrome in human pituitary hormone recipients

2.2.2 Probable CJD with recognised iatrogenic risk factor (see box)

2.3 **POSSIBLE**

Possible CJD with a recognised risk factor
(agreed at EUROCJD meeting Bled, 2006)

RELEVANT EXPOSURE RISKS FOR THE CLASSIFICATION AS IATROGENIC CJD

The relevance of any exposure to disease causation must take into account the timing of the exposure in relation to disease onset

- Treatment with human pituitary growth hormone, human pituitary gonadotrophin or human dura mater graft.
- Corneal graft in which the corneal donor has been classified as definite or probable human prion disease.
- Exposure to neurosurgical instruments previously used in a case of definite or probable human prion disease.

This list is provisional as previously unrecognised mechanisms of human prion disease transmission may occur

Abbreviations: CJD: Creutzfeldt-Jakob disease; EUROCJD: European Surveillance Network for Creutzfeldt-Jakob disease.

almost all cases of iCJD in hDM graft recipients) in neurosurgical procedures, which was particularly high in Japan (Hamaguchi *et al*., 2013). These risks have been addressed by the use of recombinant pituitary hormones and synthetic or autologous dura mater grafts respectively, so future iatrogenic exposure to CJD through these treatments are unlikely to occur.

The incubation periods in the worldwide cohort of iCJD cases are markedly variable, with the shortest incubation periods occurring in those exposed via surgical instruments or electrodes used on the CNS (1-2.3 years) and the longest occurring in human pituitary-derived hGH recipients (5-42 years) (Brown *et al*., 2012) (Table 1.8). Only 4 cases of iCJD in human gonadotrophin recipients have occurred, all in Australia (Table 1.8); one of these patients died in the UK (Figure 2.1). Estimation of incubation periods in human pituitary hormone recipients is difficult, since the patients are often treated over a period of years; the time period from the mid-point
of pituitary hormone treatment to the onset of clinical symptoms of iCJD is often used as an estimate for the incubation period (Swerdlow *et al*., 2003).

1.5.6.2. *Clinical features*

The clinical features of iCJD appear to vary according to the route of exposure. The introduction of iatrogenic infection in, on, or adjacent to the brain through contaminated neurosurgical instruments or hDM grafts leads to an illness similar to sCJD, with rapidly progressive dementia associated with ataxia and myoclonus. Accordingly, the duration of illness is similar to sCJD, often measured in a few months. Following peripheral exposure through intramuscular injections of hGH a progressive

ataxic syndrome develops accompanied by limb dysaesthesiae and followed by other cerebellar signs and symptoms, often with cognitive impairment at a relatively late stage in the illness, if at all (Rudge *et al*., 2015). The duration of illness in hGH-iCJD is longer than that for centrally acquired forms of iCJD and is often around 14 months (Rudge *et al*., 2015). Although there is relatively limited data, the clinical investigations in iCJD patients, including EEG, MR, and CSF 14-3-3, have a similar sensitivity and specificity as in sCJD (Meissner *et al*., 2009b; Rudge *et al*., 2015). The diagnostic criteria for iCJD depend on the identification of a potential risk factor for iatrogenic exposure in suspected cases of CJD or in relatively young individuals presenting with a progressive ataxic syndrome.

1.5.6.3. *Neuropathology*

Since the sCJD agent is the likely source of infection in most cases of iCJD, it is perhaps to be expected that, as for sCJD, the pathological phenotype in iCJD appears to be influenced by the patient's *PRNP* codon 129 genotype and the PrP^{res} type identified on WB of brain homogenates (Meissner *et al*., 2009b). However, some differences occur:there is a subgroup of hDM-iCJD *PRNP* codon 129 MM cases in Japan that contain amyloid plaques in the brain, which resemble kuru plaques (Yamada *et al*., 2009). In the UK, cases of hDM-iCJD occurred in *PRNP* codon 129 MM patients with type 1 PrP^{res} in the brain and no evidence of amyloid plaques (Heath *et al*., 2006).

1.5.7. Precautions to avoid future cases of iatrogenic CJD

1.5.7.1. *Control measures*

Control measures to reduce the risk of human-human transmission of prion diseases have been produced by the World Health Organisation (WHO), Geneva (http://www.who.int/ entity/ csr/resources/publications/bse/whocdscsraph2003.pdf) and in the UK by the Advisory Committee on Dangerous Pathogens (https://www.gov.uk/government/uploads/system/uploads/attachment_data/file/ 427854/Infection_controlv3.0.pdf). Similar guidelines have appeared more recently (Brown *et al*., 2012; Brown & Farrell, 2015; Bonda *et al*., 2016), including an audit of the work of the CJD Incidents Panel in the UK, which was set up to deal with any event in the UK healthcare system that might have the potential to result in the iatrogenic transmission of prion diseases (Hall *et al*., 2014). In the absence of a rapid and reliable test to detect asymptomatic infection with any form of human prion disease, the risk of human-to-human transmission of prions, either via contaminated surgical instruments, tissue-derived implants or injections, blood transfusion or organs donation, cannot be eliminated completely. Several strategies have been employed to help manage these risks:

1) Identification of symptomatic patients with any form of prion disease and asymptomatic individuals at increased risk of developing any form of prion disease and implementing a process of donor deferral for organs or tissues for transplantation, blood for transfusion (particularly for those at increased risk for vCJD) or tissues used in the manufacture of biological products.
2) Classification of tissues by their likely level of prion infectivity in human prion diseases. CNS tissues (brain, spinal cord, cranial nerves and cranial ganglia),

pituitary gland and the posterior eye (retina, retinal pigment epithelium, choroid, posterior hyaloid face, subretinal fluid and optic nerve) are considered to have the highest levels of infectivity, particularly in symptomatic patients. Spinal ganglia and olfactory epithelium are considered to have medium levels of infectivity in all forms of human prion disease, but in vCJD all lymphoid tissues (spleen, tonsil, lymph nodes, gut, appendix and thymus) and the adrenal gland are also considered to be medium infectivity tissues. All other tissues (including blood and CSF) are classified as low infectivity in all forms of human prion diseases (https://www.gov.uk/government/uploads/system/uploads/ attachment_ data/file/ 444243/Annex_A1_update.pdf).

3) Use of dedicated or single-use surgical instruments in these individuals, especially for those instruments coming into contact with high-infectivity tissues (CNS and retina), or quarantining such instruments in symptomatic patients in whom a diagnosis of CJD is being investigated, to be re-evaluated once the results of the additional investigations become available.
4) Inclusion of steps in the sterilization of certain neurosurgical and ophthalmic surgical instruments and the processing of therapeutic tissues and fluids that are designed to reduce or eliminate any potential prion infectivity.
5) Avoidance of human-derived hormones and other biological products and their replacement by recombinant equivalents whenever possible, e.g. Factor VIII.

The groups of individuals deemed to be at increased risk of CJD in the UK are summarised in Table 1.10. While the categories including the recipients of human dura mater grafts, human pituitary-derived hormones and those at a genetic risk of CJD are common to many countries, the additional category of those at increased risk of vCJD

Table 1.10.

Categorisation of individuals at increased risk of human prion disease in the UK

1. **Symptomatic patients:**

a. Patients who fulfil the diagnostic criteria for definite, probable or possible CJD (see Tables 1.4, 1.5, 1.7 and 1.9 for diagnostic criteria)
b. Patients with neurological disease of unknown aetiology, who do not fit the criteria for possible CJD, but where the diagnosis of CJD is being actively considered

2. **Patients at increased risk of genetic forms of human prion disease:**

a. Individuals who have been shown by specific genetic testing to be at significant risk of developing CJD
b. Individuals who have a blood relative known to have a genetic mutation indicative of genetic CJD
c. Individuals who have or have had two or more blood relatives affected by CJD or other prion disease

3. **Patients identified as "at increased risk" of vCJD through receipt of blood from a donor who later developed vCJD:**

a. Individuals who have received labile blood components (whole blood, red cells, white cells or platelets) from a donor who later went on to develop vCJD

4. **Patients identified as "at increased risk" of CJD through iatrogenic exposures:**

a. Recipients of hormone derived from human pituitary glands, *e.g.* growth hormone, gonadotrophin, are "at increased risk" of transmission of sporadic CJD
b. Individuals who underwent intradural brain or intradural spinal surgery before August 1992 who received (or might have received) a graft of human-derived dura mater are "at increased risk" of transmission of sporadic CJD (unless evidence can be provided that human-derived dura mater was not used)
c. Individuals who have had surgery using instruments that had been used on someone who went on to develop CJD, or was "at increased risk" of CJD
d. Individuals who have received an organ or tissue from a donor infected with CJD or "at increased risk" of CJD
e. Individuals who have been identified as having received blood or blood components from 300 or more donors since January 1990;
f. Individuals who have given blood to someone who went on to develop vCJD;
g. Individuals who have received blood from someone who has also given blood to a patient who went on to develop vCJD
h. Individuals who have been treated with certain implicated UK sourced plasma products between 1990 and 2001

Abbreviations: CJD: Creutzfeldt-Jakob disease; UK: United Kingdom.

is of special concern for the UK, particularly when the incidence of asymptomatic vCJD infection in the UK population is estimated to be as high as 1 in 2000 individuals (Gill *et al*., 2013).

1.5.7.2. *Risk reduction*

Risk reduction steps to reduce or remove prion infectivity are often challenging to implement in both clinical and laboratory settings (https://www.gov.uk/government/ uploads/system/ uploads/attachment_data/ file /427855/Annex_C_v3.0.pdf):

1. Sodium hypochlorite is considered effective at reducing infectivity, but only at concentrations (20,000ppm available chlorine for 1 hour at ambient temperature) that pose certain practical constraints, particularly in enclosed spaces.
2. Sodium hydroxide (2M for 1 hour) has a substantial effect, and will reduce infectivity to an acceptable level when used at ambient temperature. An increase in temperature will increase effectiveness.
3. Incineration is effective at removing the infectious agent and eliminating infectivity. Temperatures over 600ºC are likely to be practically effective, and 850ºC is commonly used in practice. Temperatures ≥1000 ºC can produce sterility.
4. The following autoclave methods will reduce infectivity, but cannot be relied upon to completely eliminate infectivity (either porous load or gravity displacement):

    a. 121°C for 15 minutes
    b. 134-137°C for 3 minutes

c. 134-137°C for 18 minutes

d. Six successive cycles of 3 minutes

5. Chemical disinfectants commonly used for decontamination that are ineffective at reducing prion infectivity include acids, alcohols, formaldehyde and related compounds, and phenol solutions.

Many of these methods are impractical for use on delicate or complex neurosurgical instruments. The decontamination of steel surfaces on surgical instruments is hindered by the fact that prions adhere avidly to stainless steel surfaces (Zobeley *et al*., 1999); furthermore, different strains of prions exhibit differential sensitivity to heat when used for inactivation (Fernie *et al*., 2007). However, on the basis of scenario modelling it has been suggested that after six cycles of neurosurgical instrument use with conventional cleaning and autoclaving following an index patient, subsequent patients on whom the instrument is used are highly unlikely to be at risk for iatrogenic CJD (Thomas *et al*., 2013).

The challenges of removing prions from stainless steel surfaces have been addressed by a number of new technologies, including radio-frequency gas plasma treatment (Baxter *et al*., 2005), combinations of proteolytic enzymes and detergents (Jackson *et al*., 2005) and gaseous hydrogen peroxide (Fichet *et al*., 20007). None have yet been scaled up for use in a clinical setting, even for a trial period. This disappointing failure of translation must be overcome to ensure that an effective means of decontaminating neurosurgical and ophthalmological instruments used on patients with or at increased risk of prion diseases will be available in UK hospitals.

Leucodepletion alone appears to reduce vCJD infectivity inblood by a considerable extent (Lacroux *et al*., 2012), justifying its use in the UK. However, additional "prion filters" have been unsuccessful in completely removing prion infectivity in various experimental models, including a sheep model of BSE with endogenous infectivity in blood (Lacroux *et al*., 2012; McCutcheon *et al*., 2015).

1.6. Treatment of human prion diseases

Numerous compounds have been used over many decades in attempts to treat prion diseases, initially in animal models, but now including cell culture models and cell-free prion conversion systems such as PMCA. The earliest investigations in animal models identified several compounds that appeared to have an effect in prolonging the disease incubation period, but only if administered before or at the same time as the experimental infection. None was capable of curing the disease. The background to these extensive studies has been reviewed in detail by Trevitt and Collinge (Trevitt & Collinge, 2006), who summarised the therapeutic approaches into five groups:

1. Groups of chemical agents, e.g. heparin sulphate and its analogues, tetracyclic compounds, polyene antibiotics, amyloid-binding dyes, e.g. Congo Red.
2. Immunological agents, e.g. antibodies, active and passive immunisation strategies.
3. Approaches targeting PrP^{C} expression, e.g. by RNA interference.
4. Novel compounds identified by screening approaches in vitro (cell culture and *in vitro* screens).
5. Other miscellaneous compounds including RNA aptamers and a range of unrelated compounds.

Since then, *in silico* systems have been employed to screen large numbers of compounds by a variety of modelling strategies including molecular docking to identify possible binding agents to inhibit the conversion of PrP^{C} to PrP^{Sc} (Ferreira *et al*., 2014). Some of the aryl amide compounds currently under investigation can extend survival in some prion-infected mice, but have no effect on transgenic mice infected with human prions (Giles *et al*., 2016). The development of drug resistant prion strains appears to be a problem with some of these novel compounds, e.g. 2-aminothiazole compounds (Berry *et al*., 2013). Another potential therapeutic target is the unfolded protein response, which is activated in the brain in a range of neurodegenerative diseases associated with protein misfolding. Overactivation of the protein kinase RNA-like ER kinase (PERK) branch of the unfolded protein response results in a critical reduction in protein synthesis in neurones, leading to dysfunction and ultimately cell death (reviewed in Smith & Mallucci, 2016). PERK inhibition prevents neuronal loss, spongiform change and clinical disease in prion-infected mice, but this can result in toxicity in other organs (particularly in the pancreas), which can be overcome by the use of highly selective compounds (Halliday *et al*., 2015).

1.6.1. Clinical trials

One of the major challenges in developing and evaluating potential treatments for prion diseases in that they are rare disorders, difficult to diagnose in the early stages of disease and often show rapid clinical progression with death in a few weeks or months after the onset of the first symptoms of illness (Stewart *et al*., 2008). Any drug being considered for this purpose should ideally have the capability to cross the blood-brain barrier rapidly in order to reach therapeutic levels in the CNS. A double-blind

trial of flupirtine maleate, which protects neuronal cells from apoptosis following exposure to PrP fragments and Aβ peptides, showed no significant effect on patient survival (Otto *et al*., 2004). Pentosan polysulphate, which binds to PrP^{C} and may prevent its conversion to PrP^{Sc}, does not cross the blood-brain barrier and requires intraventricular infusion (Farquhar *et al*., 1999). This compound produced no discernible clinical improvement in small numbers of sCJD, genetic CJD, GSS, iCJD and vCJD patients (Tsuboi et *al*., 2009; Bone *et al*., 2008; Newman *et al*., 2014). A patient preference trial of quinacrine, which can delay PrP^{C} conversion *in vitro* (Barret *et al*., 2003), produced no significant clinical benefits (Haik et *al*., 2004; Collinge *et al*., 2009); this was confirmed in a larger double-blind placebo-controlled trial (Geschwind *et al*., 2013). Although showing some beneficial effects in animal models, a recent clinical trial of doxycycline showed no effect on the disease course in both sCJD and genetic CJD (Haik *et al.*, 2014). Despite this disappointing outcome, this study has demonstrated that a clinical trial in this group of rare diseases is possible through international collaboration, which can serve as a model system in which other potential treatments can be evaluated (Geschwind, 2014). In a recent preventative study, asymptomatic adult carriers of the FFI mutation will undergo long-term doxycycline treatment with monitoring of PrP^{Sc} levels in olfactory mucosal brushings as a biomarker for efficacy (Forloni *et al*., 2015; Zanusso *et al*., 2016).

Improvements in early clinical diagnosis of human prion diseases will also be required if any new therapeutic agents are to be effectively evaluated in the setting of a clinical trial. In the absence of any effective curative agents, treatment of human prion diseases

currently remains symptomatic and aimed at providing as much relief and support to the patient and their families as possible, as for other fatal neurodegenerative disorders.

1.7. Prion-like mechanisms in other human neurodegenerative disorders.

The recognition that other neurodegenerative diseases are associated with the accumulation and propagation of misfolded proteins in the CNS has led to the proposal that prion-like mechanisms may also be responsible for these disorders, including AD, PD and motor neurone disease (MND) in both their sporadic and genetic forms (Jucker & Walker, 2013; Prusiner 2013). A common model of disease progression occurs in these disorders, in which abnormally folded isoforms of a disease-associated protein interact to form β sheet structures that aggregate to form a seed or nucleus that results in the formation of other abnormally folded isoforms, including neurotoxic isoforms, in a prion-like process (Goedert, 2015). In view of the lack of epidemiological evidence for disorders such as AD, PD and MND being infectious (Edgren *et al*., 2016), the term "propagon" rather than prion has been proposed for the group of proteins (including Aβ, tau and α-synuclein) that have the capacity to misfold and aggregate homotypic molecules without possessing infectivity (Eisele & Duyckaerts, 2016). Oligomeric species of these aggregates appear to have the greatest capacity for self-propagation and also are the molecular species most likely to be associated with neurotoxicity (Silveira *et al*., 2005; Aguzzi & Lakkaraju, 2016).

Histological examination of the brain in AD and PD has long established that the protein aggregates that are key components of the neuropathology – Aβ plaques and neurofibrillary tangles composed of hyperphosphorylated tau in AD and Lewy bodies

containing α-synuclein in PD – appear to spread progressively with time through the brain in highly predictable synaptically-connected neuroanatomical pathways, often correlating with the nature and severity of clinical signs and symptoms prior to death (Alafuzoff *et al*., 2009a, 2009b). These observations have led to agreed histological classification schemes to denote the extent of the neuropathological changes in these disorders to facilitate clinicopathological correlation and research (Hyman *et al*., 2012). These patterns of spread imply cell-to-cell spread of protein aggregates in the CNS, leading to progressive disease and ultimately death. The underlying mechanisms of this cell-to-cell spread are uncertain, but a number of models have been proposed, including exosomes as vehicles to carry toxic proteinaceous seeds from an affected cell to an acceptor cell, nonconventional export via direct secretion, or exchange via tunneling nanotubes (Victoria & Zurzolo, 2015).

1.7.1. Amyloid seeding

There is no convincing epidemiological evidence to date to suggest that protein misfolding disorders affecting the CNS are infectious, apart from prion diseases (Mayeux & Stern, 2012; Edgren *et al*., 2016). However, there is an increasing body of evidence to indicate that the abnormal proteins involved can be seeded *in vivo* and *in vitro*, with accumulation of the seeded deposit over time (reviewed in Moreno-Gonzalez & Soto, 2011). Intraperitoneal administration of Aβ and tau aggregates in experimental models can result in accumulation of these proteins in the brain either by vascular spread (involving crossing the blood-brain barrier, or initial spread into the regions where no blood-brain barrier exists) or by retrograde axonal transport along peripheral nerves to the CNS (Eisele *et al*., 2010; Clavaguera *et al*., 2014). Furthermore,

different strains of Aβ in AD and tau in a range of human tauopathies (AD, corticobasal degeneration, argyrophilic grain disease and frontotemporal lobar degeneration–tau) have been identified on the basis of their biological behaviour on experimental transmission, including the nature and distribution of the pathology and the timing of the appearance of the pathology in the brain (Sanders *et al*., 2014; Watts *et al*., 2014; Stohr *et al*., 2014).

These prion-like properties have potentially wide-ranging implications for our understanding of human neurodegenerative diseases in terms of cell biology, mechanisms of toxicity and opportunities for intervention and treatment (Goedert, 2015; Sanders *et al*., 2016). Another implication is the possibility of iatrogenic transmission of these disorders from one individual to another by routes known to result in iCJD. The possibility of iatrogenic transmission of Aβ, tau and α-synuclein in recipients of human growth hormone was raised by Irwin *et al*, (Irwin *et al*., 2013), since the pituitary gland can harbour deposits of Aβ and tau in patients with AD and α-synuclein in patients with PD, as well as PrP^{Sc} in CJD (Peden *et al*., 2007; Hashizume *et al*., 2013; Homma *et al*., 2014; Irwin *et al*., 2013; Jaunmuktane *et al*., 2015). This possibility was reinforced by recent evidence of Aβ seeding in the brains of 4/8 hGH recipients who died with iCJD (Jaunmuktane *et al*., 2015). However, this evidence has been questioned since the patients concerned all suffered from iCJD, with widespread accumulation of aggregated PrP^{Sc} in the brain that may have acted as an amyloid seed, resulting in co-localisation and aggregation of Aβ in the CNS. Aβ seeding around PrP^{Sc} deposits has been reported in other forms of human prion

disease, particularly in genetic prion diseases associated with the formation of PrP^{Sc} amyloid plaques (Miyazono *et al*., 1992; Bugiani *et al*., 1993; Ikeda *et al*., 1994).

Recently, further questions have been raised on the clinical background of the patients included in the study by Jaunmuktane *et al*., suggesting that the pre-existing and underlying conditions causing hGH deficiency in this patient cohort "could by themselves lead to Aβ pathology and abnormal brain structure" (Feeney *et al*., 2016). In response, Collinge *et al*. refuted this suggestion (Collinge *et al*., 2016), but both groups of authors acknowledged the need for further studies, including the examination of the brains of patients treated with hGH who did not develop iCJD.

2. Historical narrative on the production and use of hGH in the UK

The information in this section of the thesis comes from a wide ranges of sources, inevitably including records of meetings, copies of correspondence and other documents that cannot be cited as references in the published literature. Every attempt has been made to include citable references whenever possible.

2.1. Iatrogenic CJD in human growth hormone recipients in the UK

2.1.1. Background

One of the first attempts to isolate hGH from the human pituitary gland was in 1957, when Raben reported the extraction of hGH from a small series of pituitaries from humans, rhesus monkeys and pigs (Raben, 1957). Previous attempts to use animal-derived growth hormone to treat growth hormone deficiency in humans had been generally unsuccessful (Blizzard, 2012). Raben described a method in which pituitary glands were stored in acetone after autopsy (no time intervals were specified) then air dried, homogenised, washed again in acetone and desiccated in a vacuum. hGH was extracted using glacial acetic acid followed by precipitation in ethyl alcohol. Raben commented that the chemical processing using acetone, ether and hot glacial acetic acid "provided strong bactericidal and viricidal action in the extraction of human pituitaries of indeterminate origin" and that the final product was "well suited for clinical use" (Raben, 1957). Raben reported the clinical use of the extracted hGH the following year in a male "pituitary dwarf" aged 17 years, who grew 2.6 inches per year on treatment, as compared with 0.5 inches for the 18 months prior to treatment. No complications were reported (Raben, 1958).

2.1.2. Production and use of hGH

In 1959, a clinical trial on the use of pituitary-derived hGH in the treatment of primary growth hormone deficiency (either in isolation or as part of a deficiency of all anterior pituitary hormones) and secondary growth hormone deficiency (most often due to a craniopharyngioma) in the United Kingdom (UK) began under the auspices of a Medical Research Council (MRC) Working Party of the Pituitary Hormone Committee. The growth hormone was extracted from acetone-fixed pituitary glands in the Department of Biochemistry, University of Cambridge, initially using the Raben method, but later changing to a modified Wilhelmi method, which caused less degradation of hGH, gave higher hGH yields per gland and was less likely to cause anti-hGH antibody production (Mills *et al*., 1969). In 1975, an additional hGH extraction site was established at St Bartholomew's Hospital, London to help meet the increasing clinical demand for hGH. This site collected frozen pituitary glands and used the Lowry method to extract hGH, with additional gel filtration and chromatographic steps for purification of the final pyrogen-free product (Jones *et al*., 1979), and remained active until 1980.

In 1977, UK hGH production was transferred to the Therapeutic Products Laboratory in the Public Health Laboratory Service Centre for Applied Microbiology in Porton Down, where both frozen and acetone-fixed pituitary glands were collected and the hGH product underwent purification using Sephadex G-100 gel filtration. As the MRC Clinical Trial of hGH had ended in 1976, the MRC Working Group was disbanded and responsibility for the hGH service was transferred to the Department of Health and Social Security (DHSS) Human Growth Hormone Committee in 1977, which was

later reconstituted as the Joint MRC/DHSS Committee for the National Pituitary Collection (Milner *et al*., 1979). The clinical trial was considered a success: "growth hormone treatment is one of the outstanding therapeutic successes in recent years" (Milner, 1979).

2.1.3. CJD risks

When the collection of pituitary glands for hGH extraction in the UK began in 1959, there was no evidence that sCJD or GSS were infectious diseases that could be transmitted from human to human. However, this situation changed in 1968 when sCJD was transmitted experimentally to primates, and was reinforced in 1974 when the first case of iatrogenic CJD was reported in the recipient of a corneal graft from a donor who had died from sCJD (Duffy *et al*, 1974). Prior to 1974, patients with neurological diseases were not specifically excluded as donors of pituitary glands in the UK; in 1974, this exclusion was introduced for donors of frozen pituitary glands only and expanded in 1976 to cover all frozen glands in the MRC collection. The possibility of a scrapie-like "slow virus" agent contaminating the hGH production process was raised by the Agricultural Research Council (Dr A Dickinson) in 1976; Dr Dickinson also suggested a series of measures that should be put into place to help reduce the risks of CJD in the hGH preparations, but not all of these were apparently acted upon (Green, 2000). In 1977, the only CNS disorders that were identified as exclusion criteria for pituitary gland collection were meningitis, encephalitis and multiple sclerosis.

Another report of accidental CJD transmission to 2 patients via contaminated brain depth electrodes was published in 1977 (Bernoulli *et al*., 1977); the electrodes in question subsequently transmitted CJD to a chimpanzee 18 months after intracerebral implantation (Gibbs *et al*., 1994). Following this event, recommended precautions in handling material from patients with CJD were published (Gajdusek *et al*., 1977). Advice was sought in 1978 from Dr Carlton Gajdusek in the USA concerning the collection of human pituitary glands in the UK; the advice received (no name was recorded) was that tissue from patients with CJD or any other form of dementia should not be used in the preparation of hGH for human use. In 1980 the exclusion criteria for pituitary gland collection were extended to include CJD and dementia, but it is uncertain as to how compliance was monitored, if at all.

A MRC Working Group was then set up to investigate the establishment of epidemiological studies of CJD in the UK, particularly concerning the possibility that it was a naturally transmissible disease and, if so, by what means. This project was subsequently funded by MRC and awarded to Professor Bryan Matthews in the University of Oxford, who employed Dr RG Will as a Research Fellow. The first results of this retrospective study identified three cases of probable iatrogenic transmission of sCJD by contaminated neurosurgical instruments in the 1950s, along with a cluster of sCJD cases in Eastern England and the identification of a further sCJD case who had been in social contact with a patient suffering from familial CJD (Will & Matthews, 1982). In 1984, a retrospective study of CJD cases in England and Wales from 1970-79 described three main clinical phenotypes of sCJD, but no further evidence of person-to person transmission was reported (Will & Matthews, 1984).

2.1.4. Iatrogenic CJD and hGH

In the winter of 1984, the first deaths from iCJD in recipients of hGH in the USA emerged. Three of these patients had died by 1985, and later in the year the death of the first UK hGH recipient, a 23-year old female, from iCJD was reported (Koch *et al*., 1985; Gibbs *et al*., 1985; Powell- Jackson *et al*., 1985). Administration of hGH in the UK was stopped and all other pituitary hormones were withdrawn from clinical use. All hGH recipients were flagged and a follow-up project for this cohort was undertaken by Professor Michael Preece, Institute of Child Health, London. Later in 1985 a product licence for biosynthetic growth hormone (Somatonorm II) was granted to KabiVitrum and treatment of all hGH deficient patients in the UK was recommenced with this product. A publication from the groups of Dr A Dickinson and Dr P Lowry describing the preparation of hGH free from contamination with unconventional slow viruses (the recently-coined term "prion" was scrupulously avoided) appeared in the same edition of the Lancet in which the report of the first UK death from iCJD in a hGH recipient was reported (Taylor *et al*., 1985; Powell-Jackson *et al*., 1985). Later in 1985, an article warning of a potential epidemic of CJD from hGH therapy was published by the Gajdusek group (Brown *et al*., 1985). The presence of prion infectivity in hGH preparations in the USA was subsequently confirmed by experimental intracerebral inoculation of samples of pituitary-derived hGH into primates, which resulted in the onset of neurological symptoms in a squirrel monkey after an incubation period of over 5.5 years (Gibbs *et al*., 1993). Post mortem examination of the brain of this animal confirmed the presence of a spongiform encephalopathy. Further cases of hGH-iCJD have been recorded in other countries (Brown *et al*., 2012), with the largest numbers occurring in France (see below).

2.1.4.1. *Legal consequences*

In both the UK and France, legal proceedings were commenced against the bodies responsible for the administration of hGH that later resulted in cases of iCJD. In the UK, families of 8 hGH recipients who died from iCJD began a case in the High Court against the MRC and the Department of Health in 1996 (Dyer, 1996a). The judge, Mr Justice Moreland, ruled that the two bodies were negligent in not passing on concerns raised by scientists that would probably have led to suspension of hGH treatment from July 1977. This decision meant that only the families of patients dying from iCJD who started treatment after 1st July 1977 would be entitled to compensation (Dyer, 1996b). In France, an investigation began in 1993 into involuntary homicide and aggravated fraud charges on a six doctors and biochemists/pharmacists involved in the preparation and administration of hGH (Balter, 1993). In 2009, three French judges acquitted the accused and an Appeal Court hearing in 2011 dismissed all the charges (Casassus, 2009; News of the week (Science), 2011).

2.1.5. Iatrogenic CJD in hGH recipients in the UK and France

Overall, 1,849 patients from UK and Ireland were treated with hGH produced in the UK from 1959 until 1985 (Swerdlow *et al*., 2003). Over this period, it has been estimated that as many as 940,000 pituitary glands were collected for hGH extraction over this period (Dr P Adlard, personal communication), which were batched in groups of up to 35,000 for hGH extraction. The death rate for all forms of human prion disease is around 1 in 10,000 in the UK, so there was ample opportunity for at least one pituitary gland from a patient either with or incubating a prion disease (most likely sCJD) to be included in the collection for hGH extraction. Since 1985, 78 deaths from

iCJD have occurred in this cohort, the latest occurring in 2016 (Figure 2.1). It has been established that one form of UK pituitary-derived hGH (the modified Wilhelmi preparation) had been administered to all hGH recipients who had developed iCJD, albeit in varying quantities and over different time periods (Swerdlow *et al*., 2003; Rudge *et al*., 2015). Estimated incubation periods in the UK hGH-iCJD patients range from 7-40 years (Rudge *et al*., 2015); these prolonged incubation periods are reminiscent of those occurring in kuru, where incubation periods of over 40 years have been reported (Collinge *et al*., 2006). In contrast, only 8 cases of iCJD in hDM graft recipients have been reported in the UK, with incubation periods ranging from around 4-15 years (Heath *et al*., 2006).

Figure 2.1.

Annual deaths from iatrogenic CJD in the United Kingdom

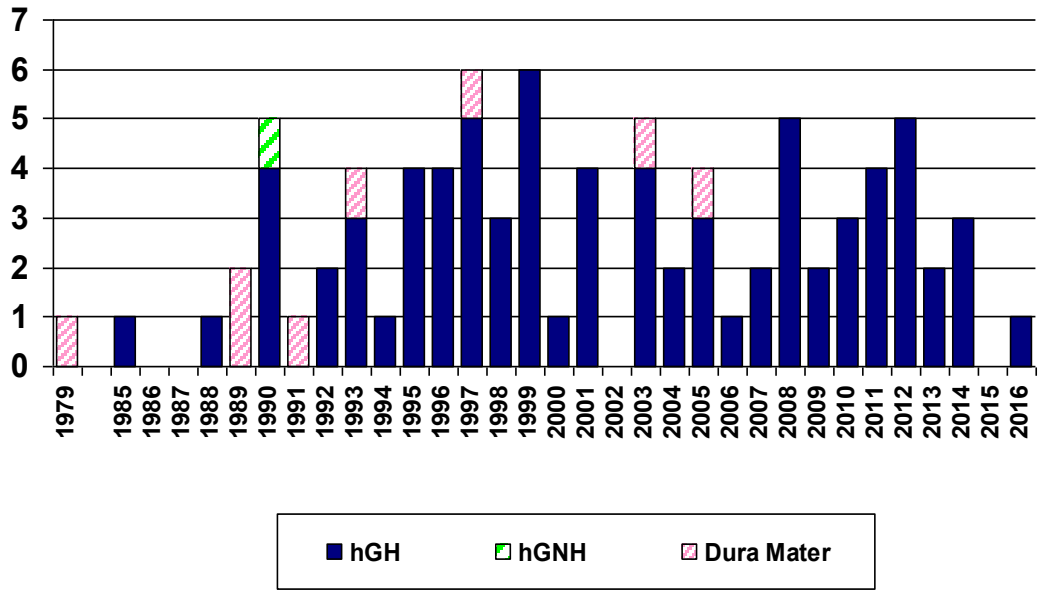

Abbreviations: CJD: Creutzfeldt-Jakob disease; dura mater: human dura mater graft-associated iatrogenic CJD hGH: human pituitary growth hormone-associated iatrogenic CJD; hGNH : human pituitary gonadotrophin-associated iatrogenic CJD (this patient was treated in Australia, but died in UK).

Courtesy of Ms Jan Mackenzie, Edinburgh, UK.

In France, 119 cases of iCJD in 1443 hGH recipients have occurred between 1991 and 2009, with no further deaths so far after this date (Brandel *et al*., 2013). The youngest patients died aged 10-11 years (Billette de Villemeur *et al.*, 2012). All were treated between December 1983 and July 1985, which has been identified as a high-risk period for hGH in France, since treatment of hGH with 8M urea was introduced at this time as a risk reduction step for prions (Brandel *et al.*, 2013). However, it is unlikely that this step would have completely eliminated any prion infectivity in the administered product.

Incubation periods in prion diseases have been studied extensively under experimental conditions and appear to be significantly influenced by both recipient (host) genetic factors and the strain properties of the infectious agent (Head *et al*., 2015). The principal human genetic factor influencing this incubation period is the *PRNP* codon 129 polymorphism of the recipient. It has long been recognised that homozygosity at this locus may predispose to both iCJD and sporadic CJD (sCJD) (Collinge *et al*., 1991; Palmer *et al*., 1991). However, differences in the frequency of the three *PRNP* codon 129 polymorphisms (MM, MV and VV) have been reported in hGH-iCJD cohorts in different countries; in particular, most cases of hGH-iCJD in France have belonged to the MM sub-group, whilst in the UK the VV and MV sub-groups predominate (Brandel *et al*., 2003). These differences may also reflect the nature of the strain(s) of CJD (presumably sCJD) that were responsible for the iatrogenic disease transmission. The average incubation period in the French iCJD hGH cohort is 9-10 years (Huillard d'Aignuax *et al*., 1999), with patients in the *PRNP* codon 129 MM subgroup having the shortest incubation periods (Brandel *et al*., 2003).

3. Objectives and Aims of the thesis:

3.1. Unanswered questions on iCJD in UK hGH recipients

Despite the fact that iCJD in hGH recipients has occurred in over 200 patients across the world, there have been very few detailed studies of the neuropathology, prion protein biochemistry and prion protein seeding activity in this form of human prion disease. There has been only a limited study of non-CNS tissues in these cases, which might inform understanding of the peripheral pathogenesis of this disease following inoculation of infected hGH preparations by intramuscular injection (Head *et al*., 2004a). Most reports from the UK describe only small numbers of cases that are not necessarily representative of the cohort in question, particularly with respect to the year of diagnosis in relation to the evolving time period since iatrogenic exposure to contaminated hGH ceased (Markus *et al*., 1992; Cordery *et al*., 2003; Jaunmuktane *et al.,* 2015).

A previous smaller study of iCJD in predominantly US hGH recipients have proposed that the prions accumulating in the brain may show an increased propagation efficiency following the secondary transmission of sporadic CJD, in a manner analogous to the shortening of disease incubation periods after cross-species transmission of scrapie prions (Xiao *et al*., 2014). Further studies on hDM-iCJD cases in Japan have proposed that the cases in *PRNP* codon 129 MM patients with amyloid plaques in the brain exhibit a "traceback phenomenon", that is to say the prions in the brain exhibit characteristics of the sCJD prion strain from which they originated, regardless of the *PRNP* codon 129 genotype of the secondary host. These characteristics will re-emerge on transmission or amplification from the secondary host to a new host with an

appropriate *PRNP* codon 129 genotype to allow the re-emergence and re-expression of these characteristics (Kobayachi *et al*., 2009, 2010). This phenomenon has been extensively investigated in sCJD and hDM-iCJD on transmission to transgenic mice, but has not yet been studied in cases of hGH-iCJD to investigate the possible sCJD strain of origin.

These two proposals can be explored using in vitro PrP^{Sc} amplification techniques in UK hGH-iCJD cases:

1. RT-QuIC will be used to measure the seeding activity of hGH-iCJD cases and to compare the findings with *PRNP* codon 129 genotype- and PrP^{Sc} isoform-matched cases of sCJD to establish whether there is evidence of increased seeding activity in the iCJD cases, corresponding to the proposed increased propagation efficiency in iCJD.

2. PMCA will be used to measure the conversion activity of PrP^{Sc} seeds from hGH-iCJD cases with *PRNP* codon 129 genotype- and PrP^{Sc} isoform-matched cases of sCJD in substrates containing PrP^{C} of either MM, VV or MV genotypes, to identify any differences in conversion activity, substrate preference and the isoform of the PrP^{Sc} generated on WB analysis. This will give an indication of any trace-back phenomenon in the hGH-iCJD cases that reflects the characteristics of the strain(s) of sCJD responsible for these cases, and will also demonstrate any increased conversion activity corresponding to the posed increased propagation efficiency in iCJD.

3.2 Objectives of the thesis

This thesis will examine the largest cohort yet collected of hGH-iCJD cases, with detailed characterisation of the PrP^{Sc} isoforms in the brain, correlation with genetic and pathological factors and an exploration of the in vitro PrP seeding activity present in different genetic sub-groups. These cases are compared with a smaller number of cases of hDM-iCJD in the UK, but also a very much larger group of sCJD cases drawn from the UK population over a similar time period. Crucially, this thesis also examine brain tissue samples from UK hGH recipients who were treated over a similar period to the hGH-iCJD patients, but who died from other causes and did not develop iCJD. Information on the hGH-iCJD patients and non-iCJD hGH recipients (e.g. sex, date of birth, date of death, duration of treatment, types of hGH administered, estimated incubation period and some genetic data) will be kindly provided from the UK National Registry of hGH recipients by Dr Peter Adlard, Institute of Child Health, London. The detailed examination of these cohorts allows a unique opportunity to ask fundamental questions about person-to-person transmission of prion disease and the molecular mechanisms involved.

3.3. Aims of the thesis

1. Determine the pathological phenotype of hGH-iCJD in the UK.
2. Explore whether the pathological phenotype is influenced by the *PRNP* codon 129 genotype and the CNS PrP^{res} isoform in the same way as in sCJD (Parchi *et al*., 1999).
3. Investigate the peripheral pathogenesis of hGH-iCJD following intramuscular inoculation.

4. Characterise the causal agent strain in hGH-iCJD and establish whether it relates to any of the known sCJD strains (Haik *et al*., 2011).
5. Seek evidence in hGH-iCJD and other non-iCJD hGH recipients for transmission/seeding of other neurotoxic proteins found in the pituitary gland - Aβ, tau, α-synuclein (Irwin *et al*., 2013; Jaunmuktane *et al*., 2015).

3.4. Hypotheses to be tested:

1. Disease phenotype: The clinicopathological phenotype of hGH-iCJD in the UK is determined by the *PRNP* codon 129 polymorphism of the patient and the PrP^{res} isoform in the CNS.
2. Increased propagation efficiency: The secondary transmission of sporadic CJD prions has led to the acquisition of greater propagation efficiency in hGH-iCJD prions (Xiao *et al*., 2014).
3. Trace-back phenomenon: The origin of the prions in hGH-iCJD can be inferred by ready reversion to their original state when given an appropriate host (Kobayashi *et al*., 2009, 2010).
4. Origin: The origin of hGH-iCJD in the UK can be inferred by the molecular and genetic changes occurring in the disease over time.
5. Co-pathology: Aβ seeding occurs in hGH recipients in the UK both with and without iCJD, resulting in the pathological accumulation of Aβ in the CNS.

4. Materials and Methods

4.1. Cases

All cases included in this study were of UK origin and were referred to the National CJD Research & Surveillance Unit (NCJDRSU) between 1991-2016 for neuropathological diagnosis and surveillance purposes (www.cjd.ed.ac.uk). Diagnoses were made according to the internationally accepted criteria for sCJD (Table 1.4), vCJD (Table 1.7) and acquired CJD (Table 1.9) on the basis of the clinical data and histological, immunohistochemical and (when unfixed frozen tissue was available) biochemical and genetic investigations. The clinical data (including the results of *PRNP* codon 129 genotype and full sequence analysis performed on blood samples taken in life) for sCJD, vCJD and iCJD were available from the clinical database in NCJDRSU with the kind help of Ms Jan Mackenzie, NCJDRSU co-ordinator. The clinical histories and details of treatment with UK hGH were kindly provided by Dr Peter Adlard, Institute of Child Health, London, who leads the National Registry of hGH recipients in the UK.

The inclusion criteria for the cases investigated in this thesis are:

1. A definite diagnosis of sCJD, vCJD, hDM-iCJD and hGH-iCJD, or a documented history of treatment with UK hGH with no clinical or neuropathological evidence of a human prion disease.
2. Appropriate consent/authorisation for use of autopsy tissues for research, or classification of autopsy tissues as Existing Holdings under the Human Tissue Act 2004 and the Human Tissue (Scotland) Act 2006. The MRC Edinburgh

Brain Bank has Research Ethics approval to provide these tissues (Edinburgh Brain Bank 16-ES-0084, IRAS project ID 199294).

4.1.1. Cases of hGH-iCJD

To date (2016) 78 cases of iCJD have occurred in the 1849 recipients of UK-produced hGH for whom records are available. Of these, 43 cases were referred to NCJDRSU for neuropathological diagnosis, three of which were brain biopsy samples in which insufficient paraffin-embedded tissue was available for research. Of the 40 autopsy cases, 35 fulfilled the inclusion criteria for research, but 2/35 had insufficient paraffin-embedded tissue available for full pathological investigation. These comprised eight female (f) and 27 male (m) patients, 21 of which had frozen brain tissue available (5f, 16m). The age at death in these 35 cases ranged from 20-46 years (y) (mean 31.2y, ± standard deviation (sd) 6.7y) (Figure 4.1). These 35 patients had been treated with hGH between 1970 and 1985 (see Appendix 1 for details of hGH treatment in this cohort).

4.1.2. Control cases

4.1.2.1. *hGH control cases*

Twelve autopsy cases with a history of hGH treatment had been referred to NCJDRSU for neuropathological diagnosis between 1991-2016, in whom there was no clinical or pathological evidence of iCJD or any other form of human prion disease. These comprised 3f and 9m patients, all with paraffin-embedded tissue available for research; 2m cases had frozen brain tissue available for research. The age at death ranged from

13-45y (mean 29.5y, ± sd 9.8y) (Figure 4.1). These patients had been treated with hGH between 1969 and 1985 (see Appendix 2 for details of hGH treatment in this cohort).

4.1.2.2 *hDM-iCJD cases*

Five autopsy cases of iCJD occurring in UK hDM graft recipients were referred to NCJDRSU for neuropathological diagnosis. These comprised 2f and 3m patients, three cases of which (2f, 1m) were available for research, but 1/3 had insufficient paraffin-embedded tissue available for full pathological investigation. The age at death ranged from 27-47y (mean 36.8y, ± sd 8.9y) (Figure 4.1). Dura mater graft surgery was performed between 1983 (month unknown) - August 1987 (Heath *et al*., 2006).

4.1.2.3. *vCJD cases.*

Thirty-three definite UK autopsy cases of vCJD with consent for research were used as age-matched controls for the paraffin-embedded tissue studies on the hGH-iCJD cases. These comprised 11f and 22m patients. The age at death ranged from 20-41y (mean 29.9y, ± sd 6.2y) (Figure 4.1).

4.1.2.4. *sCJD cases*

Fifteen definite UK autopsy cases of sCJD with consent for research were used as age-matched controls for the paraffin-embedded tissue studies on the hGH-iCJD cases. These cases included 6f and 9m patients. The age at death ranged from 20-46 y (mean 41.3y, ± 6.5y) (Figure 4.1). Data from 1,080 unselected cases of UK sCJD of known *PRNP* codon 129 genotype with deaths between 1990-2015 were used for *PRNP* genetic comparison with the UK hGH-iCJD cases. A smaller group of UK sCJD cases

(n=108) that were referred to NCJDRSU during the period 1991-2011 were used for biochemical comparison with the hGH-iCJD group. These cases were selected on the basis of sufficient frozen tissue available for research (minimal set: temporal cortex, occipital cortex, parietal cortex and thalamus) for PrP^{res} type classification according to the revised method of Parchi *et al.* (Parchi *et al.*, 2009) (see Appendix 3 for full details).

Figure 4.1.

Age distributions of hGH-iCJD and control cases (vertical bars represent the mean with standard deviation values)

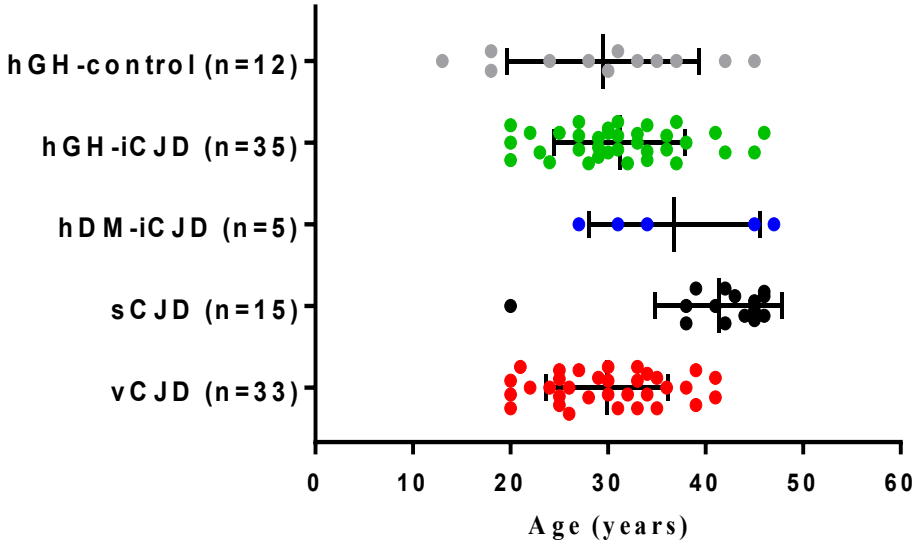

The control cases were chosen to be as close as possible in range to the hGH-iCJD cases. Cases of sCJD under the age of 50y are rare; the sCJD control cases are clustered in the 40-50y age range with higher mean age values. In contrast, cases of vCJD over the age of 40y are rare; the upper age limit for the vCJD cases is 41y.

Abbreviations: hDM: human dura mater; hGH: human growth hormone; iCJD: iatrogenic Creutzfeldt-Jakob disease; sCJD: sporadic Creutzfeldt-Jakob disease; vCJD: variant Creutzfeldt-Jakob disease.

4.2. Neuropathological examination

4.2.1. Laboratory details

All cases were examined in the Laboratory in the NCJDRSU, which has a containment suite of laboratories that have both Category 2* and Category 3 (derogation) facilities for the safe handling and storage of fixed and unfixed tissues from patients with human prion diseases. The Laboratory's premises, procedures and policies comply fully with the relevant guidance from the Advisory Committee on Dangerous Pathogens TSE Subgroup (https://www.gov.uk/government/ uploads/system/uploads /attachment _ data /file/ 209769 /Annex_K_-_Guidelines _for_pathologist_and_ pathology _ laboratories.pdf). The Laboratory is subject to regular inspection by the Health and Safety Executive and participates in the UK National External Quality Assessment Scheme for Cellular Pathology Technique – Neuropathology.

4.2.2. Tissue fixation and sampling

The 33 hGH-iCJD and 12 hGH control brains (27 whole brains, 6 half brains and 12 cases with multiple CNS tissue samples, according to the consent/authorisation status) and hDM-iCJD, vCJD and sCJD cases were all fixed in 15% unbuffered formalin for a minimum period of 3 weeks prior to weighing, external examination, dissection and sampling for histology. Extensive histological sampling included the brain regions recommended in the National Institute on Aging-Alzheimer's Association guidelines for the assessment of Alzheimer's disease (Hyman *et al*., 2012) whenever possible (Table 4.1).

Table 4.1. Brain regions sampled and assessed for ABC scoring

(modified from Hyman *et al*., 2012)

Each brain region receives a haematoxylin and eosin stain, plus additional stains/IHC as indicated.

	AD			**LBD**
	A	**B**	**C**	
Region	**4G8 and 6F/3D IHC for Aβ amyloid plaques** [4]	**AT8 IHC for NFT**	**Bielschowsky stain for NP**	**α-synuclein IHC for LB**
Medulla including DMV				1º: IHC or H&E [3]
Pons including LC				1º: IHC or H&E [3]
Midbrain including SN	3º: if 2º is +			1º: IHC or H&E [3]
Cerebellar cortex and dentate n.	3º: if 2º is +[2]			
Thalamus and subthalamic n. [1]				
Basal ganglia at level of AC with basal nucleus of Meynert [1]	2º: if 1º is +	Consider		
Hippocampus and EC [1]	2º: if 1º is +[2]	Yes	Consider	2º: IHC in at least one if 1º is +
Cingulate, anterior				
Amygdala				1º: IHC [3]
Middle frontal gyrus [1]	1º [2]	Yes	Yes	2º: IHC in at least one if 1º is +
Superior & middle temporal gyri [1]				
Inferior parietal lobule [1]				
Occipital cortex (BA 17 & 18) [1]	Consider[2]	Yes	Consider	

1 Consider taking bilateral sections if both cerebral hemispheres are available

2 Screen leptomeningeal and parenchymal vessels for cerebral amyloid angiopathy (CAA)

3 Screen for LBs with immunohistochemistry or H&E in brainstem and immunohistochemistry in amygdala. If positive, then expand immunohistochemistry for LBs in brainstem, limbic, and neocortical regions.

4 Stains for Aβ/amyloid plaques should be considered in other regions not needed for classification, such as in the precuneus or cingulate gyrus, as neuroimaging studies indicate that these sites are among the earliest to demonstrate retention of amyloid-binding molecules, a marker of fibrillar Aβ accumulation.

Abbreviations: AC: anterior commissure; AD: Alzheimer's disease; BA: Brodmann area; DMV: dorsal motor nucleus of the vagus; EC: entorhinal cortex; H&E: haematoxylin and eosin stain; IHC: immunohistochemistry; LBs: Lewy bodies; LBD: Lewy body disease; LC: locus ceruleus; n: nucleus; NP: neuritic plaques; NFT: neurofibrillary tangles; SN: substantia nigra; +: positive.

Formalin fixed, non-CNS tissue samples were available in 19/33 hGH-iCJD and 2/12 hGH control cases. These were fixed in 15% unbuffered formalin for no more than 7 days prior to sampling. All CNS and non-CNS tissue blocks were incubated in 96% formic acid for 1h as a prion risk reduction step (Brown *et al*., 1990) prior to processing into paraffin wax for microtomy (Appendix 4). Full details of the non-CNS tissues sampled for microscopy are provided in Appendix 5.

4.2.3. Histological stains

All CNS and non-CNS blocks were cut at 5μm and stained with haematoxylin and eosin (H&E). Selected CNS blocks were cut at 8μm and stained with Luxol Fast Blue/Cresyl Violet (LFB/CV) for myelin (Dawson *et al*., 2003). Sections were cut at 8μm for the Bielschowsky silver stain for neuritic plaques on the CNS blocks indicated in Table 4.1. Full details of the protocols for microtomy and histological stains are provided in Appendix 6.

4.2.4. Immunohistochemistry

Sections from all CNS blocks were labelled with two monoclonal anti-PrP antibodies recognising different epitopes of the prion protein: 12F10 (amino acids 142-160, Bioquote Ltd, UK) and KG9 (amino acids 140-180, TSE Resource Centre, Roslin Institute, UK). CNS blocks were selected for immunohistochemistry for Aβ (6F/3D and 4G8 antibodies), Aβ 1–40, Aβ 1–42, phospho-tau and α-synuclein according to the National Institute on Aging-Alzheimer's Association guidelines (Hyman *et al*., 2012); additional blocks from other regions including the spinal cord were examined when available. CNS blocks from hGH-iCJD and hGH control cases were also labelled

with antibodies to apolipoprotein E (pan-apoE), apoE-4, glial fibrillary acidic protein (GFAP), TDP-43, ubiquitin and CD68. Selected non-CNS tissues were labelled with the antibodies to PrP and Aβ.

All immunohistochemistry for a single antigen was performed in batches using the sensitive Novolink^{TM} Polymer Detection System (Leica Biosystems, UK). Details of all antibodies used, including antigen specificity, pretreatment protocols, dilutions, incubation times and positive control tissues are summarised in Table 4.2. Negative controls for immunohistochemistry were carried out by omitting the primary antibody in the reaction. Full details of the antibodies used are provided in Appendix 7 and the full protocol for immunohistochemistry is provided in Appendix 8.

4.2.5. Microscopy and photography

Tissue sections were analysed independently by two experienced assessors (Dr Diane L Ritchie and Professor James W Ironside) using a Leica DMR light microscope. Image capture was carried out with a Leica DFC 500 camera in combination with the Leica LAS image acquisition software (Leica Microsystems, Milton Keynes, UK).

Table 4.2. Antibodies and immunohistochemical protocols

Antibody clone	Antigen Specificity	1st Pre-treatment	2nd Pre-treatment	3rd Pre-treatment	Antibody dilution*/ Incubation time (mins) †	Positive control
5A9	Human apoE-4 protein	Autoclave 121ºC 10min	96% FA 5 min	-	1:600/45	AD cerebrum (*APOE* ε3/4 and ε 4/4 cases)
5B5	Human apoE-4 protein	Autoclave 121ºC 10min	96% FA 5 min	-	1:200/45	AD cerebrum (*APOE* ε3/4 and ε 4/4 cases)
D6E10	Human apoE protein	Autoclave 121ºC 10min	96% FA 5 min	-	1:2000/45	AD Hippocampus (*APOE* ε3,3 case)
11A50-B10	Human Aβ protein (1-40)	Autoclave 121ºC 10min	96% FA 5 min	-	1:400/45	AD Hippocampus
12F4	Human Aβ protein (1-42)	Autoclave 121ºC 10min	96% FA 5 min	-	1:3000/45	AD Hippocampus
6F/3D	Human Aβ (residues 8-17 with additional C-terminal cysteine)	96% FA 5 min	-	-	1:100/30	AD Hippocampus
4G8	Human Aβ (Epitope 17-24)	96% FA 5 min	-	-	1:45,000/30	AD Hippocampus
5G4	Human α-Synuclein	MW 10mmol Citric Acid (pH6.0)15 min	96% FA 1 min	-	1:1200/30	LBD Midbrain
AT8	Human PHF-Tau	MW 10mmol Citric Acid (pH6.0) 15 min	-	-	1:500/30	AD Hippocampus
11-9	Human Phospho TDP-43	MW 10mmol Citric Acid (pH6.0) 15 min	-	-	1:4000/30	MND spinal cord
12F10	Human prion protein (Epitope 142-160)	Autoclave 121ºC 10min	96% FA 5 min	PK (5µg/ml) 5 min	1:1700/60	sCJD VV2 cerebrum sCJD MV2 cerebellum
KG9	Human prion protein (Epitope 140-180)	Autoclave 121ºC 10min	96% FA 5 min	PK (5µg/ml) 5 min	1:500/60	sCJD VV2 cerebrum sCJD MV2 cerebellum
PGM1	CD 68	MW 10mmol Citric Acid (pH6.0) 15 min	-	-	1:100/30	normal tonsil
GFAP	Glial fibrillary acidic protein	-	-	-	1:1000/30	vCJD thalamus
Ubiquitin	Ubiquitin	MW 10mmol Citric Acid pH6.0,15 min	-	-	1:700/30	AD Hippocampus

Abbreviations: AD: Alzheimer's disease; CJD: Creutzfeldt-Jakob disease; FA: formic acid; LBD: Lewy body disease; min: minutes; mmol: millimolar; MND: motor neurone disease; MW: microwave; PK: Proteinase K; s: sporadic; vCJD : variant.
* All antibodies diluted in antibody diluent unless stated in the protocol (Leica Biosystems, UK: Product RE7133-CE)
† All primary antibodies are incubated at room temperature

4.2.5.1. *Assessment of CNS tissues for prion-related pathology on H&E sections*

H&E sections from all CNS regions sampled in the hGH-iCJD cases were examined for the characteristic neuropathological features of human prion diseases: spongiform change, neuronal loss, gliosis and amyloid plaque formation (Head *et al*., 2015). The distribution, severity and nature of the spongiform change (microvacuolar, confluent, mixed, status spongiosis) neuronal loss, gliosis and amyloid plaque formation (kuru-type, multicentric, florid, microplaque) were assessed and scored in a semiquantitative manner (Parchi *et al*., 2009) using 4 scores (0-absent, 1-mild, 2-moderate, 3-severe), along with assessment of the results of PrP immunohistochemistry (see below) to allow subclassification by histotyping (Parchi *et al*., 2009, 2012) to determine whether the range of neuropathological phenotypes identified in this group of patients corresponded to those occurring in the recognised sCJD subtypes (Figure 1.5), or not.

4.2.5.2. *Assessment of PrP immunoreactivity in the CNS*

All CNS sections from the hGH-iCJD cases were stained with the 12F10 and KG9 anti-PrP antibodies and examined to determine the distribution, severity and nature of the abnormal PrP accumulation (granular/synaptic, perineuronal/pericellular, plaque-like, plaques, amorphous deposits, perivascular, vascular) (Head *et al*., 2015). The findings were assessed in conjunction with those from the examination of the H&E sections (see above) to allow subclassification by histotyping (Parchi *et al*., 2009, 2012).

4.2.5.3. *Assessment of Aβ, tau and α-synuclein pathology*

Sections from the CNS of cases of hGH-iCJD, hGH controls, hDM-iCJD, vCJD controls and sCJD controls were stained by immunohistochemistry for Aβ (6F/3D and 4G8 antibodies), phospho-tau (AT8 antibody) and α-synuclein (5G4 antibody) according to the National Institute on Aging-Alzheimer Association guidelines for the neuropathological assessment of Alzheimer's disease (Hyman *et al*., 2012) (Table 4.1). An "ABC" score for the level of Alzheimer's disease neuropathology was calculated according to Hyman *et al*. (Hyman *et al*., 2012). This score is derived from the classification of the Aβ phase on sections stained using Aβ immunohistochemistry (Thal *et al*., 2002), the Braak and Braak stage for neurofibrillary tangles using immunohistochemistry for PHF-tau (Braak *et al*., 1991, 2006) and the neuritic plaque score on Bielschowsky silver-stained sections by the method of the Consortium to Establish a Registry for Alzheimer's Disease (CERAD) (Mirra *et al*., 1991). The combination of the results of these assessments in the ABC scoring method is summarised in Table 4.3.

"A" score: (Thal phase for Aβ deposits): in brief, in Thal phase 1, Aβ deposits (diffuse and non-diffuse plaques, but not including CAA) are found only in the neocortex, while in phase 2 there are additional Aβ deposits in allocortical brain regions. In Thal phase 3 there are further Aβ deposits in the diencephalon, basal forebrain and striatum. The midbrain and medulla become involved in Thal phase 4, while in phase 5 there are additional Aβ deposits in the cerebellum and pons (Thal *et al*., 2002).

"B" score: Braak & Braak stage for neurofibrillary tangles, modified for use with tau immunohistochemistry (Braak *et al*., 2006). The distribution of neurofibrillary tangles is briefly summarised as follows for the 3 groups scored in Table 4.3: in the transentorhinal region and the entorhinal region (transentorhinal stages I/II); additionally in the hippocampus and the occipito-temporal gyrus up to the medial temporal gyrus (limbic stages III/IV); additionally in the remaining neocortex, finally including the parastriate and striate cortex in the occipital lobe (neocortical stages V/VI) (Braak and Braak, 1991; Braak *et al*., 2006).

"C" score: the CERAD score for neuritic plaques is performed on Bielschowsky silver stained sections of the grey matter of the neocortex (superior and middle temporal gyri, middle frontal gyrus and the inferior parietal lobule) and examined at x100 magnification to obtain a semiquantitative assessment of the single highest number of neuritic plaques per microscopic field as follows: none; sparse (between 1-5); moderate (between 6-19); frequent (20 or more) (Mirra *et al*., 1991).

4.2.5.4. *Assessment of cerebral amyloid angiopathy*

Sections of the frontal cortex, parietal cortex, temporal cortex, occipital cortex and cerebellum from all cases of hGH-iCJD, hGH controls, hDM-iCJD, vCJD and sCJD were stained using the 6F/3D and 4G8 anti-Aβ antibodies (Table 4.2) to detect cerebral amyloid angiopathy (CAA) in vessels in the leptomeninges, the brain parenchyma and brain capillaries. CAA was scored according to the criteria of Love *et al*. (Love *et al*., 2014) (Table 4.4) and the total score for each case was recorded.

All cases with CAA were also stained with the anti-Aβ 1-40 antibody (11A50-B10) and the anti-Aβ 1-42 antibody (12F4) (Table 4.2), and the distribution of immunoreactivity for each antibody in the CAA blood vessels was recorded.

Table 4.3. ABC score for Alzheimer's disease pathology (from Hyman *et al*., 2012)

A	**Thal phase for Aβ plaques**	**B**	**Braak and Braak NFT stage**	**C**	**CERAD neuritic plaque score**
0	0	0	None	0	None
1	1 or 2	1	I or II	1	Sparse
2	3	2	III or IV	2	Moderate
3	4 or 5	3	V or VI	3	Frequent

The ABC score is derived by adding the numerical value for A, B and C for the corresponding Thal Aβ phase (Thal *et al*., 2002), the Braak and Braak stage for neurofibrillary tangles (Braak and Braak, 1991; Braak *et al*., 2006) and the CERAD neuritic plaque score (Mirra *et al*., 1991).

Abbreviations: Aβ: amyloid beta; CERAD: Consortium to Establish a Registry for Alzheimer's disease; NFT: neurofibrillary tangle.

Table 4.4. Scoring protocol for cerebral amyloid angiopathy (CAA) and CAA-associated vasculopathy (from Love *et al*., 2014)

Score	**Parenchymal CAA**	**Meningeal CAA**	**Capillary CAA**	**Vasculopathy**
0	Absent	Absent	Absent	Absent
1	Scant Aβ deposition	Scant Aβ deposition	Present	Occasional vessel
2	Some circumferential Aβ	Some circumferential Aβ		Many vessels
3	Widespread circumferential Aβ	Widespread circumferential Aβ		

Abbreviation: Aβ: amyloid beta

4.2.5.5. *Assessment of the co-localisation of PrP, phospho-tau, CD68, GFAP and Aβ pathology*

Sections of the CNS from selected cases of hGH-iCJD, sCJD and vCJD that showed immunoreactive Aβ deposits in the parenchyma and/or blood vessels were double immunostained for Aβ and either PrP or phospho-tau, CD68 or GFAP in order to determine whether co-localisation existed between these 4 proteins and the Aβ protein. Sections were double stained with the anti-PrP antibody, 12F10; the anti-phospho-tau antibody, AT8; the anti-CD68 antibody, PGM1; the anti-glial fibrillary acidic protein, GFAP and the anti-Aβ antibody, 6F3D (Table 4.2). Full details of the antibodies used are provided in Appendix 7 and the full details of the double immunohistochemistry protocol are provided in Appendix 8.

4.2.5.6. *Immunohistochemistry for apoE and apoE-4*

Sections of the CNS from cases of hGH-iCJD and hGH controls that contained immunoreactive Aβ in the parenchyma or in blood vessels and in which no frozen tissue was available for *APOE* genotype analysis were stained with antibodies to apoE and apoE-4 (Table 4.2). Immunoreactivity was compared to cases of AD of known *APOE* ε3/3 genotype as a positive control for apoE expression. AD cases of known ε3/4 and ε4/4 genotypes were used as positive controls for apoE-4 expression. Cases that showed selective labelling of AD pathology with both anti-apoE-4 antibodies were judged to be cases with an apoE4 phenotype and categorised as apoE4+(IHC); other cases were categorised as apoE4-(IHC).

4.2.6. Paraffin embedded tissue (PET) Blot

Paraffin-embedded tissue (PET) blotting was performed on formalin fixed non-CNS tissues from hGH-iCJD cases in which no frozen tissues were available for WB analysis (Ritchie *et al*., 2004). PET blots were performed using two monoclonal anti-PrP antibodies recognising different epitopes of the prion protein; 3F4 (amino acids 109-112, Cambridge Bioscience, UK) and 12F10 (amino acids 142-160, Bioquote Ltd, UK) (Appendix 6). Stained PET blot sections were analysed with a Leica $M29_5$ stereoscopic microscope and image capture carried out with a Leica DFC 320 camera in combination with the Leica LAS image acquisition software (Leica Microsystems, UK). The full protocol for the PET blot technique and microscopy is provided in Appendix 9.

4.3. Genetic analysis

4.3.1. DNA extraction from tissues

DNA was extracted from frozen tissues for *PRNP* codon 129 genotype analysis from cases in which no blood samples had been taken in life. DNA extraction from formic acid treated paraffin-embedded tissues was attempted in cases for which no frozen tissues or blood samples were available.

DNA extraction was attempted from either unfixed grey matter-enriched frozen brain tissue samples (20-30mg) of the cerebellar cortex or frontal cortex, or up to 25mg of formic acid treated paraffin-embedded tissue from the cerebellar cortex cut as 10μm unmounted sections using a Qiagen DNeasy Blood and Tissue kit (Qiagen, Hilden, Germany) using the method in the accompanying handbook (www.qiagen.com). DNA

extraction from paraffin-embedded tissues was also attempted using the method described by Nicoll *et al*. (Nicoll *et al*., 1997). Full protocols for DNA extraction from fixed and frozen tissues are provided in Appendix 10.

4.3.2. *PRNP* codon 129 analysis

PRNP codon 129 genotype analysis was performed by PCR of the *PRNP* gene, followed by restriction enzyme digestion at 37°C with NspI (New England Biolabs, UK). This enzyme cleaves the amplicon at *PRNP* codon 155 and at codon 129 only when the latter sequence codes for valine (-GTG-). This allows for discrimination of the three *PRNP* codon 129 genotypes: Homozygous methionine (MM), heterozygous (MV) and homozygous valine (VV) by agarose gel electrophoresis and staining as previously described (Bishop *et al*., 2009), but using a SYBR® Safe DNA Gel Stain (Invitrogen, Cat# S33102), (Figure 4.2). The full protocol used for *PRNP* codon 129 analysis is provided in Appendix 10.

Figure 4.2. *PRNP* codon 129 genotype interpretation

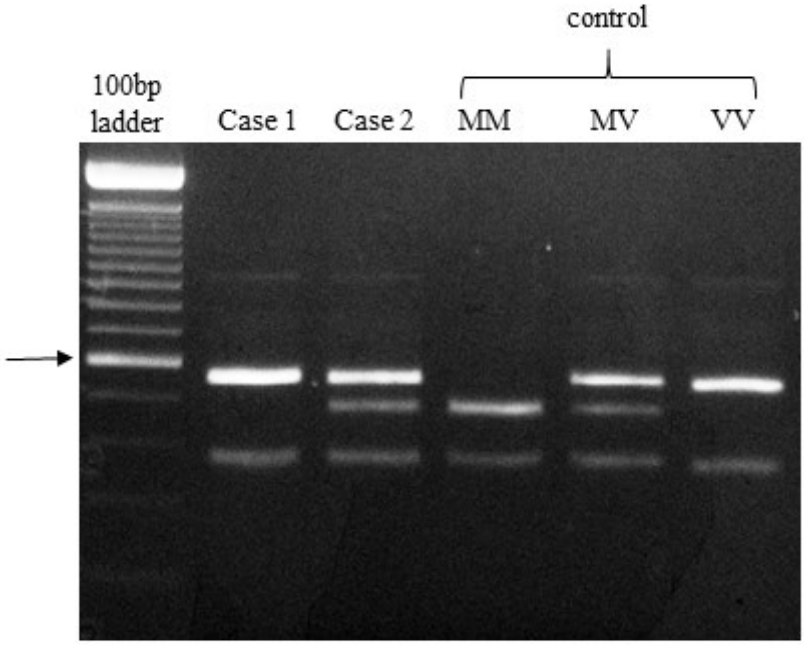

PRNP codon 129 genotyping by PCR amplification and restriction enzyme digestion. The 600 bp band on the 100 bp molecular ladder is indicated by an arrow. Controls for MM, MV and VV genotypes are included on the gel. Case 1 is from a patient with a *PRNP* codon 129 VV genotype and Case 2 is from a patient with a *PRNP* codon 129 MV genotype.

Abbreviations: bp: base pair; M: methionine: PCR: polymerase chain reaction; *PRNP*: prion protein gene; V: valine.

4.3.3. Exome sequencing and analysis

Exome sequencing and analysis, and *APOE* genotype analysis by polymerase chain reaction (PCR) were performed in the Universities of Newcastle and Cambridge by Dr Michael Keogh, Dr Wei Wei and Professor Patrick Chinnery, University of Cambridge, as part of the project "Maximising the value of MRC Brain Banks - High throughput genotype and imaging studies to enrich data available to the research community" (Medical Research Council grant MC_PC_13044; Professor JW Ironside). This summary of the methods used and the results from these investigations were kindly provided by Dr Keogh, Dr Wei and Professor Chinnery.

Genomic DNA was fragmented, exome enriched and sequenced (Nextera Rapid Exome Capture 62Mb or TruSeq rapid 37Mb kit on a HiSeq 2000 with 100bp paired-end reads). Bioinformatic analysis was performed using an in-house pipeline including alignment (human reference genome hg19, UCSC) using Burrows-Wheeler Aligner (BWA) (Langmead *et al*., 2009). Variant calling was performed using FreeBayes (Garrison, 2012). Subsequent analysis was restricted to on-target homozygous, heterozygous, and compound heterozygous variants with a minimum read depth of 10, and base quality score of 20. Further analysis selected variants in 5' untranslated region (UTR), 3' UTR or exonic regions within genes of interest that may influence the aggregation of Aβ in the CNS (*APP, C9ORF72, CHMP2B, CSFIR, FUS, GRN, ITM2B, MAPT, NOTCH3, PSEN1, PSEN2, SERPINI1, SQSTM1, TARDBP, TREM2, TYROBP, VCP*) and with a minor allele frequency <5% in the 1000 Genome Project Database (1000 Genomes Project Consortium *et al*., 2012) of European/American cases from the NHLBI ESP exomes database (NHLBI GO Exome Sequencing Project,

2013) and the ExAC server (Exome Aggregation Consortium, 2015), using Qiagen Ingenuity Variant Analysis software (Qiagen, Hilden, Germany).

4.3.4. *APOE* genotyping

APOE genotyping was performed by competitive allele-specific PCR, using KASP™ genotyping assays (LGC Genomics, Hoddesdon, UK) for both rs7412 and rs429358. Subsequent genotype data was converted into *APOE* allele status (Weisgraber *et al*., 1982). Full methods for the KASP™ genotyping platform are available from LGC Genomics (http://www.lgcgenomics.com/genotyping/kasp-genotyping-reagents/).

4.3.5. *C9orf72* PCR

Screening for the *C9ORF72* hexanucleotide repeat expansion was performed as described by Renton *et al.* (Renton *et al*., 2011) in the laboratory of Professor Stuart Pickering-Brown, University of Manchester. Positive results were confirmed by Southern blot (Beck *et al*., 2013) allowing an estimate of the repeat size.

4.4. Western blot analysis of PrP^{res} in frozen CNS tissues

4.4.1. Western blot method

Samples of frozen grey matter from the cerebral cortex (frontal, parietal, temporal and occipital cortex), cerebellar cortex, thalamus (dorsomedial region) and spinal cord were examined where available. The PrP^{res} types present in brain samples from the sCJD, hDM-iCJD and hGH-iCJD cases were determined using the refined Western blot (WB) protocol of Parchi *et al.* (Parchi *et al*., 1999). Briefly, 100mg samples of frozen CNS samples were subjected to stringent sample preparation (including strong

buffering to pH 6.9 at 37°C) and digestion with proteinase K (Roche, Lewes, UK) using 10U/ml corresponding to ~200µg/ml (depending on the batch) at 37°C for 1h prior to WB analysis. Immunodetection of PrP was carried out using monoclonal antibody 3F4 (Millipore, UK) at a final concentration of 75ng/ml or the monoclonal antibody 12B2 (Central Veterinary Institute of Wageningen UR, Lelystad, The Netherlands) at a final concentration of 200ng/ml for 1h. The full WB protocol is provided in Appendix 11.

4.4.2. PrP^{res} analysis and classification

The WB protocol allows a distinction to be made between PrP^{res} types based on the migration of the unglycosylated (bottom) band of the typical triplet glycoform pattern (Figure 1.2). Three different unglycosylated PrP^{res} fragment mobilities are recognised within the 21-19kDa range: type 1 in which the unglycosylated PrP^{res} has a molecular mass of ~21kDa; type 2 in which the unglycosylated PrP^{res} fragment has a molecular mass of ~19kDa, and an additional type with a mobility of ~20kDa migrating between type 1 and 2 and therefore referred to as type i (for intermediate) (Figure 1.2). PrP^{res} types 1, i and 2 are not mutually exclusive. Certain individual samples and cases may contain more than one PrP^{res} type; this diversity is recognised by classifying such samples and cases as 1+2, 1+i, or i+2.

4.4.3. Western blotting with sodium phosphotungstic acid (NaPTA) preciptation

WB analysis of non-CNS tissues was performed using the sodium phosphotungstic acid (NaPTA) precipitation method, which gives enhanced sensitivity for the detection of low levels of PrP^{res} in non-CNS tissues as previously described (Wadsworth *et al*.,

2001; Glatzel *et al*., 2003; Peden *et al*., 2006, 2010). Frozen, non-CNS tissue samples were available in 11/33 hGH-iCJD cases. Appendix 5 gives full details of the non-CNS tissues sampled for NaPTA analysis. 10% w/v extracts were made of 65-100mg samples of tissue by homogenising in an appropriate volume of ice-cold 2% sarkosyl/phosphate-buffered saline (PBS), pH 7.4, using the FastPrep instrument (Qbiogene, Cambridge, UK). The samples were then cleared by centrifugation at 5,200*g* for 5min at 4ºC. Cleared spleen tissue homogenate (5%) from a non-CJD patient was used as a non-CJD negative control. In addition, iCJD or sCJD brain tissue homogenate (10%, 10µl, corresponding to 100µg brain) was diluted and mixed into 1ml of 5% cleared non-CJD spleen tissue homogenate for use as positive control.

Samples (0.5ml) of the cleared lysates were diluted with a further 0.5ml of 2% sarkosyl/PBS and incubated for 10min at 37ºC. Benzonase (Sigma, Poole, UK) and MgCl2 were added at final concentrations of 50U/ml and 1mmol/l, respectively, and incubation at 37°C was continued for a further 30min. Eighty-one µl of a stock solution of 4% w/v NaPTA and 170mmol/l MgCl2, pH 7.4, were added (final concentration of NaPTA, 0.3% w/v), and precipitation was allowed to occur for 30min at 37°C. The samples were centrifuged at 20,800*g* for 30min at 37°C. The resultant supernatant was discarded and the pellets were resuspended in 20µl of 0.1% w/v sarkosyl in PBS, pH 7.4, and digested with 50µg/ml proteinase K for 30min. Digestion was terminated by the addition of 1mmol/l PefaBloc SC (Roche, Lewes, UK). Immunoblotting for proteinase resistant PrP^{Sc} following NaPTA precipitation was performed as in 4.4.1 above using the monoclonal antibody 3F4 (Millipore, UK) at a final concentration of

75ng/ml for 1h (see Appendix 11 for the full WB protocol). A full protocol for WB with NaPTA precipitation is provided in Appendix 12.

4.5. In vitro conversion assays

4.5.1. Real-time quaking-induced conversion (RT-QuIC)

The methods described by Peden *et al.* (Peden *et al.*, 2012, 2014) for the RT-QuIC PrP conversion assay were used with minor modifications. Full length hamster recombinant PrP (recPrP, aa 23–231; GenBank accession no. K02234) was used as a substrate for seeded conversion. Brain samples to seed the reactions were homogenised in phosphate buffered saline (PBS) containing 1mmol EDTA, 150mmol NaCl, 0.5 % Triton X-100 and Complete^{TM} Mini EDTA-free Protease Inhibitor Cocktail (Roche). The tissue was disrupted using one cycle of lysis (45sec, 6ms^{-1}) in a Fastprep-24 homogeniser (MP Biomedicals, USA). An appropriate volume of homogenisation buffer was used to give a final tissue concentration of 10 % (w/v). Cellular debris was cleared from the homogenates by centrifugation at 5,200*g* at 4°C. Further serial ten-fold dilutions of the cleared tissue homogenate were made using PBS.

The 100µl RT-QuIC reactions were set up in quadruplicate in the wells of a clear-bottomed black 96-well microplate (Fisher Scientific, UK). Stock solutions containing the reaction components were filtered through a 0.22µm Millex PES filter prior to making a master mix. recPrP was the final addition to the master mix, which was mixed and then dispensed into the wells in 98µl volumes. At least four replicate analyses were performed on each patient sample. The RT-QuIC reactions (final volume = 100µl, recPrP final concentration = 0.1mg/ml) were initiated by the addition of 2 µl of a 10^3-fold dilution of the 10% (w/v) brain homogenate. The plates were sealed with

film, incubated at 42^{o} C and shaken intermittently (87 sec shaking at 900rpm in a double orbital configuration followed by a 33sec rest) using a FLUOstar OMEGA microplate reader (BMG Labtech, UK). Fluorescence readings were taken at 480nm every 15min from the bottom of the wells after excitation with 20 flashes per well at 450nm.

In order to quantify prion seeding efficiency we used a method based on the one described by Shi *et al*. (Shi *et al*., 2013), where the lag time to conversion is used as an inverse measure of seeding potential. The lag time to the start of PrP^{C} conversion was taken to be the time (in hours (h)) from the start of the assay to when the RT-QuIC fluorescence reading was three times the average reading at 0.5h (the baseline). A mean lag period for four replicate analyses was thus obtained for each sample (Figure 4.3). The full protocol used for the RT-QuIC in vitro conversion assay is provided in Appendix 13.

Figure 4.3.

Diagrammatic representation of the calculation of the RT-QuIC lag time

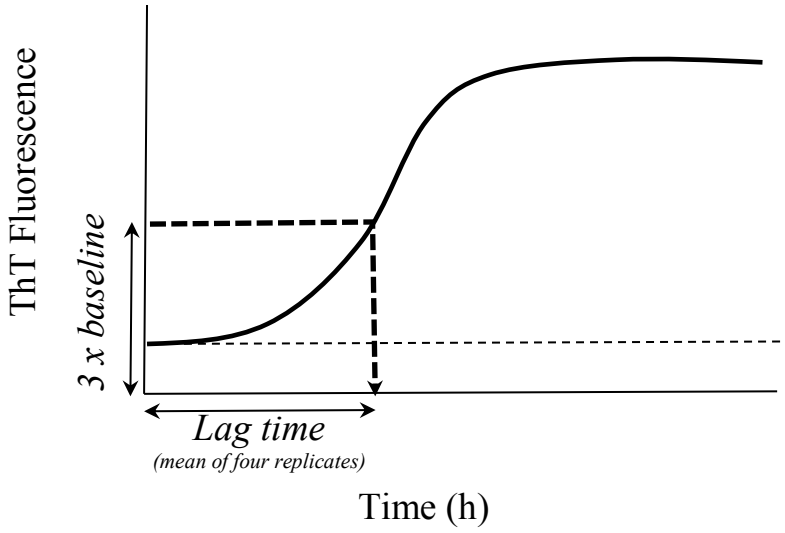

The lag time to the start of PrP^C conversion is taken to be the time (h) from the start of the assay to when the RT-QuIC fluorescence reading (Y axis) was three times the average reading at 0.5h (at least 4 replicate analyses are performed on each sample). Time (h) on the X axis starts at 0.5 h.

Abbreviations: h: hours; PrP^C: cellular prion protein; RT-QuIC: real-time quaking-induced conversion; ThT: Thioflavin T.

4.5.2. Protein misfolding cyclic amplification (PMCA)

PMCA experiments were carried out as described previously (Barria *et al*., 2014). Briefly, brain homogenates from humanised transgenic mice of *PRNP* codon 129 methionine homozygous (129MM), valine homozygous (129VV) and heterozygous (129MV) genotypes (Bishop *et al*., 2006) were prepared using a manual homogeniser and conversion buffer (phosphate-buffered saline 1X, 150mmol NaCl, 1% Triton X-100 and 1X protease inhibitors) to obtain a final 10% weight/volume solution (the

PMCA "substrate"). The homogenised tissue was cleared by centrifugation at 2,000 rpm for 40sec in a refrigerated centrifuge (4°C), and the supernatant was aliquoted and stored at −80ºC. The sCJD and iCJD brain homogenates (the PMCA "seeds") were prepared following the method used for substrate preparation.

Aliquots of 10% brain homogenate substrates were mixed with 10% CJD brain homogenates seed in PCR tubes (Figure 4.4). Low molecular weight heparin was included at 100µg/ml for all PMCA reactions. Prior to the amplification procedure, 19µl of the PMCA reaction mixture were taken (from the final volume of 120µl) for each reaction (referred to as the "frozen" sample) for comparison with the sonicated samples (referred to as the "sonicated" sample). Amplification employed cycles of sonication and incubation in a programmable sonicator (Qsonica, model Q-700) at 37°C. A total of 96 PMCA cycles were performed comprising 20sec of sonication (at an amplitude of 38%, wattage: 278-299) followed by 29min 40 sec of incubation for each cycle. Frozen and sonicated samples were digested with proteinase K (in a final concentration of 50µg/ml at 37ºC for 1h) and analysed by WB using the monoclonal antibody 3F4 as described previously (Barria *et al*., 2014). Amplification efficiency was expressed as the increase in PrP^{res} signal in the sonicated sample compared to the frozen sample, as judged by densitometry of WB images acquired and analysed using the ChemiDoc™ XRS+ System with Image Lab Software (Bio-Rad, Hemel Hempstead, UK). The full protocol used for PMCA is provided in Appendix 14.

4.6. Statistical analyses

Advice on appropriate methods for statistical analyses was kindly provided by Dr Anna Molesworth, NCJDRSU, University of Edinburgh and Catriona Graham, Lead Statistician, Edinburgh Clinical Research Facility, University of Edinburgh.

Excel (Microsoft, Reading, UK) and Prism 7.00 (GraphPad Software, Inc, La Jolla, USA, on license) were used for data storage and processing for statistical analysis of the data. The threshold used for statistical significance was $p< 0.05$. All graphs were generated using GraphPad Prism 7.00 (GraphPad Software, Inc, La Jolla, USA, on license).

5. Results

5.1. Clinical features

5.1.1. hGH-iCJD cases

The clinical features (sex, age at death, age at iCJD onset, duration of illness, duration of hGH treatment, the mid-point of treatment to death, incubation period and *PRNP* codon 129 genotype) of the 35 hGH-iCJD cases are summarised in Table 5.1. The duration of hGH treatment varied from 2-11.2y (mean 6.6y, ± sd 2.6y) and the duration of illness ranged from 2-32 months (mo) (mean 11.3mo, ± sd 6.6mo). All patients had received hGH produced by the modified Wilhelmi method for periods ranging from 0.5-8.2y.

The disease incubation period varied from 7.8-32.3y (mean 17.6y, ± sd 5.9y) and the period from the mid-point of treatment to death ranged from 8.2-32.9y (mean 18.6y, ± sd 6y). The commonest cause of hGH deficiency was idiopathic hGH deficiency (26 cases), followed by craniopharyngiomas (5 cases). Single cases of panhypopituitarism, histiocytosis X, Russell-Silver syndrome and pilocytic astrocytoma were also included. No cases had a history of head injury as a cause of hGH deficiency. Further details are provided in Appendix 1.

The distribution of *PRNP* codon 129 genotypes in relation to the year of death is shown in Figure 5.1.A for the 30/35 cases for which data are available. The *PRNP* codon 129 genotype in one case (hGH-iCJD31) was obtained from DNA extracted from a formic-acid treated paraffin block; this method was unsuccessful in the five other cases. Figure 5.1B shows the *PRNP* codon 129 genotype in relation to the year of death in the 21

cases with frozen tissue available for research; these cases appear to be representative of the total cases in Figure 5.1A. The UK hGH-iCJD group is dominated by patients of the MV and VV *PRNP* codon 129 genotypes; the 4 hGH-iCJD cases in individuals with the MM *PRNP* codon 129 genotype tended to occur in the latter part of the hGH-iCJD epidemic.

Statistically significant associations between the *PRNP* codon 129 polymorphism and the disease incubation period and the duration of illness in the hGH-iCJD patients are illustrated in Figure 5.2. Codon 129 MV patients have a significantly longer duration of illness (mean 16.3mo, ± sd 6mo) than the MM (mean 6mo, ± sd 1.4mo) and VV (mean 6.18mo, ± sd 1.8mo) patients. In contrast, the codon 129 MM patients have the longest incubation periods (mean 28.1y, ± sd 6.1y) in comparison to the MV patients (mean 18.2y, ± 4.2y) and the VV patients (mean 14.1y, ± 3.5y).

Table 5.1.

Clinical and genetic features of hGH-iCJD cases

Study ID	Sex	Age at death (years)	Age at disease onset in years (year of onset)	Duration of illness (months)	Duration of hGH treatment (years)	Midpoint of hGH treatment to death (years)	Incubation period (years)	*PRNP* codon 129 genotype
hGH-iCJD1*	m	34	33 (1989)	8	4	17.5	16.9	MV
hGH-iCJD2	m	31	30 (1991)	6	10	16.9	16.5	VV
hGH-iCJD3	m	27	26 (1992)	17	6	14.9	13.2	MV
hGH-iCJD4	m	30	29 (1992)	9	4	14.2	12.8	VV
hGH-iCJD5	m	25	25 (1993)	5	6	11.9	11.4	VV
hGH-iCJD6	f	33	32 (1994)	6	4	18.5	18.1	VV
hGH-iCJD7	f	31	30 (1995)	12	4	17.1	16.2	MV
hGH-iCJD8	m	29	28 (1996)	6	8	17.5	16.8	VV
hGH-iCJD9	m	33	32 (1985)	14	10	20.0	18.8	MV
hGH-iCJD10	m	36	36 (1996)	8	4	19.8	19.2	VV
hGH-iCJD11	m	37	35 (1996)	18	4	19.1	17.8	MV
hGH-iCJD12	m	27	27 (1998)	5	7	16.8	16.4	VV
hGH-iCJD13	m	34	32 (1997)	16	5	18.2	17.2	MV
hGH-iCJD14	m	29	28 (1997)	15	9	18.2	17.2	MV
hGH-iCJD15	m	37	37 (1999)	9	6	20.4	19.1	MV
hGH-iCJD16	m	30	28 (2000)	16	3	21.5	20	MV
hGH-iCJD17*	f	41	38 (2001)	22	10	25.2	23.7	MV
hGH-iCJD18	f	34	32 (2003)	23	8	24.1	22.6	MV
hGH-iCJD19	f	29	27 (2004)	32	7	24.5	22	MV
hGH-iCJD20	m	46	46 (2011)	5	3	29.9	29.4	MM
hGH-iCJD21	m	42	42 (2012)	8	8	31.6	31.7	MM
hGH-iCJD22	m	20	19 (1997)	7	11	8.2	7.8	VV
hGH-iCJD23	f	20	20 (1990)	2	11	15.1	10.5	VV
hGH-iCJD24	m	32	31 (1992)	13	6	14.4	13.7	MV
hGH-iCJD25	m	30	29 (1991)	16	3	13.7	12.5	N/A
hGH-iCJD26	m	27	26 (1994)	7	8	13.7	13.2	VV
hGH-iCJD27	m	24	23 (1994)	7	6	13.1	12.8	VV
hGH-iCJD28	f	22	22 (1984)	11	5	10.4	9.5	MV
hGH-iCJD29	m	20	20 (1989)	5	9	9.3	9.0	N/A
hGH-iCJD30	m	23	23 (1996)	8	5	14.2	13.6	N/A
hGH-iCJD31	m	28	28 (1997)	5	2	19.7	19.1	†MM
hGH-iCJD32	m	36	35 (1999)	9	10	22.2	21.4	N/A
hGH-iCJD33	m	31	29 (2000)	20	7	19.8	18.1	N/A
hGH-iCJD34	m	38	37 (2003)	19	10	26.9	25.4	MV
hGH-iCJD35	f	45	45 (2006)	6	9	32.9	32.3	MM

*****Insufficient paraffin-embedded tissue available for full pathological investigation
† *PRNP* codon 129 genotype was obtained from DNA extracted from a formic-acid treated paraffin block

Abbreviations: f: female; hGH: human growth hormone; iCJD: iatrogenic Creutzfeldt-Jakob disease; m: male; M: methionine; *PRNP*: prion protein gene; V: valine.

Figure 5.1.
hGH-iCJD *PRNP* codon 129 genotype in relation to year of death

A

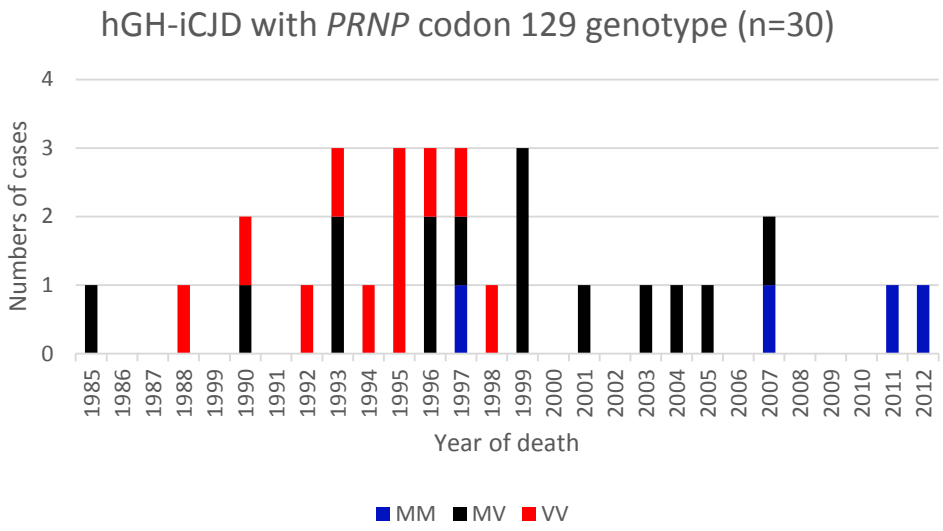

B

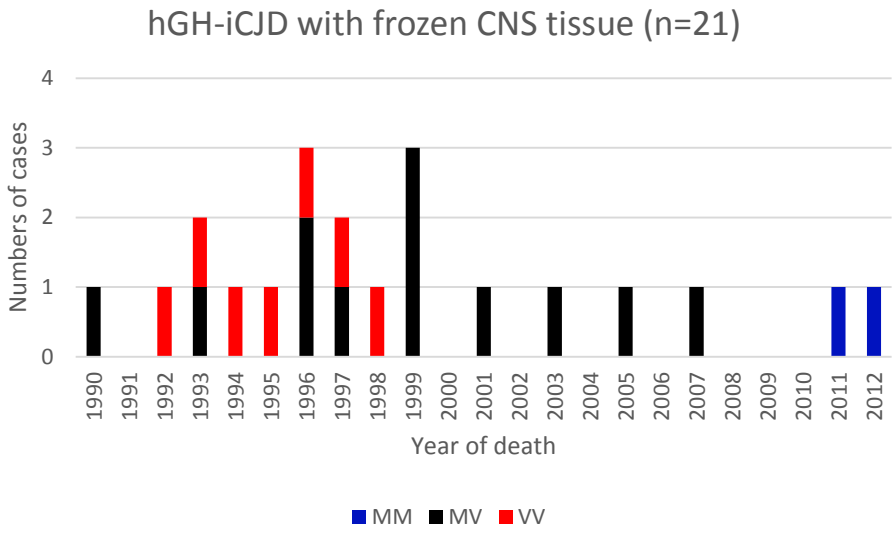

The graphs indicate that both groups of cases cover all *PRNP* codon 129 genotype within a wide time period across the hGH-iCJD epidemic and can therefore be considered as representative of the larger hGH-iCJD cohort.
Abbreviations: CNS: central nervous system; hGH: human growth hormone; iCJD: iatrogenic Creutzfeldt-Jakob disease; M: methionine; *PRNP*: prion protein gene; V: valine.

Figure 5.2.
Relationship of *PRNP* codon 129 polymorphisms to hGH-iCJD incubation period and disease duration (horizontal bars represent mean with standard deviation values)

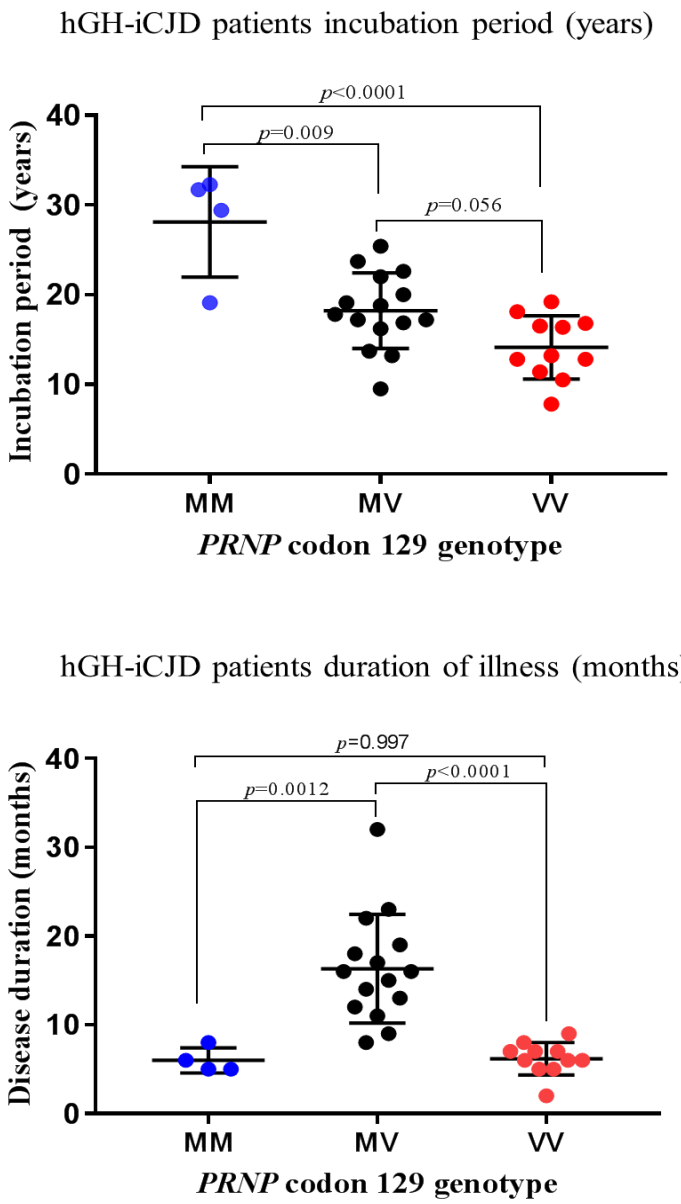

Diagram (A) shows differences in the incubation periods for hGH-iCJD in relation to *PRNP* codon 129 genotype, with the MM genotype having significantly longer incubation periods than the MV and VV genotypes. Diagram (B) shows differences in the hGH-iCJD disease duration in relation to *PRNP* codon 129 genotype, with the MM and VV genotypes having significantly shorter disease durations than the MV genotype. Statistical analyses were performed using one-way ANOVA followed by Tukey's multiple comparison test.

Abbreviations: hGH: human growth hormone; iCJD: iatrogenic Creutzfeldt-Jakob disease; M: methionine; *PRNP*: prion protein gene; V: valine.

5.1.2. hGH control cases

The clinical features (sex, age at death, duration of hGH treatment, period from mid-point of treatment to death and *PRNP* codon 129 genotype) of the 12 cases are summarised in Table 5.2. The *PRNP* codon 129 genotype in two cases was obtained from frozen tissue and in three cases from formic-acid treated paraffin blocks; the remaining seven cases have no codon 129 genotype data available (Table 5.2). The duration of treatment varied from 1-12.3y, (mean 5.1y, ± sd 3.7y) and the period from the mid-point of treatment to death ranged from 2.7-35.1y (mean 16.2y, ± sd 9.8y). 8/12 of the patients had received hGH produced by the modified Wilhelmi method for periods ranging from 0.5-6.6y. The commonest underlying disorder was craniopharyngioma (five cases), with two cases of idiopathic panhypopituitarism and single cases of idiopathic hGH deficiency, mitochondrial cytopathy, Prader-Willi syndrome, ependymoma and pilocytic astrocytoma. No cases had a history of head injury as a cause of hGH deficiency. Further details are provided in Appendix 2.

Table 5.2.
Clinical and genetic features of hGH control patients

Study ID	Sex	Age at death (years)	Duration of hGH treatment (years)	Midpoint of hGH treatment to death (years)	PRNP codon 129 genotype
hGH control1	m	18	1.0	2.7	N/A
hGH control2	f	18	2.3	5.0	N/A
hGH control3	m	13	1.0	6.4	*MV
hGH control4	m	28	3.5	8.9	*MV
hGH control5	f	24	10.3	13.4	N/A
hGH control6	f	31	7.3	19.6	N/A
hGH control7	m	30	6.3	17.5	N/A
hGH control8	m	33	5.3	16.4	*MV
hGH control9	m	42	7.5	21.6	N/A
hGH control10	m	37	3.3	16.7	MV
hGH control11	m	45	12.3	30.3	MM
hGH control12	m	35	1.0	35.1	N/A

* *PRNP* codon 129 genotype was obtained from a formic-acid treated paraffin block

Abbreviations: f: female; hGH: human growth hormone; m: male; M: methionine; N/A: data not available; *PRNP*: prion protein gene; V: valine.

5.1.3. hDM-iCJD cases

The clinical features (sex, age at death, year of dural graft, disease duration, incubation period and *PRNP* codon 129 genotype) of the five cases referred to NCJDRSU and available for research are summarised in Table 5.3. All cases underwent dura mater grafting with Lyodura between 1983-1987. The incubation periods ranged from 3.8-14.8y (mean 8.2y, ± sd 3.7y) and the duration of illness ranged from 4-33mo (mean 11.5mo, ± sd 12 mo). Three cases had *PRNP* codon 129 genotype analysis performed on blood samples taken in life. Extraction of DNA from formic-acid treated paraffin blocks for *PRNP* codon 129 analysis was unsuccessful in the remaining two cases (Table 5.3).

Table 5.3.
Clinical and genetic features of hDM-iCJD patients

Study ID	Sex	Age at death (years)	Date of Graft	Incubation period (years)	Disease duration (months)	*PRNP* codon 129 genotype
hDM-iCJD1	f	45	1983 (month unknown)	7.8 (estimate)	5	MM
hDM-iCJD2	f	27	April 1986	8.6	33	MM
hDM-iCJD3	m	34	August 1987	14.8	5	MM
hDM-iCJD4	m	31	October 1985	3.8	4	N/A
hDM-iCJD5	m	47	July 1985	7.2	11	N/A

Abbreviations: f: female; hDM: human dura mater; m: male; M: methionine; N/A: data not available; *PRNP*: prion protein gene; V: valine.

5.1.4. vCJD cases

The clinical features (sex, age at death, duration of illness and *PRNP* codon 129 genotype) of the 33 age-matched vCJD patients are summarised in Table 5.4. No cases of secondary vCJD transmission were included. The duration of illness ranged from 7-39mo (mean 14.4mo, ± sd 6.7mo). All cases were *PRNP* codon 129 MM genotypes (analysis performed on blood samples taken in life).

Table 5.4.

Clinical and genetic features of vCJD age-matched patients

Study ID	Sex	Age at death (years)	Duration of illness (months)	*PRNP* codon 129 genotype
vCJD1	f	29	11	MM
vCJD2	m	25	14	MM
vCJD3	f	24	25	MM
vCJD4	f	25	13	MM
vCJD5	m	25	14	MM
vCJD6	m	27	10	MM
vCJD7	m	21	39	MM
vCJD8	f	20	16	MM
vCJD9	m	26	10	MM
vCJD10	m	28	8	MM
vCJD11	m	25	14	MM
vCJD12	m	31	9	MM
vCJD13	f	33	30	MM
vCJD14	m	36	15	MM
vCJD15	m	39	11	MM
vCJD16	m	35	12	MM
vCJD17	m	39	14	MM
vCJD18	m	38	12	MM
vCJD19	f	30	10	MM
vCJD20	m	34	19	MM
vCJD21	m	34	17	MM
vCJD22	m	30	9	MM
vCJD23	f	32	8	MM
vCJD24	f	41	18	MM
vCJD25	m	41	7	MM
vCJD26	m	20	7	MM
vCJD27	m	20	11	MM
vCJD28	f	22	18	MM
vCJD29	m	26	12	MM
vCJD30	f	30	18	MM
vCJD31	m	33	11	MM
vCJD32	m	33	18	MM
vCJD33	f	35	14	MM

Abbreviations: f: female; m: male; M: methionine; *PRNP*: prion protein gene; vCJD: variant Creutzfeldt-Jakob disease

5.1.5. sCJD cases

The clinical features (sex, age at death, duration of illness and *PRNP* codon 129 genotype) of the 15 age-matched sCJD patients are summarised in Table 5.5. The duration of illness varied from 2-54mo (mean 16.8mo, ± sd 15mo). All cases had *PRNP* codon 129 genotype analysis performed on blood samples taken in life. Nine cases were *PRNP* codon 129 MM genotypes, two were codon 129 MV and four were codon 129 VV genotypes.

Table 5.5.
Clinical and genetic features of sCJD age-matched patients

Study ID	Sex	Age at death (years)	Duration of illness (months)	*PRNP* codon 129 genotype
sCJD1	f	44	5	MM
sCJD2	m	38	N/A	VV
sCJD3	m	42	10	VV
sCJD4	m	42	33	VV
sCJD5	f	20	54	MV
sCJD6	f	46	17	MM
sCJD7	m	39	23	MM
sCJD8	m	43	10	MM
sCJD9	f	41	21	MM
sCJD10	m	45	35	MM
sCJD11	m	46	7	VV
sCJD12	m	38	8	MV
sCJD13	m	45	6	MM
sCJD14	f	46	2	MM
sCJD15	f	45	4	MM

Abbreviations: f: female; m: male; M: methionine; N/A: data not available; *PRNP*: prion protein gene; sCJD: sporadic Creutzfeldt-Jakob disease; V: valine.

5.2. Neuropathology

5.2.1. hGH-iCJD

The neuropathological features were reviewed in all 35 hGH-iCJD patients. Records of the macroscopic brain examination of the brain were available in 34/35 cases. Whole brain weights were recorded in 26/35 cases and ranged from 825-1625g, the case with the lowest brain weight (hGH-iCJD19) corresponded to panencephalopathic CJD (Jansen *et al*., 2009) with severe grey matter atrophy and white matter degeneration. A plot of brain weights in relation to the duration of illness is provided in Figure 5.3, with comparable data for the hDM-iCJD cases and sCJD and vCJD controls.

No significant abnormalities in the cerebral hemispheres were recorded in 16/34 cases. Cerebral atrophy was present to a mild degree in 16/34 cases, with more severe atrophy recorded in 2/34 cases (hGH-iCJD19: aged 29y, brain weight 825g; and hGH-iCJD25: aged 30y, brain weight 1050g). Cerebellar atrophy, particularly involving the vermis, was present in 26/34 cases (Figure 5.4). Focal abnormalities included gliosis at the base of the brain relating to the site of neurosurgical excision of a craniopharyngioma (5 cases); the cerebellum in one case (hGH-iCJD3) showed a gliotic defect in the right hemisphere representing the site of resection of a pilocytic astrocytoma. Subsequent microscopic examination confirmed the macroscopic findings described above. No residual astrocytoma was identified in hGH-iCJD3, but the right cerebellar hemisphere showed gliosis and white matter degeneration, with vascular changes in keeping with previous irradiation. No residual or recurrent craniopharyngiomas were identified.

Figure 5.3.

Brain weights in hGH-iCJD and control cases in relation to the duration of illness

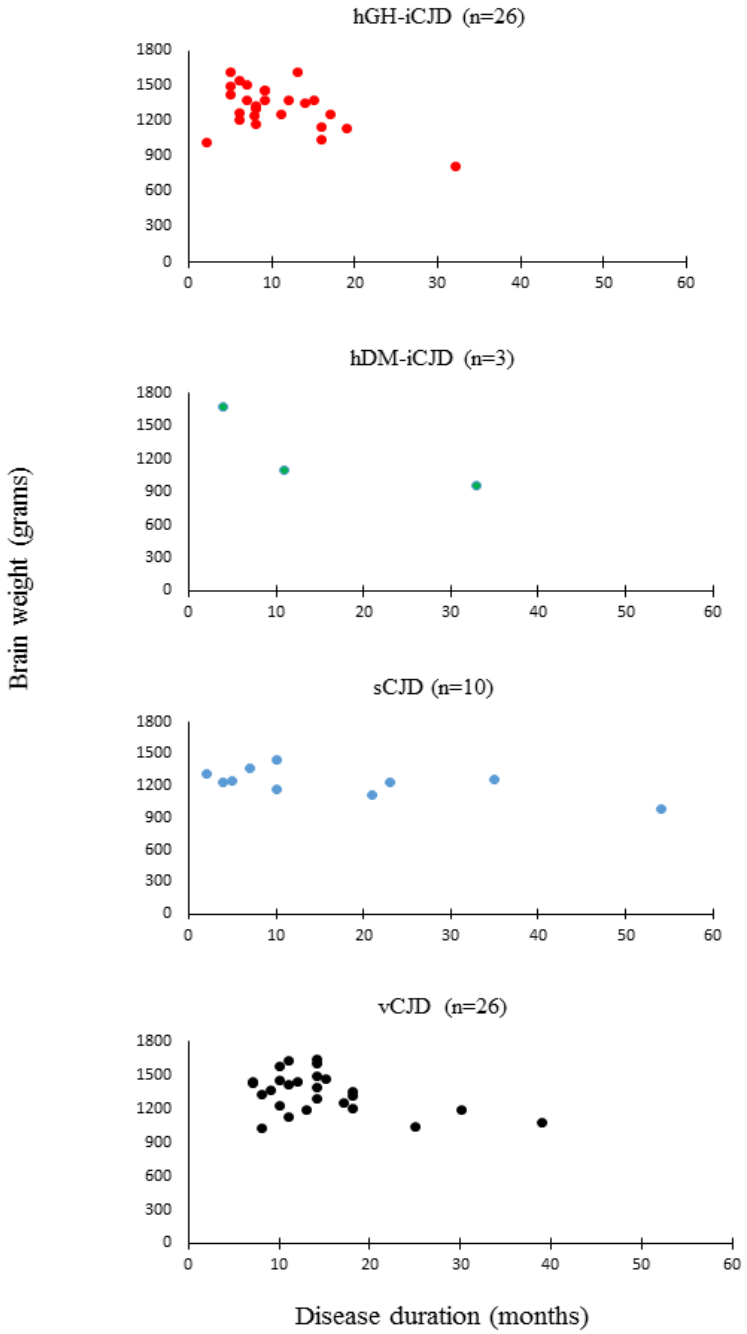

The unfixed brain weights recorded at autopsy are plotted against the disease duration for the available cases of hGH-iCJD, hDM-iCJD, sCJD controls and vCJD controls. No significant differences were found between these disease groups, but all show a trend towards a lower brain weight with increasing disease duration (adjusted R^2 test = 0.25).

Abbreviations: Abbreviations: CJD: Creutzfeldt-Jakob disease; hDM: human dura mater; hGH: human growth hormone; i: iatrogenic; s: sporadic; v: variant.

Figure 5.4.

Macroscopic cerebral and cerebellar pathology in hGH-iCJD

Macroscopic pathology in a case of hGH-iCJD (hGH-iCJD34), *PRNP* codon 129 MV, age 38y at death with a 19mo duration of illness. The cerebral hemispheres show evidence of mild atrophy of the cortex with sulcal widening. The subcortical grey matter structures are not atrophic, but the cerebellar vermis shows cortical atrophy, particularly in the superior vermis (arrow).

Abbreviations: hGH: human growth hormone; iCJD: iatrogenic Creutzfeldt-Jakob disease; M: methionine; *PRNP*: human prion protein gene; V: valine.

A widespread spongiform encephalopathy was present in all 35 cases, accompanied by variable neuronal loss and gliosis, with amyloid plaques in the cerebellum identified in 16/35 cases. The distribution, severity and nature of the spongiform change, gliosis, amyloid plaque formation and the accumulation of disease-associated prion protein on immunohistochemistry were recorded in all cases. The case with the lowest brain weight (hGH-iCJD19) exhibited status spongiosis in the cerebral cortex, with marked neuronal loss, severe gliosis and collapse of the cortical cytoarchitecture. This patient was MV at *PRNP* codon 129 and had the longest disease duration of the hGH-iCJD cases, at 32mo. A summary of the neuropathological features of each hGH-iCJD case along with the *PRNP* codon 129 genotype (where available) and PrP^{res} type (where available) is recorded in Table 5.6. In general, the distribution and nature of the pathological features in the CNS in the hGH-iCJD cases showed close similarities to those in sCJD cases with the corresponding *PRNP* codon 129 genotype, allowing a histotype to be assigned to each case (Table 5.6).

Three major histotypes were identified in relation to the established classification of subtypes of sCJD (Table 1.3 and Figure 1.5) (Parchi *et al*., 2012):

1. MV2K subtype (14 cases), with widespread spongiform change (predominantly microvacuolar) in the cerebral cortex, hippocampus, basal ganglia, thalamus and cerebellar cortex. Occasional areas of confluent spongiform change are also present in the cerebral cortex in four cases, which can be subclassified as MV2K+2C (Table 5.6). Kuru-type amyloid plaques are present in the cerebellar granular layer in all cases, but occasionally also in the

molecular layer and in the cerebral cortex. Perineuronal, plaque and plaque-like PrP deposits, particularly in the cerebellar granular and molecular layers (Figure 5.5 a-d), but also in the cerebellar white matter, basal ganglia, thalamus, hippocampus and in the cerebral cortex. One additional case for which no *PRNP* codon 129 genotype could be determined (hGH-iCJD33) had neuropathological features corresponding to the MV2K histotype.

2. VV2 subtype (11 cases), with small and medium sized vacuoles, often in a linear distribution in layer 5 of the cerebral cortex. Spongiform change is most severe in the basal ganglia and is also marked in the CA1 region of the hippocampus and the subiculum. Severe neuronal loss and gliosis is apparent in the cerebellar cortex, often resulting in cerebellar cortical atrophy. PrP immunohistochemistry shows synaptic and perineuronal deposits in the cerebral cortex in layer 5, with decoration of apical ascending dendrites (Figure 5.5 e-h). Plaque-like deposits occur in layer 3 of the cerebral cortex and in the hippocampus, basal ganglia, thalamus and cerebellar cortex, but no true amyloid plaques are present. Intense PrP labelling occurs in the cerebellar granular layer and around the neurones of the dentate nucleus. Three additional cases (hGH-iCJD29, 30 and 32) for which no *PRNP* codon 129 genotype could be determined had neuropathological features corresponding to the VV2 histotype.

3. MM/MV1 subtype (two codon 129 MM cases), with a widespread spongiform encephalopathy of microvacuolar type, most severe in the frontal and occipital

cortex. The hippocampus is relatively spared and there is variable spongiform change in the basal ganglia and medial thalamic nuclei. Patchy spongiform change occurs in the molecular layer of the cerebellar cortex, bbut no amyloid plaques are present. PrP deposition occurs in a widespread granular/synaptic pattern throughout affected grey matter regions (Figure 5.5 i-l). One additional case (hGH-iCJD25) for which no *PRNP* codon 129 genotype could be determined had neuropathological features corresponding to the MM1/MV1 histotype.

Table 5.6.

PRNP codon 129 genotype, PrP^{res} type and neuropathology in 35 hGH-iCJD cases

Study ID	*PRNP* codon 129 genotype	PrP^{res} type	Prominent neuropathological features	Histotype
*hGH-iCJD1	MV	i+2	Microvacuolation with some large confluent vacuoles; neuronal loss and gliosis most severe in the cerebellum with kuru plaques prominent in the cerebellar cortex.	MV2K+2C
hGH-iCJD2	VV	2	Microvacuolation most prominent in deeper cortical layers; PrP staining shows synaptic and perineuronal deposits with plaque-like accumulations in the cerebral and cerebellar cortex.	VV2
hGH-iCJD3	MV	i+2	Microvacuolation with synaptic and perineuronal PrP staining in all cortical layers. Kuru plaques and plaque-like accumulations prominent in the cerebral and cerebellar cortex.	MV2K
hGH-iCJD4	VV	2	Microvacuolation with some focal confluent vacuoles; PrP staining shows synaptic and perineuronal deposits with plaque-like accumulations in the cerebral and cerebellar cortex.	VV2
hGH-iCJD5	VV	2	Prominent microvacuolation with perineuronal PrP staining in addition to plaque-like accumulations in the cerebral cortex.	VV2
hGH-iCJD6	VV	2	Prominent microvacuolation with perineuronal PrP staining in addition to plaque-like accumulations in the cerebral cortex.	VV2
hGH-iCJD7	MV	i+2	Microvacuolation with some large confluent vacuoles; PrP staining shows synaptic and perineuronal PrP staining with kuru plaques and plaque-like deposits prominent in the cerebral and cerebellar cortex.	MV2K+2C
hGH-iCJD8	VV	2	Microvacuolation most prominent in deeper cortical layers with perineuronal PrP staining and numerous plaque-like deposits in the cerebral cortex.	VV2
hGH-iCJD9	MV	i+2	Microvacuolation with synaptic and perineuronal PrP staining in all cortical layers. Kuru plaques and plaque-like accumulations prominent in the cerebral and cerebellar cortex.	MV2K
hGH-iCJD10	VV	2	Prominent microvacuolation in deeper cortical layers with synaptic and perineuronal PrP staining in addition to plaque-like accumulations.	VV2
hGH-iCJD11	MV	i+2	Prominent microvacuolation with some confluent vacuolation in deeper cortical layers. Perineuronal PrP staining in addition to plaque-like accumulations. Kuru plaques prominent in the cerebellar cortex.	MV2K +2C

hGH-iCJD12	VV	2	Microvacuolation with PrP staining showing synaptic and perineuronal deposits with plaque-like accumulations in the cerebral and cerebellar cortex.	VV2
hGH-iCJD13	MV	i+2	Microvacuolation with synaptic and perineuronal PrP staining. Kuru plaques and plaque-like accumulations prominent in the cerebral and cerebellar cortex.	MV2K
hGH-iCJD14	MV	i+2	Prominent microvacuolation in deeper cortical layers with perineuronal and synaptic PrP staining in addition to plaque-like accumulations. Kuru plaques present in the cerebellar cortex.	MV2K
hGH-iCJD15	MV	i+2	Prominent microvacuolation in deeper cortical layers with perineuronal PrP staining in addition to plaque-like accumulations. Kuru plaques present in the cerebral and cerebellar cortex.	MV2K
hGH-iCJD16	MV	i+2	Prominent microvacuolation in deeper cortical layers with perineuronal PrP staining in addition to plaque-like accumulations. Kuru plaques present in the cerebral and cerebellar cortex.	MV2K
hGH-iCJD17	MV	i+2	Microvacuolation with PrP staining shows synaptic and perineuronal deposits in addition to plaque-like accumulations. Kuru plaques present in the cerebellar cortex.	MV2K
hGH-iCJD18	MV	i+2	Microvacuolation with synaptic and perineuronal PrP staining. Kuru plaques and plaque-like accumulations prominent in the cerebral and cerebellar cortex.	MV2K
hGH-iCJD19	MV	i+2	Status spongiosis with collapse of cerebral architecture. Synaptic PrP staining with plaque-like accumulations. Kuru plaques present in the cerebellar cortex.	MV2K
hGH-iCJD20	MM	i	Microvacuolation with some large confluent vacuoles; PrP staining shows synaptic and perineuronal deposits in addition to plaque-like accumulations. Kuru plaques present in the cerebral and cerebellar cortex.	Atypical – resembles MV2K+2C
hGH-iCJD21	MM	1	Microvacuolation with synaptic PrP staining in cerebral and cerebellar cortex.	MM1
hGH-iCJD22	VV	N/A	Microvacuolation most prominent in deeper cortical layers; PrP staining shows perineuronal deposits with plaque-like accumulations in the cerebral and cerebellar cortex.	Resembles VV2
hGH-iCJD23	VV	N/A	Microvacuolation with PrP staining showing synaptic and perineuronal deposits with plaque-like accumulations in the cerebral and cerebellar cortex.	Resembles VV2
hGH-iCJD24	MV	N/A	Microvacuolation with PrP staining showing synaptic and perineuronal PrP staining with kuru plaques and plaque-like accumulations prominent in the cerebral and cerebellar cortex.	Resembles MV2K

hGH-iCJD25	N/A	N/A	Status spongiosis with collapse of cerebral architecture. Severe neuronal loss and gliosis; PrP staining shows coarse synaptic accumulations.	Resembles MM/MV1
hGH-iCJD26	VV	N/A	Prominent microvacuolation in deeper cortical layers with synaptic and perineuronal PrP staining in addition to plaque-like accumulations.	Resembles VV2
hGH-iCJD27	VV	N/A	Microvacuolation with PrP staining showing synaptic and perineuronal deposits with a few plaque-like accumulations in the cerebellar cortex cortex.	Resembles VV2
hGH-iCJD28	MV	N/A	Microvacuolation with little confluent vacuolation. PrP staining shows synaptic and perineuronal deposits with a few plaque-like accumulations in the cerebral cortex.	Resembles MV2C
hGH-iCJD29	N/A	N/A	Microvacuolation with PrP staining showing weak perineuronal deposits.	Resembles VV2
hGH-iCJD30	N/A	N/A	Microvacuolation with PrP staining showing synaptic and perineuronal deposits with plaque-like accumulations in the cerebral and cerebellar cortex. cortex	Resembles VV2
hGH-iCJD31	*MM	N/A	Prominent microvacuolation in deeper cortical layers with synaptic and perineuronal PrP staining in addition to plaque-like accumulations.	Atypical: some VV2-like features
hGH-iCJD32	N/A	N/A	Prominent microvacuolation in deeper cortical layers with synaptic and perineuronal PrP staining in addition to plaque-like accumulations.	Resembles VV2
hGH-iCJD33	N/A	N/A	Mild microvacuolation with synaptic and perineuronal PrP staining with kuru plaques and plaque-like deposits prominent in the cerebral and cerebellar cortex.	Resembles MV2K
hGH-iCJD34	MV	N/A	Microvacuolation with some confluent vacuoles. Synaptic and perineuronal PrP labelling. Kuru plaques and plaque-like accumulations in the cerebral and cerebellar cortex.	MV2K+2C
hGH-iCJD35	MM	N/A	Severe microvacuolation with synaptic PrP staining in cerebral and cerebellar cortex.	MM1
*hDM-iCJD1	MM	1	Microvacuolation most marked in the cerebral cortex with relatively little cerebellar pathology.	Resembles MM1
hDM-iCJD2	MM	1	Status spongiosis with collapse of cerebral architecture. Synaptic PrP staining in cerebral and cerebellar cortex.	MM1
hDM-iCJD3	MM	1	Microvacuolation with synaptic PrP staining in cerebral and cerebellar cortex.	MM1
hDM-iCJD4	N/A	N/A	Prominent microvacuolation in deeper cortical layers with synaptic and perineuronal PrP staining in addition to plaque-like accumulations.	Resembles VV2
hDM-iCJD5	N/A	N/A	Status spongiosis with collapse of cerebral architecture. Synaptic PrP staining in cerebral and cerebellar cortex.	Resembles MM1

N/A- PrP^{res} type information not available as no frozen CNS material for analysis
* Fixed tissue not available for PrP immunohistochemical analysis
Abbreviations: C: cortical; CNS: central nervous system; hDM: human dura mater; hGH: human growth hormone; iCJD: iatrogenic Creutzfeldt-Jakob disease; K: kuru plaques; M: methionine; *PRNP*: prion protein gene; V: valine.

Figure 5.5. Typical neuropathological phenotypes in hGH-iCJD cases

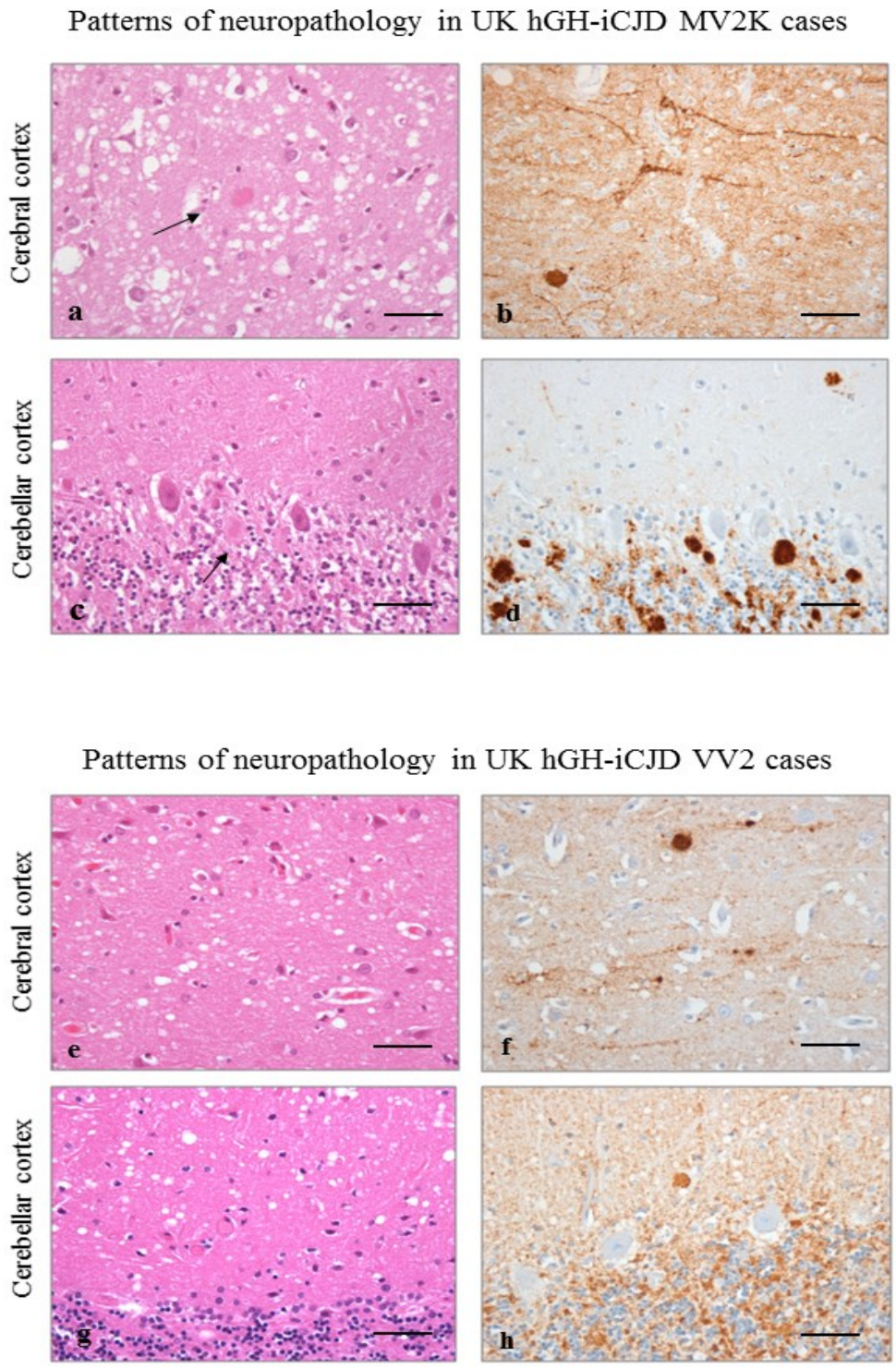

Figure 5.5. Typical neuropathological phenotypes in hGH-iCJD (continued)

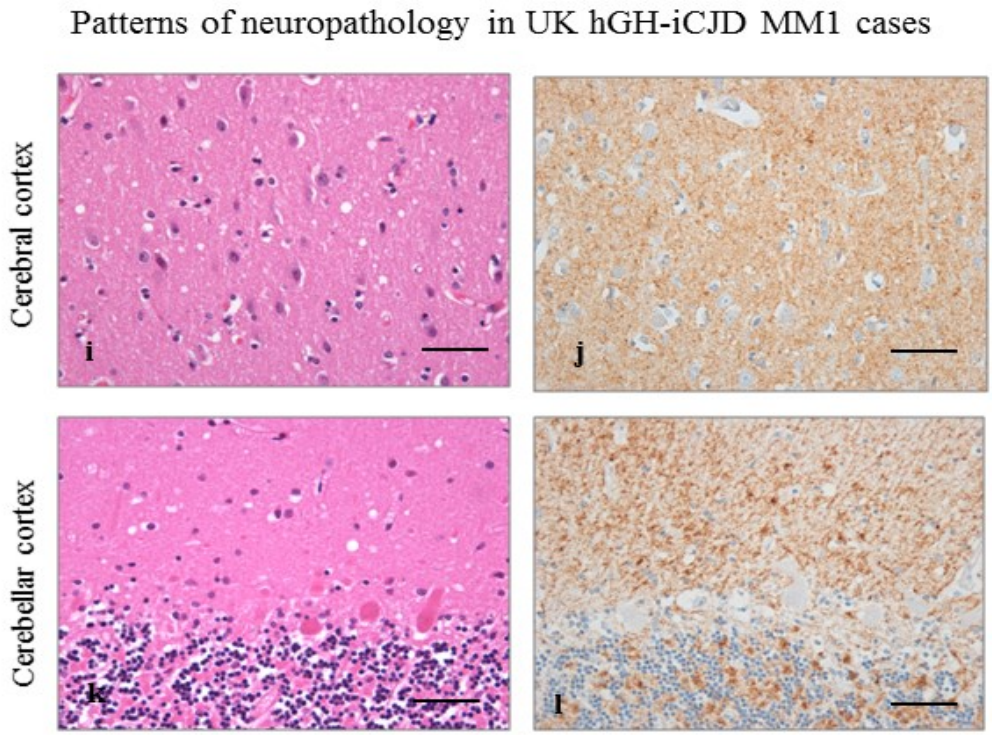

PRNP codon 129 MV hGH-iCJD cases show spongiform vacuoles of varying size, with occasional cortical kuru plaques (arrow). Coarse granular and perineuronal PrP staining in the cerebral cortex, with more intense staining of the kuru plaques (a,b). Kuru plaques are a more prominent feature in the cerebellar cortex (arrow), along with coarse granular PrP staining in the molecular layer (c,d). *PRNP* codon 129 VV hGH-iCJD cases show microvacuolation with a combination of synaptic, perineuronal and plaque-like accumulations of PrP in the cerebral and cerebellar cortex (e-h). *PRNP* codon 129 MM hGH-iCJD cases show widespread microvacuolation with a predominantly synaptic accumulation of PrP in the cerebral and cerebellar cortex (i-l). (Sections a, c, e, g, i and k are stained with haematoxylin and eosin and sections b, d, f, h, j, and l are stained by immunohistochemistry for PrP using the KG9 antibody). Scale bar=250μm.

Abbreviations: CJD: Creutzfeldt-Jakob disease; hGH: human growth hormone; i: iatrogenic; K; kuru plaque; M: methionine; *PRNP*: prion protein gene; PrP: prion protein; UK: United Kingdom; V: valine.

5.2.1.1. *Atypical neuropathological phenotypes in hGH-iCJD*

Two hGH-iCJD *PRNP* codon 129 MM cases (hGH-iCJD20 and hGH-iCJD31), exhibited neuropathological phenotypes that did not correspond to those described by Parchi *et al.* (Parchi *et al*., 1999) in sCJD cases with *PRNP* codon 129 MM. Case hGH-iCJD20 contained a mixture of both microvacuolar and confluent spongiform change in the cerebral cortex, particularly in layers 5-6, hippocampus and basal ganglia, with lesser involvement of the thalamus and cerebellum (Figure 5.6 a,c). PrP IHC showed a combination of synaptic, perineuronal and perivacuolar PrP deposits in a widespread distribution, with plaque-like deposits and kuru plaques in the cerebral and cerebellar cortex (Figure 5.6 b,d). These features most closely resemble the sCJD MV2K +C histotype (Parchi *et al*., 2012).

Case hGH-iCJD31 showed some similar features to hGH-iCJD20, with predominantly microvacuolar spongiform change in the cerebral cortex, particularly in layers 5-6, hippocampus and basal ganglia. The thalamus and cerebellum showed less spongiform change, but no kuru-type plaques were identified in the cerebellum (Figure 5.6 e,g). PrP immunohistochemistry showed a combination of synaptic, perineuronal and plaque-like PrP deposits in a widespread distribution, including the cerebral and cerebellar cortex, basal ganglia, hippocampus and thalamus. An occasional plaque-like deposit was present in the parietal cortex, with intense labelling on PrP immunohistochemistry. (Figure 5.6 f,h). This phenotype was distinct from both the MM/MV1-like phenotype and the MV2-like phenotype in hGH-iCJD, and from MM1 and MV2 cases of sCJD. However, there are some similarities to the VV2 phenotype in both sCJD and hGH-iCJD.

Figure 5.6. Atypical neuropathological phenotypes in hGH-iCJD MM cases

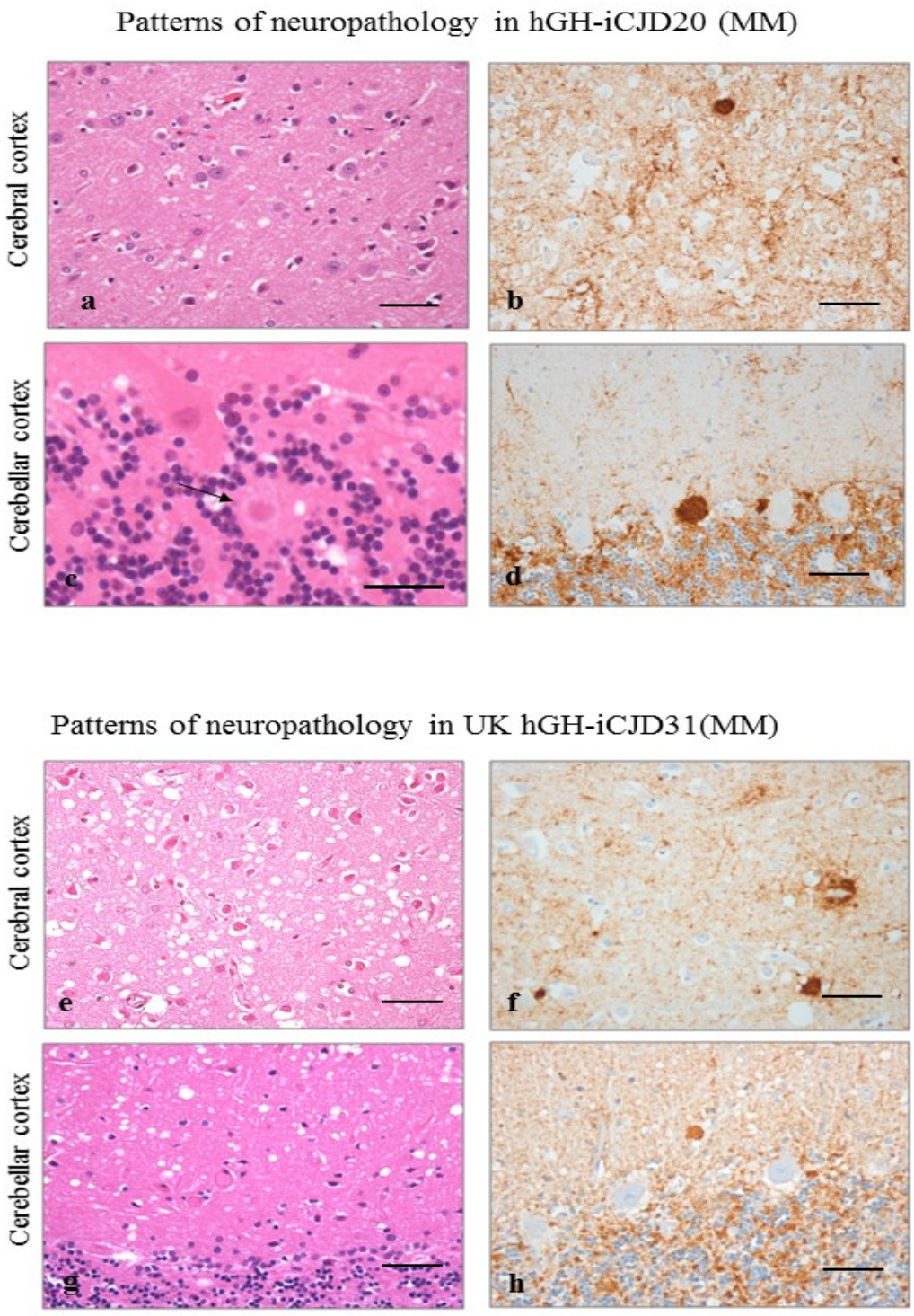

Legend to Figure 5.6.

Both cases have atypical neuropathological features in comparison with the codon 129 MM hGH-iCJD cases in Figure 5.5 i-l. Case hGH-iCJD20 has a mixture of microvacuolar and confluent vacuolation and occasional large PrP positive kuru plaques in the cerebral cortex (a,b). Kuru plaques (arrow) are also present in the cerebellum, with dense PrP labelling and coarse PrP positivity in the granular layer (c,d), resembling the MV2K+C histotype. Case hGH-iCJD31 has microvacuolation in the lower layers of the cerebral cortex and in the cerebellar cortex (e,g), with a combination of synaptic, perineuronal and plaque-like accumulations of PrP in the cerebral and cerebellar cortex (f,h). No kuru-type amyloid plaques were present in any brain region. These features show some similarities to the VV2 histotype in sCJD. (Sections a, c, e, and g, are stained with haematoxylin and eosin and sections b, d, f, and h are stained by immunohistochemistry for PrP using the KG9 antibody).

Scale bar=250μm.

Abbreviations: CJD: Creutzfeldt-Jakob disease; hGH: human growth hormone; i: iatrogenic; K; kuru plaque; M: methionine; *PRNP*: prion protein gene; PrP: prion protein; UK: United Kingdom; s: sporadic; V: valine.

5.2.2 hGH control cases

Most (10/12) of the hGH-control cases were not examined initially in NCJDRSU. Records of the macroscopic pathology are available for 9/12 cases, although most of these are incomplete. The brain weights varied from 1042-1640g; the lowest weight occurred in a 24 year-old patient with a recurrent craniopharyngioma (case hGH-control5). Craniopharyngiomas had also been resected in four other patients, two of whom (hGH-control2 and hGH-control5) had recurrent craniopharyngiomas at the time of death. No residual ependymoma was present in the gliotic cerebellum in a patient (hGH-control10) who had undergone neurosurgical resection with post-operative radiotherapy. However, a recurrent pilocytic astrocytoma was identified in the 3rd ventricle in patient hGH-control1, who had undergone neurosurgical resection.

The microscopic neuropathology ranged from no significant abnormalities (two cases with idiopathic panhypopituitarism, and single cases of idiopathic growth hormone deficiency, mitochondrial cytopathy and the Prader-Willi syndrome) to focal abnormalities with tissue disruption and gliosis in cases with resected neoplasms. The presence of recurrent craniopharyngiomas in hGH-controls 2 and 5, and a recurrent pilocytic astrocytoma in hGH-control1 was confirmed. No recurrent ependymoma was identified in hGH-control10, but the cerebellum showed white matter degeneration with macrophage infiltration and vascular changes in keeping with previous radiotherapy. A small focus of neuronal loss with gliosis was also present in the right inferior temporal cortex. No evidence of a spongiform encephalopathy or prion protein immunoreactivity was found in any of the hGH control cases.

5.2.3 hDM-iCJD cases

Records of the macroscopic pathology are available for 3/5 cases. The brain weights varied from 958-1675g, with the lowest weight recorded in hDM-iCJD2, who had the longest duration of illness (33mo). This case showed severe cerebral and cerebellar atrophy, corresponding to panencephalopathic CJD (Figure 5.6 a-d). The three hDM-iCJD cases with frozen tissue available and *PRNP* genotype data all showed microscopic features in keeping with the MM1 histotype (Figure 5.7 e,h). Of the two cases with no frozen tissue available, hDM-iCJD5 also showed the features of the MM/MV1 histotype, while hDM-iCJD4 resembled the VV2 histotype. Kuru-type amyloid plaques were not observed in any hDM-iCJD cases (Table 5.6).

Figure 5.7. Neuropathological phenotypes in hDM-iCJD MM cases

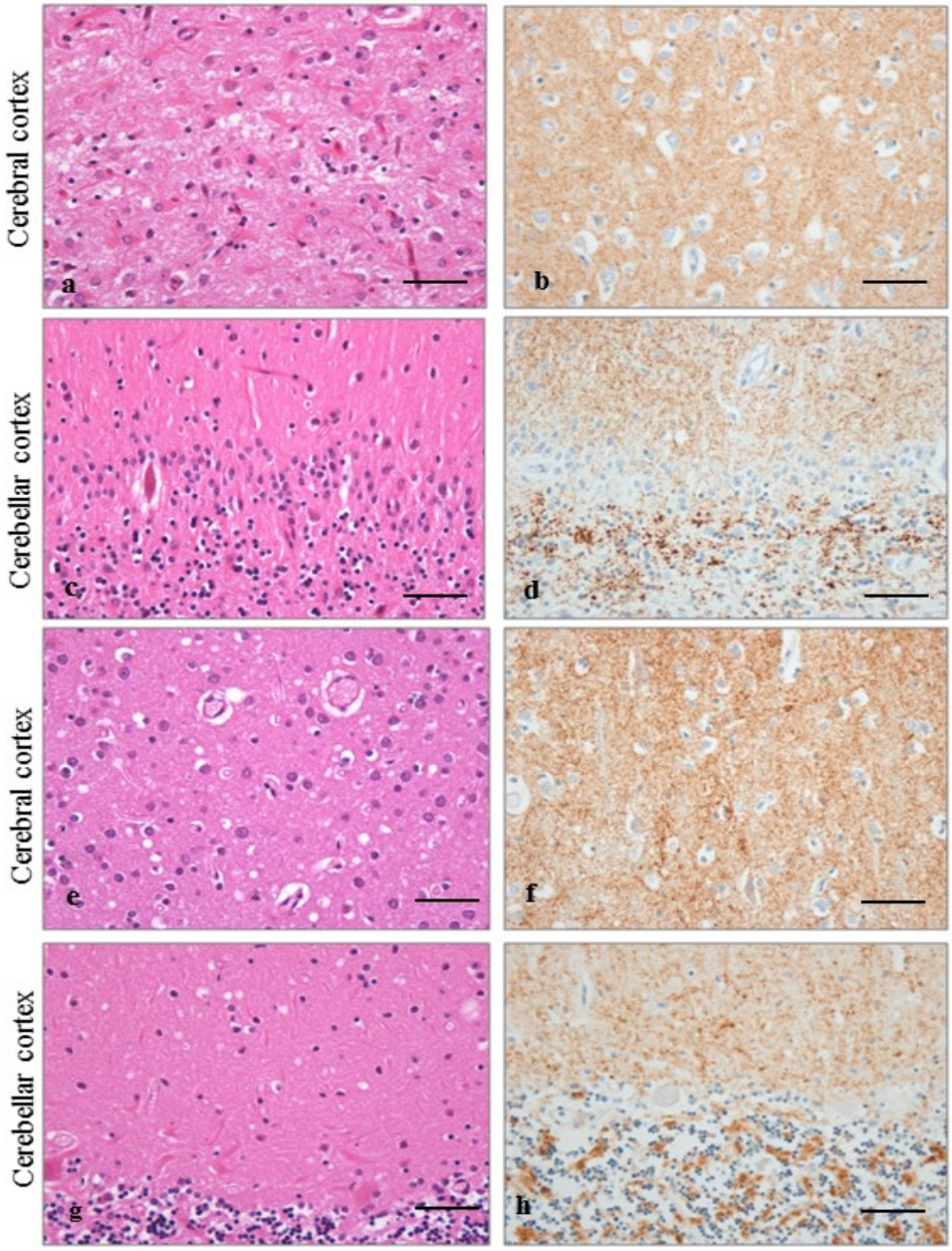

PRNP codon 129 MM hDM-iCJD2 shows severe cerebral and cerebellar neuronal loss and gliosis in keeping with panencephalopathic CJD, with a predominantly synaptic accumulation of PrP in the cerebral and cerebellar cortex (a- d). The other codon 129 MM hDM-iCJD cases have less severe neuronal loss and gliosis and show microvacuolar spongiform change with granular/synaptic PrP accumulation, resembling the sCJD MM1 histotype (e-h). (Sections a, c, e, and g, are stained with haematoxylin and eosin and sections b, d, f, and h are stained by immunohistochemistry for PrP using the KG9 antibody). Scale bar=250µm.

Abbreviations: CJD: Creutzfeldt-Jakob disease; hDM: human dura mater; i: iatrogenic; M: methionine; *PRNP*: prion protein gene; PrP: prion protein; UK: United Kingdom.

5.3. Co-pathology

5.3.1. Aβ pathology in hGH-iCJD

Aβ was detected as cerebral amyloid angiopathy (CAA) and/or CNS parenchymal deposits by IHC in 18/33 hGH-iCJD cases with sufficient paraffin-embedded tissue for analysis. 6/18 Aβ positive cases had CAA alone, 4/18 had parenchymal deposits without CAA and 8/18 had both CAA and parenchymal deposits (Figure 5.8). All cases with parenchymal deposits contained diffuse (immature) plaques. Variable numbers of cored plaques, some with a surrounding corona of diffuse Aβ, were detected by Aβ IHC. Neuritic plaques were identified with the Bielschowsky silver stain in five cases (Figure 5.9 a-d). Patchy diffuse subpial Aβ deposits were also present in five cases (Figure 5.9 g,h), but other forms of diffuse Aβ (such as lake-like or fleecy deposits) were absent. No Aβ deposits were identified in the entorhinal cortex, hippocampus, basal ganglia, thalamus, brain stem, cerebellum, spinal cord or white matter. Two cases had diffuse Aβ plaques in the anterior cingulate gyrus in addition to the neocortex, but the full Thal phase 2 distribution of Aβ deposits was absent e.g. in the entorhinal cortex and hippocampus. These were therefore recorded as Thal phase 1* in the ABC scores (see Table 5.7), as recently reported in hDM-iCJD cases (Kovacs *et al*., 2016a).

Focal Aβ deposits (diffuse and cored plaques, neuritic plaques and subpial deposits) occurred in the cerebral cortex in an unpredictable and varied distribution, either singly or in clusters, in one or more cortical regions. No evidence of a selective laminar distribution of plaques was found and no areas of pancortical involvement were identified. The plaque frequency varied from occasional diffuse grey mater plaques to more numerous diffuse and neuritic plaques (up to CERAD score 2). The neurites

around the cored plaques were relatively sparse on IHC with the AT8 antibody (Figure 5.10a). However, ubiquitin IHC showed more widespread neurites (Figure 5.10b). Reactive astrocytes surrounded the cored/neuritic plaques with extensive processes and microglial cells were present in both the plaque cores and the periphery (Figure 5.10 c,d). No neurofibrillary tangles were identified in the cortical regions with neuritic plaques or in any other brain regions with the Bielschowsky silver stain and tau IHC.

CAA varied from occasional focal Aβ deposits in meningeal vessel walls to more extensive circumferential deposition in meningeal and intraparenchymal vessels, with variable perivascular Aβ accumulation (Figure 5.11 a-d). None of the cases showed vasculopathy related to CAA. Case hGH-iCJD18 displayed sparse capillary CAA in addition to parenchymal and meningeal CAA. CAA was present most often in the occipital meningeal vessels and occipital cortex, but occasional cases had isolated CAA in the parietal or frontal cortex. A single case also had CAA in the cerebellar meningeal vessels, with no cerebellar parenchymal involvement (Figure 5.11c). CAA was absent in the hippocampus, basal ganglia, thalamus or brain stem in all cases.

Immunohistochemistry for Aβ 1-40 showed preferential labelling of CAA and plaque cores, while the Aβ1-42 antibody showed more labelling of diffuse Aβ deposits in the subpial region, diffuse plaques and the diffuse corona around some cored plaques (Figure 5.11 e,f). Capillary CAA lesions labelled with the antibody to Aβ 1-42, with less intense labelling with the Aβ 1-40 antibody. Perivascular diffuse Aβ deposits were present in the cases with most widespread intraparenchymal CAA (Figure 5.11d), with some dyshoric vessels identified.

Figure 5.8.

Frequency of Aβ accumulation in hGH-iCJD and control cases

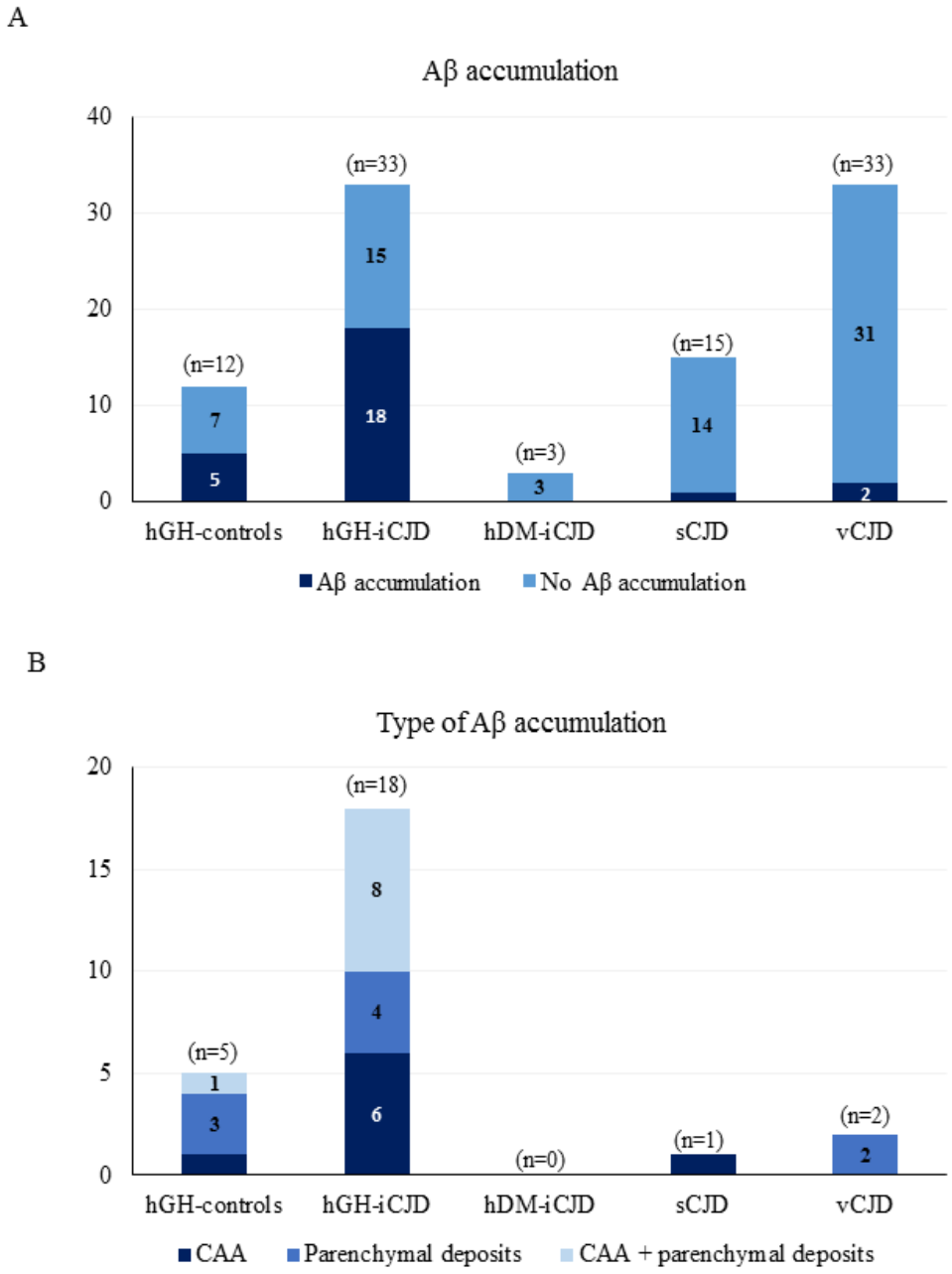

There is a significant difference in the percentage of cases with CNS Aβ deposition in the two groups treated with hGH (51%) compared to the three groups not treated with hGH (6%); $p<0.001$ (Fisher's exact test). Comparison of the hGH-iCJD, hGH control and non hGH-treated groups confirms the association between CNS Aβ accumulation and hGH treatment; $p<0.001$ (Chi-squared test).

Abbreviations: Aβ: amyloid beta; CAA: cerebral amyloid angiopathy; CNS: central nervous system; CJD: Creutzfeldt-Jakob disease; hGH: human growth hormone; i: iatrogenic; s: sporadic; v: variant

Figure 5.9. CNS Aβ deposition in hGH-iCJD cases

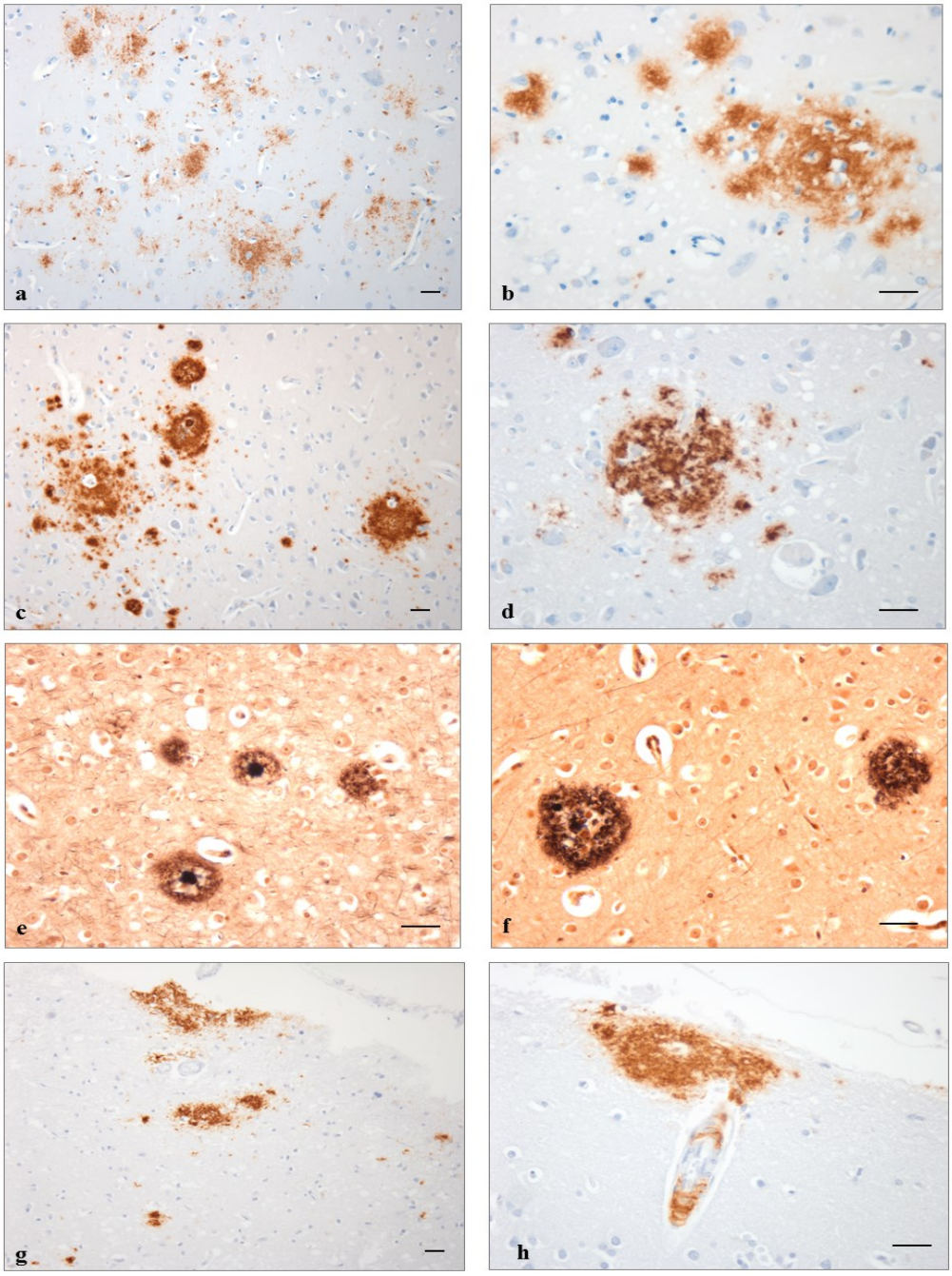

Aβ IHC (6F/3D antibody) (a-d, g,h) and Bielschowsky silver stain (e,f) showing the range of Aβ plaques in hGH-iCJD cases. Diffuse plaques (a,b) were a feature of all hGH-iCJD cases in which CNS Aβ deposition was observed. Cored plaques were less frequently observed following Aβ immunohistochemistry (c,d). Neuritic plaques were demonstrated with the Bielschowsky silver stain in 5 cases (e,f). Patchy diffuse subpial Aβ deposits (g,h) were also identified in 5 cases by IHC. Scale bar=250µm.

Abbreviations: Aβ: amyloid beta; CJD: Creutzfeldt-Jakob disease; hGH: human growth hormone; i: iatrogenic; IHC: immunohistochemistry.

Figure 5.10 Aβ plaque reactions in hGH-iCJD cases

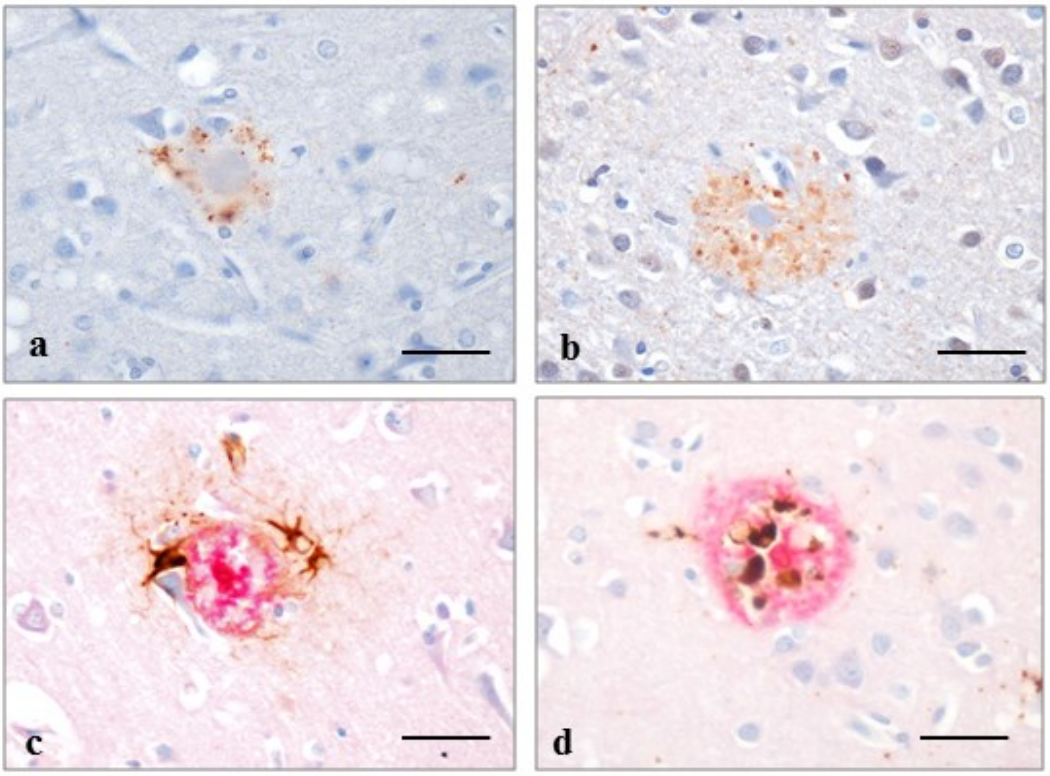

The AT8 anti-tau antibody labels sparse neurites around a cored Aβ plaque (a). The ubiquitin antibody labels extensive neurites around a cored Aβ plaque (b). Reactive astrocytes around a cored Aβ plaque revealed on double IHC for Aβ (6F/3D antibody-red) and GFAP (GFAP antibody-brown) (c). Double IHC for Aβ (6 F/3D antibody-red) and CD 68 (PGM1 antibody-brown) shows microglial cells around and within a cored Aβ plaque (d). Scale bar=250µm.

Abbreviations: Aβ: amyloid beta; CJD: Creutzfeldt-Jakob disease; GFAP: glial fibrillary acidic protein; hGH; human growth hormone; i: iatrogenic; IHC: immunohistochemistry.

Figure 5.11. CAA in hGH-iCJD cases

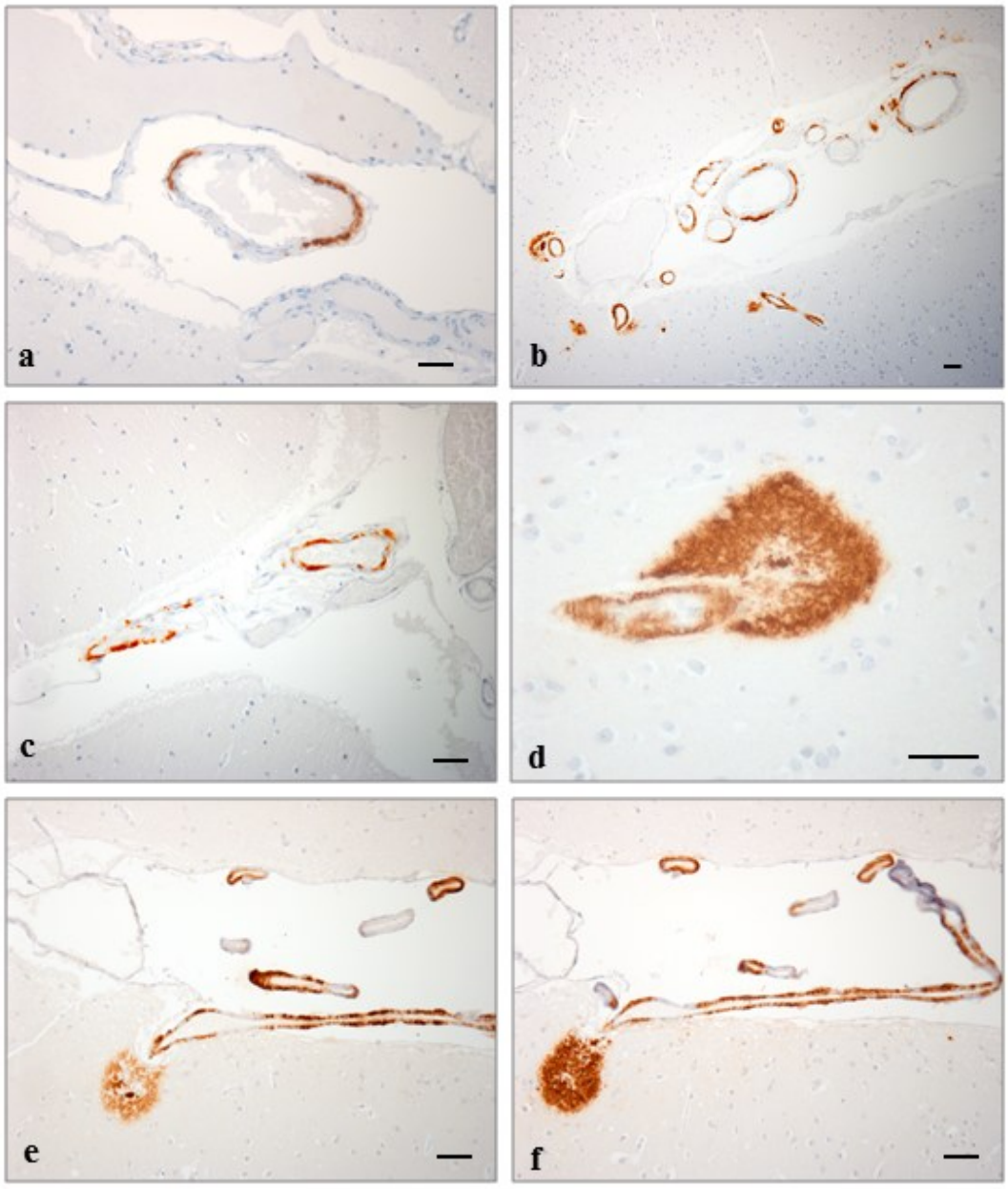

Patchy deposition of Aβ in the wall of a meningeal vessel (a). More extensive Aβ deposition in occipital vessels of varying size in the meninges and adjacent cortex (b). Patchy Aβ deposition in the wall of meningeal vessels overlying the cerebellar cortex (c). Circumferential deposition in a cortical arteriole with extensive perivascular Aβ forming a cored plaque-like structure (d). (f). IHC with Aβ 1-40 (e) and 1-42 (f) antibodies on adjacent sections. The 1-40 antibody shows intense labelling of vessels and plaque cores, while the 1-42 antibody shows intense labelling of a large diffuse Aβ deposit. Scale bar=250µm. The 6F/3D anti-Aβ antibody was used in a-d.

Abbreviations: Aβ: amyloid beta; CAA: cerebral amyloid angiopathy; CJD: Creutzfeldt-Jakob disease; hGH; human growth hormone; i: iatrogenic; IHC: immunohistochemistry.

5.3.2 Aβ pathology in control cases

5.3.2.1 *hGH controls*

Similar patterns of CNS Aβ accumulation were identified in 5/12 hGH control cases, with 3/5 cases containing parenchymal Aβ deposits only, and a single case with meningeal and intraparenchymal CAA, but no parenchymal deposits or capillary CAA (Figure 5.12 a,b). The remaining case had extensive meningeal and intraparenchymal CAA with capillary CAA and widespread diffuse and neuritic cerebral cortical plaques with scanty neurites (up to CERAD score 2), and patchy subpial Aβ deposits (Figure 5.12 c-d). Dyshoric CAA vessels were also present and occasional Aβ-laden vessels exhibited splitting of the vessel wall (Figure 5.12 e-g). The distribution of these lesions was very similar to those in the hGH-iCJD cases, with no plaques or CAA identified in the entorhinal region, hippocampus, basal ganglia, thalamus, brain stem, cerebellum or spinal cord in any of the cases examined. Two cases were scored as Thal phase 1* (see section 5.3.1 above).

Immunohistochemistry for Aβ1-40 and Aβ-42 gave similar results to the hGH-iCJD cases (Figure 5.12h). No neurofibrillary tangles were identified on the Bielschowsky silver stain or tau IHC in relation to the Aβ pathology. However, numerous tau-positive neurites were identified around cored Aβ plaques and around Aβ deposits surrounding intraparenchymal blood vessels (Figure 5.13 a,b). Reactive astrocytes and microglial cells were also identified around and within the cored Aβ plaques (Figure 5.13 c,d).

5.3.2.2. *hDM-iCJD cases*

No Aβ labelling was identified in either the CNS parenchyma or blood vessels (Figure 5.7). This may reflect the periods of survival following dura mater graft surgery; all died within 20y of surgery, while all the hDM-iCJD cases with CNS Aβ accumulation reported by Frontzek *et al*. (Frontzek *et al*., 2015) had survived surgery for over 20 y.

5.3.2.3. *vCJD control cases*

Two vCJD cases (vCJD22 and vCJD32) showed occasional diffuse Aβ plaques in the occipital and parietal cortex (Figure 5.13 f,g). The Aβ deposits appeared to co-localise with the PrP amyloid in some florid plaques, but double IHC with antibodies to Aβ and PrP showed some separation of the diffuse deposits (Figure 5.13g). No cored or neuritic Aβ plaques were identified and no meningeal or parenchymal CAA was present. No Aβ deposits were present in any subcortical grey matter regions.

5.3.2.4. *sCJD control cases*

A single sCJD control case (sCJD14) showed focal Aβ deposits in the walls of occasional small to medium sized meningeal blood vessels over the occipital and temporal lobes and in the superficial occipital cortex (Figure 5.13h), with very few vessels exhibiting circumferential deposition. No Aβ deposits were found in the cerebral cortex or any subcortical grey matter regions.

The results of the ABC and CAA scores for the hGH control, vCJD and sCJD cases are summarised in Table 5.7.

Figure 5.12. Aβ deposits and CAA in hGH control cases

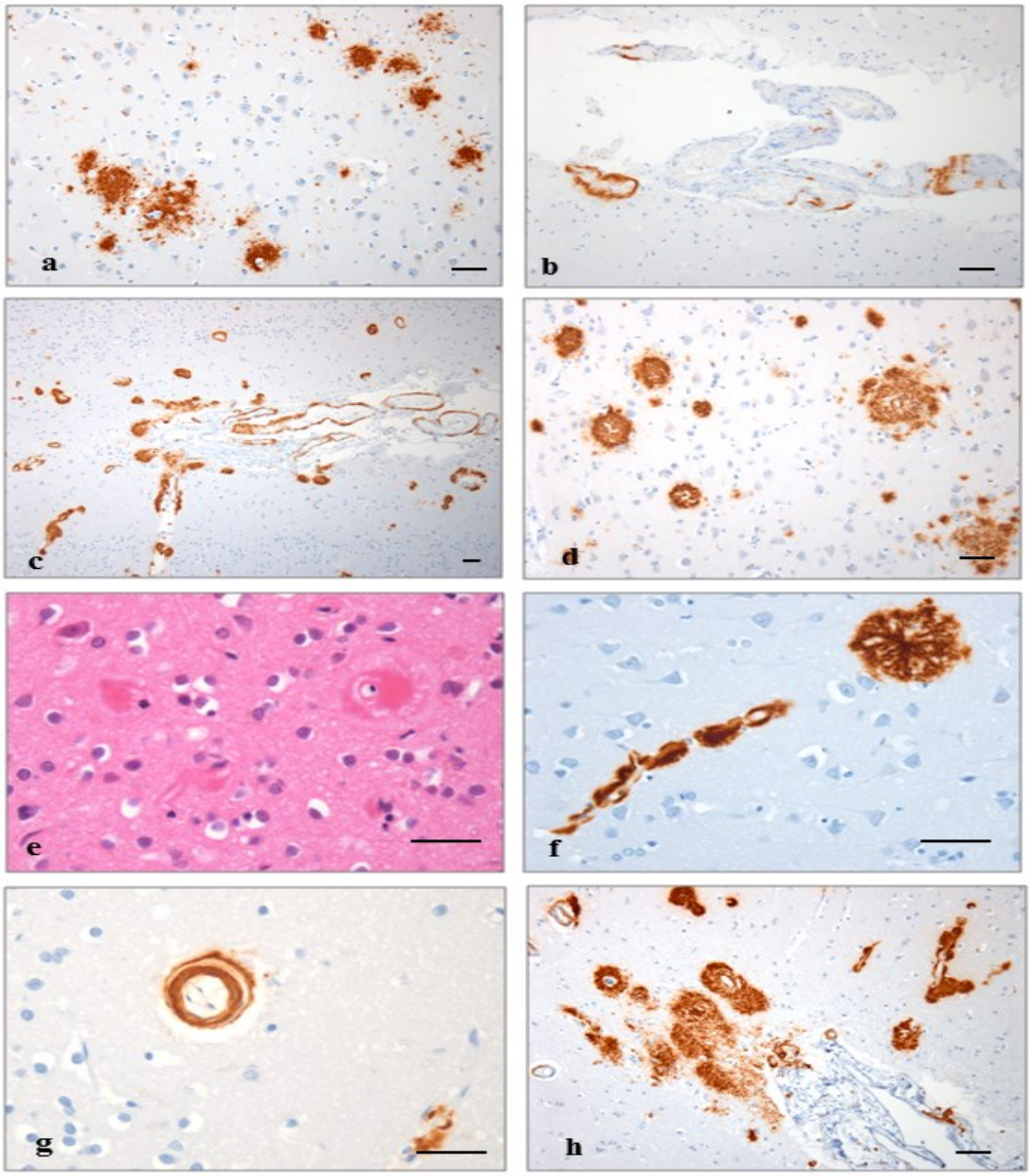

Diffuse Aβ deposits and plaques in the frontal cortex (a). CAA with patchy meningeal deposits and circumferential deposition in a superficial cortical vessel (b). Extensive CAA in meninges and cortex with diffuse and perivascular Aβ deposits (c). Multiple cored plaques and smaller diffuse Aβ deposits. Severe capillary CAA with marked thickening of vessel walls (e). A dyshoric cortical vessel and an adjacent cored plaque (f). Vasculopathy with splitting of an intracortical arteriole wall (g). Meningeal and intracortical CAA with diffuse subpial deposits, perivascular deposits and diffuse and cored Aβ plaques. Scale bar=250µm. The 6F/3D antibody was used for Aβ IHC in a-d and f-h.

Abbreviations: Aβ: amyloid beta; CAA: cerebral amyloid angiopathy; CJD: Creutzfeldt-Jakob disease; hGH; human growth hormone; i: iatrogenic; IHC: immunohistochemistry.

Figure 5.13. Aβ pathology in hGH control, vCJD and sCJD cases

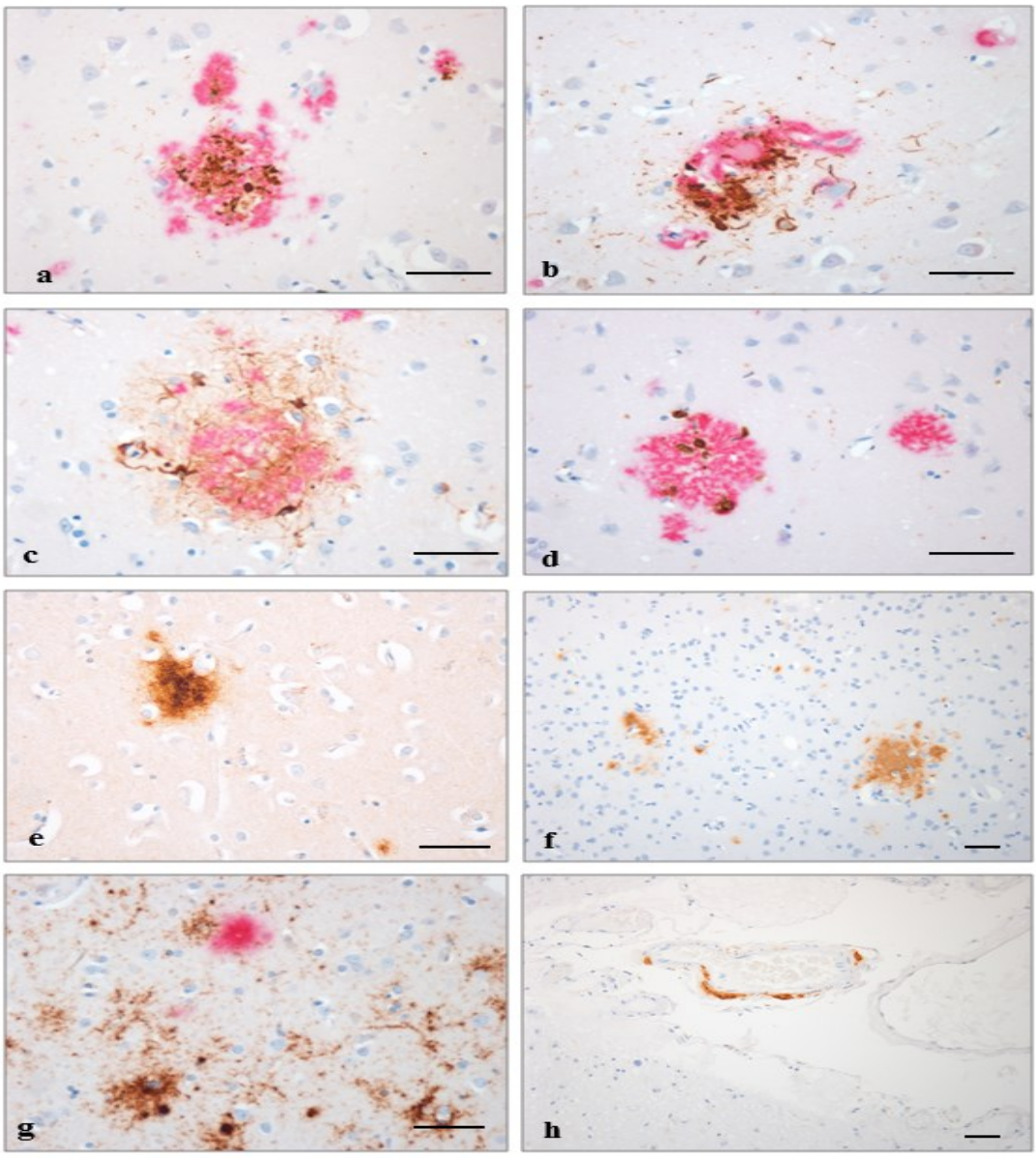

Tau positivity (brown) in neurites around Aβ (red) in (a) a cored plaque (b) a dyshoric vessel with CAA (b) in hGH control11. Astrocytes (brown) surround a cored Aβ plaque (red) (c) and microglial cells (brown) are present within a cored Aβ plaque (red) in a hGH control10 (d). apoE-4 positivity in diffuse Aβ deposits in hGH control6 (e). Diffuse Aβ deposits in the parietal cortex in vCJD22 (f). The diffuse cortical Aβ deposits in vCJD 37 (red) do not all colocalise with the abundant PrP deposits (brown) (g). Patchy localised meningeal CAA in the occipital region in sCJD14 (h). Scale bar=250µm.

Antibodies used for IHC: 6F/3D (Aβ): a-d, f-h; AT8 (tau): a,b; GFAP: c; CD 68: d; 5A9 (apoE-4): e; KG9 (PrP): g.

Abbreviations: Aβ: amyloid beta; CAA: cerebral amyloid angiopathy; CJD: Creutzfeldt-Jakob disease; hGH; human growth hormone; i: iatrogenic; IHC: immunohistochemistry.

Table 5.7.
ABC scores for Alzheimer pathology and CAA scores for hGH-iCJD, hGH control, sCJD and vCJD cases

Study ID	ABC score (Hyman *et al*., 2012)			Hybrid protocol (from Love *et al*., 2014)			
	A	B	C	Parenchymal CAA	Meningeal CAA	Capillary CAA	Vasculo -pathy
hGH-iCJD 4	1	0	0	0	0	0	0
hGH-iCJD 5	0	0	0	0	1	0	0
hGH-iCJD 6	0	0	0	1	2	0	0
hGH-iCJD 8	0	0	0	2	2	0	0
hGH-iCJD 9	0	0	0	1	2	0	0
hGH-iCJD 10	1	0	1	2	2	0	0
hGH-iCJD 12	1	0	0	0	0	0	0
hGH-iCJD 15	1	0	0	2	2	0	0
hGH-iCJD 16	1	0	2	1	2	0	0
hGH-iCJD 18	1*	0	2	2	2	1	0
hGH-iCJD 19	1	0	0	2	2	0	0
hGH-iCJD 26	0	0	0	0	1	0	0
hGH-iCJD 29	0	0	0	2	2	0	0
hGH-iCJD 31	1	0	1	1	2	0	0
hGH-iCJD 32	1	0	1	2	3	0	0
hGH-iCJD 33	1	0	0	2	2	0	0
hGH-iCJD 34	1	0	0	0	0	0	0
hGH-iCJD 35	1*	0	0	0	0	0	0
hGH-control6	1 *	0	0	0	0	0	0
hGH-control7	1	0	0	0	0	0	0
hGH-control9	0	0	0	2	2	0	0
hGH-control10	1	0	0	0	0	0	0
hGH-control11	1*	0	2	3	3	1	1
sCJD14	0	0	0	1	2	0	0
vCJD22	1	0	0	0	0	0	0
vCJD32	0	0	0	0	0	0	0

1*: Thal phase 1 with anterior cingulate gyrus involvement, but not the entorhinal cortex, insular cortex or hippocampus.

Abbreviations: A: Thal phase score; B; Braak stage score; C: CERAD score; CAA: cerebral amyloid angiopathy; CJD; Creutzfeldt-Jakob disease; hGH: human growth hormone; i: iatrogenic; s: sporadic; v:variant.

5.3.3. Tau pathology

Tau immunolabelling was present in all cases of hGH-iCJD, hDM-iCJD, sCJD and vCJD cases in the form of small neuritic dots in the neuropil in affected grey matter regions as previously described (Kovacs *et al*., 2016b). Additional labelling of fine neuritic processes was noted around PrP amyloid plaques, including kuru-type plaques in the hGH-iCJD cases and sCJD controls, and florid plaques in the vCJD controls (Figure 5.14 a,b). No neurofibrillary tangles, pretangles or other structures were labelled by the AT8 antibody or the Bielschowsky silver stain in the brain stem, entorhinal region, hippocampus or subcortical nuclei in the hGH-iCJD cases, hGH controls, hDM-iCJD, sCJD and vCJD cases. No glial tau pathology was identified.

However, small numbers of AT8-positive pretangles and occasional neurofibrillary tangles were identified in the gliotic region in the inferior right temporal cortex in hGH-control10, who had undergone resection of an ependymoma (Figure 5.11c).
This localised abnormality was not associated with Aβ deposition and did not involve the entorhinal region or the hippocampus. No glial tau positivity was present, and no tau positivity was identified in the subcortical nuclei or brain stem. Case hGH-iCJD31 (a patient with idiopathic hGH deficiency) had a small number of AT8-positive pretangles that were not labelled by the Bielschowsky silver stain in a localised area of the superior frontal cortex. No Aβ deposition or other adjacent pathology was evident. No glial tau positivity was present and no tau positivity was identified in the entorhinal region, hippocampus, subcortical nuclei or brain stem.

Figure 5.14. Non-Aβ related tau pathology in hGH-iCJD and control cases

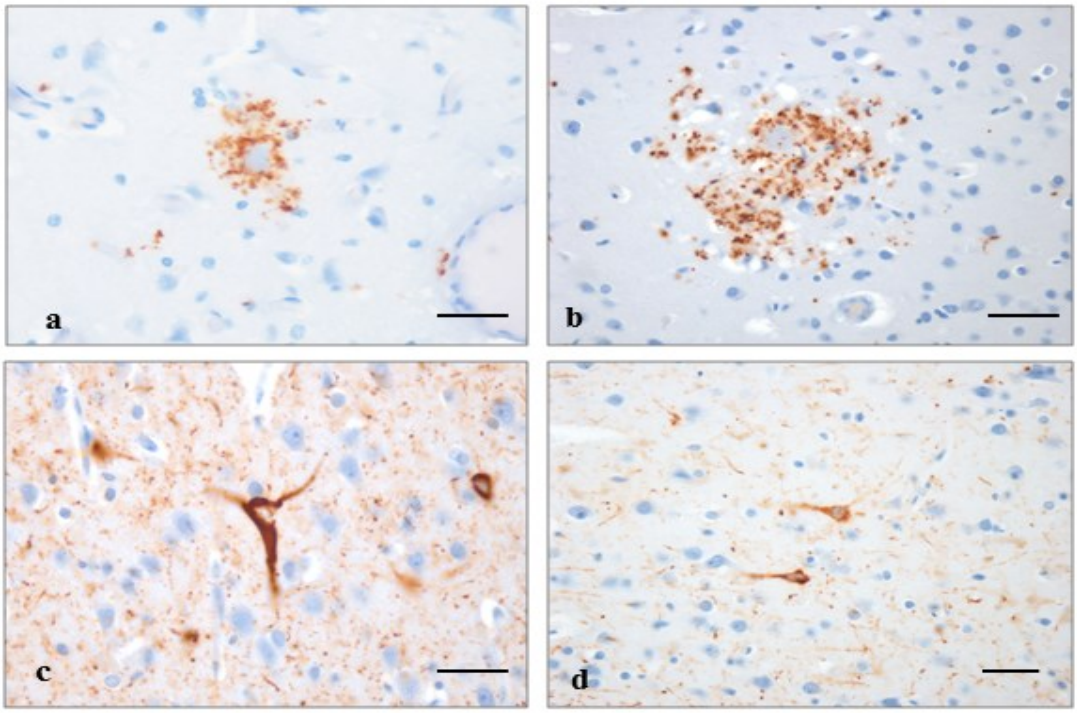

Small neurites around a kuru-type plaque in hGH-iCJD (a). Numerous small rounded neurites and threads are present around a florid plaque in vCJD (b). Occasional neurofibrillary tangles and numerous neuropil threads are present in the focally gliotic temporal cortex in hGH control10 (c). Occasional pretangles and neuropil threads are present in a small region within the superior frontal cortex in hGH-iCJD31. No glial positivity was identified (e). All sections were stained with the AT8 anti-phosphotau antibody. Scale bar=250μm.

Abbreviations: Aβ: amyloid beta; CJD: Creutzfeldt-Jakob disease; GFAP: glial fibrillary acidic protein; hGH; human growth hormone; i: iatrogenic; s: sporadic; v: variant.

5.3.4. α-synuclein and TDP-43 pathology

No evidence of Lewy body disease was identified in any of the hGH-iCJD cases, hGH control cases, hDM-iCJD cases and sCJD and vCJD control cases. Immunohistochemistry for α-synuclein showed no labelling of Lewy bodies or neurites in any of the cases examined. No TDP-43 labelling was found in any of the cases examined, regardless of whether CJD and/or Aβ pathology was present or not.

5.3.5. Correlations with Aβ pathology

5.3.5.1. *Aβ pathology and age at death*

The frequency of Aβ positive cases in both the hGH-iCJD and hGH control groups are significantly higher than in the sCJD and vCJD age-matched groups (Figure 5.7). The age range at death for the 18/33 hGH-iCJD cases with CNS Aβ deposition ranged from 20-45y. The 15 Aβ negative hGH-iCJD patients ranged from 20-46y at death. The differences in the age ranges in these two groups of hGH-iCJD patients is not statistically significant (Figure 5.15). The 5/12 hGH control cases with CNS Aβ deposition ranged from 30-45y at death, while the seven Aβ negative patients ranged from 13-35y at death. The difference between the age ranges in these two groups of hGH control patients is statistically significant (Figure 5.15). The single Aβ positive sCJD case was 46 years old at death, while the 13 negative sCJD patients ranged from 20-46y at death. The 2 Aβ positive vCJD cases were aged 30y and 33y at death, while the 31 Aβ negative vCJD cases ranged from 20-41y at death.

5.3.5.2. *Time, duration and type of treatment*

The timelines for the dates of first treatment and the dates of the midpoint of treatment for the hGH-iCJD and hGH control patients are shown in Figure 5.16. No significant differences in the dates of first treatment or the treatment midpoint were identified between the Aβ positive and Aβ negative hGH-iCJD cases, but there are non-significant trends for the Aβ positive hGH control cases to have been treated earlier and for longer than the Aβ negative control cases. No significant difference was found

in the time intervals from the end of treatment to death between the Aβ positive and Aβ negative hGH control cases (Figure 5.17).

5.3.5.3 *Duration of illness and incubation period for hGH-iCJD*

The iCJD disease incubation period and duration of the iCJD illness in the hGH-iCJD patients are displayed in relation to Aβ positivity in Figure 5.18. No significant differences were found in these parameters between the two groups.

Figure 5.15. CNS Aβ accumulation and age at death in hGH-iCJD and hGH-control cases (horizontal bars represent mean with standard deviation values)

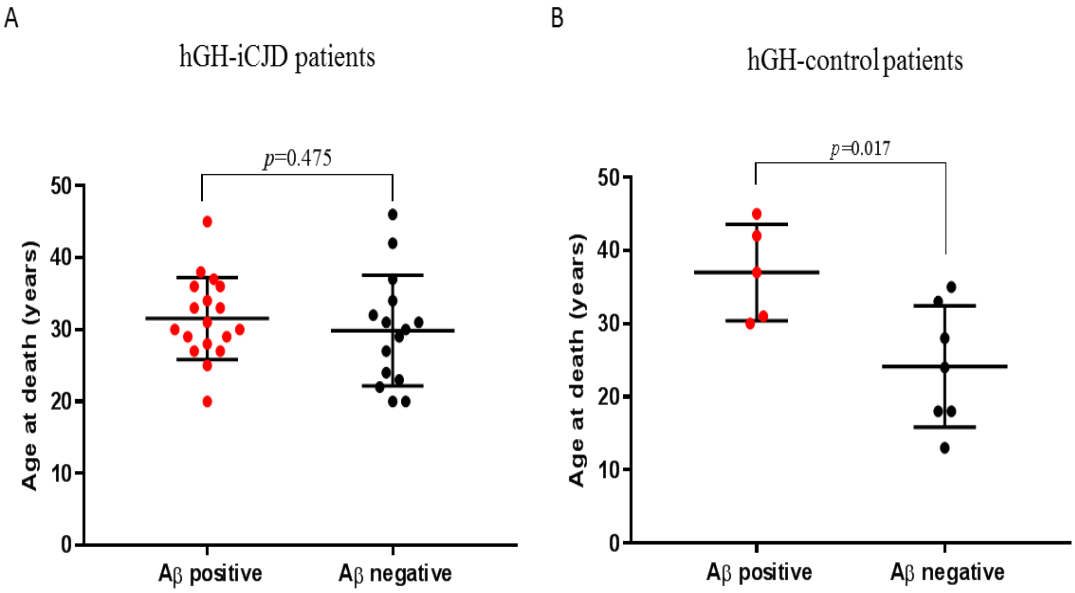

Comparisons of the age at death for (A) hGH-iCJD and (B) hGH-control patients in relation to accumulation of Aβ. No significant difference in the age at death was found between the Aβ positive and Aβ negative hGH-iCJD cases. However, a significant difference was found between the Aβ positive and Aβ negative hGH control cases, with the Aβ positive cases showing a higher age at death. Statistical analysis was performed an unpaired t-test.

Abbreviations: Aβ; amyloid beta: hGH: human growth hormone; iCJD: iatrogenic Creutzfeldt-Jakob disease.

Figure 5.16. Timelines for dates of first treatment and midpoint of treatment in relation to CNS Aβ positivity in hGH-iCJD and hGH control groups (vertical bars represent mean with standard deviation values)

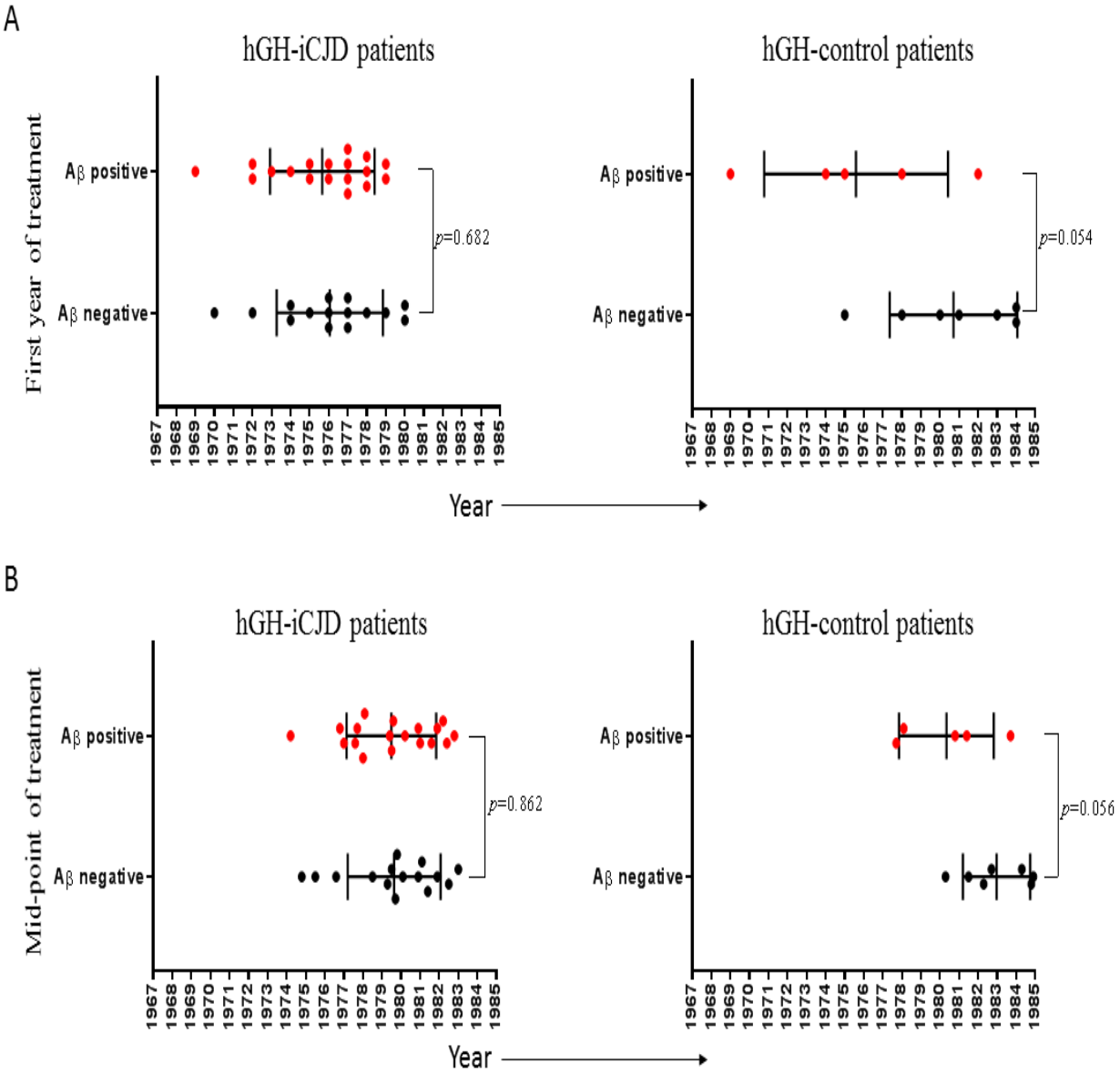

(A) Year of first treatment and in the (B) mid-point of treatment for hGH-iCJD and hGH-control patients in relation to accumulation of Aβ. Differences were found in both the year of first hGH treatment and the mid-point of treatment in the hGH control cases with and without CNS Aβ accumulation, but these did not reach levels of statistical significance. Statistical analysis was performed using an unpaired t-test.

Abbreviations: Aβ; amyloid beta: hGH: human growth hormone; iCJD: iatrogenic Creutzfeldt-Jakob disease.

Figure 5.17. Duration of hGH treatment and period between the midpoint of hGH treatment and date of death (D.O.D) in hGH-iCJD cases and hGH controls (horizontal bars represent mean with standard deviation values)

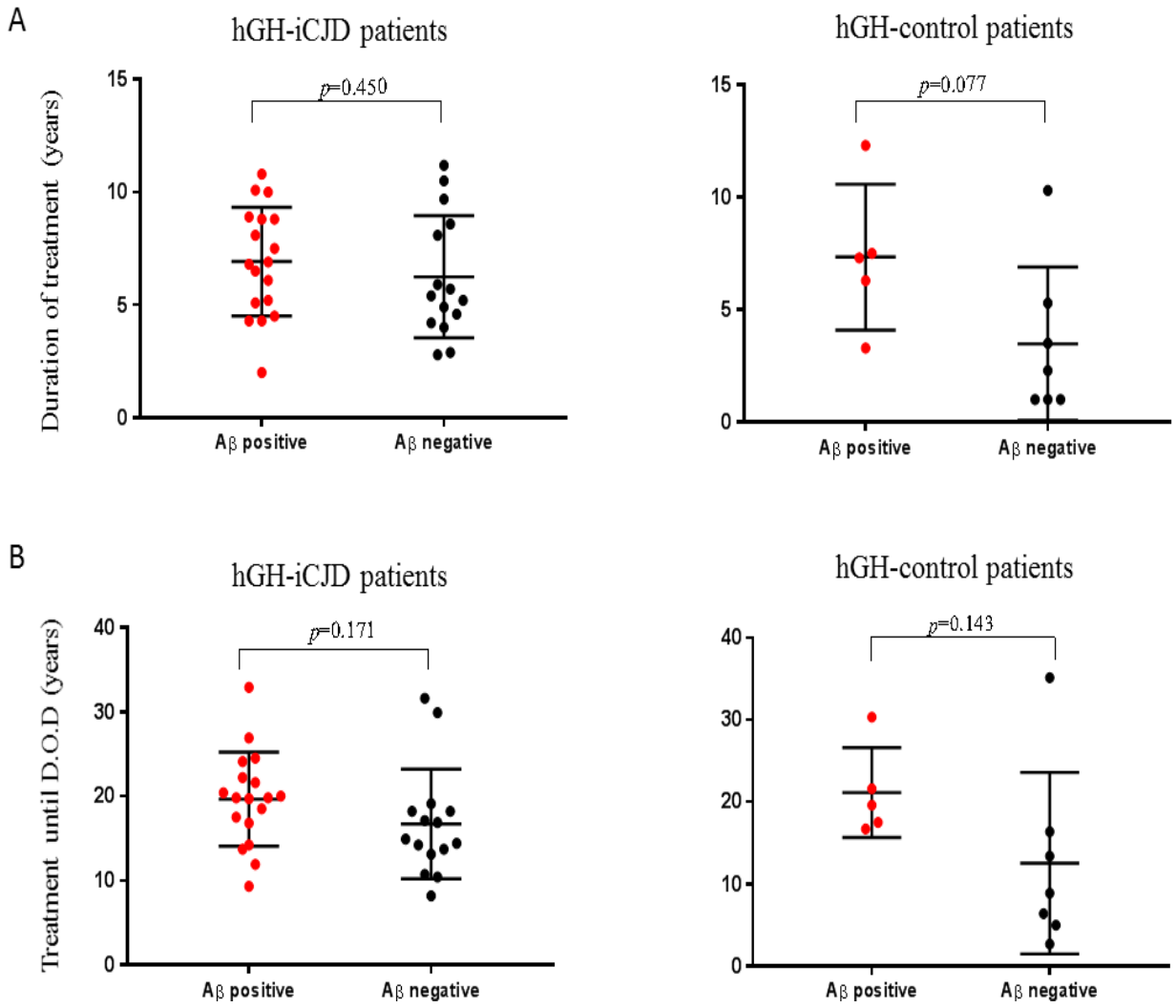

(A) Duration of treatment and (B) time period from the mid-point of treatment until death for hGH-iCJD and hGH-control patients in relation to CNS Aβ accumulation. Differences were found in both the duration of treatment and mid-point of treatment until D.O.D in the hGH-iCJD cases with and without CNS Aβ accumulation, but these did not reach levels of statistical significance. Statistical analysis was performed using an unpaired t-test.

Abbreviations: Aβ; amyloid beta: D.O.D; date of death: hGH: human growth hormone; iCJD: iatrogenic Creutzfeldt-Jakob disease.

Figure 5.18. Disease incubation period and duration of iCJD illness in hGH-iCJD cases in relation to CNS Aβ positivity (horizontal bars represent mean with standard deviation values)

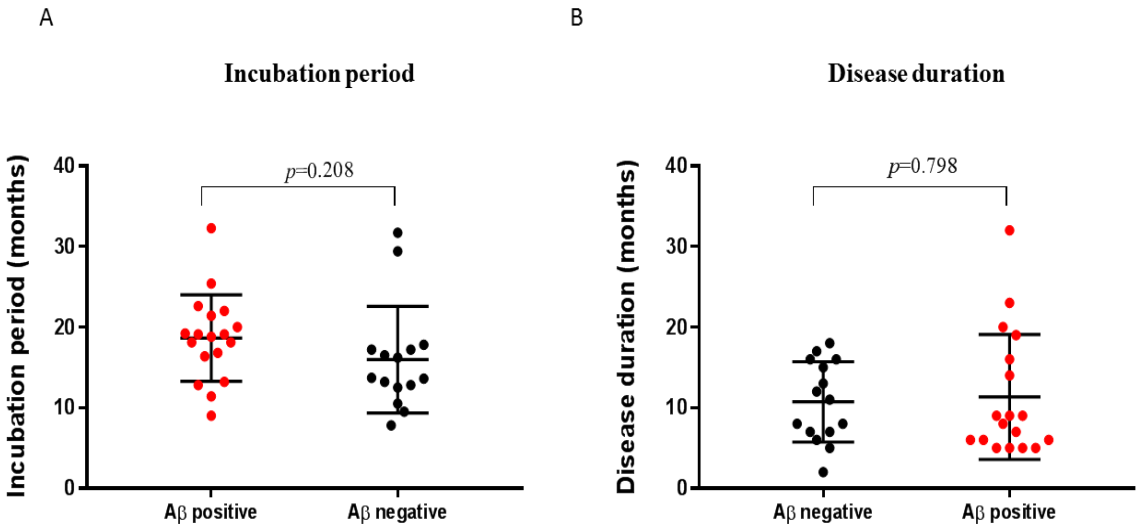

(A) Incubation periods and (B) durations of disease for hGH-iCJD in relation to CNS Aβ accumulation. Differences were found in the incubation period and the disease duration between the Aβ positive and Aβ negative hGH-iCJD groups, but these did not reach statistical significance. Statistical analysis was performed using an unpaired t-test

Abbreviations: Aβ; amyloid beta: CNS: central nervous system; D.O.D; date of death: hGH: human growth hormone; iCJD: iatrogenic Creutzfeldt-Jakob disease.

5.3.5.4. Predisposing medical factors.

No predisposing risk factors for Aβ deposition were identified in the clinical histories available in the hGH-iCJD, hGH-control, sCJD and vCJD cases. No Aβ pathology was identified in 4/6 hGH-iCJD patients with brain tumours (5 craniopharyngiomas and 1 astrocytoma), and 5/7 hGH control patients with brain tumours (5 craniopharyngiomas, 1 astrocytoma and 1 ependymoma). In the four cases with brain tumours and Aβ deposition in the CNS, there was no relationship between the sites of Aβ deposition and the sites of neurosurgery. However, one hGH control case with a resected ependymoma had localised AT8-positive pretangles and occasional neurofibrillary tangles in a small focal gliotic area in the right inferior temporal cortex (see 5.3.3).

5.3.2.5. *Predisposing genetic factors*

APOE genotype analysis was available for 13/18 Aβ-positive hGH-iCJD cases, 9/15 Aβ-negative hGH-iCJD cases, 2/5 Aβ-positive hGH controls, 2/2 Aβ positive vCJD controls and the single Aβ-positive sCJD control case (Table 5.7). No *APOE* ε4 homozygous cases were found in any of these groups. See section 5.6.4 below for further data on *APOE* genotype and apoE-4 phenotype analysis. The results of exome sequencing in hGH-iCJD, hGH controls, sCJD and vCJD cases with frozen tissue available found no major genetic risk factors for Aβ deposition in the brain in any of the cases studied. See section 5.6.3 below for further data from the exome sequencing results.

5.4. hGH-iCJD and hGH control non-CNS tissues

5.4.1. PrP immunohistochemistry and PET blot analysis

Twenty-one different non-CNS tissues from 19 hGH-iCJD and two hGH controls were available for investigation in this study. There was considerable variability of both fixed and frozen tissue for each individual case. Analysis of formalin fixed tissues was carried out by PrP IHC and PET blot analysis, with frozen tissues analysed by Western blotting following NaPTA precipitation. Full details of the tissues analysed in each case are presented in Appendix 5. The results of the combined IHC, PET blot and NaPTA analysis of these tissues are summarised in Table 5.8.

Accumulation of the disease associated prion protein was detected in sensory ganglia, with intense staining of ganglion cells in the trigeminal ganglia and dorsal root ganglia in all hGH-iCJD cases investigated (Figure 5.19a). In addition, PrP immunopositivity was found in the adrenal gland in three hGH-iCJD cases, generally in the chromaffin cells of the adrenal medulla (Figure 5.19b). PrP accumulation was also observed in lymphoreticular tissue, with labelling of the germinal centres of numerous lymphoid follicles in abdominal lymph nodes in a single hGH-iCJD case (hGH-iCJD15) (Figure 5.19c).

Most of the pituitary glands appeared histologically unremarkable. The glands from cases with panhypopituitarism tended to be smaller in size, but contained a normal population of cells in the adenohypophysis. No other abnormalities were noted. Over half of the pituitary glands from hGH-iCJD cases showed PrP immunoreactivity, with focal PrP^{res} deposition in the neurohypophysis as previously described (Peden *et al*.,

2007). PrP immunoreactivity was also observed in a single skeletal muscle sample (hGH-iCJD15), in a linear pattern with a distribution and morphology consistent with that of a small nerve (Figure 5.19d), as previously observed (Peden *et al*., 2006). No labelling of muscle spindles or motor end plates was observed. No PrP immunoreactivity was observed in the appendix, duodenum, large intestine, peripheral nerve, small intestine, spleen, sympathetic chain or tonsil in the hGH-iCJD patients or in the hGH control tissues by either IHC or PET blot analysis.

5.4.2. Aβ immunohistochemistry

Immunohistochemistry for Aβ using the 6F/3D antibody showed no labelling in any of the non-CNS tissues from the hGH-iCJD and hGH control cases, including the pituitary gland (Figure 5.19 e). However, the anti-Aβ 4G8 antibody showed fine granular labelling with more intensely labelled dot-like structures within the cytoplasm of many endocrine cells in the anterior pituitary glands from both groups (Figure 5.19 f). It has been reported recently that the 4G8 antibody recognises a sequence-independent epitope associated with α-synuclein and pancreatic islet amyloid polypeptide amyloid fibrils (Hatami *et al*., 2016). Peptide and protein hormones in secretory granules of pituitary endocrine cells are stored in an amyloid-like cross-β-sheet rich conformation, which may represent a functional amyloid that contributes to normal endocrine cell physiology (Maji *et al*., 2009). It is conceivable that these conformations could contain the sequence-independent epitope recognised by 4G8, which would explain this unexpected observation. The 4G8 positivity in the anterior pituitary gland therefore cannot be considered as evidence of intracellular accumulation of Aβ.

Figure 5.19. Results of immunohistochemistry and PET blot analysis on non-CNS tissues in hGH-iCJD cases

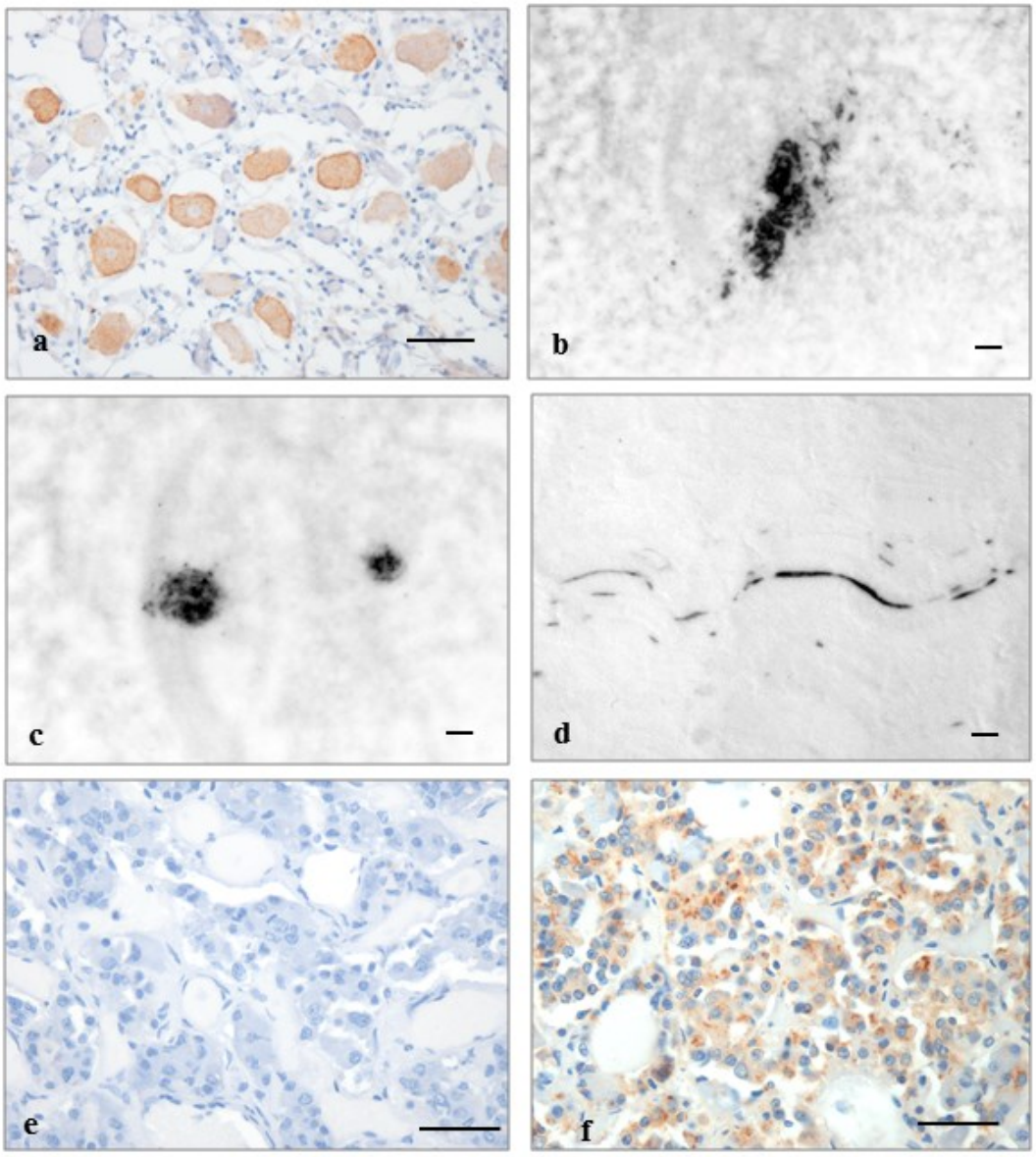

IHC with the KG9 anti-PrP antibody shows labelling of the ganglion cells in a dorsal root ganglion (a). PET blot analysis with the 12F10 anti-PrP antibody shows intense labelling (black) of a group of chromaffin cells within the adrenal medulla (b), in germinal centres within an abdominal lymph node (c) and in a small nerve within skeletal muscle (d). Aβ IHC using the 6F/3D antibody shows no labelling in the anterior pituitary gland (e), but the 4G8 anti-Aβ antibody shows some diffuse fine granular and discrete dot-like intracellular positivity in the endocrine cells (f).

Abbreviations: Aβ: amyloid beta; CJD: Creutzfeldt-Jakob disease; hGH; human growth hormone; i: iatrogenic; IHC: immunohistochemistry; PET: paraffin embedded tissue; PrP: prion protein.

5.4.3. Western blot analysis using NaPTA precipitation

All the frozen non-CNS tissues listed in Appendix 5dys were investigated by Western blot analysis following NaPTA precipitation (NaPTA WB). Only four samples gave unequivocal positive reactions: dorsal root ganglion in a single case and the pituitary gland in three cases (Figure 5.20). Two of the pituitary glands were found to have a type 2 PrP^{res} isoform (similar to that in the corresponding brain). The remaining case had a type 1 isoform, which was also present in the brain. Densitometric analysis indicated that the levels of PrP^{res} in the pituitary gland and dorsal root ganglion were around 0.8% and 0.04% respectively in comparison with brain PrP^{res} levels in a control hGH-iCJD case. Several other tissues gave indeterminate results on NaPTA WB, when two of the usual three PrP^{res} bands were visible, including adrenal gland, bone marrow, kidney, heart, lung, lymph node, skeletal muscle and peripheral nerve. Skeletal muscle from one hGH-iCJD case had previously found to be positive on NaPTA WB, and also gave a positive signal for PrP^{res} on PET blot analysis (see Figure 5.19d) (Peden *et al*., 2006). Repeat NaPTA WB analysis of the indeterminate cases was attempted, but was restricted in some cases by tissue sample availability. None of the repeat NaPTA WB tests altered the classification of these samples.

The results for PrP IHC, PET blot and NaPTA WB are summarised in Table 5.8.

Table 5.8. Summary of PrP immunohistochemistry, PET blot and WB NaPTA results in non-CNS tissues in hGH-iCJD and control cases

	hGH-iCJD (n=19)			hGH-control (n=2)		
	IHC	PET blot	NaPTA	IHC	PET blot	NaPTA
AG	3/5	4/5	0/1	0/1	0/1	0/0
AP	0/4	0/4	0/1	0/2	0/2	0/0
BM	0/0	0/0	0/1	0/0	0/0	0/0
DR	3/3	3/3	1/1	0/0	0/0	0/0
DU	0/1	0/1	0/0	0/0	0/0	0/0
HE	0/0	0/0	0/1	0/0	0/0	0/0
KI	0/0	0/0	0/2	0/0	0/0	0/0
LI	0/1	0/1	0/2	0/1	0/1	0/0
LN	1/6	1/6	0/3	0/1	0/1	0/0
MU	1/8	1/8	0/5	0/1	0/1	0/0
PA	0/0	0/0	0/2	0/0	0/0	0/0
PI	6/10	6/10	3/5	0/1	0/1	0/0
PN	0/7	0/7	0/3	0/0	0/0	0/0
SG	0/0	0/0	0/1	0/0	0/0	0/0
SI	0/1	0/1	0/1	0/0	0/0	0/0
SP	0/10	0/10	0/6	0/1	0/1	0/0
SY	0/2	0/2	0/1	0/0	0/0	0/0
TG	2/2	2/2	0/0	0/0	0/0	0/0
TO	0/3	0/3	0/1	0/2	0/2	0/0
TY	0/0	0/0	0/1	0/0	0/0	0/0

Abbreviations: AG: adrenal gland; AP: appendix; BM: bone marrow; DR: dorsal root ganglion; DU: duodenum: HE: heart; hGH: human growth hormone; iCJD: iatrogenic Creutzfeldt-Jakob disease; IHC: immunohistochemistry; KI: kidney; LI: large intestine; LN: lymph node; LU: Lung; LV: liver; MU: muscle; NaPTA: sodium phosphotungstic acid; PA: pancreas; PET: paraffin embedded tissue; PI: pituitary; PN: peripheral nerve; PrP: prion protein; SG: salivary gland; SI: small intestine; SP: spleen; SY: sympathetic chain; TG: trigeminal ganglion; TO: tonsil; TY: thyroid; WB: western blot

Figure 5.20. Western blots with NaPTA precipitation on non-CNS tissues

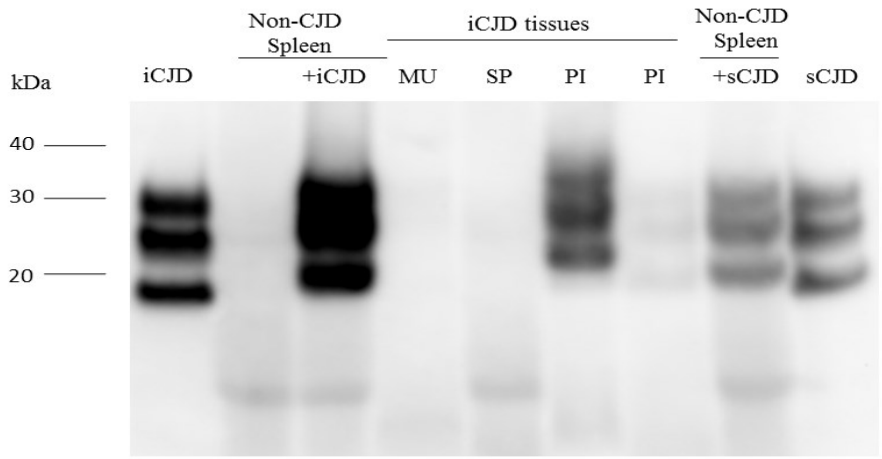

30second exposure XRS

Western blot after NaPTA precipitation showing (left to right) iCJD brain, non-CJD spleen, non-CJD spleen spiked with iCJD brain, iCJD muscle, iCJD spleen, iCJD pituitary 1, iCJD pituitary 2, non-CJD spleen spiked with sCJD brain, sCJD brain. iCJD pituitary 1 gives a strong positive signal, with a weaker signal for iCJD pituitary 2 (confirmed on a longer exposure). No signal is seen in the lanes for iCJD muscle and spleen.

Abbreviations: CJD: Creutzfeldt-Jakob disease; i: iatrogenic; kDa: kilodaltons; MU: muscle; PI: pituitary; s: sporadic; SP: spleen

5.5. CNS Biochemistry

The results of the biochemical and genetic investigations and *in vitro* conversion assays described below are included in the recent publication by Ritchie *et al*. (Ritchie *et al*., 2016), a copy of which is provided in Appendix 15.

5.5.1. Western blot analysis and classification of PrP^{res} types in the CNS

Western blot analysis of all available CNS samples from the 21 cases of hGH-iCJD for protease resistant prion protein (PrP^{res}) was undertaken. Four PrP^{res} types (types 1, i, i+2 and 2) were identified in the hGH-iCJD cases, differing in mobility and in the number of unglycosylated bands found. Representative examples of the PrP^{res}

types 1, i, i+2 and 2 are shown in Figure 5.21; sample Western blots for each individual case of hGH-iCJD and hDM-iCJD are shown in Figure 5.22.

The majority of cases contained the 19kDa type 2 PrP^{res} band (19/21 cases). However, in 12/19 cases the 20kDa type i PrP^{res} band was also present. The relative abundance of the 19kDa type 2 PrP^{res} band and the 20kDa type i PrP^{res} band was variable, but the 19kDa type 2 PrP^{res} band usually predominated (Figure 5.22). Type i was found to predominate overall in only one hGH- iCJD case (hGH-iCJD20) and the 21kDa type 1 PrP^{res} was found in only one hGH-iCJD case (hGH-iCJD21). In contrast, all three cases of hDM-iCJD contained type 1 PrP^{res} exclusively. Where assessed, regional PrP^{res} variation within the brain was largely confined to the presence or absence of the PrP^{res} types i band and the relative abundance of PrP^{res} types i and 2 bands (Table 5.9). Comparison of the immunoreactivity of the 21kDa type 1, 20kDa type i, and 19kDa type 2 bands using the 3F4 antibody (epitope 106-112) with the 12B2 antibody (epitope 89-93) showed that the 21kDa type 1 PrP^{res} and the 20kDa type i PrP^{res} fragments both retain the 12B2 epitope, whereas type 2 PrP^{res} fragments does not (Figure 5.21(b)).

Analysis of the PrP^{res} types in the CNS of 108 sCJD cases showed type 1, type 2, type i+2 and cases in which type 1 and type 2 were found in individual brains, either in the same or in different regions. The latter cases were designated type 1+2, irrespective of the relative abundance and location of the two types. The breakdown of these 108 sCJD cases according to the combination of CNS PrP^{res} type and *PRNP* codon 129 genotype is shown in Appendix 13.

Figure 5.21. PrP^{res} types found in the hGH-iCJD cases

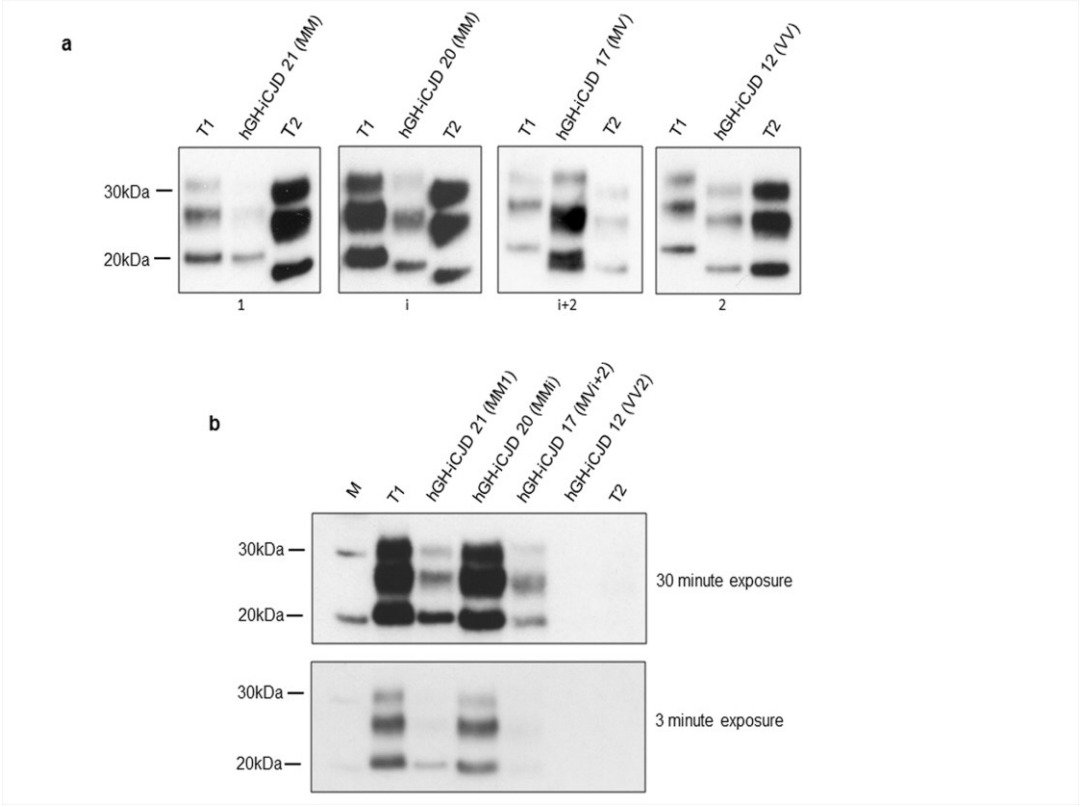

(a) Four PrP^{res} molecular types were detected by Western blot analysis of proteinase K treated brain extracts of hGH-iCJD patients: type 1, type i, type i+2 and type 2. Representative blots of each PrP^{res} type are shown. Each sample (middle lane) is flanked by type 1 (T1) (left lane) and type 2 (T2) (right lane) reference standards from sCJD MM1 and VV2 subtype cases, respectively. Case number and codon 129 *PRNP* genotype are indicated above each blot whilst PrP^{res} type is indicated below. The most informative exposure for the test and reference standard samples from a series of timed exposures is shown. Blots were probed using the monoclonal antibody 3F4.

(b) Western blot analysis of proteinase K treated samples of PrP^{res} types detected in hGH-iCJD patients using the monoclonal antibody 12B2, which detects type 1 PrP^{res}.

The approximate molecular mass is shown in kDa in (a) and (b). The immunoblots shown are representative of at least three technical repeats.

Abbreviations: hGH: human growth hormone; iCJD: iatrogenic Creutzfeldt-Jakob disease; kDa: kilodaltons; M: methionine; *PRNP*: prion protein gene; PrP^{res}: protease-resistant prion proteins; sCJD sporadic Creutzfeldt-Jakob disease; V: valine.

Figure 5.22. PrP^{res} typing of 21 hGH-iCJD cases and 3 hDM-iCJD cases

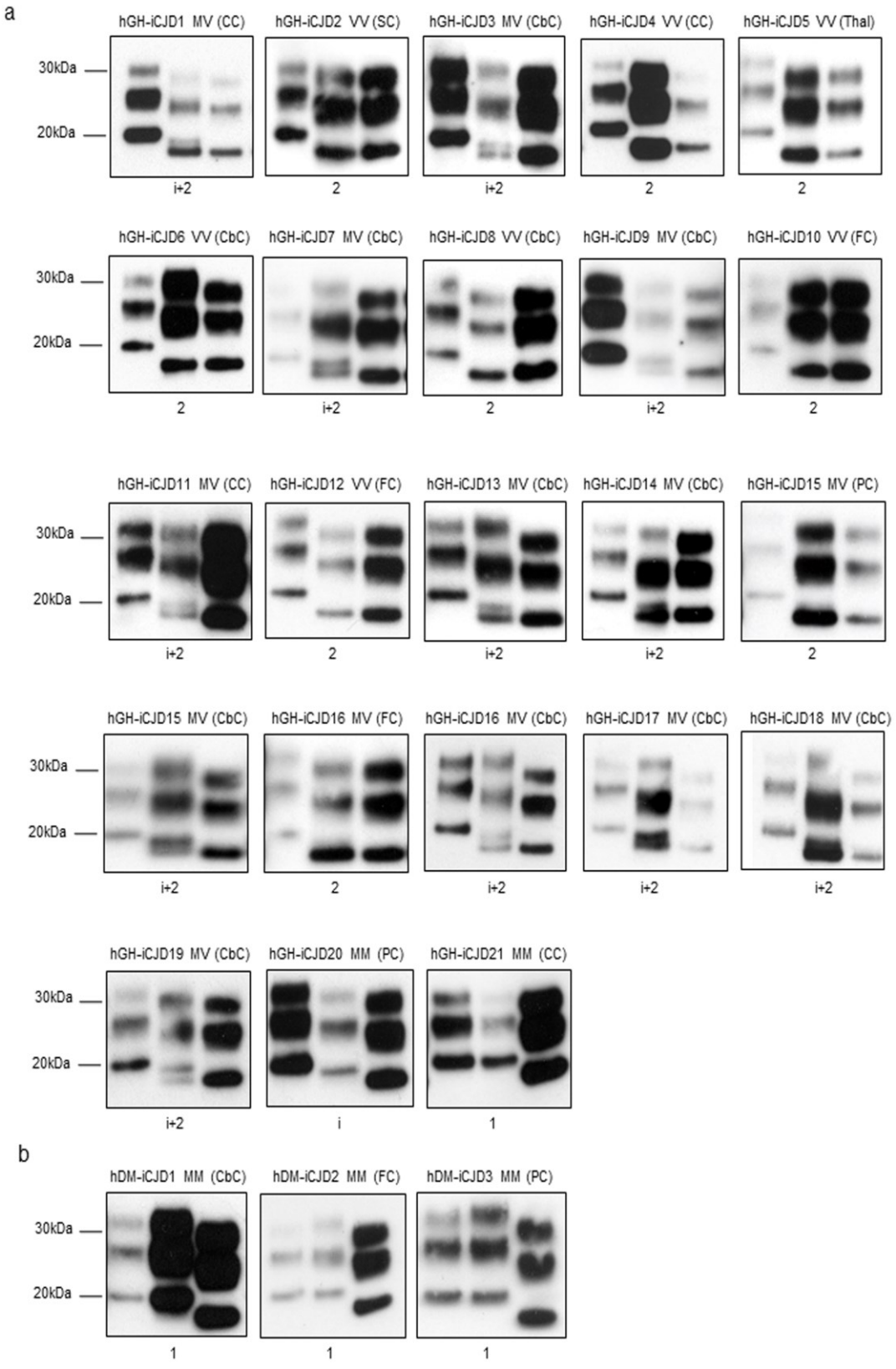

Legend to Figure 5.22.

PrP^{res} typing of (a) hGH-iCJD cases 1-21 and (b) hDM-iCJD cases 1-3. Each sample (middle lane) was run between a type 1 (left lane) and type 2 (right lane) reference standard from sCJD MM1 and VV2 subtype cases, respectively. Study identification number and brain region are indicated above each blot and PrP^{res} type is indicated below. The immunoblots shown are representative of at least three technical repeats for each sample. Regional differences in PrP^{res} types are illustrated for case hGH-iCJD 15 and case hGH-iCJD 16.

Abbreviations: CbC: cerebellar cortex; FC: frontal cortex; hDM: human dura mater; hGH: human growth hormone; iCJD: iatrogenic Creutzfeldt-Jakob disease; M: methionine; PC: parietal cortex; PrP^{res}: protease-resistant prion proteins; SC: spinal cord; sCJD sporadic Creutzfeldt-Jakob disease; TC: temporal cortex; V: valine.

Table 5.9.

PrP^{res} types found in each available CNS region of the iCJD cases examined

Study ID	PrP^{res} type							
	FC	TC	PC	OC	CbC	Th	SC	Consensus
hGH-iCJD1	i+2	-	-	-	-	-	-	i+2
hGH-iCJD2	-	2	-	-	-	-	2	2
hGH-iCJD3	-	-	-	-	i+2	-	-	i+2
hGH-iCJD4	2	-	-	-	2	-	-	2
hGH-iCJD5	2	2	2	2	2	2	-	2
hGH-iCJD6	-	-	-	-	2	-	-	2
hGH-iCJD7	i+2	-	-	-	i+2	-	-	i+2
hGH-iCJD8	2	-	-	-	2	-	-	2
hGH-iCJD9	i+2	-	-	-	-	-	-	i+2
hGH-iCJD10	2	-	-	-	2	-	-	2
hGH-iCJD11	i+2	-	-	-	-	-	-	i+2
hGH-iCJD12	2	2	-	-	2	-	-	2
hGH-iCJD13	i+2	-	-	-	i+2	-	-	i+2
hGH-iCJD14	i+2	-	-	-	i+2	-	-	i+2
hGH-iCJD15	i+2	2	2	i+2	i+2	i+2	-	i+2
hGH-iCJD16	2	-	-	-	i+2	-	-	i+2
hGH-iCJD17	i+2	-	-	-	i+2	-	-	i+2
hGH-iCJD18	i+2	-	-	-	i+2	-	-	i+2
hGH-iCJD19	i+2	i+2	-	i+2	i+2	-	-	i+2
hGH-iCJD20	i	i	i	i	i	i	-	i
hGH-iCJD21	-	1	-	-	-	-	-	1
hDM-iCJD1	1	-	-	-	-	-	-	1
hDM-iCJD2	1	1	1	1	1	1	-	1
hDM-iCJD3	1	-	1	-	1	-	-	1

Abbreviations: Cb: cerebellum; CC: cerebral cortex (unspecified); CNS: central nervous system; FC: frontal cortex; hDM: human dura mater; hGH: human growth hormone; iCJD: iatrogenic Creutzfeldt-Jakob disease; OC: occipital cortex; PC: parietal cortex; PrP^{res}: protease-resistant prion protein; SC: spinal cord; TC: temporal cortex; Th: thalamus; -: not tested.

5.6. Genetics

5.6.1. *PRNP* codon 129 genotype

Comparison of the *PRNP* codon 129 genotype distribution in the hGH-iCJD and sCJD cohorts shows striking differences. The MM *PRNP* codon 129 genotype is the most frequently occurring group within the UK sCJD group and occurs throughout the period of the hGH-iCJD epidemic (Figure 5.23A). In contrast, the *PRNP* codon 129 MV and VV genotypes predominate in the hGH-iCJD cohort; the MM genotype is uncommon and occurs later in the epidemic (Figure 5.1).

When considered as a whole, the distribution of codon 129 genotypes of the 21 available hGH-iCJD cases and the 108 sCJD cases selected for biochemical analysis differ from each other and from the normal UK population, but appear to be broadly representative subsets of the larger hGH-iCJD and sCJD cohorts (Figure 5.23B).
The *PRNP* genotype results of the hGH controls are incomplete even after attempts to extract DNA from formic acid pretreated paraffin blocks; the available results for 5/12 cases show 4 *PRNP* codon 129 MV cases and 1 codon 129 MM case (Table 5.2).

Figure 5.23.

PRNP codon 129 genotype distribution in hGH-iCJD, sCJD and the UK population

a

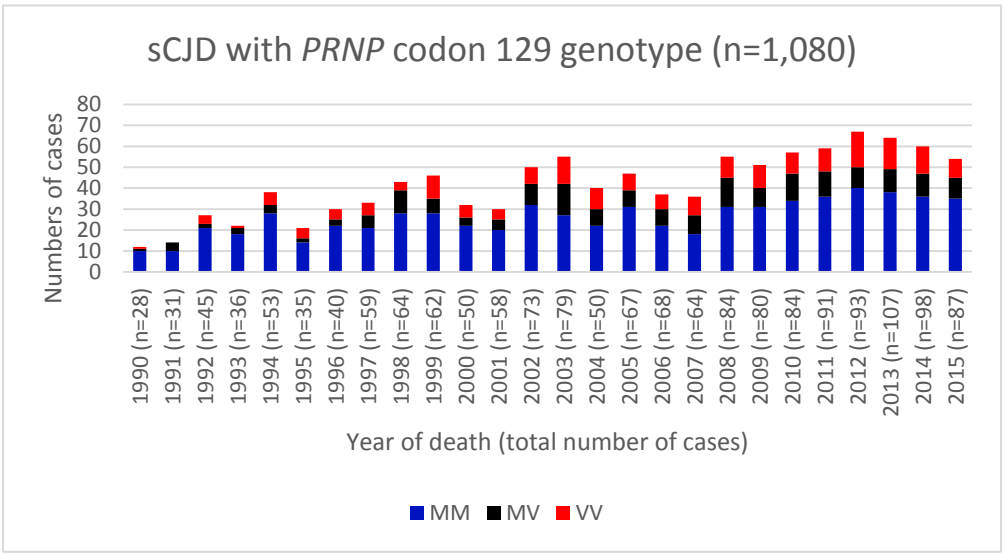

b

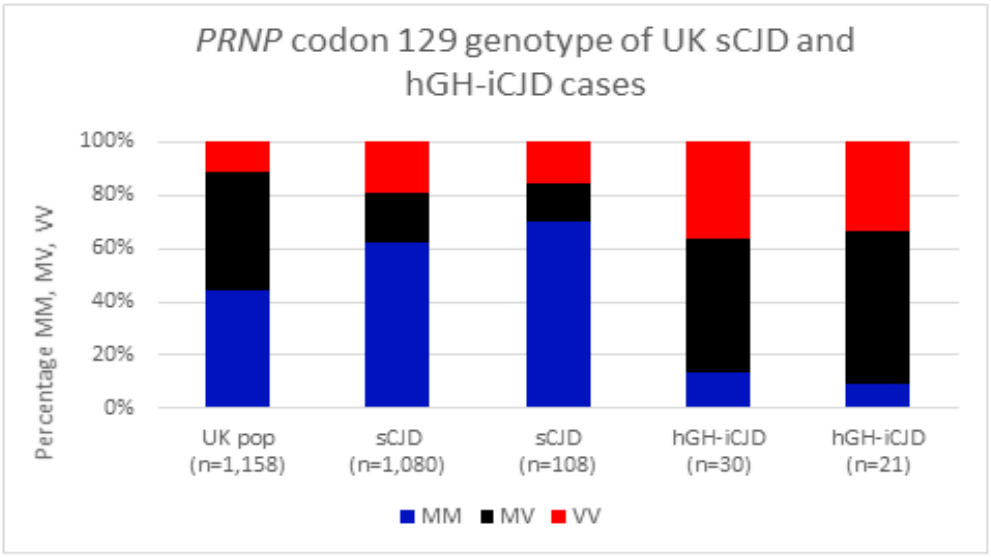

The *PRNP* codon 129 distribution by year of death for the 1,080 UK sCJD cases from 1990 to 2015 is shown in (a). (b) compares the *PRNP* codon 129 distribution of the hGH-iCJD (n=21) and sCJD (n=108) cases with frozen tissue analysed with the larger cohorts of hGH-iCJD (n=37) and sCJD (n=1080) cases of which they are representative subsets. The UK normal population results are shown for reference.

Abbreviations: hGH: human growth hormone; iCJD: iatrogenic Creutzfeldt-Jakob disease; M: methionine; pop: population; *PRNP*: prion protein gene; sCJD: sporadic Creutzfeldt-Jakob disease; UK: United Kingdom; V: valine.

5.6.2. *PRNP* codon 129 genotype and PrP^{res} type in iCJD and sCJD cases

When the 21 cases of hGH-iCJD were grouped according to the combination of *PRNP* genotype and CNS PrP^{res} type (Figure 5.24A) all *PRNP* codon 129 VV hGH-iCJD cases (7/7) were found to have type 2 PrP^{res} exclusively. All of the hGH-iCJD *PRNP* codon 129 MV genotype cases were found to have type i+2 PrP^{res} (12/12). One of the *PRNP* codon 129 MM cases contained type 1 PrP^{res} while the other contained type i PrP^{res}. However, within the 108 sCJD cases those with type 1 PrP^{res} and a *PRNP* codon 129 MM genotype predominated (50/108); cases with type 1+2 PrP^{res} were relatively common (26/108), but no examples of type i PrP^{res} alone were found (Figure 5.24B). All three hDM-iCJD cases occurred in individuals of the *PRNP* codon 129 MM genotype and each had PrP^{res} type 1 in the CNS, in keeping with their neuropathological features resembling the sCJD MM1 histotype.

Figure 5.24.

PrP^{res} type and *PRNP* codon 129 genotype of the hGH-iCJD and sCJD groups

A

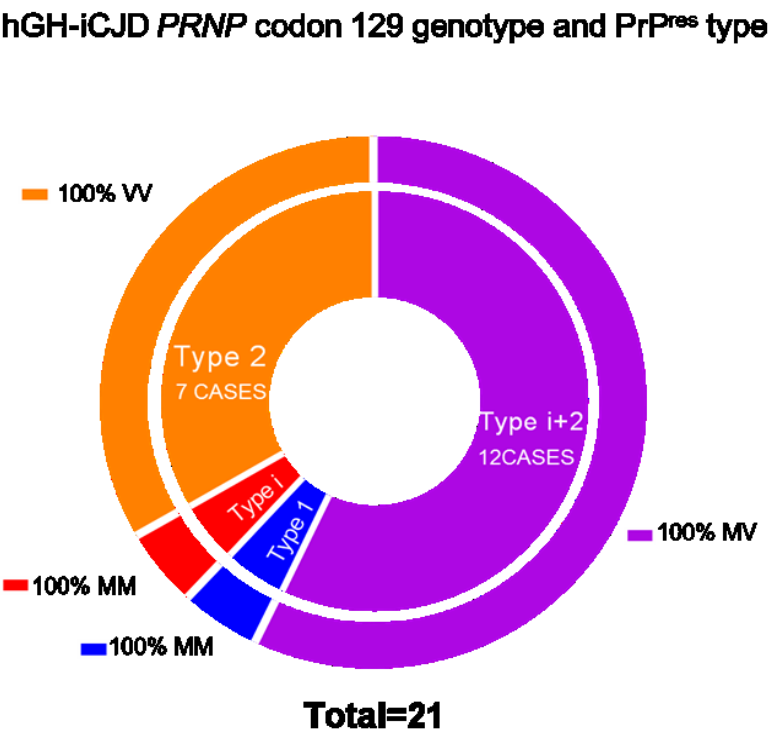

B

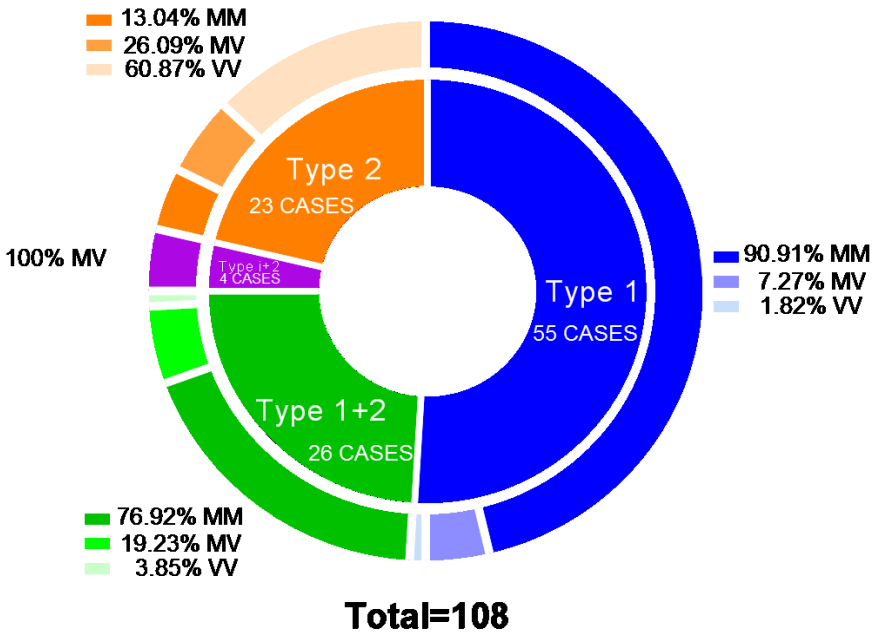

Legend to Figure 5.24.

Diagram A shows the classification of cases in the hGH-iCJD group (n=21) according to the combination of PrP^{res} type (inner ring) and *PRNP* codon 129 genotype (outer ring). Diagram B shows the classification of cases in the sCJD group (n=108) according to the combination of PrP^{res} type (inner ring) and *PRNP* codon 129 genotype (outer ring).

Abbreviations: hGH: human growth hormone; iCJD: iatrogenic Creutzfeldt-Jakob disease; M: methionine; *PRNP*: prion protein gene; PrP^{res}: protease-resistant prion protein; sCJD: sporadic Creutzfeldt-Jakob disease; V: valine.

5.6.3. Exome sequencing

Exome sequence analysis data for the hGH-iCJD cases, hGH-controls and sCJD cases with frozen tissue available found no coding, non-coding or 3- or 5-prime untranslated variants in genes that were likely to be associated with Aβ accumulation in the CNS (*APP, C9ORF2, CHMP2B, CSFIR, FUS, GRN, ATM2B, MAPT, NOTCH3, PSEN1 PSEN2, SERPINI1, SQTM1, TARDBP, TREM2, TYROBP, VCP*).

One of the hGH-iCJD cases (hGH-iCJD35) had a *NOTCH3* variant (p.H1133Q) that appears to be non-pathogenic (Schmidt *et al*., 2011). One of the hDM-iCJD cases (hDM-iCJD2) had the *TREM2* p.R62H variant that has been reported as a risk factor for AD (Jin *et al*., 2014), but showed no evidence of CNS Aβ deposition. No other variants were detected in the hDM-iCJD cases. One of the vCJD cases (vCJD22) with diffuse Aβ deposits in the brain had the *PSEN1* p.E318G variant that increases the risk of AD in *APOE* ε4 carriers (Benitez *et al*., 2013) and a -48 C/T polymorphism in the *PSEN1* promoter that is as genotype associated with an increased risk of AD and an increased Aβ load in the brain (Lambert *et al*., 2001). Neither can be considered as

highly penetrant monogenic alleles causing disease. No other variants were detected in the vCJD cases.

5.6.4 *APOE* genotype and apoE-4 phenotype analysis

APOE genotype data was available for 22/33 hGH-iCJD cases and 2/12 hGH control cases (Table 5.10). No *APOE* ε4/4 genotypes were identified and a mixture of *APOE* ε2/3, *APOE* ε3/3 and *APOE* ε3/4 genotypes was present in the hGH-iCJD cases. Immunohistochemistry for apoE-4 in 4 hGH-iCJD cases with CNS Aβ accumulation found no positives (Table 5.10). In the 5 hGH control cases with CNS Aβ accumulation there was a single case with the *APOE* ε3/3 genotype and another with the *APOE* ε3/4 genotype. Immunohistochemistry for apoE-4 in the 3 remaining hGH control cases with CNS Aβ accumulation found a single positive case: hGH control6 (Figure 5.13e) (Table 5.10). No information on the *APOE* genotype or apoE-4 phenotype can be obtained on the remaining 6 hGH-iCJD cases and 7 hGH control cases with no CNS Aβ accumulation, due to a lack of frozen tissue samples.

The relationship of the *APOE* ε4 genotype and the apoE-4+(IHC) phenotype to Aβ deposition in the CNS in all the hGH-iCJD and the hGH control cases with CNS Aβ accumulation and the age at death is summarised in Figure 5.25. These data indicate that there are no significant differences in *APOE* genotypes between the Aβ positive and Aβ-negative hGH-iCJD cases; comparisons between the Aβ –positive and Aβ- negative hGH control cases are hampered by a lack of *APOE* genotype data for the Aβ-negative cases.

The 2 vCJD cases with diffuse Aβ parenchymal deposits included one case with the *APOE* ε3/4 genotype (vCJD32) and one case with the *APOE* ε2/3 genotype (vCJD22). Genomic analysis of the latter found the *PSEN1* p.E318G variant and the -48 C/T polymorphism in the *PSEN1* promoter (see section 5.6.3 above).

Table 5.10.

APOE genotypes in hGH-iCJD and hGH-control cases

***APOE* genotype and apoE-4 phenotype**	**hGH-iCJD**		**hGH control**	
	CNS Aβ accumulation		**CNS Aβ accumulation**	
	Positive	**Negative***	**Positive**	**Negative***
2/2	0	0	0	0
2/3	1	1	0	0
2/4	0	0	0	0
3/3	8	6	1	0
3/4	4	2	1	0
4/4	0	0	0	0
apoE-4+(IHC)$^{+}$	0	0	1	0
apoE-4 –(IHC)$^{+}$	5	0	2	0
Total	18	9	5	0

$^{+}$apoE-4 phenotypes were determined on paraffin sections of the brains from 5 hGH-iCJD and 3 hGH-control cases with CNS Aβ accumulation using immunohistochemistry for the apoE-4 protein.

*No data on the *APOE* genotype or apoE-4 phenotype on 6 hGH-iCJD cases and 7 hGH control cases with no CNS Aβ accumulation, due to a lack of frozen tissue and an absence of Aβ pathology.

Abbreviations: Aβ: amyloid beta; *APOE*: apolipoprotein E gene; apoE-4: apolipoprotein E4; CNS: central nervous system; hGH: human growth hormone; iCJD: iatrogenic Creutzfeldt-Jakob Disease: IHC: immunohistochemistry.

Figure 5.25.

Distribution of *APOE* ε3/4 genotypes and apoE-4 positive phenotypes in relation to age at death and CNS Aβ accumulation in hGH-iCJD and hGH control cases (horizontal bars represent mean with standard deviation values)

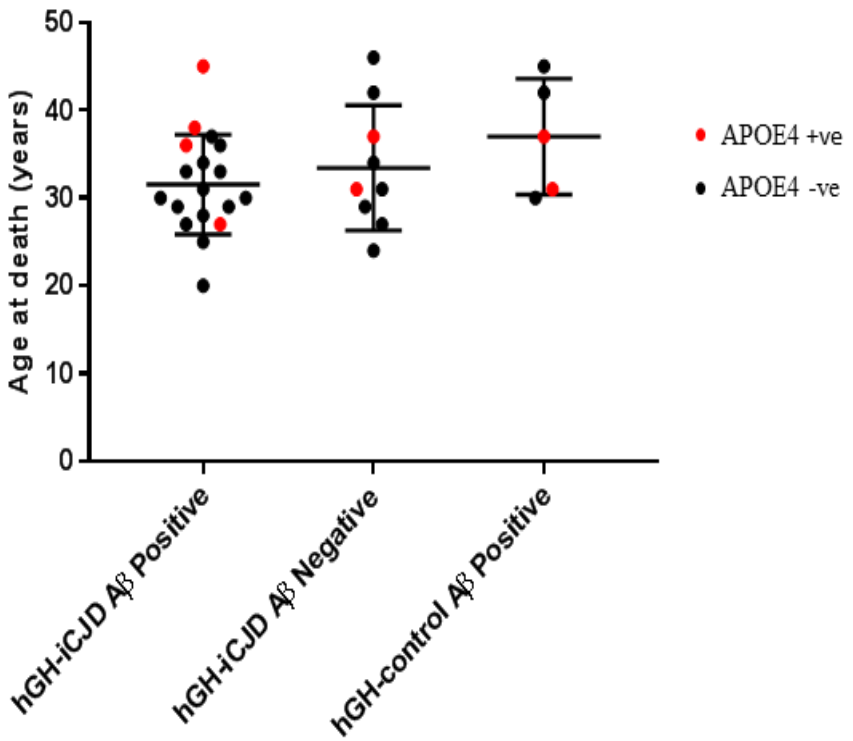

There is no evidence of a difference in the percentage of APOE4+ve hGH-iCJD cases in the Aβ positive and Aβ negative groups; p=1.00 (Fisher's exact test). There is no evidence of a significant difference in the percentage of APOE4+ve cases between the Aβ positive hGH-iCJD group and the Aβ positive hGH control group; p=0.576 (Fisher's exact test). No apparent relationship between age and APOE4 status is detected.

Abbreviations: Aβ: amyloid beta; APOE4: *APOE* e3/4 genotype or apoE-4 phenotype on immunohistochemistry; hGH: human growth hormone; iCJD: iatrogenic Creutzfeldt-Jakob disease.

5.7 *In vitro* conversion assays

5.7.1. RT-QuIC analysis

The amyloid seeding activity of hGH-iCJD and sCJD cases was compared using the RT-QuIC assay. hGH-iCJD cases were selected on the basis of availability of cerebral cortex samples (n=20). sCJD cases (n=28) were selected on the basis of PrP^{res} type and *PRNP* codon 129 genotype to match, as far as possible, those found in the hGH-iCJD cohort. RT-QuIC assays were seeded with CJD cerebral cortex homogenate diluted by a factor of 2×10^{-5} (each 100 μl RT-QuIC reaction was seeded with the equivalent of 2×10^{-7} g brain) and the seeding activity for each patient was assumed to be inversely proportional to the mean lag period (Figure 4.3). The hGH-iCJD and sCJD seed amounts were determined empirically to be within the range for quantifying seeding activity by the lag time method. Figure 5.26 (a) shows that the hGH-iCJD group as a whole (and their subgroups) have a lower median seeding activity than the sCJD group (and their matched subgroups). The difference is significant for the hGH-iCJD group as a whole and for the VV and MV subgroups. The two *PRNP* codon 129 MM hGH-iCJD cases had noticeably different lag times in this assay (hGH-iCJD20 at 43.5 hrs and hGH- iCJD21 at 27.5hrs) (Figure 5.26b). Three hDM-iCJD cases were also analysed by RT-QuIC and their median lag period (34.2hrs) was also greater than the sCJD MM1 subgroup, but this difference was not statistically significant (Figure 5.26B).

Figure 5.26.

RT-QuIC analysis of iCJD and sCJD cases

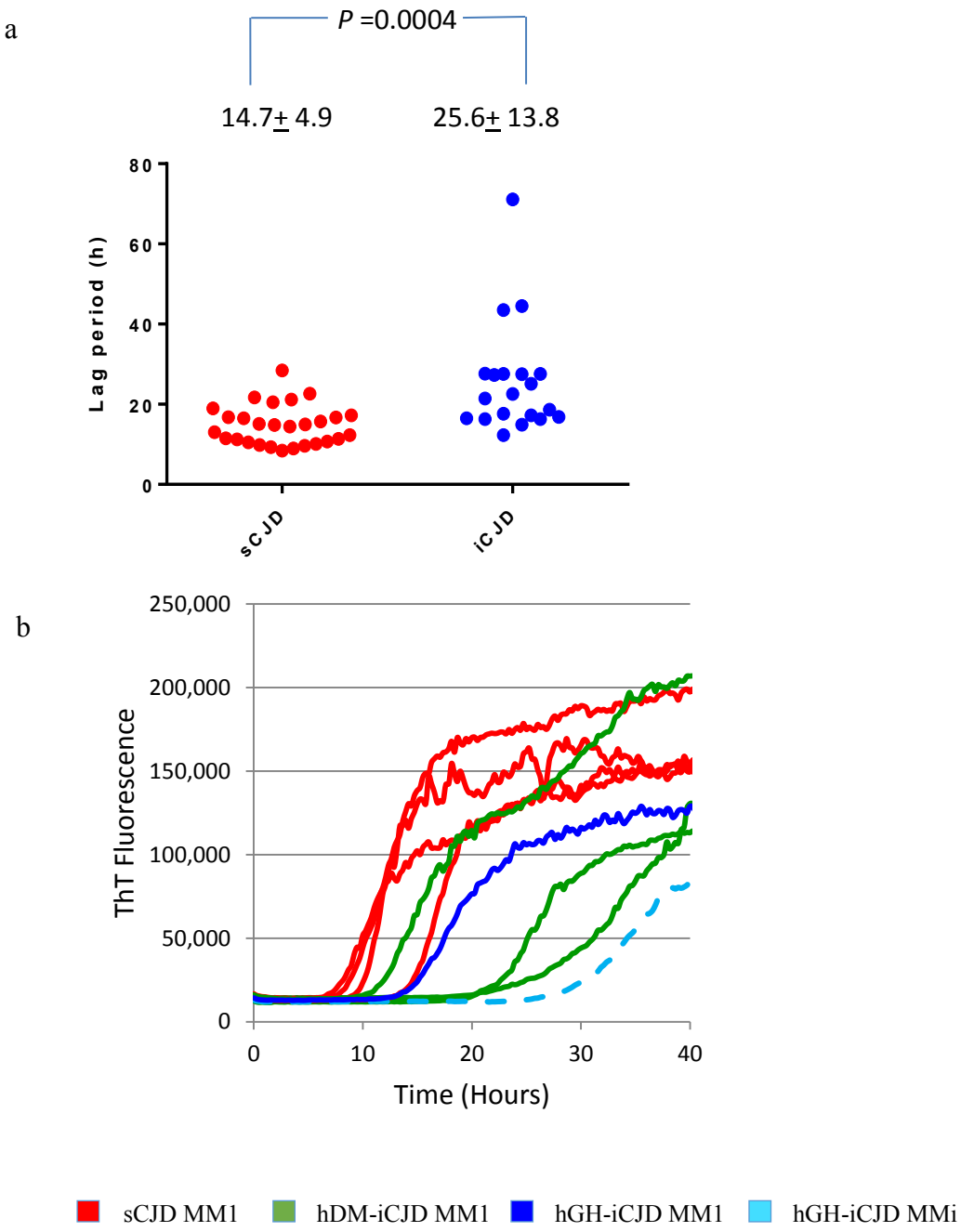

Legend for Figure 5.26.

Diagram (a) shows the differences in the lag time between a group of 28 sCJD cases including MM1, VV2 and MV2 subtypes (red) and 20 hGH-iCJD cases with similar *PRNP* codon 129 genotypes and PrP^{res} types (blue). The mean lag time for the iCJD cases as a group is significantly longer than that for the sCJD cases (Student's t-test, p=0.0004), indicating that there is no evidence of enhanced propagation of hGH-iCJD PrP^{Sc} seeds as assessed by RT-QuIC PrP substrate conversion.
Diagram (b) shows the differences in the RT-QuIC reactions for 3 sCJD MM1 cases (red), 3 hDM-iCJD MM1 cases (green), the single hGH-iCJD MM1 case (dark blue) and the single hGH-iCJD MMi case (light blue). The sCJD MM1 cases appear to have the shortest lag times in comparison with the iCJD cases as a group, as also demonstrated in diagram (A) above. However, there are differences between the hGH-iCJD cases, with the MMi case showing a more prolonged lag time and slower RT-QuIC reaction course than the MM1 case.

The Shapiro-Wilk normality test was used to determine whether or not the RT-QuIC lag periods in the various iCJD and sCJD subgroups were normally distributed. In the statistical analysis of RT-QuIC data, a two-sided Mann-Whitney test was used to assess the statistical significance of differences between the median RT-QuIC lag periods of sCJD versus hGH-iCJD or hDM-iCJD cases. The Kruskal-Wallis test was used for the combined analysis of sCJD (VV2, MV2, MM1) and hGH-iCJD (VV2, MV2) subgroups.

Abbreviations: hDM: human dura mater; hGH: human growth hormone; i: intermediate; iCJD: iatrogenic Creutzfeldt-Jakob disease; M: methionine; *PRNP*: prion protein gene; PrP^{res}: protease-resistant prion protein; PrP^{Sc}: disease-associated misfolded prion protein; RT-QuIC: real-time quaking-induced conversion; sCJD: sporadic Creutzfeldt-Jakob disease; V: valine.

5.7.2. Protein misfolding cyclic amplification (PMCA)

The seeding characteristics of the two divergent hGH-iCJD *PRNP* codon 129 MM cases (hGH-iCJD20 and hGH-iCJD21) were further examined using PMCA. Samples of cerebral cortex were used to seed matched (*PRNP* codon 129 MM, designated HuMM) and mis-matched (*PRNP* codon 129 VV and codon 129 MV) humanised transgenic mouse brain substrates, (designated HuVV and HuMV respectively) and the results compared with those from seeds of sCJD MM1, MV2 and VV2 subtypes and hDM-iCJD MM1 seeds. PMCA reactions seeded with cerebral cortex samples from cases of sCJD of the MM1 subtype amplified poorly under the conditions used, whether in matched (MM) or mismatched (VV) humanised transgenic mouse brain substrate (Figure 5.27a). This was also true for the seeds from the three hDM-iCJD cases (hDM-iCJD1-3) (Figure 5.27a). The sCJD MV2 and hGH-iCJD MV2 seeds also gave similar results.

Seeding of PMCA reactions with cerebral cortex samples from cases of sCJD of the VV2 subtype amplified more efficiently under these same conditions, with the amplification levels higher in the matched (VV) than in the mis-matched (MM) humanised transgenic mouse brain substrate (Figure 5.27a). The two hGH-iCJD *PRNP* codon 129 MM cases gave divergent results: hGH-iCJD20 amplified well and more efficiently in the HuVV substrate than the MM and MV substrates, whereas hGH-iCJD21 failed to seed any of the three substrates efficiently (Figure 5.27b). This difference in amplification efficiency and substrate preference between hGH-iCJD20 and hGH-iCJD21 was independent of seeding dilution (Figure 5.27a, b).

Figure 5.27.

PMCA reactions in Tg human *PRNP* codon 129 MM, MV and VV mouse brain substrates seeded with sCJD and iCJD brain homogenates

a

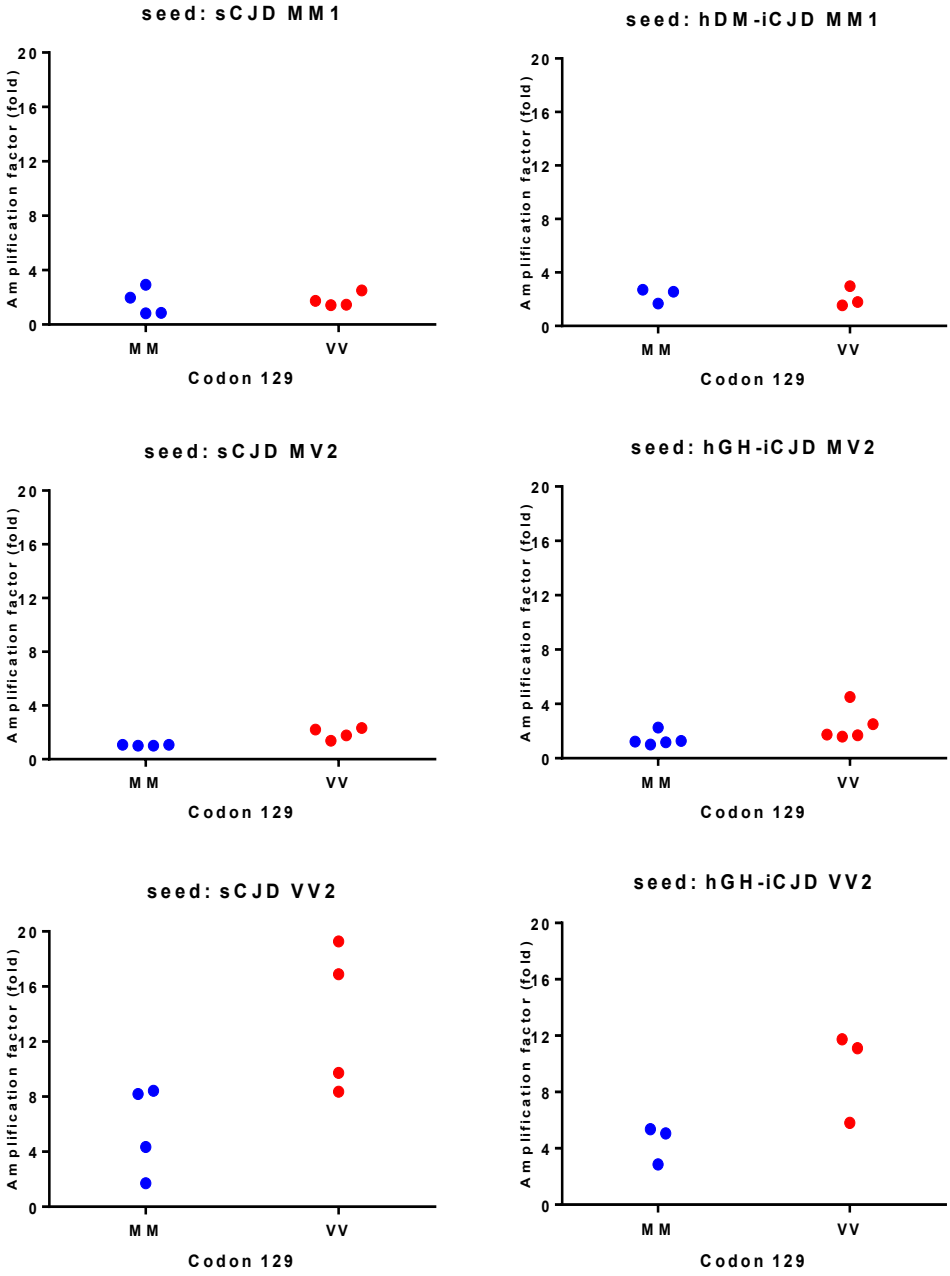

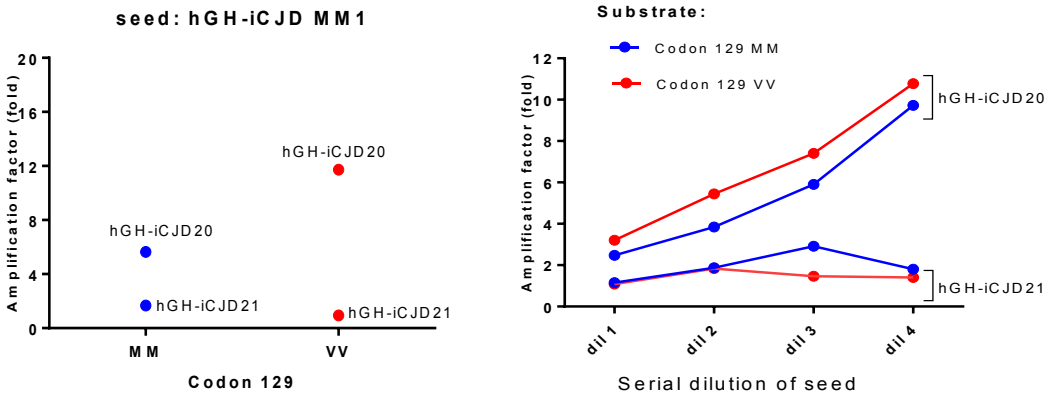
seed: hGH-iCJD MM1
Amplification factor (fold)
20
16
12
8
4
0
hGH-iCJD20
hGH-iCJD20
hGH-iCJD21
hGH-iCJD21
MM
VV
Codon 129
Substrate:
Codon 129 MM
Codon 129 VV
Amplification factor (fold)
12
10
8
6
4
2
0
hGH-iCJD20
hGH-iCJD21
dil 1
dil 2
dil 3
dil 4
Serial dilution of seed

b

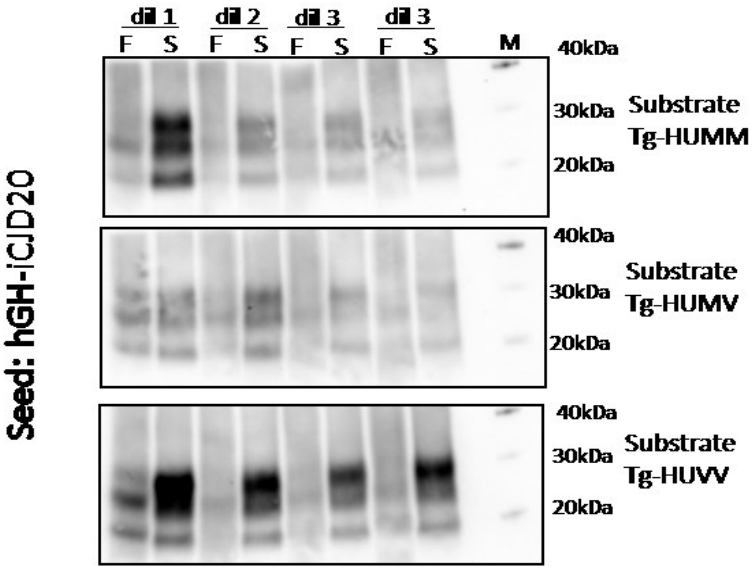
Seed: hGH-iCJD20
dil 1
dil 2
dil 3
dil 3
F S F S F S F S
M
40kDa
30kDa
20kDa
Substrate
Tg-HUMM
Substrate
Tg-HUMV
Substrate
Tg-HUVV

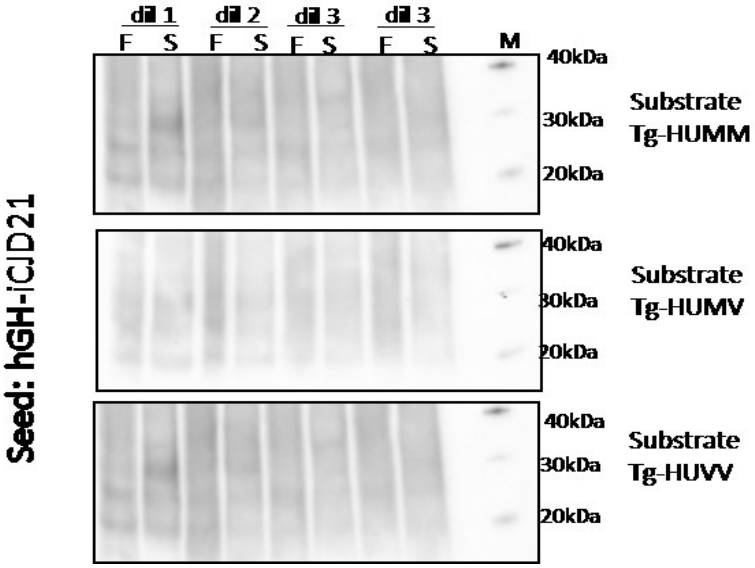
Seed: hGH-iCJD21
dil 1
dil 2
dil 3
dil 3
F S F S F S F S
M
40kDa
30kDa
20kDa
Substrate
Tg-HUMM
Substrate
Tg-HUMV
Substrate
Tg-HUVV

Legend for Figure 5.27.

In (a) hGH-iCJD, hDM-iCJD and sCJD brain homogenate (seeds) were diluted in humanised transgenic mouse brain homogenate (substrates) of *PRNP* codon 129 MM and VV genotypes. The PMCA amplification factor is shown as relative increase (fold) in PrP^{res} signal after a single round of PMCA as determined by densitometry of the Western blot signal. PMCA reactions were normalised by seed PrP^{res} amount.

Similar low levels of amplification are seen with sCJD MM1 and hDM-iCJD MM1 seeds in the Tg MM and VV substrates, and with sCJD MV2 and hGH-iCJD MV2 seeds. In contrast, the sCJD VV2 and hGH-iCJD VV2 seeds show amplification in Tg MM and VV substrates, although the levels of amplification with the hGH-iCJD seeds are lower. Amplification results are shown for sCJD MM1, MV2 and VV2 seeds, hDM-iCJD MM1 seeds and hGH-iCJD MV2, VV2, MM1 (hGH-iCJD21) and MMi (hGH-iCJD20) seeds in Tg mouse brain MM (blue) and VV (red) substrates.

Diverse results are seen with amplification of the two hGH-iCJDMM cases. Case hGH-iCJD21 (MM1) shows low levels of amplification in Tg mouse brain MM and VV substrates. However, case hGH-iCJD20 (MMi) shows higher levels of amplification in the Tg MM and VV substrates, similar to those seen with sCJD VV2 and hGH-iCJD VV2 seeds (a). Humanised transgenic mouse brain homogenate (substrate) of the *PRNP* codon 129 MM (red) or VV (blue).

These differences were maintained on PMCA of serial dilutions of the hGH-iCJD MM seeds in all three Tg mouse brain substrates: Tg MM, MV and VV (hGH-iCJD20: 1/50, 1/100, 1/200, 1/400 and hGH-iCJD21: 1/4, 1/8, 1/16, 1/32). Results are shown as Western blots for all three Tg mouse substrates (b). PMCA experiments seeded with hGH-iCJD, hDM-iCJD and sCJD samples were performed twice independently and repeated at least 4 times for the hGH-iCJD MM cases.

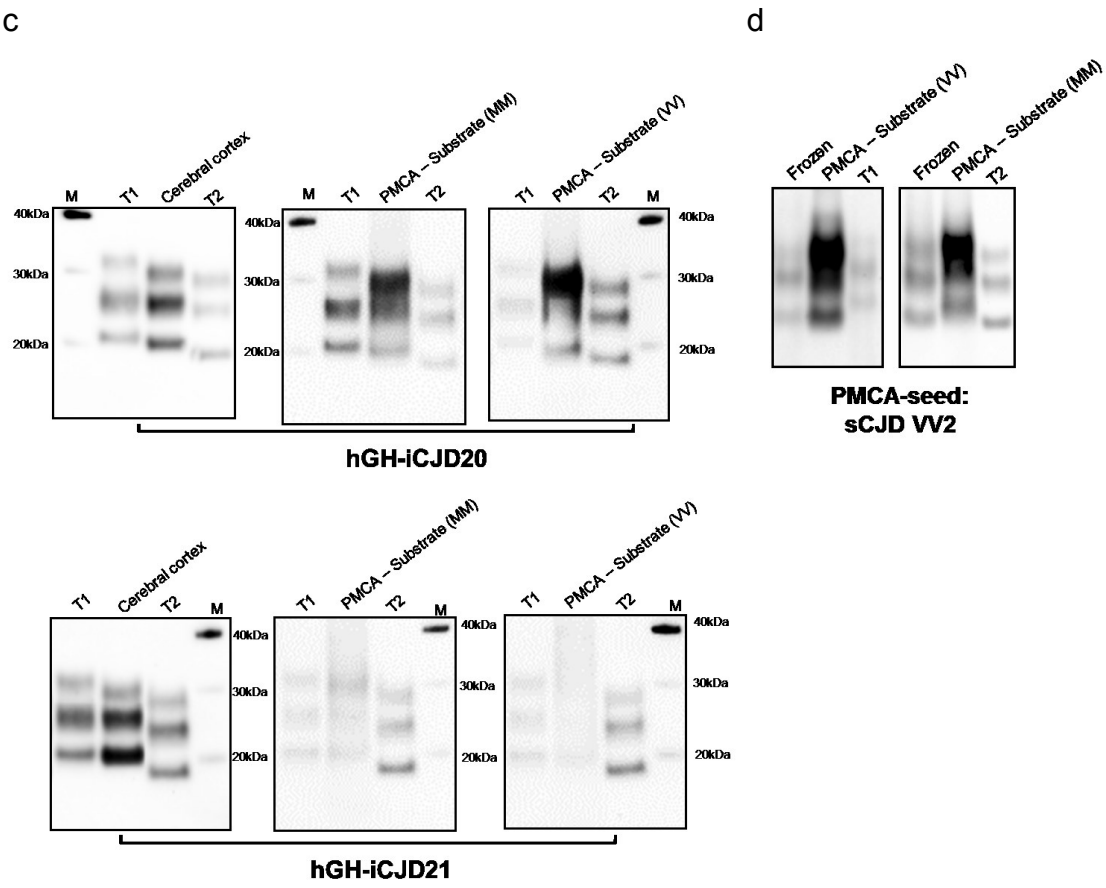

In (c), the PrP^{res} types of MM hGH-iCJD cases 20 and 21 are assessed before and after PMCA. PMCA reactions employed matched (MM) and mis-matched (VV) *PRNP* Tg mouse brain substrates. Each sample was run between a type 1 (left lane) and type 2 (right lane) reference standards from sCJD MM1 and VV2 subtype cases respectively (T1 and T2). Study identification numbers of the hGH-iCJD MM cases are indicated.

In (d), PrP^{res} analysis of sCJD VV2 PMCA products detected by Western blot. sCJD VV2 brain homogenate was diluted and amplified in matched (MM) and mismatched (VV) codon 129 substrate by a single round of PMCA. Samples corresponding to unamplified (Frozen) and amplified (PMCA) aliquots are shown with reference standards as described above. A total of 25 biological replicates of hGH-iCJD, hDM-iCJD and sCJD were analysed.

Abbreviations: hDM: human dura mater; hGH: human growth hormone; i: intermediate; iCJD: iatrogenic Creutzfeldt-Jakob disease; M: methionine; PMCA: protein misfolding cyclical amplification; *PRNP*: prion protein gene; PrP^{res}: protease-resistant prion protein; sCJD: sporadic Creutzfeldt-Jakob disease; Tg: transgenic; V: valine.

In the case of hGH-iCJD20, the choice of *PRNP* codon 129 substrate (HuMM or HuVV) also had an effect on the PrP^{res} type of the PMCA product when analysed by Western blotting (Figure 5.27c). The cerebral cortex sample from hGH-iCJD20 was PrP^{res} type i, but matching of the MMi seed with the HuMM substrate resulted in an up-shift in mobility of the reaction product, whereas mismatching the MMi seed with the HuVV substrate resulted in an apparent down-shift in mobility of the reaction product. hGH-iCJD21 amplified only poorly, and there was no evidence of any change in the type 1 PrP^{res} when the PMCA products were analysed by Western blotting (Figure 5.27c). The possibility that PrP^{res} type i results from replication of sCJD with type 2 PrP^{res} in an individual with a *PRNP* codon 129 MM genotype was then modelled. When sCJD VV2 subtype brain homogenate was used to seed the HuMM substrate, an upward shift was seen, whereas amplification of the same seed in a *PRNP* codon 129 VV genotype resulted in conservation of the type 2 PrP^{res} (Figure 5.27d).

5.7.3. Comparison of the two hGH-iCJD *PRNP* codon 129 MM cases

PRNP codon 129 MM is the rarest genotype within the UK hGH-iCJD cohort and tends to occur later during the epidemic. The two hGH-iCJD *PRNP* codon 129 MM cases with frozen tissue available to this study were divergent in their neuropathology, PrP^{res} type and amplification potential in both the RT-QuIC and PMCA assays. In each of these respects hGH-iCJD21 resembled the sCJD MM1 subtype (and the limited number of hDM-iCJD MM1 cases analysed), whereas hGH-iCJD20 more closely resembled the sCJD MV2 or VV2 subtype, despite its *PRNP* codon 129 MM genotype. A summary of the key differences between cases hGH-iCJD20 and hGH-iCJD21 is provided in Table 5.11.

Table 5.11.

Comparison of hGH-iCJD20 and hGH-iCJD21

	hGH-iCJD20	**hGH-iCJD21**
Age at death (y)	46	42
Sex	Male	Male
Underlying cause of GH deficiency	Idiopathic hGH deficiency	Craniopharyngioma
Duration of hGH treatment (y)	2.8	8.1
Duration of HWP-hGH treatment (y)	0.5	3.3
Incubation period (y)	29.4	31.7
***APOE* genotype**	ε3/3	ε3/3
***PRNP* codon 129 genotype**	MM	MM
Neuropathology	PrP positive kuru plaques present (similar to MV2K sCJD).	Diffuse PrP positivity (resembling MM1 sCJD and hDM-iCJD).
CNS Aβ accumulation	Negative	Negative
RT-QuIC seeding activity	Long lag time	Shorter lag time (closer to MM1 sCJD)
PrP^{res}	type i (~20kDa)	type 1 (~21kDa)
PMCA efficiency	Greater	Poor
PMCA substrate preference	VV > MM	None
PMCA product PrP^{res} mobility	Substrate MM → Upshift Substrate VV → Downshift	type 1

Abbreviations: Aβ: amyloid beta; *APOE*: apolipoprotein E gene; CAA: cerebral amyloid angiopathy; hDM: human dura mater; hGH: human growth hormone; HWP-hGH: human growth hormone produced using the Hartree modification of the Wilhelmi protocol; i: intermediate; iCJD: iatrogenic Creutzfeldt-Jakob disease; K: kuru plaque; kDa: kilodalton; M: methionine; PMCA: protein misfolding cyclical amplification; *PRNP*: prion protein gene; PrP^{res}: protease-resistant prion protein; RT-QuIC: real-time quaking-induced conversion; sCJD: sporadic Creutzfeldt-Jakob disease; Tg: transgenic; V: valine; y: years.

6. Discussion

6.1. Introduction

This thesis describes the findings of a detailed neuropathological and molecular genetic study of the largest series of iCJD cases occurring in recipients of hGH in the UK (or indeed in any other country). Without Coroners and Procurators Fiscal instructing an autopsy to be performed on these patients to determine the cause of death, or clinicians seeking consent for a hospital autopsy and, most importantly, the generosity of the relatives of the deceased in giving consent/authorisation for the subsequent retention of the brain and use of the retained tissue and accompanying clinical data in research, this study could not have taken place.

6.2. hGH-iCJD epidemiology, genetics and prion strains

6.2.1. hGH-iCJD epidemiology and genetics

The results of this study indicate that hGH-iCJD epidemic in the UK occurred first in patients with the *PRNP* codon 129 VV and MV genotypes, and later emerged in the codon 129 MM genotype, in keeping with the recent findings of Rudge *et al*. (Rudge *et al*., 2015). A report of eight recent UK hGH-iCJD cases not included in this study comprised six codon 129 MV and two codon 129 MM cases, but no codon 129 VV cases (Jaunmuktane *et al*., 2015). The *PRNP* codon 129 genotype has a major effect on the hGH-iCJD disease incubation period, with codon 129 MM cases having the longest incubation periods (up to 32y) (Table 5.1; Figure 5.2). This polymorphism also influences the duration of the illness, with codon 129 MV cases having the longest clinical duration (up to 32mo) (Table 5.1; Figure 5.2). This polymorphism also influenced the disease incubation period in kuru, with the longest incubation periods

(over 40 years) occurring in codon 129 MV patients (Collinge *et al*., 2006). However, the codon 129 MM kuru cases had the shortest incubation periods, in contrast to the UK hGH-iCJD cases. In another acquired human prion disease, vCJD, all but one of the definite cases occurring worldwide were codon 129 MM patients, but the most recent UK patient (who died in 2016) had the codon 129 MV genotype (Figure 1.6). The incubation periods in cases of vCJD are still uncertain; it is entirely possible that further cases of vCJD will emerge in the MV and the VV genotypes in the UK.

The *PRNP* codon 129 polymorphism also has a major influence on the clinicopathological phenotype in sCJD and some forms of genetic CJD (Head *et al*., 2015). In sCJD, six major subgroups are defined by the combination of this polymorphism and the brain PrP^{res} type (Table 1.3). In contrast to UK hGH-iCJD, the codon 129 MM genotype occurs most frequently in sCJD, but within this genotype the duration of illness is greatly influenced by the brain PrP^{res} isoform: MM1 cases have a median duration of illness of 3mo, while MM2 patients have a median duration of illness of 17mo (Table 1.3). The four codon 129 MM hGH-iCJD cases in this study have a median duration of illness of 5.5mo (range 5-8mo). Only two of these cases had frozen tissue available to determine the brain PrP^{res} isoform; the MM1 case had a duration of illness of 8mo, while the MMi case had a duration of illness of 5mo (Table 5.10). No hGH-iCJD MM2 cases were found in this study.

6.2.2. Prion contamination of hGH preparations

Iatrogenic CJD in hGH recipients is believed to result from contamination of hGH preparations for intramuscular injection with prions present in the pituitary glands

collected from hGH extraction. PrP^{res} is detectable in the pituitary gland in sCJD and vCJD (Peden *et al*., 2007) and this study also identified PrP^{res} in the pituitary gland in patients with hGH-iCJD (Figure 5.20). The most likely source of prions in hGH preparations is sCJD, which is the commonest form of human prion disease and occurs most frequently in elderly patients, who account for the majority of the hospital autopsies that were the main source of pituitary glands collected for hGH extraction. Another possible, but less likely, source of prion infectivity in pituitary glands collected in the UK is genetic CJD, which accounts for around 10% of all CJD cases, but tends to occur at a younger age than sCJD (Head *et al*., 2015). The first case of vCJD in the UK presented in 1995, so it is highly unlikely that any of the UK hGH preparations were infected with vCJD prions. Although the very large number of pituitary glands collected for hGH extraction in the UK up to 1985 may have included glands from more than a single case of CJD of either sporadic or genetic origin, this thesis proposes that infection with a single prion strain is the most likely explanation for the epidemiology and genetic features of hGH-iCJD in the UK.

6.2.3. Prion strains in hGH-iCJD

Prion transmission is substantially influenced by the strain of the infectious prion and the host prion protein genotype, which interact to determine disease susceptibility, incubation period and clinicopathological phenotype. The results of this study reflect these influences; both the incubation period and the duration of illness in the hGH-iCJD cases are influenced by the *PRNP* codon 129 polymorphism, which also influences the neuropathological phenotype in conjunction with the PrP^{res} isoform in the brain. According to the concept of molecular strain typing, brain PrP^{res} isoforms

are surrogate markers for agent strain, since they reflect the differences in PrP^{Sc} conformation that are responsible for individual strain properties (Parchi *et al*., 1999; Haik *et al*., 2011). The commonest form of sCJD is the MM1 subtype, in which the M1 strain of sCJD prions has been identified, while the second commonest sCJD prion strain, the V2 strain, is identified in both sCJD VV2 and sCJD MV2 (see section 1.5.1.5). It is therefore conceivable that the predominance of hGH-iCJD patients in the *PRNP* codon 129 VV and MV genotypes in the UK might result from infection with the V2 sCJD strain, while the predominance of hGH-iCJD patients in the *PRNP* codon 129 MM genotype in France (see section 2.1.5) might result from infection with a different strain of sCJD prions (Brandel *et al*., 2003), specifically the M1 strain. Experimental transmission studies of hGH-iCJD cases of differing *PRNP* codon 129 genotype from both France and the UK are required to address these possibilities; such experiments are currently underway (Andreoletti *et al*., 2016).

6.3. hGH-iCJD neuropathology and biochemistry

6.3.1. Neuropathology

The neuropathological phenotype in sCJD is determined largely by the *PRNP* codon 129 genotype of the patient and the PrP^{res} isoform in the brain (Figure 1.5). Since sCJD is the most likely source of the prion infectivity responsible for hGH-iCJD, the question arises as to whether the neuropathological phenotype in hGH-iCJD is subject to similar influences. The results in the 21 hGH-iCJD cases with frozen brain tissue available for biochemical analysis show that many of the hGH-iCJD cases showed a similar neuropathological phenotype to the recognised sCJD subtypes. This was particularly true for the seven *PRNP* codon 129 VV hGH-iCJD cases, which had both

a neuropathological phenotype very similar to the sCJD VV2 subtype and an identical PrP^{res} brain isoform (type 2) on Western blot examination. The neuropathological features of the sCJD MV2 subtype are variable and can be subclassified according to the presence of kuru-type plaques in the cerebellum (MV2K) or the presence of confluent vacuolation in the cerebral cortex with perivacuolar PrP accumulation on IHC, but no kuru–type plaques (MV2C). Some cases of sCJD MV2 contain both kuru-type plaques in the cerebellum and confluent vacuolation in the cerebral cortex, when the term MV2K+C is used (Parchi *et al*., 1999). In addition to this neuropathological heterogeneity, there is also biochemical heterogeneity in this subgroup. The MV2K sCJD subtype is characterised by PrP^{res} type i+2 (a doublet of approximately 20 kDa (intermediate) and 19 kDa (type 2)) in the brain, whereas the MV2C subtype is characterised by a type 2 brain PrP^{res} only (Parchi *et al*., 2009; Kobayashi *et al*., 2013). The 12 codon 129 MV hGH-iCJD cases all showed a neuropathological phenotype similar to the sCJD MV2K subtype, with characteristic kuru-type plaques present in the cerebellum and occasionally in the cerebrum. All these cases contained a mixture of type 2 and intermediate (20 kDa) brain PrP^{res} isoforms, but only 3/12 showed confluent vacuolation in the cerebral cortex.

6.3.1.1. *Atypical neuropathological phenotypes*

The two *PRNP* codon 129 MM cases with frozen tissue available for brain PrP^{res} analysis in this study showed divergent neuropathological phenotypes, with case hGH-iCJD21 exhibiting the typical features of sCJD MM1, accompanied by brain PrP^{res} type 1 on Western blot examination. In contrast, case hGH-iCJD20 showed an atypical phenotype with kuru-type plaques in the cerebellum and cerebral cortex, and confluent

vacuolation in the cerebral cortex, resembling sCJD MV2K+C. Western blot examination found an intermediate (20 kDa) brain PrP^{res} isoform alone in all six brain regions examined, with no type 1 or type 2 PrP^{res} identified. The two additional hGH-iCJD cases with *PRNP* codon 129 MM (but no frozen tissue available for WB analysis) also showed a divergent neuropathological phenotype; case hGH-iCJD35 showed neuropathological features similar to the sCJD MM1 subtype, while
hGH-iCJD31 showed atypical features, with some similarities to the sCJD VV2 histotype, perhaps reflecting incomplete adaptation of the infecting V2 prion strain in this codon 129 patient.

6.3.1.2. *The significance of kuru-type plaques in iCJD*

In a recent report, three *PRNP* codon 129 MM genotype hGH-iCJD cases from the USA all had a type 1 brain PrP^{res} isoform (Cali *et al.*, 2015). However, one of the cases (case 1) had kuru-type plaques in the brain and other neuropathological similarities to the MMi case in this study, while the others resembled the sCJD MM1 phenotype. The apparent discrepancy between the brain PrP^{res} isoforms between the USA and UK codon 129 MM cases with kuru-type plaques is likely to reflect methodological differences in the Western blotting technique used in these studies, since the technique used in the USA study is not optimised for the detection of intermediate-sized PrP^{res} isoforms.

Kuru-type amyloid plaques have reported in other cases of *PRNP* codon 129 MM genotype hGH-iCJD in France (Billette de Villemeur *et al*., 1994; Delisle *et al*., 1993) and in the UK (Markus *et al*., 1992); however, not all of the French codon 129 MM

hGH-iCJD cases contain kuru plaques (Billette de Villemeur *et al*., 1994). No data on brain PrP^{res} isoforms is available in these studies. The authors of these reports and the recent USA report (Cali *et al*., 2015) noted that the disease duration in the French and USA codon 129 MM cases with kuru plaques (10-36mo) was longer than in the two USA codon 129 MM cases without plaques (2mo). However, this is not the case for an additional codon 129 MM hGH-iCJD case resembling sCJD MM1 from the Netherlands (Croes *et al*., 2002), who died 11mo after the onset of the first symptoms of the disease. In this study, the codon 129 MM cases resembling sCJD MM1 and without kuru-type plaques had durations of illness of 6mo and 8mo, while the two codon MM cases with atypical neuropathology containing kuru-type plaques each had a duration of illness of 5mo, indicating that the relationship between atypical neuropathology with kuru plaques and the duration of the clinical illness is not predictable.

Similar neuropathological diversity has also been described in the 142 cases of hDM-iCJD in Japan. The majority (68%) resemble the sCJD MM1 subtype in terms of the clinical features, neuropathology and brain PrP^{res} isoform. The remaining 32% contain kuru-type amyloid plaques in the brain and are referred to as plaque-type dura mater-associated iCJD (Kobayashi *et al*., 2014); these cases also contain an intermediate (20kDa) brain PrP^{res} band on Western blot examination. The experimental transmission properties and *in vitro* conversion properties in both the non-plaque and plaque hDM-iCJD cases in Japan have been extensively investigated (see below). The three UK cases of hDM-iCJD with data on brain PrP^{res} isoforms in this study all belonged to the codon 129 MM group and all had PrP^{res} type 1 in the brain (Table 5.6).

The neuropathology in all three cases resembled that of the sCJD MM1 subtype, with no kuru-type plaques present.

Kuru-type amyloid plaques have also been reported on several occasions in atypical cases of sCJD in *PRNP* codon 129 MM patients, sometimes in the white matter alone (Schoene *et al*., 1981; Ishida *et al*., 2003; Kobayashi *et al*., 2008; Gelpi *et al*., 2013; Berghoff *et al*., 2015). On the basis of the identification of the plaque hDM-iCJD cases in Japan, it has been suggested that the presence of kuru-type places in an apparent sporadic CJD case in a *PRNP* codon 129 MM patient should raise the possibility of an iatrogenic origin, particularly if the intermediate 20kDa brain PrP^{res} isoform is also detected (Kobayashi *et al*., 2016); this suggestion has been explored further by experimental transmission studies and *in vitro* conversion studies.

6.3.1.3. *Neuropathological comparisons in hGH-iCJD and sCJD*

Despite this suggestion, it is clear from this study that most cases of hGH-iCJD in the UK have a neuropathological and biochemical phenotype that is indistinguishable from sCJD when it occurs in VV2, MVi+2 and MM1 patients (Table 5.6), which as a group account for 20/21 the hGH-iCJD cases in which both *PRNP* codon 129 genotype and PrP^{res} isoform data are available. Of the remaining 14 cases, only one case (hGH-iCJD 31) had an atypical neuropathological phenotype, while the others could all be assigned a histotype that corresponded to one of the recognised sCJD histotypes. Particular care must be taken in interpreting the neuropathological findings in the five cases in which neither *PRNP* codon 129 genotype nor PrP^{res} isoform data are available (hGH-iCJD25, 29, 30, 32 and 33) (Table 5.6). Case 25 resembled the sCJD MM/MV1

histotype, while cases 29, 30 and 32 resembled the sCJD VV2 histotype. Case 33 resembled the sCJD MM/MV2K histotype; however, the possibility that this case could have a MM genotype and an intermediate PrP^{res} brain isoform (as in case 20, Table 5.6) cannot be excluded. Even if this were so, over 90% (32/35) of the UK hGH-iCJD cases would have neuropathological and biochemical features that are indistinguishable from one of the sCJD histotypes; a detailed clinical history of iatrogenic exposure to CJD prions is therefore essential for diagnosis.

Rudge *et al*. (Rudge *et al*., 2015) have reported that the UK hGH-iCJD patients tend to have a clinical history that begins with gait ataxia and lower limb dysaesthesiae rather than the rapidly progressive dementia that is typical, but by no means universal, in sCJD. Patients in the sCJD VV2 subtype and, to a lesser extent, the MV2 subtype can have a clinical presentation with gait ataxia (see section 1.5.1.3). The clinical features noted by Rudge *et al*. may therefore simply reflect the large predominance of VV2 and MVi+2 cases in the UK hGH-iCJD cohort, rather than specific features indicative of hGH-iCJD.

6.3.2. Biochemistry and experimental transmission

6.3.2.1. *The concept of the traceback phenomenon*

A molecular traceback phenomenon was proposed Kitamoto and co-workers to explain the phenotypic diversity of MV2 sCJD cases, and the transmission properties and origin of hDM-iCJD in Japan (Kobayashi *et al*., 2007, 2010, 2013). These experiments are represented diagrammatically in Figure 6.1. Transmission of the V2 prion strain from sCJD VV2 into transgenic mice expressing human *PRNP* codon 129

MM was only achieved after a lengthy incubation period. Examination of these mouse brains found amyloid plaques (not present in human sCJD VV2) and an intermediate PrP^{res} type, termed type i. Subsequent passage into transgenic mice expressing either human *PRNP* codon 129 MM or codon 129 VV found that the codon 129 VV mice were highly susceptible to infection in comparison with the codon 129 MM mice. The prions generated in the initial transmission of sCJD VV2 into codon 129 MM transgenic mice (which were necessarily composed of PrP^{Sc} with methionine at codon 129) exhibited a traceback phenomenon on subsequent passage, since they transmitted preferentially to transgenic mice with the codon 129 VV genotype from which they originated. We have modelled the traceback phenomenon in hGH-iCJD prions using PMCA reactions with *PRNP* codon 129 MM and VV substrates in place of the corresponding transgenic mice used by Kobayashi *et al*.

6.3.2.2. The traceback phenomenon in hGH-iCJD: in vitro modelling

The molecular mechanism of the traceback phenomenon is not fully understood, but the data of Kitamoto and co-workers indicates that PrP^{res} type i is a key component of this phenomenon and may indicate a transitional phase of prion adaptation in a host of differing codon 129 genotype (Kobayashi *et al*., 2007, 2013). PrP^{res} type i is also associated with the presence of kuru-type PrP amyloid plaques in the brains of both transgenic mice and humans, perhaps reflecting a high propensity for β-sheet formation and higher order aggregation of this intermediate prion isoform.

Figure 6.1. The molecular traceback phenomenon in experimental prion transmission studies (modified from Kobayashi *et al*., 2014)

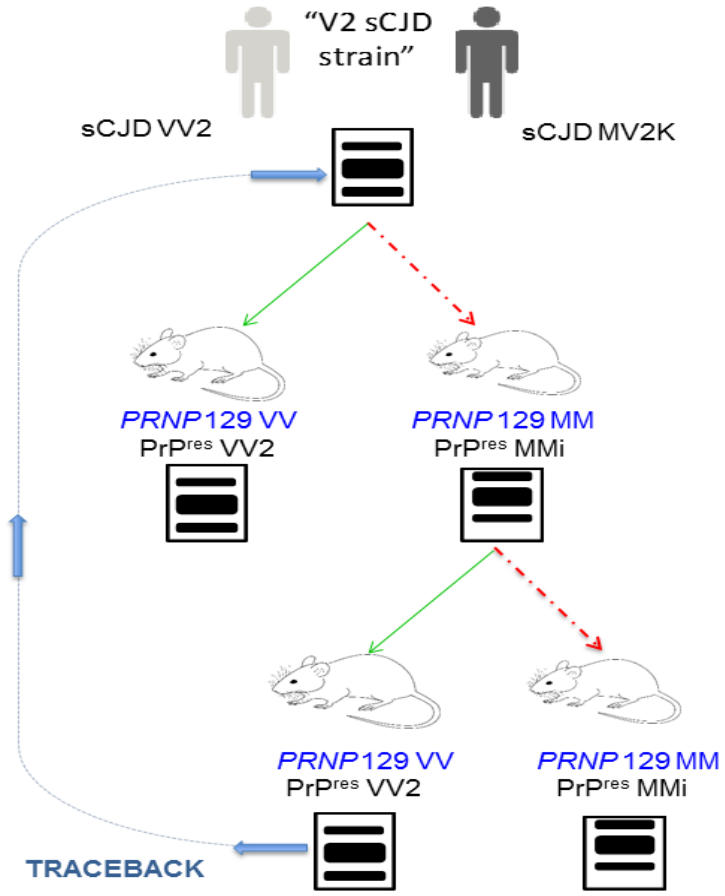

Inoculation of the sCJD V2 strain into humanised transgenic mice with different *PRNP* codon 129 genotypes found rapid transmission (green) into the VV mice, generating VV2 prions, but inefficient transmission (red) across the genotypic barrier to the MM mice, generating MMi prions. Subsequent transmissions of these MMi prions found rapid transmission across the genotypic barrier (green) to the VV mice, generating VV2 prions, but inefficient transmission (red) with no genotypic barrier to the MM mice. The preference of MMi prions to replicate in VV mice and produce VV2 prions demonstrates a molecular traceback to the original sCJD V2 prion strain.

Abbreviations: i: intermediate type PrP^{res}; M: methionine; *PRNP*: human prion protein gene; PrP^{res}: protease-resistant prion protein; sCJD: sporadic Creutzfeldt-Jakob disease; V: valine.

This group has also proposed that kuru plaques in *PRNP* codon 129 MM apparent sCJD cases can be used as an indication of an iatrogenic aetiology with a traceback potential (Kobayashi *et al*., 2015, 2016). The neuropathological and biochemical characterisation of case hGH-iCJD20 in this study supports this proposal and extends the traceback phenomenon to include UK hGH-iCJD in addition to hDM-iCJD in Japan. The association of a *PRNP* codon 129 MM genotype with kuru plaques in three national independent hGH-iCJD cohorts (France, USA and UK) adds further weight to this phenomenon. The data reported in this study from PMCA experiments (Figure 5.19) confirm that the traceback phenomenon in hGH-iCJD can be modelled in cell-free systems in addition to animal transmission studies, as predicted for hDM-iCJD by Kobayashi *et al*. (Kobayashi *et al*., 2016) and subsequently demonstrated by Takeuchi *et al*. (Takeuchi *et al*., 2016) using PMCA.

6.3.2.3. *In vitro modelling: implications for human to human transmission*

The results of the in vitro conversion studies using RT-QuIC and PMCA did not support the hypothesis that human to human transmission of CJD results in acquired replicative efficiency (Xiao *et al*., 2014), but instead indicated the opposite. The RT-QuIC assay showed consistently reduced seeding activity in hGH-iCJD and hDM-iCJD in comparison to matched sCJD subtypes, indicating that secondary transmission of sCJD in human does not result in an enhanced propensity for PrP^{C} conversion. Similar findings were noted in the PMCA studies, where the amplification factors achieved by the hGH-iCJD seeds were never higher than the corresponding matched sCJD seeds in identical substrates.

While these results may appear reassuring in terms of any public health concerns over the secondary transmission of prion infectivity from hGH-iCJD patients, the current steps to identify hGH recipients who are about to undergo surgery or donate blood should remain in place (see section 1.5.7.1). The (admittedly preliminary) novel finding in this study of abnormal prion protein accumulation in lymph nodes in hGH-iCJD (Table 5.9) indicates a potential for prion infectivity in non-CNS tissues in hGH-iCJD.

The UK experience with hGH-iCJD and other acquired human prion diseases indicates that the consequences of exposure can be manifested over a considerable period of time, not only as a result of primary exposure to the infectious prions, but also to secondary transmission as a consequence of prion infectivity in non-CNS tissues, as has occurred in the cases of secondary vCJD associated with blood transfusion. These prolonged consequences also reflect the lengthy incubation periods in acquired human prion diseases, which in turn are influenced by the *PRNP* codon 129 genotypes in the exposed population. The occurrence of a new case of vCJD in the *PRNP* codon 129 MV genotype in 2016, some three years after the last *PRNP* codon 129 MM patient (Figure 1.6) and twenty years after vCJD was first identified (Will *et al*., 1996) exemplifies this point.

6.3.3. Origin of the UK hGH-iCJD epidemic

The data presented in this thesis support the hypothesis that the hGH-iCJD epidemic in the UK results from infection with the V2 sCJD strain. The *PRNP* genotypes of the hGH treated patient cohort, if similar to the UK blood donor population would be 44%

MM, 45% MV and 11% VV (Bishop *et al*., 2009). Exposure of the *PRNP* codon 129 VV hGH-iCJD recipients to the V2 sCJD strain cases could explain the early emergence of iCJD in this subgroup in the absence of a genotypic barrier and relatively short incubation periods. The subsequent appearance of more cases in *PRNP* codon 129 MV recipients may reflect both a larger genotypic barrier to transmission and the larger numbers of *PRNP* codon 129 MV individuals in the hGH treated patient group. Finally, the appearance of a limited number of *PRNP* codon 129 MM hGH-iCJD cases later in the epidemic could be interpreted as evidence of a substantial *PRNP* codon 129 genotypic barrier to transmission of V2 sCJD strain, resulting in prolonged incubation periods.

Although the possibility of a mixture of other contaminating prion strains (e.g. the M1 strain) during the period hGH was administered in the UK cannot be excluded, the relatively late appearance of the codon 129 MM hGH-iCJD cases argues against this possibility. Since the V2 sCJD strain appears to be responsible for both VV2 and MV2 sCJD, distinguishing between these sources as the cause of the UK hGH-iCJD epidemic is difficult. This difficulty is reinforced by the recent finding that the proportion of PrP^{res} derived from the two *PRNP* M and V alleles can vary dramatically in sCJD, so heterozygous sCJD cases might in effect contain only PrP^{res} derived from the 129 V or the 129 M alleles (Moore *et al*., 2016). The proposed sources, mechanisms and resulting chronological sequence of UK hGH-iCJD cases are depicted in Figure 6.2.

Figure 6.2.

Proposed model for the UK hGH-iCJD epidemic and the study outcomes

a

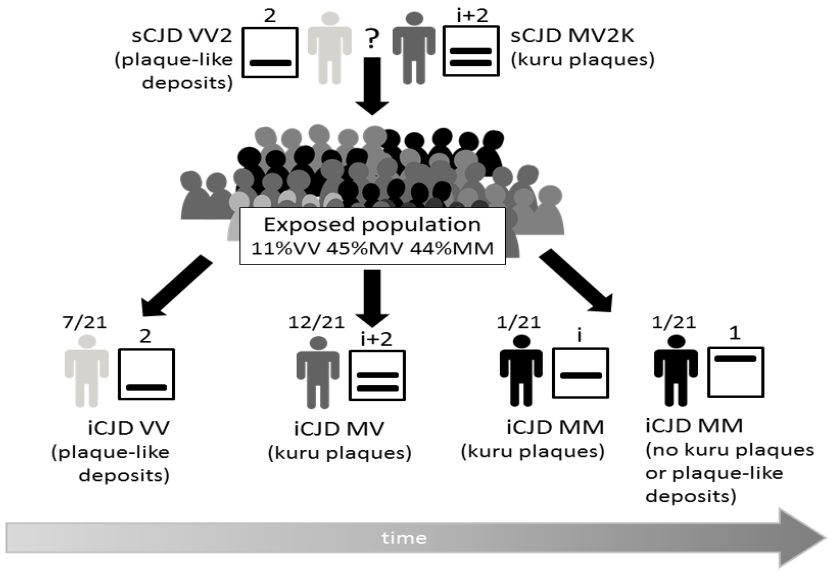

b

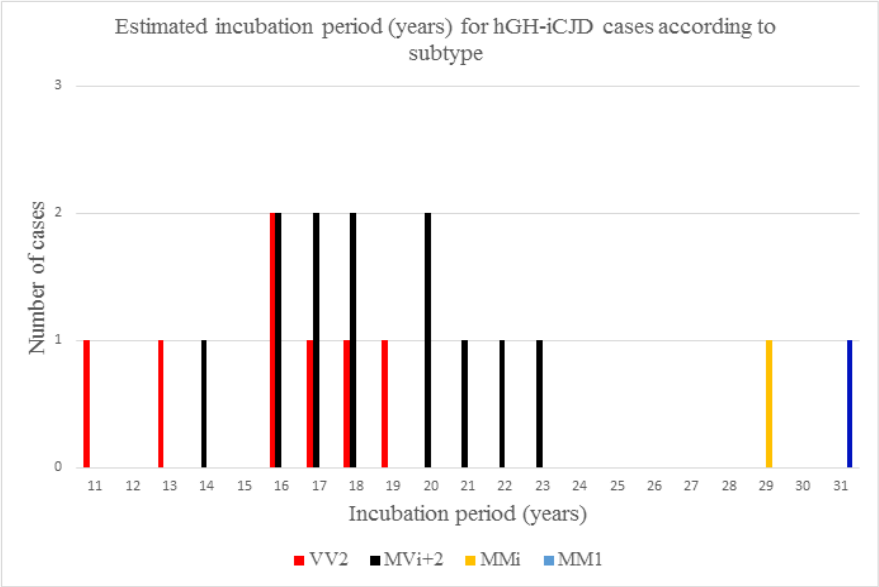

(a) A summary of the molecular and genetic findings in the 21 hGH-iCJD cases with frozen tissue available, showing correlations between *PRNP* codon 129 genotype, PrP^{res} type and pathology, the genetics of the exposed patient group and the proposed causative V2 sCJD strain (from either a sCJD VV2 or a sCJD MV2 case).

(b) Graphic representation of the numbers of hGH-iCJD subtypes (*PRNP* codon 129 genotype and PrP^{res} type) in the 21 hGH-iCJD cases with frozen tissue available plotted according to increasing estimated incubation period.

Abbreviations: CJD: Creutzfeldt-Jakob disease; hGH: human growth hormone; i: iatrogenic; M: methionine; *PRNP*: prion protein gene; PrP^{res}: protease-resistant prion protein; s: sporadic; V: valine.

6.3.4. Route and pathogenesis of hGH-iCJD infection

The route of hGH administration was by intramuscular injection, raising the question of how the infectious prions in the inoculum reach the CNS during a prolonged incubation period. Data from experimental prion transmissions by a variety of non-CNS) routes (including intramuscular and subcutaneous routes) have found variations in the peripheral pathogenesis that may reflect agent strain (Kimberlin & Walker, 1988; Mabbott & MacPherson, 2008). Some prion strains (including vCJD) replicate in lymphoid tissues (e.g. spleen, tonsil) before invading the CNS (Peden *et al*., 2004). CNS spread may occur via the blood-borne route, or by slow retrograde spread along autonomic nerve to the spinal cord and/or brainstem, then spreading to the brain itself (Mabbott & MacPherson, 2008). These complex mechanisms partly explain the lengthy incubation period in prion diseases (Kimberlin & Walker, 1988).

The results of this study on this limited amount of non-CNS tissues available give some support for involvement of the peripheral nervous system (nerves, dorsal root ganglia and trigeminal ganglia) and, in a single case, involvement of lymphoid tissues, with evidence of PrP^{res} accumulation in the germinal centres within lymph nodes. It may be that hGH-iCJD has some similarities to vCJD in terms of its peripheral pathogenesis, but the levels of PrP^{res} detected in lymphoid and peripheral nervous system structures appear lower and more restricted in distribution than in vCJD. Nevertheless, these novel findings merit further study in a relevant experimental model, which may provide support for the development of biomarkers of asymptomatic hGH-iCJD infection.

6.4. Co-pathology in hGH-iCJD

6.4.1. Pathogenesis of CNS Aβ accumulation in hGH recipients

When attempting to understand the pathogenesis of the CNS Aβ accumulation observed in the hGH-iCJD and hGH control cases in this study, the following points should be considered:

1. Source of the Aβ: this is presumed to originate from Aβ in the pituitary glands collected for hGH extraction (Irwin *et al*., 2013; Jaunmuktane *et al*., 2015), many of which are likely to have been derived from elderly patients undergoing autopsy, including patients with AD pathology and symptomatic AD (no restrictions were made on the collection of glands from patients with dementia or most other neurological disorders until 1980). The processing of the glands for hGH extraction using the modified Wilhelmi protocol may have had some effect on the Aβ aggregates in the pituitary gland, but it appears to have neither removed nor denatured the Aβ sufficiently for it to lose its capacity to act as a propagon (Eisele & Duyckaerts, 2016).
2. The investigations of the limited numbers of non-CNS tissues in this study yielded no information on the involvement of these systems in the spread of Aβ to the CNS. Possible routes include retrograde spread via the peripheral nervous system or vascular spread, as for prions.
3. The pathogenesis of CAA in AD is considered to result from failure of perivascular drainage of soluble Aβ from the brain (Keable *et al*., 2016). The similarities of the CAA in this study to that occurring in AD are considerable and include a predominant involvement of the occipital region, affecting arterioles, venules and capillaries. This implies a similar pathogenesis and

suggests that soluble Aβ accumulates in the brain before CAA becomes established in hGH recipients. CAA in hGH recipients therefore cannot be taken to provide evidence of a vascular route of spread to the CNS.

4. Analysis of co-pathology in the brains of the cohorts studied is complicated by the other existing pathologies: widespread CJD-related pathology (in hGH-iCJD, sCJD and vCJD cases) and other pathologies relating to the medical history and cause of death in the hGH controls, including recurrent brain tumours, neurosurgery and radiotherapy. Nevertheless, it has been possible to assess fully the co-pathology in these cases by performing a detailed analysis by two independent observers using internationally accepted standardised assessment criteria and recording the results in relation to the other existing pathologies, as in the cases of hDM-iCJD described by Kovacs *et al*. (Kovacs *et al*., 2016a):

6.4.2. CNS Aβ accumulation in hGH-iCJD cases and hGH controls

CNS Aβ accumulation in the cerebral cortex and/or meningeal and intraparenchymal blood vessels (including capillaries) was identified in 18/33 hGH-iCJD patients and 5/12 hGH controls. In both groups of patients, the cortical pathology varied from occasional diffuse Aβ plaques in one or more cortical regions to more widespread involvement with diffuse subpial and perivascular Aβ deposits and diffuse and neuritic Aβ plaques. No parenchymal Aβ deposition was identified in the entorhinal cortex, hippocampus, basal ganglia, thalamus, brain stem, cerebellum or spinal cord in any of these cases. The vascular Aβ pathology varied in both groups from patchy focal deposition with only occasional circumferential deposits in the meningeal vessels

(generally arterioles) to extensive deposition in meningeal and intraparenchymal vessels, including arterioles, veins and capillaries, with dyshoric vessels. One hGH control case also showed early vasculopathy, with splitting of occasional vessel walls. Overall, there were no major differences in the nature or range of severity of the pathology between the hGH-iCJD and hGH control groups (Table 5.7).

No significant differences were found between the Aβ positive and Aβ negative cases in hGH-iCJD and hGH control groups in terms of the time period or duration of their hGH treatment, although there was a trend for the hGH controls with Aβ pathology to have been treated with hGH in an earlier time period ($p=0.054$) and for longer ($p=0.077$) than the Aβ negative cases. The most severe Aβ pathology tended to occur in the patients who had survived for longest after the end of their hGH treatment, perhaps reflecting a lengthier period for Aβ propagation and seeding in the CNS prior to death.

6.4.3. CNS Aβ and tau accumulation in hGH recipients compared to AD

A number of differences between the Aβ and tau accumulation in the CNS of hGH recipients and the neuropathology of AD are apparent:

1. The Aβ deposits in the hGH recipients resembled some of the deposits found in AD (Duyckaerts *et al*., 2009), with diffuse Aβ deposits, focal deposits (diffuse plaques and neuritic plaques) and CAA present. Stellate deposits were not identified.
2. Diffuse Aβ deposits were found in the subpial region in a minority of cases. However, the "lake-like" diffuse deposits in the presubiculum and the "fleecy"

diffuse deposits in the entorhinal cortex found in AD (Duckaerts *et al*., 2009) were entirely absent.

3. Focal Aβ deposits included diffuse plaques and cored/neuritic plaques, as in AD. The neuritic plaques had short neurites that labelled with antibodies to ubiquitin and tau. Cored plaque formation around vessels with CAA was relatively common; these plaques and the adjacent perivascular Aβ deposits were also surrounded by tau-positive neurites. Reactive astrocytes also surrounded the cored plaques and microglial cells were identified in the core region and the periphery of these plaques.
4. The anatomical distribution of the focal and cored/neuritic plaques was more restricted than in AD; most cases had patchy collections of plaques in an unpredictable distribution in the neocortex, corresponding to Thal phase 1. In the few cases where the cingulate cortex was also involved there was never accompanying involvement of the entorhinal cortex or hippocampus, as included in Thal phase 2, so a provisional designation of Thal phase 1* was made. No evidence of laminar involvement of the cerebral cortex with Aβ deposits was identified.
5. CAA pathology was similar to that occurring in AD, but cored plaques occurred commonly adjacent to the larger intraparenchymal vessels with CAA and perivascular Aβ.
6. The accompanying tau pathology was restricted to short neurites around cored/neuritic plaques and perivascular deposits with cored plaques. Very occasional neuropil threads were identified in the cortical grey matter, but neurofibrillary tangles, neurites and neuropil threads were absent in the

entorhinal cortex and hippocampus, making it impossible to assign a Braak stage for neurofibrillary pathology.

The other main differences from AD are the age of the individuals involved and the absence of a clinical history of slowly progressive cognitive impairment. Most hGH recipients with CNS Aβ accumulation were under the age of 40y, most of whom did not have the *APOE* ε3/4 genotype or were negative for apoE-4 on IHC (see below).

6.4.4. Genetic factors influencing CNS Aβ accumulation

None of the hGH-iCJD cases or hGH controls with frozen tissue available for full exome sequencing had any evidence of a genetic abnormality on a wide range of genes affecting Aβ accumulation in the CNS (including *APP*, *PS1* and *PS2*). The use of apoE-4 IHC to identify individuals with an apoE-4 phenotype is not novel (Saki *et al*., 2014) and was performed by using two different apoE-4 antibodies, controlled and validated with a pan-apoE antibody and the use of appropriate AD controls of known *APOE* genotypes. The results of the *APOE* genotype analysis and apoE-4 IHC did not find any significant association between *APOE* ε4 or apoE4+IHC and Aβ accumulation in the brain; most of the cases with CAA in this study had the *APOE* ε3/3 genotype and the two cases with capillary CAA in this study both had the *APOE* ε3/3 genotype. The hGH-iCJD case with the greatest amount of Aβ positivity (hGH-iCJD18) had the *APOE* ε3/3 genotype (combined ABC and CAA score: 8), as did the hGH control case (hGH-control11) with the greatest amount of Aβ accumulation in the CNS (combined ABC and CAA score: 11). The *PRNP* genotype also had no significant association with Aβ accumulation in the CNS in hGH-iCJD cases.

The single sCJD case with CAA had the *APOE* ε3/4 genotype, while the two vCJD cases with diffuse Aβ parenchymal deposits comprised one case with the *APOE* ε3/4 genotype and one case with the *APOE* ε2/3 genotype. The latter (vCJD 27) was identified on exome sequencing to have the *PSEN1* p.E318G variant that increases the risk of AD in *APOE* ε4 carriers (but possibly not relevant in the *APOE* ε2/3 genotype) (Benitez *et al*., 2013), and the -48 C/T polymorphism in the *PSEN1* promoter that is associated with an increased risk of AD and an increased Aβ load in the brain (Lambert *et al*., 2001), which might be of relevance to the finding of sparse diffuse Aβ brain parenchymal deposits at 30y of age.

6.4.5. Age and *APOE* genotype/apoE-4 phenotype

In a recent study of the brains of 154 individuals between the ages of 30-50y (Pletnikova *et al*., 2015), Aβ deposition was not identified in any individuals under the age of 40y, but was present in the brains of 13 individuals aged between 40-49y in the form of diffuse plaques throughout the cerebral cortex. Of these, 5/13 cases had subtle tau positivity in the entorhinal cortex and/or hippocampus. None of the cases with Aβ positivity had clinical evidence of dementia or mild cognitive impairment. All individuals with Aβ positivity carried 1 or 2 *APOE* ε4 alleles; however, of the 28 individuals aged 40-50y with the *APOE* ε3/4 genotype, 10 (36%) had Aβ deposition in the brain, but 18 (64%) did not, indicating that the Aβ deposition in the brain before the age of 50y occurs in only around 1/3 of non-demented individuals with the *APOE* ε3/4 genotype. In the earlier study by Braak and Braak (Braak & Braak, 1997), Aβ deposits were found in the brains of only 9/280 individuals under the age of 45y

(five at amyloid stage stage A and four at amyloid stage B, with no cases at amyloid stage C). CAA was not assessed in this publication. These results in this study (Figure 5.20) indicate no apparent influence of the *APOE* ε3/4 genotype or the apoE-4 phenotype on the presence of either parenchymal or vascular Aβ accumulation in the groups of hGH-iCJD and hGH control patients, which include a patient as young as 20y of age with CAA and an apoE-4-ve(IHC) phenotype.

6.4.6. Other factors influencing CNS Aβ accumulation in hGH recipients

6.4.6.1. *hGH preparations used for inoculation*

The lack of a relationship between the duration of hGH treatment and the development of Aβ pathology suggests that the amount of Aβ contaminating the hGH inocula was variable and unpredictable. The same can be said for the lack of a relationship between the development of iCJD and the duration of hGH treatment; prion contamination of the hGH inocula must also have been variable and unpredictable. It has been observed that hGH recipients who developed iCJD were all treated for at least six months with hGH produced using the modified Wilhelmi protocol, which was used to treat hGH deficiency in the UK between 1967-1980 (Swerdlow *et al*., 2003). This study has found that all the hGH recipients with CNS Aβ accumulation had also been treated (for varying periods of time) with this preparation. While not all patients treated with this preparation developed either hGH-iCJD or CNS Aβ accumulation, the four patients who were never treated with this hGH preparation did not develop either iCJD or CNS Aβ accumulation.

Subsequent studies of the hGH produced by the modified Wilhelmi protocol were reported in 1982 (Stein *et al*., 1982). Using polyacrylamide gel electrophoresis and amino acid analysis of the high molecular weight fraction of this preparation, the investigators found that it contained "aggregated hGH as well as other material not separated from hGH by the purification procedure" Could this "other material" have included PrP^{Sc} and Aβ? None of these preparations are available to investigate this possibility either by protein analysis or by experimental transmission into relevant animal models, so it is not possible to investigate this intriguing question further.

6.4.6.2. *Other potential factors*

In relation to the doubts raised by Feeney *et al*. (Feeney *et al*., 2016) concerning potential predisposing factors for Aβ deposition in the 8 hGH-iCJD patients described by Jaunmuktane *et al*. (Jaunmuktane *et al*., 2015), there was no history or neuropathological evidence of traumatic brain injury as the cause of the hGH deficiency in the first two groups. Further to the additional questions raised by Feeney *et al*. (2016) concerning more generalised disorders that can be associated with Aβ deposition in the CNS, no history or neuropathological evidence of epilepsy, fragile X syndrome, Down's syndrome or Parkinson's disease was evident for any of the patients included in this study. The morphology and distribution of Aβ lesions and relative lack of tau pathology argue against an underlying traumatic aetiology for the Aβ pathology reported in this study, as does the lack of any morphological evidence of previous trauma e.g. axonal bulbs, microglial accumulation, or white matter degeneration. In the two cases with incidental focal isolated tau pathology (pretangles and occasional tangles) unrelated to areas of Aβ deposition, the localised abnormalities

did not match the recent proposed diagnostic criteria for chronic traumatic encephalopathy (McKee *et al*., 2016) and did not resemble the early stages of tauopathies such as corticobasal degeneration (Uchihara, 2014). In hGH-control10, the accompanying neuronal loss and gliosis indicates longstanding focal brain tissue damage that may relate to previous neurosurgery. The pretangles in hGH-iCJD 31 are more difficult to explain, but might represent a local reaction to a previous focal insult no longer apparent in the post mortem brain. Pretangles in the brains of very young individuals were identified in a large study by Braak *et al.* (Braak *et al*., 2011) in subcortical sites, but not in the cerebral cortex. However, subcortical pretangles or tangles were not found in this or any other case examined.

6.5 Comparison of the co-pathology with findings in other iCJD studies

CNS Aβ accumulation in patients with different forms of iCJD has been reported in 4/8 recent cases of UK hGH-iCJD (Jaunmuktane *et al*., 2015) and 5/7 cases of hDM-iCJD in Europe (Frontzek *et al*., 2015; Kovacs *et al*., 2016a), while a recent study of 16 Japanese hDM-iCJD cases reported a significant association with subpial Aβ deposition and meningeal amyloid angiopathy (Hamaguchi *et el*., 2016). The report on the eight UK hGH-iCJD cases claimed in the title that the findings provided "Evidence for human transmission of amyloid-β pathology", provoking a reaction in the media and scientific journals that included "Seeds of neuroendocrine doubt" (Feeney *et al*., 2016). Most of this reaction resulted from use of the term "transmission" in the title. which implies a prion-like process, but did not include any apparent clinical manifestations of the Aβ pathology. The reaction to the articles on hDM-iCJD has been more measured, perhaps due to the absence of the term "transmission" in their

titles, but perhaps also because it was considered that Aβ spread from a human dura mater graft to the underlying cerebral cortex did not constitute an unimaginable possibility due to its anatomical proximity. Table 6.1 summarises the key findings in these reports and compares their findings with those from this study. All four previous papers provide evidence of CNS Aβ accumulation in cases of hGH-iCJD and hDM-iCJD, but the level of detail varies both in the descriptive pathology of the CNS and the results of associated genetic investigations.

This study adds considerably to these reports in terms of the number of cases studied, the inclusion of hGH control cases without iCJD, and in the young age of the patients included. The detailed neuropathological description provided is comparable with that in Kovacs *et al*. (Kovacs *et al*., 2016a), particularly in relation to the nature and localisation of the Aβ deposition and its relationship to AD. This study has found more evidence of tau deposition in relation to Aβ deposits, but this still falls short of resembling a full AD neuropathological phenotype, particularly in the conspicuous absence of neurofibrillary tangles. CNS Aβ accumulation in hGH recipients is not indicative of AD, but rather represents a partial phenotype that is restricted in both the nature and anatomical distribution of Aβ and tau lesions. This study also found no evidence of the subcortical forms of tau accumulation that appear to represent part of the preclinical phase of the pathological processes underlying AD (Braak et al., 2011).

Table 6.1 Comparison of results with other studies on CNS Aβ accumulation in iCJD (modified from Kovacs, 2016)

Study Reference	Jaunmuktane *et al*., 2015	Frontzek *et al*., 2015	Kovacs *et al*., 2016a	Hamaguchi *et al*., 2016	This study	
Clinical phenotype	CJD	CJD	CJD	CJD	CJD	Not CJD
Cause of iCJD	hGH	hDM	hDM	hDM	hGH	None
Number of cases	8	7	2*	16	33	12
Other autopsy tissues examined	No	No	Yes	No	Yes	Yes
Non-CJD autopsy tissues examined	Pituitary gland: 55 cases	No	Dura mater: 84 cases	No	hGH control cases – see Table 5.8	
Genetic analysis	*APOE* + AD genes	No	*APOE* + AD genes	*APOE*	*APOE* + AD genes	
Number with Aβ parenchymal deposits	4 + 2 focal	5	2*	13	12	4
Morphology + distribution of Aβ deposits described	Yes, with quantitative analysis	No	Yes, in detail	Subpial Aβ accumulation Plaque morphology not included	Yes, in detail	
Age of cases with parenchymal Aβ	5th decade-51y	28-63	28,33	35-81	27-45	30-45
Age of cases <40 y with parenchymal Aβ	36 (focal deposits)	28,33	28,33	35, 39	27-38	30-37
Number with Aβ CAA	3 +1 focal	5	2*	11	14	2
Age of cases with Aβ CAA	5th decade-51y	28-63	28,33	35-81	20-37	42-45
Age of cases <40 y with Aβ CAA	None	28,33	28-33	35-39	20-37	None
AD - related tau pathology	No	No	No	Yes-details given	Yes-details given	
Statistical difference from sCJD	Yes	Yes	Yes	Yes	Yes – and also from vCJD	

Abbreviations: Aβ: amyloid beta: AD; Alzheimer's disease; *APOE*: apolipoprotein E gene; CAA: cerebral amyloid angiopathy; CJD: Creutzfeldt-Jakob disease; hDM: human dura mater; hGH: human growth hormone: i: iatrogenic; s: sporadic; v: variant: y:years; *: cases also included in the study by Frontzek *et al*., 2015

6.6. Conclusions of this study

6.6.1. How the results address the Aims of the thesis

1. Determine the pathological phenotype of hGH-iCJD in the UK.

The pathological phenotype of hGH-iCJD in the UK is diverse. All cases exhibit a spongiform encephalopathy with predominantly microvacuolar spongiform change in a variety of distributions (see 2 below). Amyloid plaque formation is a prominent part of the pathology in some cases of hGH-iCJD, with kuru-type plaques present in the cerebellar cortex and occasionally also in some other brain regions including the cerebral cortex, and basal ganglia. In approximately 50% of hGH-iCJD cases there is co-existing Aβ pathology (CAA, diffuse and cored plaques, or both CAA and plaques) that cannot readily be explained by the *APOE* genotype and other genetic factors (see 5. below). No evidence of significant accompanying α-synuclein or TDP-43 pathology was identified.

2. Explore whether the pathological phenotype is influenced by the *PRNP* codon 129 genotype and CNS PrP^{res} isoform in the same way as in sCJD (Parchi *et al*., 1999).

The pathological phenotype in UK hGH-iCJD is strongly influenced by the *PRNP* codon 129 genotype and the brain PrP^{res} isoform. In the codon 129 VV2 and MV2 subtypes of hGH-iCJD, the neuropathology, PrP immunohistochemistry and brain PrP^{res} isoform are similar to those in the corresponding VV2 and MV2 sCJD subtypes. However, the MM subgroup shows a divergent phenotype, with the MM1 cases resembling the sCJD MM1 subtype in terms of neuropathology, PrP

immunohistochemistry and brain PrP^{res} isoform. However, the MMi subtype of hGH-iCJD shows neuropathological, immunohistochemical and brain PrP^{res} isoform features more similar to the MV2 sCJD subgroup. This combination of features has not been described in UK cases of either hDM-iCJD or sCJD with *PRNP* codon 129 MM, but they have been described in cases of hDM-iCJD in Japan in *PRNP* codon 129 MM genotype patients. Kobayashi *et al*. (Kobayshi *et al*., 2016) have suggested that the combination of a *PRNP* codon 129 genotype and the presence of kuru plaques in the cerebellum and cerebral cortex in a patient with apparently sporadic CJD should lead to a suspicion of an iatrogenic source of infection.

3. Investigate the peripheral pathogenesis of hGH-iCJD following intramuscular inoculation.

The PET blot studies and WB studies using NaPTA precipitation in this thesis show that PrP^{res} can be detected in the peripheral nervous system (peripheral nerves, adrenal medulla, dorsal root ganglia and trigeminal ganglia), the lymphoreticular system (lymph nodes) and the pituitary gland in hGH-iCJD. This evidence is incomplete and patchy in terms of the number of positive tissues from a limited selection of non-CNS tissues in a total of 19 patients. However, it does give an indication that both the peripheral nervous system and lymphoreticular system are possible routes through which the infectious agent may spread to the CNS after intramuscular inoculation. These routes are also involved the spread of infection in vCJD in humans and in experimental scrapie in rodents. In contrast, no evidence of Aβ accumulation was found in any of the non-CNS tissues in this study.

4. Characterise the causal agent strain in hGH-iCJD and establish whether it relates to any of the known sCJD strains (Haik *et al*., 2011).

From the combination of data concerning the neuropathological phenotype of UK hGH-iCJD, the brain PrP^{res} isoforms and the chronological sequence of *PRNP* codon 129 genotype involvement, it seems most likely that the causative agent is the V2 strain of sCJD (Bishop *et al*., 2010; Haik *et al*., 2011). This possibility is reinforced by the result of the PMCA experiments on the hGH-iCJD codon 129 MM cases, in which evidence demonstrating a traceback phenomenon to a VV2 origin for the MMi hGH-iCJD case was obtained (Kobayshi *et al*., 2009, 2010). In a separate study, experimental transmission of UK iCJD hGH-iCJD cases and sCJD cases to transgenic mice over-expressing human *PRNP* codon 129 genotypes is being undertaken as part of an ongoing collaboration to determine the disease transmission characteristics and establish whether further evidence of a traceback phenomenon can be obtained *in vivo* (Andreoletti *et al*., 2016)

5. Seek evidence in hGH-iCJD and other non-iCJD hGH recipients for transmission/seeding of other neurotoxic proteins found in the pituitary gland - Aβ, tau, α–synuclein (Irwin *et al*., 2013; Jaunmuktane *et al*., 2015).

The results of this study indicate that CNS Aβ deposition occurs in around 50% of all UK hGH recipients, regardless of whether they died from hGH-iCJD or not, as a likely consequence of Aβ seeding from contaminated hGH extracts. These findings also indicate a trend towards an association between the length of survival from the end date of the period of hGH treatment and the presence of Aβ seeding and accumulation in the CNS, but this was not statistically significant. No clear association with the

APOE genotype or any other genetic predisposing factors was identified. The Aβ pathology in the CNS occur as parenchymal deposits (diffuse subpial deposits, diffuse plaques and cored/neuritic plaques) and as CAA, or both CAA and parenchymal deposits. Plaques occur in the cerebral cortex in a patchy distribution that does not appear to resemble the pattern that is characteristic of Alzheimer's disease, but is more similar to the patterns of Aβ pathology described in hDM-iCJD graft patients (Kovacs *et al*., 2016a). Accompanying tau accumulation occurs in neuritic processes and sparse neuropil threads, but no neurofibrillary tangles were identified. No α-synuclein or TDP-43 pathology was observed, but evidence of an astrocytic and microglial reaction to the Aβ deposits was present. The CAA involved both meningeal and intraparenchymal vessels, including capillaries; occasional cases had dyshoric intraparenchymal vessels and one had evidence of vasculopathy.

The full neuropathological phenotype of AD was not present in these cases; in particular, there was an absence of neurofibrillary tangles. These findings are in keeping with the clinical data, particularly for the hGH controls, where no evidence of progressive cognitive decline was recorded. This incomplete phenotype cannot be regarded as a model for AD, but confirms the capacity of Aβ to act as a propagon in humans (Eisele & Duyckaerts, 2016) and to produce a range of CNS Aβ pathology, with tau pathology and glial reactions apparently occurring as secondary phenomena (Kovacs, 2016).

6.6.2. Advantages and limitations of this study

This study has a number of advantages beyond its size. The cases have occurred across the entire timescale of the hGH-iCJD epidemic in the UK (Figure 2.1) and are therefore more likely to be representative of the epidemic as a whole, unlike the small series of recent UK hGH-iCJD cases reported by Jaunmuktane *et al*. (Jaunmuktane *et al*., 2015). The wider temporal distribution of cases in this study also contains cases of all three possible *PRNP* codon 129 genotypes (unlike the study by Jaunmuktane *et al*.), allowing the molecular biology of prion transmission from UK hGH to be studied across all *PRNP* codon 129 polymorphic barriers across a wide period of time in a well-characterised patient cohort.

Another advantage is the availability of a clinical database in the Institute of Child Health, London that contains many details of the individual patients, including their date of birth and gender, the underlying disease causing their growth hormone deficiency, dates of hGH treatment (including use of the Hartree-modified Wilhelmi preparation of hGH), the date of onset of hGH-iCJD and their date of death. These data allow the incubation period for the hGH-iCJD infection to be estimated (Table 5.1). This wealth of clinical data on is supplemented by additional data from the NCJDRSU, in particular the results of analysis of the codon 129 polymorphism in the prion protein gene. Brain tissue from the cases in this study was referred to the NCJDRSU for diagnosis as part of the National CJD Surveillance Project. The brain tissue from each case was examined and sampled in a standardised way and a diagnosis made using consistent clinical and neuropathological criteria (Table 1.9). The requirement for unfixed frozen brain tissue samples for Western blot analysis for PrP^{res} to confirm a

diagnosis of iCJD allowed frozen tissue samples to be retained for research (when appropriate consent was provided) in the MRC Edinburgh Brain Bank (EBB). The frozen tissue available for this study was essential for the genetic, biochemical and molecular biological components of this study. Some hGH-iCJD cases had multiple frozen tissue samples from different brain areas available to investigate regional variation in brain PrP^{res} isoforms (Table 5.9), which has not been described in any previous study of hGH-iCJD.

This study also benefits from the availability of similar data and brain tissue samples from the EBB for use as controls for the hGH-iCJD cases. In particular, brain tissue samples were available from a group of patients who were also treated over a similar time period with UK hGH, but who did not develop hGH-iCJD and died instead from complications of the underlying conditions causing their GH deficiency, the most common of which were intracranial neoplasms. These cases provide an ideal control group for the hGH-iCJD cases when investigating the co-pathology (AD, CAA, LB and TDP-43 pathology) in the brain, since the influence of co-existing iCJD pathology can be assessed. Cases of sCJD and vCJD were also available for use as age-matched controls of other forms of human prion disease of different pathogenesis (respectively idiopathic and acquired from a bovine source), who had never been treated with hGH.

This study does have its limitations; it is necessarily an observational study that was conducted in retrospect using pre-existing tissue samples and data that were not collected for this specific purpose. The most significant disadvantage is the lack of frozen brain tissue samples in some cases, which precludes any biochemical, genetic

or molecular biological studies. This disadvantage is partly overcome by the ability to perform *PRNP* codon 129 analysis successfully in a small number of cases from DNA extracted from the formic acid-pretreated paraffin-embedded brain tissue blocks, and the use of antibodies to apoE-4 to determine the apoE-4 phenotype in hGH-iCJD and hGH control cases with co-existing AD pathology. Fortunately, cases without frozen brain tissue were in the minority, and the full range of the investigative techniques employed in this study were used on the majority (21) of the hGH-iCJD cases.

6.7. Tests of the stated hypotheses of this thesis:

1. Disease phenotype: The clinicopathological phenotype of hGH-iCJD in the UK is determined by the *PRNP* codon 129 polymorphism of the patient and the PrP^{res} isoform in the brain.

This hypothesis is supported by the evidence of a statistically significant association between *PRNP* codon 129 polymorphisms and both the disease incubation period and duration of clinical illness, and by the observation of a strong influence of the *PRNP* codon 129 genotype and the brain PrP^{res} isoform on the pathological phenotype in UK hGH-iCJD.

2. Increased propagation efficiency: The secondary transmission of sporadic CJD prions has led to the acquisition of greater propagation efficiency in hGH-iCJD prions (Xiao *et al*., 2014).

This hypothesis is not supported by the results of the in vitro conversion assays in this thesis. The RT-QuiC assays did not show the shortened lag time for hGH-iCJD cases or hDM-iCJD cases that would indicate increased propagation efficiency; the lag times for the hGH-iCJD cases were found to be significantly slower than for the sCJD cases. Similarly, the PMCA assays did not show evidence of an increased amplification of iCJD seeds in comparison to sCJD seeds of all possible *PRNP* codon 129 genotypes in identical PMCA substrates.

3. Traceback phenomenon: The origin of the prions in hGH-iCJD can be inferred by ready reversion to their original state when given an appropriate host genotype (Kobayashi *et al*., 2009, 2010).

This hypothesis is supported by the results of the PMCA assays, which show evidence to support a traceback phenomenon for the hGH-iCJD MMi case. The PMCA seed prepared from this case amplified more efficiently in a VV substrate than a MM substrate, consistent with an origin from a V2 strain of sCJD. In contrast, the hGH-iCJD MM1 case and the sCJD MM1 cases did not amplify efficiently in either substrate.

4. Origin: The origin of hGH-iCJD in the UK can be inferred by the molecular and genetic changes occurring in the disease over time.

This hypothesis is supported by the data in this thesis, which indicate from the results referred to in (3) above that an origin of UK hGH-iCJD from a V2 strain of sCJD

appears likely. This is reinforced by the temporal distribution of *PRNP* codon 129 genotypes in the UK hGH-iCJD cohort; recipients with the matching *PRNP* codon 129VV genotype are affected first, followed by the MV genotype and eventually the MM genotype. The latter are phenotypically heterogeneous in terms of their neuropathology, possibly indicating incomplete adaption of the V2 strain in the MMi hGH-iCJD cases.

5. Co-pathology: Aβ seeding occurs in hGH recipients in the UK both with and without iCJD, resulting in the pathological accumulation of Aβ in the CNS.

This hypothesis is supported by the data from this study, with around 50% of UK hGH recipients showing evidence of Aβ accumulation in the CNS as cerebral amyloid angiopathy, parenchymal deposits including diffuse and cored plaques, or both CAA and parenchymal deposits. No clear association with *APOE* genotype or other genetic predisposing factors was identified. For the first time, CNS Aβ accumulation in hGH recipients who died from causes other than iCJD has been demonstrated, indicating that Aβ seeding in the CNS is not dependent on co-existing prion infection. The Aβ pathology in the hGH-iCJD cases and hGH controls is very similar in each group, and has undoubted similarities to the pathology of AD. However, there are also major pathological differences from AD in terms of the restricted distribution of the Aβ deposits in the brain, a relative paucity in the number of tau-positive neurites around neuritic plaques, and the absence of neurofibrillary tangles.

6.8. Wider implications of the results in this thesis

The findings of this study indicate that Aβ can behave as a propagon in humans, able to spread to the CNS following intramuscular injection and subsequently seed in the parenchyma of the brain and in cerebral blood vessels, but not resulting in AD or any other apparent clinical manifestations. CNS Aβ accumulation occurred in around 50% of hGH-iCJD and hGH control cases, and is therefore not dependent on co-existing PrP^{Sc} accumulation or other CJD pathology. This behaviour of Aβ as a propagon in humans has possible broader implications when other opportunities for the potential exposure to Aβ may occur, for example in the re-use of Aβ-contaminated neurosurgical instruments previously used on the brains of elderly patients, or via blood transfusions from elderly donors who may have increased levels of plasma Aβ (Blennow *et al*., 2010). Recent epidemiological studies have found no evidence of either previous surgery or blood transfusion as risk factors for AD (Vanderweyde *et al*., 2010; Edgren *et al*., 2016), but the possibility that such scenarios could occur as rare events after prolonged incubation periods requires further consideration.

These findings also indicate that a significant number of the remaining survivors in the cohort of UK hGH recipients are at increased risk of CNS Aβ accumulation and, although they may not progress to symptomatic AD, they may subsequently develop vascular complications. The severe CAA found in the older hGH control patients in this study suggests that surviving hGH recipients may be at future risk of the complications of CAA, including spontaneous lobar cerebral haemorrhage, perivascular inflammation and cognitive impairment (Gahr *et al*., 2013).

Although human growth hormone therapy in the UK was abandoned over thirty years ago, cases of hGH-iCJD still occur- the most recent patient died earlier this year. These findings indicate that unrecognised or poorly assessed risks associated with medical interventions can have very long-term ramifications when it comes to patient safety. The study also underscores the importance of continued CJD surveillance and deep phenotyping of cases of this rare but fatal and transmissible condition in order to determine their precise cause and to help protect public health.

7. References

1. 1000 Genomes Project Consortium: Abecasis GR, Auton A *et al*. An integrated map of genetic variation from 1,092 human genomes. *Nature* 2012;**491**:56-65.

2. Abid K, Morales R, Soto C. Cellular factors implicated in prion replication. *FEBS Lett* 2010;**584**:2409-14.

3. Advisory Committee on Dangerous Pathogens Transmissible Spongiform Encephalopathy Working Group. Infection prevention and control of CJD and variant CJD in healthcare and community settings. 2015: (https://www.gov.uk/government/uploads/system/uploads/attachment_data/file/ 427854/Infection_controlv3.0.pdf).

4. Aguzzi A, Falsig J. Prion propagation, toxicity and degradation. *Nat Neurosci* 2012;**15**:936-9.

5. Aguzzi A, Lakkaraju AKK. Cell biology of prions and prionoids: a status report. *Trends Cell Biol* 2016;**26**;40-51.

6. Alafuzoff I, Ince PG, Arzberger T *et al*. Staging/typing of Lewy body related alpha-synuclein pathology: a study of the BrainNet Europe Consortium. *Acta Neuropathol* 2009a;**117**:635-52.

7. Alafuzoff I, Thal DR, Arzberger T *et al*. Assessment of beta-amyloid deposits in human brain: a study of the BrainNet Europe Consortium. *Acta Neuropathol* 2009b;**117**:309-20.

8. Alcalde-Cabero E, Almazan-Isla J, Brandel J-P *et al*. Health professionals and risk of sporadic Creutzfeldt-Jakob disease, 1965 to 2010. *Eurosurveillance* 2012;**17**:pii:20144.

9. Alfonso DS, Adriana Z, Philippe D. Structural and hydration properties of the partially unfolded states of the prion protein. *Biophys J* 2007;**93**:1284-92.

10. Alper T, Cramp WA, Haig DA, Clarke MC. Does the agent of scrapie replicate without nucleic acid? *Nature* 1967;**214**:764-6.

11. Alper T, Haig DA, Clark MC. The scrapie agent: evidence against its dependence for replication on intrinsic nucleic acid. *J Gen Virol* 1978;**41**:503-16.

12. Andreoletti O, Lacroux C, Cassard H *et al*. Prion strain diversity in French and British iatrogenic CJD cases. *Clin Neuropathol* 2016;**35**:204.

13. Ansoleaga B, Garcia-Esparcia P, Lloerns F *et al*. Altered mitochondria, protein synthesis machinery, and purine metabolism are molecular contributors to the pathogenesis of Creutzfeldt-Jakob disease. *J Neuropathol Exp Neurol* 2016; Jun 12.p11:nlw048.

14. Antonacopoulou AG, Grivas PD, Skarlas L *et al*. POLR2F, ATP6V0A1 and PRNP expression in colorectal cancer: new molecules with prognostic significance? *Anticancer Res* 2008;**28**:1221-7.

15. Antonacopoulou AG, Palli M, Marousi S *et al*. Prion protein expression and the M129V polymorphism of the PRNP gene in patients with colorectal cancer. *Mol Carcinog* 2010;**49**:693-9.

16. Atarashi R, Satoh K, Sano K *et al*. Ultrasensitive human prion detection in cerebrospinal fluid by real-time quaking induced conversion. *Nat Med* 2011; **17**:175-8.

17. Atkinson CJ, Zhang K, Munn AL *et al*. Prion protein scrapie and the normal cellular prion protein. *Prion* 2016;**10**:63-82.

18. Balter M. French scientists may face charges over CJD outbreak. *Science* 1993;**261**:543.

19. Barbot C, Castro L, Oliveira C, Carpenter C. Variant Creutzfeldt-Jakob disease: the first confirmed case from Portugal shows early onset, long duration and unusual pathology. *J Neurol Neurosurg Psychiatry* 2010;**81**:112-5.

20. Barret A, Tagliavini F, Forloni G *et al*. Evaluation of quinacrine treatment for prion diseases. *J Virol* 2003;**77**:8462-9.

21. Barria M, Mukherjee A, Gonzale-Romero *et al*. De novo generation of infectious prions in vitro produces a new disease phenotype. *PLoS Pathog* 2009;**5**:e10000421.doi 10.1371.

22. Barria MA, Balachandran A, Morita M *et al*. Molecular barriers to zoonotic transmission of prions. *Emerg Infect Dis* 2014;**20**:88-97.

23. Baxter HC, Campbell GA, Whittaker AG *et al*. Elimination of transmissible spongiform encephalopathy infectivity and decontamination of surgical instruments by using radio-frequency gas-plasma treatment. *J Gen Virol* 2005;**86**:2393-9.

24. Baylis M, Goldmann W. The genetics of scrapie in sheep and goats. *Curr Mol Med* 2004;**4**:385-96.

25. Beck J, Poulter M, Hensman D *et al*. Large C orf72 hexanucleotide repeat expansions are seen in multiple neurodegenerative syndromes and are more frequent than expected in the UK population. *Am J Hum Genet* 2013;**92**:345-53.

26. Beekes M, McBride PA. The spread of prions through the body is naturally acquired transmissible spongiform encephalopathies. *FEBS J* 2007;**274**:588-605.

27. Benitez BA, Karch CM, Cai Y *et al*. The *PSEN1*,p.E318G variant increases the risk of Alzheimer's disease in *APOE*-ε4 carriers. *PLoS Genet* 2013;9: e1003685. doi: 10.1371/journal.pgen.1003685.

28. Berghoff AS, Trummert A, Unterberger U *et al*. Atypical sporadic CJD-MM phenotype with white matter kuru plaques associated with intranuclear inclusion body and argyrophilic grain disease. *Neuropathology* 2015;**35**:336-42.

29. Beringue V, Vilotte JL, Laude H. Prion agent diversity and species barrier.*Vet Res* 2008;**39**: 47. doi:10.1051/vetres:2008024. Epub 2008 Jun 3.

30. Bernoulli C, Sigfried J, Baungarten G *et al*. Danger of accidental person to person transmission of Creutzfeldt-Jakob disease by surgery. *Lancet* 1977;**1**:478-9.

31. Berry DB, Lu D, Geva M *et al*. Drug resistance confounding prion therapeutics. *Proc Natl Acad Sci USA* 2013; **110**:E4160-9.doi:10.1073/pnas.1317164110.

32. Bessen RA, Marsh RF. Distinct PrP properties suggest the molecular basis of strain variation in transmissible mink encephalopathy. *J Virol* 1994;**68**:7859-68.

33. Biasini E, Turnbaugh JA, Unterberger U, Harris DA. Prion protein at the crossroad of physiology and disease. *Trends Neurosci* 2012;**35**:92-103.

34. Billette de Villemeur T, Gourmelen M, Beauvais P *et al*. Creutzfeldt-Jakob disease in 4 children treated with growth hormone. *Rev Neurol (Paris)* 1992;**148**:328-34.

35. Binelli S, Agazzi P, Giaccone G *et al*. Periodic electroencephalogram complexes in a patient with variant Creutzfeldt-Jakob disease. *Ann Neurol* 2006;**59**:423-7.

36. Bishop MT, Diack A, Ritchie D *et al*. Prion infectivity in the spleen of a PRNP heterozygous individual with subclinical variant Creutzfeldt-Jakob disease. *Brain* 2013;**136**:1139-45.

37. Bishop MT, Hart P, Aitchison L *et al*. Predicting susceptibility and incubation time of human-to-human transmission of vCJD. *Lancet Neurol* 2006;**5**:393-8.

38. Bishop MT, Pennington C, Heath CA *et al*. PRNP variation in UK sporadic and variant Creutzfeldt-Jakob disease highlights genetic risk factors and a novel non-synchronous polymorphism. *BMC Med Genet* 2009;**10**:146. doi: 10.1186/1471-2350-10-146.

39. Bishop MT, Ritchie Dl, Will RG *et al*. No major change in vCJD agent strain after secondary transmission via blood transfusion. *PLoS One* 2008;**3**:e2878.doi:10.1371/jornal.pone.0002878.

40. Bishop MT, Will RG, Manson JC. Defining sporadic Creutzfeldt-Jakob disease strains and their transmission properties. *Proc Natl Acad Sci* USA 2010;**107**:12005-10.

41. Blennow K, Hampel H, Weiner M, Zetterberg H. Cerebrospinal fluid and plasma biomarkers in Alzheimer's disease. *Nat Rev Neurol* 2010;**6**:131-44.

42. Blizzard R M. History of growth hormone therapy. *Ind J Pediatr* 2012;**79**:87-91.

43. Boelle P-Y, Cesbron J-Y, Valleron A-J. Epidemiological evidence of higher susceptibility to vCJD in the young. *BMC Infect Dis* 2004;4:doi:10.1186/1471-2334/4/26.

44. Bonda DJ, Manjila S, Mhndiratta P *et al*. Human prion diseases: surgical lessons learned from iatrogenic prion transmission. *Neurosurg Focus* 2016;**41**:E10.2016.

45. Bone I, Belton L, Walker AS, Darbyshire J. Intraventricular pentosan polysulphate in human prion diseases: an observational study in the UK. *Eur J Neurol* 2008;**15**:458-64.

46. Borchelt DR, Scott M, Taraboulos A *et al*. Scrapie and cellular prions differ in their kinetics of synthesis and topology in cultured cells. *J Cell Biol* 1990;**110**:743-52.

47. Botsios S, Manuelidis L. CJD and scrapie require agent-associated nucleic acids for infection. *J Cell Biochem* 2016;**117**:1947-58.

48. Braak H, Alafuzoff I, Arzberger T *et al*. Staging of Alzheimer disease-associated neurofibrillary pathology using paraffin sections and immunohistochemistry. *Acta Neuropathol* 2006;**112**:389-404.

49. Braak H, Braak E. Frequency of stages of Alzheimer-related lesions in different age categories. *Neurobiol Aging* 1997;**18**:351-7.

50. Braak H, Braak E. Neuropathological staging of Alzheimer-related changes. *Acta Neuropathol* 1991;**82**:239-59.

51. Braak H, Thal DR, Ghebremedhin E, del Tredici K. Stages of the pathologic process in Alzheimer disease: age categories from 1 to 100 years. *J Neuropathol Exp Neurol* 2011:**70**:960-9.

52. Brandel J-P, Preece M, Brown P *et al*. Distribution of codon 129 genotype in human growth hormone-treated CJD patients in France and the UK. *Lancet* 2003;**362**:128-30.

53. Brandel J-P, Peckeu L, Haik S. The French surveillance network of Creutzfeldt-Jakob disease. Epidemiological data in France and worldwide. *Transfus Clin Biol* 2013;**20**:395-7.

54. Brandner S, Isenmann S, Raeber A *et al*. Normal host prion protein is necessary for scrapie-induced neurotoxicity. *Nature* 1996a;**379**:339-43.

55. Brandner S, Raeber A, Sailer A *et al*. Normal host prion protein (PrPC) is required for scrapie spread within the central nervous system. *Proc Natl Acad Sci USA* 1996b;**93**:13148-51.

56. Brandner S, Whitfield J, Boone K *et al*. Central and peripheral pathology of kuru: pathological analysis of a recent case and comparison with other forms of human prion disease. *Philos Trans R Soc Lond B Biol Sci*;**363**:3755-63.

57. Brown D, Qin, Herms JW *et al*. The cellular prion protein binds copper in vivo. *Nature* 1997;**390**:684-7.

58. Brown P, Bradley R. 1755 and All That: a historical primer of transmissible spongiform encephalopathy. *BMJ* 1998;**317**:1688-92.

59. Brown P, Brandel J-P, Sato T *et al*. Iatrogenic Creutzfeldt-Jakob disease, final assessment. *Emerg Infect Dis* 2012;**18**:901-7.

60. Brown P, Cervenakova L, Boellaard JW *et al*. Identification of a PRNP gene mutation in Jakob's original Creutzfeldt-Jakob disease family. *Lancet* 1994;**344**:130-1.

61. Brown P, Farrell M. A practical approach to avoiding iatrogenic Crutzfeldt-Jakob disease from invasive instruments. *Infect Control Hosp Epidemiol* 2015;**36**:844-8.

62. Brown P, Gajdusek DC, Gibbs CJ, Asher DA. Potential epidemic of Creutzfeldt-Jakob disease from human growth hormone therapy. *N Engl J Med* 1985;**313**:728-31.

63. Brown P, Wolff A, Gajdusek DC. A simple and effective method for inactivating virus infectivity in formalin-fixed tissue samples from patients with Creutzfeldt-Jakob disease. *Neurology* 1990;**40**:887-90.

64. Bruce ME. Scrapie strain variation and mutation. *Br Med Bull* 1993;**49**:822-38.

65. Bruce ME. TSE strain variation. *Br Med Bull* 2003;**66**:99-108.

66. Bruce M, Chree A, McConnell I *et al*. Transmission of bovine spongiform encephalopathy and scrapie to mice: strain variation and the species barrier. *Philos Trans R Soc Lond B Biol Sci* 1994;**343**:405-11.

67. Bruce ME, McConnell I, Will RG *et al*. Detection of variant Creutzfeldt-Jakob disease infectivity in extraneural tissues. *Lancet* 2001;**358**:208-9.

68. Bruce ME, Will RG, Ironside JW *et al*. Transmissions to mice indicate that "new variant" CJD is caused by the BSE agent. *Nature* 1997;**389**: 498-501.

69. Bugiani O, Giaccone G, Verga L *et al*. Beta APP participates in PrP-amyloid plaques of Gerstmann-Straussler-Scheinker disease, Indiana kindred. *J Neuropathol Exp Neurol* 1993;**52**:64-70.

70. Butler DA, Scott MR, Bockman JM *et al*. Scrapie-infected murine neuroblastoma cells produce protease-resistant prion proteins. *J Virol* 1988;**62**:1558-64.

71. Cali I, Miller CJ, Parisi JE, *et al*. Distinct pathological phenotypes of Creutzfeldt-Jakob disease in recipients of prion-contaminated growth hormone. *Acta Neuropathol Commun* 2015;**3**:DOI 10.1186/s40478-015-1324-2.

72. Casassus B. Acquittals in CJD trial divide French scientists. *Science* 2009;**323**:446.

73. Castilla J, Saa P, Hetz C *et al*. In vitro generation of infectious scrapie prions. *Cell* 2005;**121**:195-206.

74. Castilla J, Saa P, Morales R *et al*. Protein misfolding cyclic amplification for diagnosis and prion propagation studies. *Method Enzymol* 2006;**412**:3-21.

75. Caughey B. Prion protein conversions: insight into mechanisms, TSE transmission barriers and strains. *Br Med Bull* 2003;**66**:109-20.

76. Caughey B, Raymond GJ. The scrapie-associated form of PrP is made from a cell surface precursor that is both protease- and phospholipase-sensitive. *J Biol Chem* 1991;**226**:18217-23.

77. Chandler RL. Encephalopathy in mice produced by inoculation with scrapie brain material. *Lancet* 1961;**1**:1378-9.

78. Chapuis J, Moudjou M, Reine F *et al*. Emergence of two prion subtypes in ovine PrP transgenic mice infected with human MM2-cortical Cruetzfeldt-Jakob disease prions. *Acta Neuropathol Comm* 2016; 4:10. doi: 10.1186/s40478-016-0284-9.

79. Clavaguera F, Hench J, Lavenir I *et al*. Peripheral administration of tau aggregates triggers intracerebral tauopathy in transgenic mice. Acta Neuropathol 2014;**127**:299-301.

80. Colby DW, Prusiner SB. De novo generation of prion strains. *Nat Rev Microbiol* 2011a;**9**:771-777.

81. Colby DW, Prusiner SB. Prions. *Cold Spring Harb Perspect Biol* 2011b;**3**:a006833.

82. Collie DA, Summers DM, Sellar RJ *et al.* Diagnosing variant Creutzfeldt-Jakob disease with the pulvinar sign: MR imaging findings in 86 neuropathologically confirmed cases. *Am J Neuroradiol* 2003;**24**:1560-69.

83. Collinge J. Molecular neurology of prion disease. *J Neurol Neurosurg Psychiatry* 2005;**76**:906-19.

84. Collinge J, Gorham M, Hudson F *et al*. Safety and efficacy of quinacrine in human prion disease (PRION-1 study): a patient preference trial. *Lancet Neurol* 2009;**8**:334-44.

85. Collinge J, Jaunmuktane Z, Mead S *et al*. Reply to "Seeds of neuroendocrine doubt". *Nature* 2016;**535**:E2-3.

86. Collinge J, Palmer MS, Dryden AJ. Genetic predisposition to iatrogenic Creutzfeldt-Jakob disease. *Lancet* 1991;**337**:1441-2.

87. Collinge J, Sidle KCL, Meads J *et al*. Molecular analysis of prion strain variation and the aetiology of 'new variant' CJD. *Nature* 1996;**383**:685-90.

88. Collinge J, Whitfield J, McKintosh E *et al*. Kuru in the 21st century – an acquired human prion disease with very long incubation periods. *Lancet* 2006;**367**:2068-74.

89. Concha-Marambio L, Pritzkow S, Moda F *et al*. Detection of prions in blood of variant Creutzfeldt-Jakob disease patients. *Sci Transl Med* (in press).

90. Cooper JD, Bird SM. 2002. UK dietary exposure to BSE in beef mechanically recovered meat: by birth cohort and gender. *J Cancer Epidemiol Prevent* 2002;**7**:59-70.

91. Cooper JK, Andrews N, Ladhani K *et al*. Evaluation of a test for its suitability in the diagnosis of variant Creutzfeldt-Jakob disease. *Vox Sang* 2013;**105**:196-204.

92. Cordery RJ, Hall M, Ciplotti L *et al*. Early cognitive decline in Creutzfeldt-Jakob disease associated with human growth hormone treatment. *J Neurol Neurosurg Psychiatry* 2003;**74**:412-6.

93. Cousens SN, Zeidler M, Esmonde TF *et al*. Sporadic Creutzfeldt-Jakob disease in the United Kingdom: analysis of epidemiological surveillance data for 1970-96. *BMJ* 1997;**315**:389-95.

94. Creutzfeldt HG. Uber eine eigenartige herdformige erkrankung des zentralnervensystems. *Z Gesamte Neurol Psychiatr* 1920;**57**:1-18.

95. Croes EA, Roks G, Jansen GH *et al*. Creutzfeldt-Jakob disease 38 after diagnostic use of human growth hormone. *J Neurol Neurosurg Psychiatry* 2002;**72**:792-3.

96. Cuillé J, Chelle PL. Pathologie animale: la maladie dite de la tremblante du mouton: est-elle inoculable? *C.R. Acad Sci (Paris)* 1936;**203**:1552-4.

97. Daude N, Lehmann S, Harris DA. Identification of intermediate steps in the conversion of a mutant prion protein to a scrapie-like form in cultured cells. *J Biol Chem* 1997;**272**:11604-12.

98. Dawson TP, Neal JW, Llewellyn L, Thomas C. *Neuropathology Techniques*. London: Edward Arnold, 2003.

99. de Almeida CJ, Chiarini LB, da Silva JP *et al*. The cellular prion protein modulates phagocytosis and inflammatory response. *J Leukoc Biol* 2005;**77**:238-46.

100. de Pedro Cuesta J, Mahillo-Fernandez I, Rabano A *et al*. Nosocomial transmission of sporadic Creutzfeldt-Jakob disease: results from a risk-based assessment of surgical interventions. *J Neurol Neurosurg Psychiatry* 2011;**82**: 204-12.

101. de Pedro Cuesta J, Ruiz Tovar M, Ward H *et al*. Sensitivity to biases of case-control studies on medical procedures, particularly surgery and blood transfusion, and risk of Creutzfeldt-Jakob disease. *Neuroepidemiology* 2012;**39**: 1-18.

102. del Rio JA, Gavin R. Functions of the cellular prion protein, the end of Moore's law, and Ockham's razor theory. *Prion* 2016;**10**:25-40.

103. Deleault NR, Harris BT, Rees JR, Supattapone S. Formation of native prions from minimal components in vitro. *Proc Natl Acad Sci USA* 2007;**104**:9741-6.

104. Deleault NR, Lucassen RW, Supattapone S. RNA molecules stimulate prion protein conversion. *Nature* 2003;**425**:717-20.

105. Delisle MB, Fabre N, Rochiccioli P *et al*. Creutzfeldt-Jakob disease after treatment with human extracted growth hormone. A clinicopathological study. *Rev Neurol (Paris)* 1993;**149**:524-7.

106. Department of the Environment, Food and Rural Affairs. Active TSE Surveillance in Great Britain (2002-2017): https://www.gov.uk/government/statistics/active-tse-surveillance-statistics

107. Diack AB, Ritchie DL, Peden AH *et al*. Variably protease-sensitive prionopathy, a unique prion variant with inefficient transmission properties. *Emerg Infect Dis* 2014;**20**:1969-79.

108. Donaldson DS, Kobayashi A, Ohno H *et al*. M-cell depletion blocks oral prion disease pathogenesis. *Mucosal Immunol* 2012;**5**:216-25.

109. Dorsey KZS, Schonberger LB, Sullivan M *et al*. Lack of evidence of transfusion transmission of Creutzfeldt-Jakob disease in a US surveillance study. *Transfusion* 2009;**49**:977-84.

110. Douet J-Y, Zafar S, Perret-Liaudet A *et al*. Detection of infectivity in blood of persons with variant and sporadic Creutzfeldt-Jakob disease. *Emerg Infect Dis* 2014; **20**: 114-7.

111. Duyckaerts C, Delatour B, Potier M-C. Classification and basic pathology of Alzheimer disease. *Acta Neuropathol* 2009;**118**:5-36.

112. Duffy P, Wolf J, Collins G *et al*. Possible person-to-person transmission of Creutzfeldt-Jakob disease. *N Engl J Med* 1974;**290**:692-3.

113. Dyer C. Trial begins into victims of CJD growth hormone. *BMJ* 1996a;**312**:1057.

114. Dyer C. Growth hormone deaths blamed on MRC and DoH. *BMJ* 1996b;**313**:185.

115. Edgeworth JA, Farmer M, Sicilia A *et al*. Detection of prion infection in variant Creutzfeldt-Jakob disease: a blood-based assay. *Lancet* 2011;**377**:487-93.

116. Edgren G, Hjalgrim H, Rostgaard K *et al*. Transmission of neurodegenerative disorders through blood transfusion. A cohort study. *Ann Intern Med* 2016; doi: 10.7326/M15-2421.

117. Eisele YS, Duyckaerts C. Propagation of Aβ pathology: hypotheses, discoveries, and yet unresolved questions from experimental and human brain studies. *Acta Neuropathol* 2016; **131**:5-25.

118. Eisele YS, Obermüller U, Heilbronner G *et al*. Peripherally applied Abeta-containing inoculates induce cerebral beta-amyloidosis. *Science* 2010;**330**:980-2.

119. el Tawil S, Mackay G, Davidson L *et al*. Variant Creutzfeldt-Jakob disease in older patients. *J Neurol Neurosurg Psychiatry* 2015;**86**:1279-80.

120. Exome Aggregation Consortium (ExAC). [Version 0.3.1 cited March 2016]; http://exac.broadinstitute.org.

121. Farquhar C, Dickinson A, Bruce M. Prophylactic potential of pentosan polysulphate in transmissible spongiform encephalopathies. *Lancet* 1999; **353**: 117.

122. Feeney C, Scott GP, Cole JH *et al*. Seeds of neuroendocrine doubt. *Nature* 2016;**535**:E1-2.

123. Fernie K, Steele PJ, Taylor DM, Somerville RA. Comparative studies on the thermostability of five strains of transmissible-spongiform-encephalopathy agent. *Biotechnol Appl Biochem* 2007;**47**:175-83.

124. Ferreira NC, Marques IA, Conceição WA *et al*. Anti-prion activity of a panel of aromatic chemical compounds: in vitro and in silico approaches. *PLoS One* 2014;**9**: e84531. doi: 10.1371/journal.pone.0084531. eCollection 2014.

125. Fichet G, Antloga K, Comoy E *et al*. Prion inactivation using a new gaseous hydrogen peroxide sterilisation process. *J Hosp Infect* 2007;**67**:278-86.

126. Forloni GF, Tettamanti M, Lucca U *et al*. Preventative study in subjects at risk of fatal familial insomnia: Innovative approaches to rare diseases. *Prion* 2015;**9**:75-9.

127. Frontzek K, Lutz M, Aguzzi A, Kovacs GG, Budka H. Amyloid β-pathology and cerebral angiopathy are frequent after iatrogenic Creutzfeldt-Jakob disease after dural grafting. *Swiss Med Wkly* 2016;**146**:w14287 doi:10.4414/smw.2016.14287.

128. Gahr M, Nowak DA, Connemann B, Schonfeldt-Lecuona C. Cerebral amyloid angiopathy – a disease with implications for neurology and psychiatry. *Brain Res* 2013;**1519**:19-30.

129. Gajdusek DC, Gibbs CJ, Alpers DM. Experimental transmission of a Kuru-like syndrome to chimpanzees. *Nature* 1966;**209**:794-6.

130. Gajdusek DC, Gibbs CJ, Asher DM *et al*. Precautions in medical care of, and in handling materials from, patients with transmissible virus dementia (Creutzfeldt-Jakob disease). *N Engl J Med* 1977;**297**:1253-8.

131. Gajdusek DC, Zigas V. Degenerative disease of the central nervous system in New Guinea: the endemic occurrence of 'kuru' in the native population. *N Engl J Med* 1957;**257**:974-8.

132. Gajdusek DC, Zigas V. Kuru; Clinical, pathological and epidemiological study of an acute progressive degenerative disease of the central nervous system among natives of the Eastern Highlands of New Guinea. *Am J Med* 1959;**26**:442-69.

133. Gambetti P, Cali I, Notari S *et al*. Molecular biology and pathology of prion strains in sporadic human prion diseases. *Acta Neuropathol* 2011;**121**:79-90.

134. Gambetti P, Dong Z, Yuan J *et al*. A novel human disease with abnormal prion protein sensitive to protease. *Ann Neurol* 2008;**63**:697-708.

135. Gambetti P, Kong Q, Zou W *et al*. Sporadic and familial CJD: classification and characterisation. *Br Med Bull* 2003;**66**:213-39.

136. Garrison E, Marth G. Haplotype-based variant detection from shortread sequencing. *arXiv*, 2012: p. 1207.3907v2.

137. Garske T, Ghani AC. Uncertainty in the tail of the variant Creutzfeldt-Jakob disease epidemic in the UK. *PLoS One* 2010;**5**:15626.doi: 10.1371/journal.pone.0015626.

138. Gelpi E, Insa JMS, Parchi P *et al*. Atypical neuropathological sCJD-MM phenotype with abundant white matter Kuru-type plaques sparing the cerebellar cortex. *Neuropathology* 2013;**33**:204-8.

139. Gerstmann J, Straussler E, Scheinker I. Uber eine eigenartige hereditar-familiare erkrankung des zentralnervensystems. Zugleich ein beitrag zur frage des vorzeitigen localen alterns. *Z Neurol Psychiat* 1936;**154**:736-62.

140. Geschwind MD. Doxycycline for Creutzfeldt-Jakob disease: a failure, but a step in the right direction. *Lancet Neurol* 2014;**13**:130-2.

141. Geschwind MD, Kuo AL, Wong KS *et al*. Quinacrine treatment trial for sporadic Creutzfeldt-Jakob disease. *Neurology* 2013;**81**:2015-23.

142. Ghetti B, Dlouhy SR, Giaccone G *et al*. Gerstmann-Sträussler-Scheinker disease and the Indiana kindred. *Brain Pathol* 1995;**5**:61-75.

143. Ghetti B, Piccardo P, Frangione B *et al*. Prion protein amyloidosis. *Brain Pathol* 1996;**6**:127-45.

144. Gibbs CJ, Asher DM, Brown PW *et al*. Creutzfeldt-Jakob disease infectivity of growth hormone derived from human pituitary glands. *N Engl J Med* 1993;**328**:358-9.

145. Gibbs CJ, Asher DM, Kobrine A *et al*. Transmission of Creutzfeldt-Jakob disease to a chimpanzee by electrodes contaminated during neurosurgery. *J Neurol Neurosurg Psychiatry* 1994;**57:**757-8.

146. Gibbs CJ, Gajdusek DC, Asher DM *et al*. Creutzfeldt-Jakob Disease (spongiform encephalopathy): transmission to the chimpanzee. *Science* 1968;**161**:388-9.

147. Gibbs CJ, Joy A, Heffner R *et al*. Clinical and pathological features and laboratory confirmation of Creutzfeldt-Jakob disease in a recipient of pituitary-derived human growth hormone. *N Engl J Med* 1985;**313**:734-8.

148. Giles K, Berry DB, Condell C *et al*. Optimization of aryl amides that extend survival in prion-infected mice. *J Pharmacol Exp Ther* 2016; Jun 17. pii: jpet.116.235556.

149. Gill AC, Agarwal S, Pinheiro TJ, Graham JF. Structural requirements for efficient prion conversion: cofactors may promote a conversion-competent structure for PrP(C). *Prion* 2010;**4**:235-42.

150. Gill ON, Spencer Y, Richard-Loendt A *et al*. Prevalent abnormal prion protein in human appendixes after bovine spongiform encephalopathy epizootic: large scale survey. *BMJ* 2013;**347**: f5675. doi: 10.1136/bmj.f5675.

151. Glatzel M, Abela E, Maissen M *et al*. Extraneural pathologic prion protein in sporadic Creutzfeldt-Jakob disease. *N Engl J Med* 2003;**349**:1812-20.

152. Goedert M. Alzheimer's and Parkinson's diseases: the prion concept in relation to assembled Aβ, tau and α-synuclein. *Science* 2015;**349**:601-10.

153. Goldfarb LG, Petersen RB, Tabaton M *et al.* Fatal familial insomnia and familial Creutzfeldt-Jakob disease: disease phenotype determined by a DNA polymorphism. *Science* 1992;**258**:806-8.

154. Gonzalez L, Martin S, Begara-McGorum I *et al*. Effects of agent strain and host genotype on PrP accumulation in the brain of sheep naturally and experimentally affected with scrapie. *J Comp Path* 2002;**126**:17-29.

155. Green A, Sanchez-Juan P, Ladogana A *et al*. CSF analysis in patients with sporadic CJD and other transmissible spongiform encephalopathies. *Eur J Neurol* 2007;14:121-4.

156. Green AJE, Thompson EJ, Stewart GE *et al*. Use of 14-3-3 and other brain-specific proteins in CSF in the diagnosis of variant Creutzfeldt-Jakob disease. *J Neurol Neurosurg Psychiatry* 2001;**70**:744-8.

157. Green E. A wonder drug that carried the seeds of death. Los Angeles Times, 21st May 2000. http://articles.latimes.com/2000/may/21/news/mn-32419/5.

158. Griffith JS. Self replication and scrapie. *Nature* 1967;**215**:1043-4.

159. Hadlow WJ. Scrapie and Kuru. *Lancet* 1959;**2**:289-90.

160. Haik S, Brandel J-P. Biochemical and strain properties of CJD prions: complexity versus simplicity. *J Neurochem* 2011;**119**:251-61.

161. Haik S, Brandel JP, Salomon D *et al*. Compassionate use of quinacrine in Creutzfeldt-Jakob disease fails to show significant effects. *Neurology* 2004; **63**: 2413-5.

162. Haik S, Faucheux BA, Sazdovitch *et al*. The sympathetic nervous system is involved in variant Creutzfeldt-Jakob disease. *Nat Med* 2003;**9**:1121-3.

163. Haik S, Marcon G, Malle A *et al*. Doxycycline in Creutzfeldt-Jakob disease: a phase 2, randomised, double-blind, placebo-controlled trial. *Lancet Neurol* 2014;**13**:150-8.

164. Hall V, Brookes D, Nacul L *et al*. Managing the risk of iatrogenic transmission of Creutzfeldt-Jakob disease in the UK. *J Hosp Infect* 2014;**88**:22-7.

165. Halliday M, Radford H, Sekine Y *et al*. Partial restoration of protein synthesis rates by the small molecule ISRIB prevents neurodegeneration without

pancreatic toxicity. *Cell Death Dis* 2015;**6**: e1672. doi: 10.1038/cddis.2015.49.

166. Hamaguchi T, Sakai K, Noguchi-Shinohara M *et al*. Insight into the frequent occurrence of dura mater graft-associated Creutzfeldt-Jakob disease in Japan. *J Neurol Neurosurg Psychiatry* 2013;**84**:1171-5.

167. Hamaguchi T, Taniguchi Y, Sakai K *et al*. Significant association of cadaveric dura mater grafting with subpial Aβ deposition and meningeal amyloid angiopathy. *Acta Neuropathol* 2016;**132**:313-5.

168. Harder A, Jendroska K, Kreuz F *et al*. Novel twelve-generation kindred of fatal familial insomnia from Germany representing the entire spectrum of disease expression. *Am J Med Genet* 1999;**87**:11-6.

169. Harris DA, Peters PJ, Taraboulos V, *et al*. Cell Biology of Prions. In: Prusiner SB ed. *Prion Biology and Diseases Second Edition*. New York: Cold Spring Harbor Laboratory Press, 2004: 483–544.

170. Hashizume M, Takagi J, Kanehira T *et al*. Histologic study of age-related change in the posterior pituitary gland focusing on abnormal deposition of tau protein. *Pathol Int* 2011;**61**:13-8.

171. Hatami A, Monjazeb S, Glabe C. The anti-amyloid-β monoclonal antibody 4G8 recognises a generic sequence-independent epitope associated with α-synuclein and islet amyloid polypeptide amyloid fibrils. *J Alzheimers Dis* 2016;**50**:517-25.

172. Head MW, Bunn TJR, Bishop MT *et al*. Prion protein heterogeneity in sporadic but not variant Creutzfeldt-Jakob disease: UK cases 1991-2002. *Ann Neurol* 2004a;**55**:851-9.

173. Head MW, Ironside JW. Creutzfeldt-Jakob disease: prion protein type, disease phenotype and agent strain. *Neuropathol Appl Neurobiol* 2012;**38**:296-310.

174. Head MW, Ironside JW, Ghetti B *et al*. Prion diseases. In: Love S, Budka H, Ironside JW, Perry A eds. *Greenfield's Neuropathology Ninth Edition*. Boca Ratan: CRC Press, 2015: 1016-1086.

175. Head MW, Ritchie D, Smith N *et al*. Peripheral tissue involvement in sporadic, iatrogenic and variant Creutzfeldt-Jakob disease: an immunohistochemical, quantitative and biochemical study. *Am J Pathol* 2004b;**164**:143-53.

176. Head MW, Yull HM, Ritchie DL *et al*. Variably protease-sensitive prionopathy in the UK: a retrospective review 1991-2008. *Brain* 2013;**136**: 1102-15.

177. Heath CA, Barker RA, Esmonde TFG *et al*. Dura mater-associated Creutzfeldt-Jakob disease: experience from surveillance in the UK. *J Neurol Neurosurg Psychiatry* 2006; **77**:880-2.

178. Heath CA, Cooper SA, Murray K *et al*. Diagnosing variant Creutzfeldt-Jakob disease: a retrospective analysis of the first 150 cases in the UK. *J Neurol Neurosurg Psychiatry* 2011;**82**:646-51.

179. Heppner FL, Christ AD, Klein MA *et al*. Transepithelial prion transport by M cells. *Nature Med* 2001;**7**:976-7.

180. Herms J, Tings T, Gall S *et al*. Evidence of presynaptic location and function of the prion protein. *J Neurosci* 1999;**19**:8866-75.

181. Hill AF, Butterworth RJ, Joiner S *et al.* Investigation of variant Creutzfeldt-Jakob disease and other human prion diseases with tonsil biopsy samples. *Lancet* 1999;**353**:183-89.

182. Hilton DA, Fathers E, Edwards P *et al*. Prion immunoreactivity in appendix before clinical onset of variant Creutzfeldt-Jakob disease. *Lancet* 1998;**352**:703-4.

183. Hilton DA, Ghani AC, Conyers L *et al*. Prevalence of lymphoreticular prion protein accumulation in UK tissue samples. *J Pathol* 2004a;**203**:733-9.

184. Hilton DA, Sutak J, Smith MEF *et al*. Specificity of lymphoreticular accumulation of prion protein for variant Creutzfeldt-Jakob disease. *J Clin Pathol* 2004b;**57**:300-2.

185. Homma T, Mochizuki Y, Mizutani T. Phosphorylated α-synuclein immunoreactivity in the posterior pituitary lobe. *Neuropathology* 2012;**32**:385-9.

186. Hooper NM. Glycosylation and GPI anchor storage of the prion protein. *Adv Exp Med Biol* 2005;**564**:95-6.

187. House of Commons Science & Technology Committee: After the storm: UK blood safety and the risk of variant Creutzfeldt-Jakob disease. http://www.publications.parliament.uk/pa/cm201415/cmselect/cmsctech/327/32702.htm 2014.

188. Hsiao K, Baker HF, Crowe TJ *et al*. Linkage of a prion protein missense variant to Gerstmann-Sträussler syndrome. *Nature* 1989;**338**:342-5.

189. Huillard d'Aignaux J, Costagliola D, Maccario J *et al*. Incubation period of Creutzfeldt-Jakob disease in human growth hormone recipients in France. *Neurology* 1999;**53**:1197-201.

190. Hunter N, Moore L, Hosie BD *et al*. Association between natural scrapie and PrP genotype in a flock of Suffolk sheep in Scotland. *Vet Rec* 1997;**140**:59-63.

191. Hyman BT, Phelps CH, Beach TG *et al*. National Institute on Aging-Alzheimer's Association guidelines for the neuropathologic assessment of Alzheimer's disease. *Alzheimers Dement* 2012;**8**:1-13.

192. Ikeda SI, Yanagisawa N, Allsop D, Glenner GG. Gerstmann- Sträussler-Scheinker disease showing beta-protein type cerebellar and cerebral amyloid angiopathy. *Acta Neuropathol* 1994;**88**:262-6.

193. Ironside JW. Prion diseases in man. *J Pathol* 1998;**186**:227-34.

194. Ironside JW, Head MW, Bell JE *et al*. Laboratory diagnosis of variant Creutzfeldt-Jakob disease. *Histopatholog**y*** 2000;**37**:1-9.

195. Ironside JW, McCardle L, Horsburgh A *et al*. Pathological diagnosis of variant Creutzfeldt-Jakob disease. *APMIS* 2002;**11**:79-87.

196. Ironside JW, Ritchie DL, Head MW. Phenotypic variability in human prion diseases. *J Neuropathol Appl Neurobiol* 2005;**21**:565-79.

197. Ironside JW, Bishop MT, Connolly K *et al*. Variant Creutzfeldt-Jakob disease: prion protein genotype analysis of positive appendix tissue samples from a retrospective prevalence study. *Brit Med J* 2006;**332**:1186-8.

198. Irwin DJ, Abrams JY, Schonberger LB *et al*. Evaluation of potential infectivity of Alheimer and Parkinson disease proteins in recipients of cadaver-derived human growth hormone. *JAMA Neurol* 2013;**70**:462-8.

199. Ishida C, Kakushima A, Okino S *et al*. Sporadic Creutzfeldt-Jakob disease with MM1-type prion protein and plaques. *Neurology* 2003;**60**:514-7.

200. Jackson GS, McKintosh E, Flechsig E *et al*. An enzyme-detergent method for effective prion decontamination of surgical steel. *J Gen Virol* 2005;**86**:869-78.

201. Jakob A. Über eigenartige erkrankungen des zentralnervensystems mit bemerkenswertem anatomischen befunde (spastische pseudosklerose-encephalomyelopathie mit disseminierten degenerationsherden). *Deutches Z fur Nervenheilkunde* 1921a;**70**:132-46.

202. Jakob A. Über eigenartige erkrankungen des zentralnervensystems mit bemerkenswertem anatomischen befunde (spastische pseudosklerose-encephalomyelopathie mit disseminierten degenerationsherden). *Z Ges Neurol Psychiatrie* 1921b;**64**:147-228.

203. Jakob A. Spastische pseudosklerose. In: Foerster O, Wilmanns K eds. *Die Extrapyramidalen Erkrankungen.* Berlin: Julius Springer, 1923:215-345.

204. Jansen C, Head MW, Rozemuller AJ, Ironside JW. Panencephalopathic Creutzfeldt-Jakob disease in the Netherlands and the UK: clinical and pathological characteristics of nine patients. *Neuropathol Appl Neurobiol* 2009;**35**:272-82.

205. Jarosz-Griffiths HH, Noble E, Rushworth JV, Hooper NM. Amyloid-β receptors: the good, the bad, and the prion protein. *J Biol Chem* 2016;**291**:3174-83.

206. Jaunmuktane Z, Mead S, Ellis M *et al*. Evidence for human transmission of amyloid-β pathology and cerebral amyloid angiopathy. *Nature* 2015;**525**:247-50.

207. Jin SC, Benitez BA, Karch CM *et al*. Coding variants in *TREM2* increase risk for Alzheimer's disease. *Hum Mol Genet* 2014;**23**:5838-46.

208. Jones M, Peden AH, Head MW, Ironside JW. The application of in vitro cell-free conversion systems to human prion diseases. *Acta Neuropathol* 2011;**121**:135-43.

209. Jones RL, Benker G, Salacinski PR *et al*. Large-scale preparation of highly purified pyrogen-free human growth hormone for clinical use. *J Endocrinol* 1979;**82**:77-86.

210. Jucker M, Walker LC. Self-propagation of pathogenic protein aggregates in neurodegenerative diseases. *Nature* 2013;**501**:45-51.

211. Keable A, Fenna K, Yuen HM *et al*. Deposition of amyloid β in the walls of human leptomeningeal arteries in relation to perivascular drainage pathways in cerebral amyloid angiopathy. *Biochim Biophys Acta* 2016;**1862**:1037-46.

212. Kim JI, Cali I, Surewiscz K *et al*. Mammalian prions generated from bacterially expressed prion protein in the absence of any mammalian cofactors. *J Biol Chem* 2010;**285**:14083-7.

213. Kimberlin RH, Walker CA. Pathogenesis of experimental scrapie. *Ciba Found Symp* 1988;**135**:37-62.

214. Kirkwood JK, Cunningham AA. Epidemiological observations on spongiform encephalopathies in captive wild animals in the British Isles. *Vet Rec* 1994;**135**:296-303.

215. Kirschbaum WR. Zwei eigenartige erkrankugen des zentralnervensystems nach art der spastischen pseudosklerose (Jakob). *Z Ges Neurol Psychiatrie* 1924;**92**:175-220.

216. Klatzo I, Gajdusek DC, Zigas V. Pathology of Kuru. *Lab Invest* 1959**;8**:799-847.

217. Klohn PC, Stoltze L, Flechsig E *et al*. A quantitative, highly sensitive cell-based infectivity assay for mouse scrapie prions. *Proc Natl Acad Sci USA* 2003;**100**:11666-73.

218. Kobayashi A, Arima K, Ogawa M *et al*. Plaque-type deposition of prion protein in the damaged white matter of sporadic Creutzfeldt-Jakob disease MM1 patients. *Acta Neuropathol* 2008;**116**:561-6.

219. Kobayashi A, Asano M, Mohri S, Kitamoto T. Cross-sequence transmission of sporadic Creutzfeldt-Jakob disease creates a new prion strain. *J Biol Chem* 2007;**282**:30022-8.

220. Kobayashi A, Asano M, Mohri S, Kitamoto T. A traceback phenomenon can reveal the origin of prion infection. *Neuropathology* 2009;**29**:619-24.

221. Kobayashi A, Iwasaki Y, Otsuka H *et al*. Deciphering the pathogenesis of sporadic Creutzfeldt-Jakob disease with codon 129 M/V and type 2 abnormal prion protein. *Acta Neuropathol Commun* 2013;**1**:74.doi 10.1186/2051-2960-1-74.

222. Kobayashi A, Matsuura Y, Mohri S, Kitamoto T. Distinct origins of dura mater graft-associated Creutzfeldt-Jakob disease; past and future problems. *Acta Neuropathol Commun* 2014;**2**:32 doi: 10.1186/2051-5960-2-32.

223. Kobayashi A, Parchi P, Yamada M *et al*. Transmission properties of atypical Creutzfeldt-Jakob disease: a clue to disease etiology? *J Virol* 2015;**89**:3939-46.

224. Kobayashi A, Parchi P, Yamada M *et al*. Neuropathological and biochemical criteria to identify acquired Creutzfeldt-Jakob disease among presumed sporadic cases. *Neuropathology* 2016;**36**:305-10.

225. Kobayashi A, Sakuma N, Matsuura Y *et al*. Experimental verification of a traceback phenomenon in prion infection. *J Virol* 2010;**84**:3230-8.

226. Koch TK, Berg BO, DeArmond SJ *et al*. Creutzfeldt-Jakob disease in a young adult with idiopathic hypopituitarism. *N Engl J Med* 1985;**313**:731-3.

227. Kocisko DA, Come JH, Priola SA *et al*. Cell-free formation of protease-resistant prion protein. *Nature* 1994;**370**:471-4.

228. Kong Q, Surewicz WK, Petersen RB, W *et al*. Inherited prion diseases. In: Prusiner SB ed. *Prion Biology and Diseases Second Edition*. New York: Cold Spring Harbor Laboratory Press, 2004: 673 - 776.

229. Kovacs GG. Can Creutzfeldt-Jakob disease unravel the mysteries of Alzheimer? *Prion* 2016 Sep 20:0. Epub ahead of print.

230. Kovacs GG, Lutz ML, Ricken R, *et al*. Dura mater is a potential source of Aβ seeds. *Acta Neuropathol* 2016a;**131**:911-23.

231. Kovacs GG, Puopolo M, Ladogana A *et al*. Genetic prion disease: the EUROCJD experience. *Hum Genet* 2005;**118**:166-74.

232. Kovacs GG, Rahimi J, Strobel T, *et al*. Tau pathology in Creutzfeldt-Jakob disease revisited. *Brain Pathol* 2016b Jul 5. doi: 10.1111/bpa.12411.

233. Krejciova Z, Pells S, Cancellotti E *et al*. Human embryonic stem cells rapidly take up and then clear exogenous human and animal prions in vitro. *J Pathol* 2011;**223**:635-45.

234. Kudo W, Lee HP, Zou WQ *et al*. Cellular prion protein is essential for oligomeric amyloid-β-induced neuronal cell death. *Hum Mol Genet* 2012;**21**:1138-44.

235. Küffer A, Lakkaraju AK, Mogha A *et al*. The prion protein is an agonistic ligand of the G protein-coupled receptor Adgrg6. *Nature* 2016;**536**:464-8.

236. Lacroux C, Bougard D, Litaise C *et al*. Impact of leucocyte depletion and prion reduction filters on TSE blood borne transmission. *PLoS One* 2012;**7**: e42019. doi: 10.1371/journal.pone.0042019. Epub 2012 Jul 31.

237. Lacroux C, Comoy E, Moudjou M *et al*. Preclinical detection of variant CJD and BSE prions in blood. *PLoS Pathogens* 2014;**10**: e1004202. doi: 10.1371/journal.ppat.1004202. eCollection 2014.

238. Ladogana A, Puopolo M, Croes EA *et al*. Mortality from Creutzfeldt-Jakob disease and related disorders in Europe, Australia and Canada. *Neurology* 2005;**64**:1586-91.

239. Lambert JC, Mann DM, Harris JM *et al*. The -48 C/T polymorphism in the presenilin 1 promoter is associated with an increased risk of developing Alzheimer's disease and an increased Abeta load in brain. *J Med Genet* 2001;**38**:353-5.

240. Langmead B, Trapnekk C, PopM, Slazberg SL. Ultrafast and memory-efficient alignment of short DNA sequences to the human genome. *Genome Biol* 2009;**10**: R25. doi: 10.1186/gb-**2009**-10-3-r25. Epub **2009** Mar 4.

241. Lasmezas CI, Deslys JP, Robain O *et al*. Transmission of the BSE agent to mice in the absence of detectable prion protein. *Science* 1997;**275**:402-5.

242. Lasmezas CI, Comoy E, Hawkins S *et al*. Risk of oral infection with bovine spongiform encephalopathy agent in primates. *Lancet* 2005;**365**:781-3.

243. Lee IY, Westaway D, Smit AFA *et al*. Complete genomic sequence and analysis of the prion protein gene region from three mammalian species. *Genome Res* 1998;**8**:1022-37.

244. Lee KS, Caughey B. A simplified recipe for prions. *Proc Natl Acad Sci USA* 2007;**104**:9551-2.

245. Lee YJ, Baskakov IV. The cellular form of the prion protein guides the differentiation of human embryonic stem cells into neuron-, oligodendrocyte- and astrocyte-committed lineages. *Prion* 2014;**8**:266-75.

246. Legname G, Baskakov IV, Nguyen HO *et al*. Synthetic mammalian prions. *Science* 2004;**305**:673-6.

247. Liberski PP, Budka H, Sluga E *et al*. Tubulovesicular structures in Creutzfeldt-Jakob disease. *Acta Neuropathol* 1992;**84**:238-43.

248. Liberski PP, Sikorska B, Brown P. Kuru: the first prion disease. Adv Exp Mol Neurol 2012;**724**:143-53.

249. Liberski PP, Streichenberger N, Giraud P *et al*. Ultrastructural pathology of prion diseases revisited: brain biopsy studies. *Neuropathol Appl Neurobiol* 2005;**31**:88-96.

250. Linden R, Martins VR, Prado MA *et al*. Physiology of the prion protein. *Physiol Rev* 2008;**88**:673-728.

251. Linsell L, Cousens SN, Smith PG *et al.* A case-control study of sporadic Creutzfeldt-Jakob disease in the United Kingdom: Analysis of clustering. *Neurology* 2004;**63:**2077-83.

252. Love S, Chalmers K, Ince P *et al*. Development, appraisal, validation and implementation of a consensus protocol for the assessment of cerebral amyloid angiopathy in post-mortem brain tissue. *Am J Neurodegener Dis* 2014;**3**:19-32.

253. Mabbott NA, MacPherson GG. Prions and their lethal journey to the brain. *Nat Rev Microbiol* 2006;**4**:201-11.

254. Mahal SP, Asante EA, Antoniou M, Collinge J. Isolation and functional characterisation of the promoter region of the human prion protein gene. *Gene* 2001;**268**:105-14.

255. Maji SK, Perrin MH, Sawaya MR *et al*. Functional amyloids as natural storage of peptide hormones in pituitary secretory granules. *Science* 2009;**325**:328-32.

256. Makarava N, Kovacs GG, Bocharova O *et al*. Recominant prion protein induces a new transmissible prion disease in wild-type animals. *Acta Neuropathol* 2010;**119**:177-87.

257. Mangé A, Béranger F, Peoc'h K *et al*. Alpha- and beta- cleavages of the amino-terminus of the cellular prion protein. *Biol Cell* 2004;**96**:125-32.

258. Manson JC, West JD, Thomson V *et al*. The prion protein gene: a role in mouse embryogenesis? *Development* 1992;**115**:117-22.

259. Markus HS, Duchen LW, Parkin EM *et al.* Creutzfeldt-Jakob disease in recipients of human growth hormone in the United Kingdom - a clinical and radiographic study. *Q J Med* 1992; **82**: 43-51.

260. Masters CL, Gajdusek DC. The spectrum of Creutzfeldt-Jakob disease and the virus-induced subacute spongiform encephalopathies. In: Smith WT, Cavanagh JB eds. *Recent Advances in Neuropathology Second Edition*. Edinburgh: Churchill Livingstone, 1982:139-63.

261. Masters CL, Gajdusek DC, Gibbs CJ. Creutzfeldt-Jakob disease virus isolations from the Gerstmann-Sträussler syndrome with an analysis of the various forms of amyloid plaque deposition in the virus-induced spongiform encephalopathies. *Brain* 1981;**104**;559-88.

262. Mastrianni JA, Nixon R, Layzer R *et al*. Prion protein conformation in a patient with sporadic fatal insomnia. *N Engl J Med* 1999;**340**:1630-8.

263. Mattei V, Garofalo T, Misasi R *et al*. Prion protein is a component of the multimolecular signaling complex involved in T cell activation. *FEBS Lett* 2004;**560**:14-8.

264. Mayeux R, Stern Y. Epidemiology of Alzheimer disease. *Cold Spring Harb Perspect Med* 2012;**2**: pii: a006239. doi: 10.1101/cshperspect.a006239.

265. Mays CE, Soto C. The stress of prion disease. *Brain Res* 2016; doi: 10.1016/j.brainres.2016.04.009.

266. McBride PA, Schultz-Schaeffer WJ, Donaldson M *et al*. Early spread of scrapie from the gastrointestinal tract to the central nervous system involves autonomic fibers of the splanchnic and vagus nerves. *J Virol* 2001;**75**:9320-7.

267. McCutcheon S, Blanco ARA, Tan BC *et al*. A prion reduction filter does not completely remove endogenous prion infectivity from sheep blood. *Transfusion* 2015;**55**:2123-33.

268. McGuire LI, Poleggi A, Poggiolini I *et al*. CST RT-QuIC is a robust and reliable test for sporadic CJD: an international study. *Ann Neurol* 2016;**80**:160-5.

269. McKee AC, Cairns NJ, Dickson DW *et al*. The first NINDS/NBIB consensus meeting to define neuropathological criteria for the diagnosis of chronic traumatic encephalopathy. *Acta Neuropathol* 2016: **131**:75-86.

270. McKinley MP, Hay B, Lingappa VR *et al*. Developmental expression of prion protein gene in the brain. *Dev Biol* 1987;**121**:105-10.

271. McKinnon C, Goold R, Andre R *et al*. Prion-mediated neurodegeneration is associated with early impairment of the ubiquitin-proteasome system. *Acta Neuropathol* 2016;**131**:411-425.

272. McLean CA, Ironside JW, Alpers MP *et al*. Comparative neuropathology of kuru with the new variant of Creutzfeldt-Jakob disease: evidence for strain of agent predominating over genotype of host. *Brain Pathol* 1998;**8**:429-37.

273. Mead S, Poulter M, Beck J *et al*. Inherited prion disease with six octapeptide repeat insertional mutation – molecular analysis of phenotypic heterogeneity. *Brain* 2006;**129**:2297-317.

274. Mead S, Whitfield J, Poulter M *et al*. A novel prion protein variant that colocalises with kuru exposure. *N Engl J Med* 2009:**361**:2056-65.

275. Medori R, Tritschler HJ, LeBlanc A *et al*. Fatal familial insomnia, a prion disease with a mutation at codon 178 of the prion protein gene. *N Eng J Med* 1992;**326**:444-9.

276. Meissner B, Kallenberg K, Sanchez-Juan P *et al*. MRI lesion profiles in sporadic Creutzfeldt-Jakob disease. *Neurology* 2009a;**72**:1994-2001.

277. Meissner B, Kallenberg K, Sanchez-Juan P *et al*. MRI and clinical syndrome in dura mater-related Creutzfeldt-Jakob disease. *J Neurol* 2009b;**256**: 355-63.

278. Mills JB, Ashworth RB, Wilhelmi AE, Hartree AS. Improved method for the extraction and purification of human growth hormone. *J Clin Endocrinol Metab* 1969;29:1456-9.

279. Milner RD. Human growth hormone (UK). *Archiv Dis Child* 1979;**54**:733-4.

280. Milner RD, Russell-Fraser T, Brook CG *et al*. Experience with growth hormone in Great Britain: the report of the MRC Working Party. *Clin Endocrinol (Oxf)* 1979;**11**:15-38.

281. Minikel EV, Vallabh SM, Lek M *et al*. Quantifying prion disease penetrance using large population control cohorts. Sci Transl Med 2016;**8**: 322ra9. doi: 10.1126/scitranslmed.aad5169.

282. Mirra S, Heyman A, McKeel D *et al*. The Consortium to Establish a Registry for Alzheimer's Disease (CERAD). Part II. Standardization of the neuropathologic assessment of Alzheimer's disease. *Neurology* 1991;**41**:479-86.

283. Miyazono M, Kitamoto T, Iwaki T, Tateishi J. Colocalisation of prion proteion and beta protein in the same amyloid plaques in patients with Gerstmann-Sträussler syndrome. *Acta Neuropathol* 1992;**83**:333-9.

284. Mobley WC, Neve RL, Prusiner SB, McKinley MP. Nerve growth factor increases mRNA levels for the prion protein and the beta-amyloid protein precursor in developing hamster brain. *Proc Natl Acad Sci USA* 1988;**85**:9811-5.

285. Moda F, Gambetti P, Notari S *et al*. Prions in the urine of patients with variant Creutzfeldt-Jakob disease. *N Engl J Med* 2014;**371**:530-9.

286. Moda F, Suardi S, Di Fede G *et al*. MM2-thalamic Creutzfeldt-Jakob disease: neuropathological, biochemical and transmission studies reveal a distinctive prion strain. *Brain Pathol* 2012;**22**:662-9.

287. Moore RA, Head MW, Ironside JW *et al*. The distribution of prion protein allotypes differs between sporadic and iatrogenic Creutzfeldt-Jakob disease patients. *PLOS Pathog* 2016;**12**:e1005496.

288. Moore RC, Hope J, McBride PA *et al*. Mice with gene targeted prion protein alterations show that Prnp, Sinc and Prni are congruent. *Nat Genet* 1998;**18**:118-25.

289. Morales R, Duran-Aniotz C, Diaz-Espinoza R *et al*. Protein misfolding cyclic amplification of infectious prions. *Nat Protoc* 2012;**7**;1397-409.

290. Moreno JA, Radford H, Peretti D *et al*. Sustained translational repression by elF2α-P mediates prion neurodegeneration. *Nature* 2012;**485**:507-11.

291. Moreno-Gonzales I, Soto C. Misfolded protein aggregates: mechanisms, structures and potential for disease transmission. *Semin Cell Dev Biol* 2011;**22**:482-7.

292. Nevin S, McMenemey WH, Behrman S, Jones DP. Subacute spongiform encephalopathy - a subacute form of encephalopathy attributable to vascular dysfunction (spongiform cerebral atrophy). *Brain* 1960; **83**: 519-63.

293. Newman PL, Todd NV, Scoones D *et al*. Postmortem findings in a case of variant Creutzfeldt-Jakob disease treated with intraventricular pentosan polysulfate. *J Neurol Neurosurg Psychiatry* 2104;**85**:921-4.

294. News of the week. Scientists in growth hormone scandal found blameless. *Science* 2011;**332**:772.

295. NHLBI GO Exome Sequencing Project (ESP). [cited 2013 12/12/2013]; Available from: URL: http://evs.gs.washington.edu/EVS.

296. Nicoll JAR, Burnett C, Love S *et al*. High frequency of Apolipoprotein E ε2 allele in hemorrhage due to cerebral amyloid angiopathy. *Ann Neurol* 1997;**41**:716-21.

297. Notari S, Moleres FJ, Hunter SB *et al*. Multiorgan detection and characterization of protease-resistant prion protein in a case of variant CJD examined in the United States. *PLoS One* 2010;**5**: e8765. doi: 10.1371/journal.pone.0008765.

298. Notari S, Xiao X, Espinosa JC *et al*. Transmission characteristics of variably protease-sensitive prionopathy. *Emerg Infect Dis* 2014;**20**:2006-14.

299. Oechs B, Westaway D, Walchli M *et al*. A cellular gene encodes scrapie PrP 27-30 protein. *Cell* 1985;**40**:735-46.

300. Orru CD, Wilham JM, Hughson AG *et al*. Human variant Creutzfeldt-Jakob disease and sheep scrapie PrP^{res} detection using seeded conversion of recombinant prion protein. *Protein Eng Des Sel* 2009;**22**:515-21.

301. Otto M, Cepek L, Ratzka P *et al*. Efficacy of flupirtine on cognitive function in patients with CJD. A double blind study. *Neurology* 2004;**62**:714-8.

302. Owen F, Poulter M, Lofthouse R *et al*. Insertion in prion protein gene in familial Creutzfeldt-Jakob disease. *Lancet* 1989;**1**:51-2.

303. Palmer MS, Dryden AJ, Hughes JT, Collinge J. Homozygous prion protein genotype predisposes to sporadic Creutzfeldt-Jakob disease. *Nature* 1991;**352**:340-2.

304. Parchi P, Capellari S, Chen SG *et al*. Typing prion isoforms. *Nature* 1997;**386**:232-34.

305. Parchi P, Castellani R, Capellari S *et al.* Molecular basis of phenotypic variability in sporadic Creutzfeldt-Jakob disease. *Ann Neurol* 1996;**39:**767-78.

306. Parchi P, Cescatti M, Notari S *et al*. Agent strain variation in human prion disease: insights from a molecular and pathological review of the National Institutes of Health series of experimentally transmitted disease. *Brain* 2010;**133**:3030-42.

307. Parchi P, de Boni L, Saverioni D *et al*. Consensus classification of human prion disease histotypes allows reliable identification of molecular subtypes: an inter-rater study among surveillance centres in Europe and USA. *Acta Neuropathol* 2012;**124**:517-29.

308. Parchi P, Giese A, Capellari S *et al.* Classification of sporadic Creutzfeldt-Jakob disease based on molecular and phenotypic analysis of 300 subjects. *Ann Neurol* 1999;**46:**224-33.

309. Parchi P, Petersen RB, Chen SG *et al*. Molecular pathology of fatal familial insomnia. *Brain Pathol* 1998;**8**:539-48.

310. Parchi P, Strammiello R, Notari S *et al*. Incidence and spectrum of sporadic Creutzfeldt-Jakob disease variants with mixed phenotype and co-occurrence of PrPSc types: an updated classification. *Acta Neuropathol* 2009;**118**:659-71.

311. Parchi P, Zou W, Wang W *et al*. Genetic influence on the structural variations of the abnormal prion protein. *Proc Natl Acad Sci USA* 2000;**97**:10168-72.

312. Peden AH, Head MW, Ritchie DL *et al*. Preclinical vCJD after blood transfusion in a PRNP codon 129 heterozygous patient. *Lancet* 2004;**364**:527-9.

313. Peden AH, McCardle L, Head MW *et al*. Variant CJD in the spleen of a neurologically asymptomatic UK adult patient with haemophilia. *Haemophilia* 2010;**16**:296-304.

314. Peden AH, McGuire LI, Appleford NE *et al*. Sensitive and specific detection of sporadic Creutzfeldt-Jakob disease brain prion protein using real-time quaking-induced conversion. *J Gen Virol* 2012;**93**:438-49.

315. Peden AH, Ritchie DL, Head MW *et al*. Detection and localization of PrP^{Sc} in the skeletal muscle of patients with variant, iatrogenic, and sporadic forms of Creutzfeldt-Jakob disease. *Am J Pathol* 2006;**168**:927-35.

316. Peden A, Ritchie D, Udin HP *et al*. Abnormal prion protein in the pituitary gland in sporadic and variant Crutzfeldt-Jakob disease. *J Gen Virol* 2007;**88**:1068-72.

317. Peden A, Sarode D, Mulholland C *et al*. The prion protein protease sensitivity, stability and seeding activity in variably protease sensitive prionopathy brain tissue suggests molecular overlaps with sporadic Creutzfeldt-Jakob disease. *Acta Neuropathol Comm* 2014; **2**:doi:10.1186/s40478-014-0152-4.

318. Peters PJ, Mironov A, Peretz D *et al*. Trafficking of prion proteins through a caveolae-mediated endosomal pathway. *J Cell Biol* 2003;**162**:703-17.

319. Piccardo P, Dlouhy SR, Lievens PMJ *et al*. Phenotypic variability of Gerstmann-Sträussler-Scheinker disease is associated with prion protein heterogeneity. *J Neuropathol Exp Neurol* 1998;**57**:979-88.

320. Pletnikova O, Rudow GL, Hyde TM *et al*. Alzheimer lesions in the autopsied brains of people 30 to 50 years of age. *Cogn Behav Neurol* 2015;**28**:144-52.

321. Powell-Jackson J, Weller RO, Kennedy P *et al*. Creutzfeldt-Jakob disease after administration of human growth hormone. *Lancet* 1985;**2**:244-6.

322. Prusiner SB. Novel proteinaceous particles cause scrapie. *Science* 1982;**216**:136-44.

323. Prusiner SB. Prions. *Proc Natl Acad Sci USA* 1998a;**95**:13363-83.

324. Prusiner SB. The prion diseases. *Brain Pathol* 1998b;**8**:499-513.

325. Prusiner SB. Biology and genetics of prions causing neurodegeneration. *Ann Rev Genet* 2013;**47**:601-23.

326. Prusiner SB, Hadlow WJ, Garfin DE *et al*. Partial purification and evidence for multiple molecular forms of the scrapie agent. *Biochemistry* 1978;**17**:4993-9.

327. Public Health England. Summary results of the third national survey of abnormal prion prevalence in archived appendix specimens. *Health Protection Report* 2016; **10** (26):11-12, 12th August 2016. https://www.gov.uk/government/uploads/system/uploads/attachment_data/file/546883/hpr2616.pdf.

328. Puopolo M, Ladogana A, Vetrugno V, Pocchiari M. Transmission of sporadic Creutzfeldt-Jakob disease by blood transfusion: risk factor or possible biases. *Transfusion* 2011;**51**:1556-66.

329. Raben MS. Preparation of growth hormone from pituitaries of man and monkey. *Science* 1957;**125**:883-4.

330. Raben MS. Treatment of a pituitary dwarf with human growth hormone. *J Clin Endocrinol Metab* 1958;**18**:901-3.

331. Raymond GJ, Hope J, Kocisko DA *et al*. Molecular assessment of the potential transmissibilities of BSE and scrapie to humans. *Nature* 1997;**388**:285-8.

332. Renton AE, Majounie E, Waite A *et al*. A hexanucleotide repeat expansion in C9ORF72 is the cause of chromosome 9p21-linked ALS-FTD. *Neuron* 2011;**72**: 257-68.

333. Richt JA, Hall SM. BSE case associated with a prion gene mutation. *PLoS Pathog* 2008;**4**: e1000156. doi: 10.1371/journal.ppat.1000156.

334. Ritchie DL, Barria MA, Peden AH *et al*. UK iatrogenic Creutzfeldt-Jakob disease: investigating human prion transmission across genotypic barriers using human tissue-based and molecular approaches. Acta Neuropathol 2016; Nov 3. Epub ahead of print. DOI 10.10007/s00401-016-1638-x.

335. Ritchie DL, Head MW, Ironside JW. Advances in the detection of prion protein in peripheral tissues of variant Creutzfeldt-Jakob disease patients using paraffin-embedded tissue blotting. *Neuropathol Appl Neurobiol* 2004;**30**:360-8.

336. Robinson MM, Cheevers WP, Burger D, Gorham JR. Organ-specific modification of the dose-response relationship of scrapie infectivity. *J Infect Dis* 1990;**161**:783-6.

337. Rudge P, Jaunmuktane Z, Adlard P *et al*. Iatrogenic CJD due to pituitary-derived growth hormone with genetically determined incubation times of up to 40 years. *Brain* 2015;**138**.3386-99.

338. Saa P, Castillo J, Soto C. Presymptomatic detection of prions in blood. *Science* 2006; **313**: 92-4.

339. Saa P, Cervenakova L. Protein misfolding cyclic amplification (PMCA): current status and future directions. *Virus Res* 2014;**207**:47-61.

340. Saborio GP, Permanne B, Soto C. Sensitive detection of pathological prion protein by cyclic amplification of protein misfolding. *Nature* 2001;**411**:810-3.

341. Safar JG, Geschwind MD, Deering C *et al*. Diagnosis of human prion disease. *Proc Natl Acad Sci USA* 2005;**102**:3501-6.

342. Sakai K, Boche D, Carare R *et al*. Aβ immunotherapy for Alzheimer's disease: effects on apoE and cerebral vasculopathy. *Acta Neuropathol* 2014;**128**:777-89.

343. Sakudo A, Onodera T. Prion protein (PrP) gene-knockout cell lines: insight into the functions of the PrP. *Front Cell Dev Biol* 2015;**2**: 75. doi: 10.3389/fcell.2014.00075. eCollection 2014.

344. Salahuddin P, Fatima MT, Abdelhameed AS *et al*. Structure of prion oligomers and their mechanisms of toxicities: targeting amyloid oligomers using novel therapeutic approaches. *Eur J Med Chem* 2016;**114**:41-58.

345. Sanders DW, Kaufman S DeVos SL *et al*. Distinct tau prion protein strains propagate un mice and define different tauopathies. *Neuron* 2014;**82**:1271-88.

346. Sanders DW, Kaufman SK, Holmes BB, Diamond MI. Prions and protein assemblies that convey biological information in health and disease. *Neuron* 2016;**89**:433-48.

347. Sawyer EB, Edgeworth JA, Thomas C *et al*. Preclinical detection of infectivity and disease-specific PrP in blood throughout the incubation period of prion disease. Sci Rep 2015;**5**: 17742. doi: 10.1038/srep17742.

348. Schmidt H, Zeginigg M, Wiltgen M *et al*. Genetic variants of the *NOTCH3* gene in the elderly and magnetic resonance imaging correlates of age-related cerebral small vessel disease. *Brain* 2011;**134**:3384-97.

349. Schmitz M, Dittmar K, Llorens F *et al*. Hereditary human prion diseases: an update. *Mol Neurobiol* 2016; Jun 20. [Epub ahead of print].

350. Schoene WC, Masters CL, Gibbs CJ *et al*. Transmissible spongiform encephalopathy (Creutzfeldt-Jakob disease). Atypical clinical and pathological findings. *Arch Neurol* 1981;**38**:473-77.

351. Scott MR, Will R, Ironside J *et al*. Compelling transgenetic evidence for transmission of bovine spongiform encephalopathy prions to humans. *Proc Natl Acad Sci USA* 1999;**96**:15137-42.

352. Shi S, Mitteregger-Kretzschmar G, Giese A, Kretzschmar H. Establishing quantitative real-time quaking-induced conversion (qRT-QuIC) for highly sensitive detection and quantification of PrPSc in prion-infected tissues. *Acta Neuropathol Comm* 2013; **1**:44.doi: 10.1186/2051-5960-1-44.

353. Sigurdsson B. Rida, a chronic encephalitis of sheep: with general remarks on infections which develop slowly and some of their special characteristics. *Brit Vet J* 1954:**110**:255-70.

354. Silva CJ, Vazquez-Fernandez E, Onisko B, Requena JR. Proteinase K and the structure of PrP^{Sc}: the good, the bad and the ugly. *Virus Res* 2015;**207**:120-6.

355. Silveira JR, Raymond GJ, Hughson AG *et al*. The most infectious prion particles. *Nature* 2005;**437**:257-61.

356. Simoneau S, Rezaei H, Sales N *et al*. In vitro and in vivo neurotoxicity of prion protein oligomers. *PLoS Pathog* 2007;**3**:e125.

357. Smith HL, Mallucci GR. The unfolded protein response: mechanisms and therapy of neurodegeneration. *Brain* 2016;**139**:2113-21.

358. Smith PG, Bradley R. Bovine spongiform encephalopathy (BSE) and its epidemiology. *Br Med Bull* 2003;**66**:185-98.

359. Solassol J, Crozet C, Lehmann S. Prion propagation in cultured cells. *Br Med Bull* 2003;**66**:87-97.

360. Sparkes RS, Simon M, Cohn VH *et al*. Assignment of the human and mouse prion protein genes to homologous chromosomes. *Proc Natl Acad Sci USA* 1986;**83**:7358-62.

361. Spielmeyer W. Histopathologie des Nervensystems. Berlin: Springer: 1922.

362. Stein J, Lester J, Fosten A, Shownkeen RC, Hartree AS. Studies of a human growth hormone preparation used for clinical treatment in Great Britain. *J Endocrinol* 1982;**94**:203-10.

363. Stewart LA, Rydzewska LHM, Keogh GF, Knight RSG. Systematic review of therapeutic interventions in human prion disease. *Neurology* 2008;**70**:1272-81.

364. Stöhr J, Condello C, Watts JC *et al*. Distinct synthetic Aβ prion strains producing different amyloid deposits in bigenic mice. *Proc Natl Acad Sci USA* 2014;**111**:10329-34.

365. Swerdlow AJ, Higgins CD, Adlard P *et al*. Creutzfeldt-Jakob disease in United Kingdom patients treated with human pituitary growth hormone. *Neurology* 2003;**61**:783-91.

366. Takeuchi A, Kobayashi A, Parchi P *et al*. Distinctive properties of plaque-type dura mater graft-associated Creutzfeldt-Jakob disease in cell-protein misfolding cyclic amplification. *Lab Invest* 2016;**96**:581-7.

367. Taraboulos A, Scott M, Semenov A *et al*. Cholesterol depletion and modification of COOH-terminal targeting sequence of the prion protein inhibit formation of the scrapie isoform. *J Cell Biol* 1995;**129**:121-32.

368. Taylor DM, Dickinson AG, Fraser H *et al*. Preparation of growth hormone free from contamination with unconventional slow viruses. *Lancet* 1985;**2**:260-2.

369. Telling G, Scott M, Mastrianni J *et al*. Prion propagation in mice expressing human and chimeric PrP transgenes implicates the interaction of cellular PrP with another protein. *Cell* 1995;**83**:79-90.

370. Thal DR, Rub U, Orantes M, Braak H. Phases of Abeta-deposition in the human brain and its relevance for the development of AD. *Neurology* 2002;**58**:1791-800.

371. Thomas JG, Chenoweth CE, Sullivan SE. Iatrogenic Creutzfeldt-Jakob disease via surgical instruments. *J Clin Neurosci* 2013;**20**:1207-12.

372. Trevitt C, Collinge J. A systematic review of prion therapeutics in experimental models. *Brain* 2006;**129**:2241-65.

373. Tsuboi Y, Doh-ura K, Yamada T. Continuous intraventricular infusion of pentosan polysulfate: clinical trial against prion diseases. *Neuropathology* 2009;**29**:632-6.

374. Turner M. Transfusion safety with regards to prions: ethical, legal and social considerations. *Transfus Clin Biol* 2006;**13**:317-9.

375. Uchihara T. Pretangles and neurofibrillary changes: similarities and differences ewtween AD and CBD based on molecular and morphological evolution. *Neuropathology* 2014;**34**:571-7.

376. Urwin P, Mackenzie J, Llewelyn CA *et al*. Creutzfeldt-Jakob disease and blood transfusion: updated results of the UK Transfusion Medicine Epidemiological Review study. *Vox Sang* 2016;**110**:310-6.

377. Valleron AJ, Boelle PY, Will R, Cesbron JY. Estimation of epidemic size and incubation time based on age characteristics of vCJD in the United Kingdom. *Science* 2001;**294**:1726-8.

378. van der Merwe J, Aiken J, Westaway D, McKenzie D. The standard scrapie cell assay: development, utility and prospects. *Viruses* 2015;**7**:180-98.

379. Vanderweyde T, Bednar MM, Forman SA, Wolozin B. Iatrogenic risk factors for Alzheimer's disease: surgery and anaesthesia. *J Alzheimers Dis* 2010;**22**Suppl3:91-104.

380. Vazquez-Fernandez E, Alonso J, Pastrana MA *et al*. Structural organization of mammalian prions as probed by limited proteolysis. *PLoS One* 2012:**7**;e50111. doi: 10.1371/journal.pone.0050111. Epub 2012 Nov 20.

381. Victoria GS, Zurzolo C. Trafficking and degradation pathways in pathogenic conversion of prions and prion-like proteins in neurodegenerative diseases. *Virus Res* 2015;**207**:146-54.

382. Wadsworth JDF, Joiner S, Hill AF *et al*. Tissue distribution of a protease resistant prion protein in variant Creutzfeldt-Jakob disease using a highly sensitive immunoblotting assay. *Lancet* 2001;**358**:171-80.

383. Wadsworth JDF, Joiner S, Linehan JM *et al*. Kuru prions and sporadic Creutzfeldt-Jakob disease prions have equivalent transmission properties in transgenic and wild-type mice. *Proc Natl Acad Sci* USA 2008;**105**:3885-90.

384. Ward HJT, Everington D, Croes EA *et al.* Sporadic Creutzfeldt-Jakob disease and surgery: A case-control study using community controls. *Neurology* 2002;**59:**543-8.

385. Ward HJT, Everington D, Cousens SN *et al*. Risk factors for variant Creutzfeldt-Jakob disease: A case-control study. *Ann Neurol* 2006;**59**:111-20.

386. Watts JC, Condello C, Stöhr J *et al*. Serial propagation of distinct strains of Aβ prions from Alzheimer's disease patients. *Proc Natl Acad Sci* USA 2014;**111**:10329-43.

387. Weisgraber KH, Innerarity TL, Mahley AW. Abnormal lipoprotein receptor-binding activity of the human E apoprotein due to cysteine-arginine interchange at a single site. *J Biol Chem* 1982;**257**:2518-21.

388. Wells GA, Scott AC, Johnson CT *et al*. A novel progressive spongiform encephalopathy in cattle. *Vet Rec* 1987;**121**:419-20.

389. Wells GA, Wilesmith JW. The neuropathology and epidemiology of bovine spongiform encephalopathy. *Brain Pathol* 1995;**5**:91-103.

390. Will RG, Matthews WB. Evidence for case-to-case transmission of Creutzfeldt-Jakob disease. *J Neurol Neurosurg Psychiatry* 1982; **45**: 235-8.

391. Will RG, Matthews WB. A retrospective study of Creutzfeldt-Jakob disease in England and Wales 1970-79 I: Clinical features. *J Neurol Neurosurg Psychiatry* 1984;**47**:134-40.

392. Will RG, Ironside JW, Zeidler M *et al*. A new variant of Creutzfeldt-Jakob disease in the UK. *Lancet* 1996;**347**:921-5.

393. World Health Organization. *WHO Infection Control Guidelines for Transmissible Spongiform Encephalopathies.* Geneva: World Health Organization,1999. http://www.who.int/entity/csr/resources/publications/bse/whocdscsraph2003.pdf.

394. Xiao X, Yuan J, Qing L *et al*. Comparative study of prions in iatrogenic and sporadic Creutzfeldt-Jakob disease. *J Clin Cell Immunol* 2014;**5**; pii: 240.

395. Xiao X, Yuan J, Zou WQ. Isolation of soluble and insoluble PrP oligomers in the normal human brain. *J Vis Exp* 2012;**68**: pii: 3788. doi: 10.3791/3788.

396. Yamada M. The first Japanese case of variant Creutzfeldt-Jakob disease showing periodic electroencephalogram. *Lancet* 2006;**367**:874.

397. Yamada M, Noguchi-Shinohara M, Hamaguchi T *et al*. Dura mater graft-associated Creutzfeldt-Jakob disease in Japan: Clinicopathological and

molecular characterization of the two distinct subtypes. *Neuropathology* 2009;**29**:609-18.

398. Yuan J, Xiao X, McGeehan J *et al*. Insoluble aggregates and protease-resistant conformers of prion protein in uninfected human brains. *J Biol Chem* 2006;**281**:34848-58.

399. Zanusso G, Monaco S, Pocchiari M, Caughey B. Advanced tests for early and accurate diagnosis of Creutzfeldt-Jakob disease. *Nature Rev Neurol* 2016;**12**:325-33.

400. Zeidler M, Johnstone EC, Bamber RWK *et al*. New variant Creutzfeldt-Jakob disease: psychiatric features. *Lancet* 1997a;**350**: 908-10.

401. Zeidler M, Stewart GE, Barraclough CR *et al*. New variant Creutzfeldt-Jakob disease: neurological features and diagnostic tests. *Lancet* 1997b;**350**: 903-7.

402. Zerr I, Pocchiari M, Collins S *et al*. Analysis of EEG and CSF 14-3-3 proteins as aids to the diagnosis of Creutzfeldt-Jakob disease. *Neurology* 2000;**55**:811-5.

403. Zhao Y, You H, Liu F *et al*. Differentially expressed gene profiles between multidrug resistant gastric adenocarcinoma cells and their parental cells. *Cancer Lett* 2002;**185**:211-8.

404. Zhou M, Ottenber G, Sferrazza GF *et al*. Neuronal death induced by misfolded prion protein is due to NAD^+ depletion and be relieved *in vitro* and *in vivo* by NAD^+ replenishment. *Brain* 2015;**138**:992-1008.

405. Zobeley E, Flechsig E, Cozzio A *et al*. Infectivity of scrapie prions bound to a stainless steel surface. *Mol Med* 1999;**5**:240-3.

406. Zou WQ, Puoti G, Xiao X *et al*. Variably protease-sensitive prionopathy: a new sporadic disease of the prion protein. *Ann Neurol* 2010;**68**:162-72.

Appendices.

Appendix 1. Details of hGH-iCJD cases from Dr Peter Adlard, Institute of Child Health

Study number	Sex	Period of hGH treatment (years)	Duration of HWP-hGH treatment (years)	Incubation Period (years)	Duration of illness (months)	Age at Death (years)	Cause of GH deficiency
hGH-iCJD 1	m	1970-1974	2.5	16.9	8	34	CP
hGH-iCJD 2	m	1970-1980	4	16.5	6	31	IGHD
hGH-iCJD 3	m	1975-1981	3.8	13.2	17	27	astrocytoma
hGH-iCJD 4	m	1977-1981	3.5	12.8	9	30	IGHD
hGH-iCJD 5	m	1979-1985	1.8	11.4	5	25	IGHD
hGH-iCJD 6	f	1974-1978	3	18.1	6	33	IGHD
hGH-iCJD 7	f	1977-1981	3.3	16.2	12	31	IGHD
hGH-iCJD 8	m	1975-1983	1	16.8	6	29	IGHD
hGH-iCJD 9	m	1972-1982	5.8	18.8	14	33	IGHD
hGH-iCJD 10	m	1975-1979	4.3	19.2	8	36	IGHD
hGH-iCJD 11	m	1976-1980	4	17.8	18	37	IGHD
hGH-iCJD 12	m	1978-1985	0.8	16.4	5	27	IGHD
hGH-iCJD 13	m	1978-1983	3.2	17.2	16	34	IGHD
hGH-iCJD 14	m	1976-1985	4	17.2	15	29	histiocytosis X
hGH-iCJD 15	m	1976-1982	3.8	19.1	9	37	IGHD
hGH-iCJD 16	m	1978-1985	1.8	20	16	30	IGHD
hGH-iCJD 17	f	1973-1983	6	23.7	22	41	IPHP
hGH-iCJD 18	f	1977-1985	4.3	22.6	23	34	IGHD
hGH-iCJD 19	f	1980-1985	1.5	22	32	29	IGHD
hGH-iCJD 20	m	1980-1983	0.5	29.4	5	46	IGHD
hGH-iCJD 21	m	1977-1985	3.3	31.7	8	42	CP
hGH-iCJD 22	m	1974-1985	5.5	7.8	7	20	IGHD
hGH-iCJD 23	f	1974-1985	8.2	10.5	2	20	IGHD
hGH-iCJD 24	m	1976-1982	4.7	13.7	13	32	IGHD
hGH-iCJD 25	m	1977-1985	2.3	12.5	16	30	IGHD
hGH-iCJD 26	m	1977-1985	2	13.2	7	27	IGHD
hGH-iCJD 27	m	1979-1985	1	12.8	7	24	IGHD
hGH-iCJD 28	f	1972-1977	1.5	9.5	11	22	CP
hGH-iCJD 29	m	1976-1985	3.8	9	5	20	CP
hGH-iCJD 30	m	1980-1985	1	13.6	8	23	IGHD
hGH-iCJD 31	m	1977-1979	2	19.1	5	28	IGHD
hGH-iCJD 32	m	1972-1982	5	21.4	9	36	CP
hGH-iCJD 33	m	1978-1985	3.8	18.1	20	31	IGHD
hGH-iCJD 34	m	1973-1983	4.3	25.4	19	38	IGHD
hGH-iCJD 35	f	1969-1978	3.5	32.3	6	45	RSS

Abbreviations: CP: craniopharyngioma; f: female; GH: growth hormone; hGH: human growth hormone; HWP-hGH: human growth hormone produced using the Hartree modification of the Wilhelmi protocol; iCJD: iatrogenic Creutzfeldt-Jakob disease; IGHD: isolated growth hormone deficiency; IPHP: idiopathic hypopituitarism; m: male. RSS: Russell-Silver syndrome

Appendix 2. Details of hGH control cases from Dr Peter Adlard, Institute of Child Health

Study number	Sex	Period of hGH treatment (years)	Duration of HWP-hGH treatment (years)	Age at Death (years)	Cause of GH deficiency
hGH-control1	m	1981-1982	0	18	astrocytoma
hGH-control2	f	1983-1985	0	18	craniopharyngioma
hGH-control3	m	1984-1985	0	13	craniopharyngioma
hGH-control4	m	1978-1981	3	28	craniopharyngioma
hGH-control5	f	1975-1985	5.2	24	craniopharyngioma
hGH-control6	f	1975-1981	6	31	Prader Willi syndrome
hGH-control7	m	1978-1983	1.8	30	craniopharyngioma
hGH-control8	m	1980-1985	0.5	33	mitochondrial cytopathy
hGH-control9	m	1974-1981	3.2	42	idiopathic panhypopituitarism
hGH-control10	m	1982-1985	0.3	37	ependymoma
hGH-control11	m	1969-1981	6.6	45	IGHD
hGH-control12	m	1984-1985	0	35	idiopathic panhypopituitarism

Abbreviations: f: female; GH: growth hormone; hGH: human growth hormone; HWP-hGH: human growth hormone produced using the Hartree modification of the Wilhelmi protocol; IGHD: isolated growth hormone deficiency; m: male.

Appendix 3. Details of 108 sCJD cases according to the combination of CNS PrP^{res} type and *PRNP* codon 129 genotype

Study ID	***PRNP* codon 129 genotype**	**PrP^{res} type**				
		TC	**PC**	**OC**	**Th**	**Consensus**
sCJD1	MM	2	1	1	1	1+2
sCJD2	MM	1+2	1+2	1+2	0	1+2
sCJD3	MM	1	1	1	1	1
sCJD4	MM	0	1	0	0	1
sCJD5	MM	1	1	1	0	1
sCJD6	MV	2	2	2	1+2	1+2
sCJD7	VV	2	2	2	2	2
sCJD8	MM	1	1	1	1	1
sCJD9	VV	1	1	1	1	1
sCJD10	MM	1	1	1	1	1
sCJD11	MM	1	1	1	1	1
sCJD12	MV	1+2	1+2	2	1+2	1+2
sCJD13	MM	0	1	1	0	1
sCJD14	MM	1	1	1	1	1
sCJD15	MM	1	1	1	0	1
sCJD16	MM	1	1	1	1	1
sCJD17	MM	1+2	1	1	1	1+2
sCJD18	MM	1	1	1	1	1
sCJD19	MM	1	1	1	1	1
sCJD20	MM	2	2	2	0	2
sCJD21	MM	2	2	2	2	2
sCJD22	MM	1	1	1	1	1
sCJD23	MV	i+2	2	2	i+2	i+2
sCJD24	VV	2	2	2	2	2
sCJD25	MM	1	1+2	1	1+2	1+2
sCJD26	MM	1	1	1	1	1
sCJD27	MM	1	1	1	1	1
sCJD28	MM	1	1	1	0	1
sCJD29	MM	1+2	2	2	2	1+2
sCJD30	MM	0	2	2	1+2	1+2
sCJD31	MM	1	1	1	1	1
sCJD32	VV	2	2	2	2	2
sCJD33	MM	1	1	1	1	1
sCJD34	MV	1	1	1	1	1
sCJD35	MM	1	1	1	1	1
sCJD36	VV	2	2	2	2	2

sCJD37	MM	1	1	1	0	1
sCJD38	VV	2	2	2	2	2
sCJD39	MV	2	2	2	i+2	i+2
sCJD40	VV	2	2	2	2	2
sCJD41	MM	1	1	1	1	1
sCJD42	MM	1	1	1+2	1+2	1+2
sCJD43	MV	2	2	2	2	2
sCJD44	MM	1	1	1	1	1
sCJD45	MV	1	1	1	1	1
sCJD46	MM	1	1	1	1	1
sCJD47	MM	1	1	1	1	1
sCJD48	MM	1	1	1	0	1
sCJD49	MM	1	1	1+2	1	1+2
sCJD50	MM	1	1	1	1	1
sCJD51	MM	1	1	1	1+2	1+2
sCJD52	MM	1	1	1	1	1
sCJD53	MM	1	1	1	1	1
sCJD54	MM	1	1	1	1	1
sCJD55	MV	2	2	2	i+2	i+2
sCJD56	MM	1	1	1	1	1
sCJD57	MM	1	1	1	1+2	1+2
sCJD58	MV	2	1+2	1+2	1+2	1+2
sCJD59	MM	1	1	1	0	1
sCJD60	MM	1	1	1	1	1
sCJD61	MM	1	1	1	1	1
sCJD62	MM	1+2	1+2	1+2	1+2	1+2
sCJD63	VV	2	2	2	2	2
sCJD64	MM	1	1+2	1+2	1+2	1+2
sCJD65	MV	0	0	0	1	1
sCJD66	MV	i+2	i+2	2	i+2	i+2
sCJD67	MM	2	2	0	1+2	1+2
sCJD68	MM	2	2	2	2	2
sCJD69	MM	1	1+2	1+2	1	1+2
sCJD70	MV	1+2	1	1+2	1+2	1+2
sCJD71	MM	1+2	1+2	1+2	1+2	1+2
sCJD72	MM	1	1	1	1	1
sCJD73	MM	1	1	1	1	1
sCJD74	MM	1	1	1	1	1
sCJD75	MM	1	1	1	1	1
sCJD76	MV	2	2	2	2	2
sCJD77	VV	2	2	2	2	2
sCJD78	VV	2	2	2	2	2
sCJD79	VV	2	2	2	2	2

sCJD80	MV	2	2	2	2	2
sCJD81	MM	1	1+2	1+2	1	1+2
sCJD82	VV	0	2	2	2	2
sCJD83	VV	0	0	0	2	2
sCJD84	MV	0	0	0	2	2
sCJD85	MV	1	1	1	0	1
sCJD86	MM	1	1	1	1	1
sCJD87	VV	2	2	2	2	2
sCJD88	MM	1+2	1+2	1	1+2	1+2
sCJD89	MM	1	1	1	1	1
sCJD90	MM	1	1+2	1+2	1	1+2
sCJD91	MV	1+2	1+2	1+2	1+2	1+2
sCJD92	MM	1	1	1	1	1
sCJD93	MM	1	1	1	1	1
sCJD94	MM	1	1	1	0	1
sCJD95	MV	2	2	2	2	2
sCJD96	VV	1	1+2	0	1+2	1+2
sCJD97	MM	1	1	1	1	1
sCJD98	MM	1+2	1+2	1	1+2	1+2
sCJD99	VV	2	2	0	2	2
sCJD100	MV	2	2	2	0	2
sCJD101	MM	1	1	0	1	1
sCJD102	MM	1	1	1	1	1
sCJD103	MM	1	1	1	1	1
sCJD104	MM	1	1	0	0	1
sCJD105	MM	1	1	1	1	1
sCJD106	MM	1	1	1	1	1
sCJD107	MM	2	1+2	1	1+2	1+2
sCJD108	MM	1	1	1	1	1

Abbreviations: Cb: cerebellum; M: methionine; OC: occipital cortex, PC: parietal cortex, *PRNP*: prion protein gene; sCJD: sporadic Creutzfeldt-Jakob disease; TC: temporal cortex, Th: thalamus; V: valine

Appendix 4. Tissue processing

4.1. *CNS tissue processing*

Using the Class 1 Cabinet, the 15% unbuffered formalin (GENTA MEDICAL, York, UK, catalogue F40050) from the trimmed tissue blocks and cassettes was drained and replaced with 96% formic acid (Fischer Scientific, Loughborough, UK, catalogue 10478020), for 1h. Following formic acid treatment, the tissue and cassettes were washed with 2 or 3 changes of tap water (5min each), and placed into stainless steel baskets for processing. The processing schedule for CNS tissue using the Tissue Tek VIP 6 (Sakura, Thatcham, UK, catalogue 6032) was as follows:

Solution	**Time**	**Temperature (C)**	**Pressure/Vacuum Cycle**
15% formaldehyde	2 h	35°	YES
80% alcohol	2 h	35°	YES
90% alcohol	2 h	35°	YES
74° IMS	2 h	35°	YES
Absolute alcohol (3 changes)	2 h	35°	YES
Xylene (3 changes)	2 h	35°	NO
Wax	2 h	60°	NO
Wax (3 changes)	2 h	60°	YES

Total processing time = 28 h

(h: hours, C: centigrade, IMS: Industrial methylated spirit)

Once the cycle was completed the baskets were removed and the tissue placed into fresh wax (Tek III paraffin wax, Sakura, Thatcham, UK, catalogue 4509) in the Tissue-Tek 5 Embedding Centre and coldplate (Sakura, Thatcham, UK, catalogue 5229).

Processing fluids: Formaldehyde 40%, Ethanol solution (IDA 99%) and Xylene all from Genta Medical, York, UK, (catalogue numbers F40050, 199050 and XYL050), Ethanol 100% from Haymankimia, Witham, UK (catalogue DRA 00020001).

4.2. *Non-CNS tissue processing*

Using the Class 1 Cabinet, the 15% unbuffered formalin (GENTA MEDICAL, York, UK, catalogue F40050) from the trimmed tissue blocks and cassettes was drained and replaced with 96% formic acid (Fischer Scientific, Loughborough, UK, catalogue 10478020), for 1h. Following formic acid treatment, the tissue and cassettes were washed with 2 or 3 changes of tap water (5min each), and placed into stainless steel baskets for processing. The processing schedule for CNS tissue using the Tissue Tek VIP 6 (Sakura, Thatcham, UK, catalogue 6032) was as follows:

Solution	**Time**	**Temperature (C)**	**Pressure/Vacuum Cycle**
15% formaldehyde	1 h	40°	YES
80% alcohol	1 h	40°	YES
90% alcohol	1 h	40°	YES
74° IMS	1 h	40°	YES
Absolute alcohol (3 changes)	1 h	40°	YES
Xylene (3 changes)	1 h	40°	YES
Paraffin wax (4 changes)	0.75 h	60°	YES

Total time = 13 h

(h: hours, C: centigrade, IMS: Industrial methylated spirit)

Once the cycle was completed the baskets were removed and the tissue placed into fresh wax (Tek III paraffin wax, Sakura, Thatcham, UK, catalogue 4509) in the Tissue-Tek 5 Embedding Centre and coldplate (Sakura, Thatcham, UK, catalogue 5229). Processing fluids were obtained from the sources listed above.

Appendix 5. Non-CNS tissues sampled for histology and biochemistry

Case	Fixed tissues	Frozen tissues
hGH-iCJD2	LN, SP, TG	MU, LN, PN, SP
hGH-iCJD3	DR, MU, PN, PI	
hGH-iCJD4	PI	
hGH-iCJD5	AG, LN, MU, PI, PN, SP, SY, TG	LN, MU, PI, PN, SP
hGH-iCJD6	AG, MU, PI, PN, SP	MU, PN, SP
hGH-iCJD7		PI
hGH-iCJD8	AG, LN, MU, SP	
hGH-iCJD9	PI	
hGH-iCJD10		PI
hGH-iCJD11	LN, SP, TO	
hGH-iCJD12		PI
hGH-iCJD13		KI, LU, LV, PA
hGH-iCJD14	AP, LN, PI, SP, TO	
hGH-iCJD15	AG, AP, DR, DU, LI, LN, MU, PI, PN, SP, SY, TO	AG, AP, BM, DR, HE, K, LN, LU, LV, MU, PA, PN, SG, SP, TY, TO
hGH-iCJD19	AP, MU, PN, PI, SPL, TON	SP
hGH-iCJD20	PI	PI
hGH-iCJD24	PI	
hGH-iCJD27	AG, DR, MU, PN	MU, SP
hGH-iCJD28	PI	
hGH-iCJD29	MU, SI, SP	
hGH-iCJD30	PI	
hGH-iCJD34	SP	
hGH-iCJD35	AP, LN, PI, SP	
hGH-control8	AP, LI, LN, MU, SI, TO	
hGH-control10	AG, AP, PN, SP	

Abbreviations: AG: adrenal gland; AP: appendix; BM: bone marrow; DR: dorsal root ganglion; DU: duodenum: HE: heart; hGH: human growth hormone; KI: kidney; LI: large intestine; LN: lymph node; LU: Lung; LV: liver; MU: muscle; PA: pancreas; PI: pituitary; PN: peripheral nerve; SG: salivary gland; SI: small intestine; SP: spleen; SY: sympathetic chain; TG: trigeminal ganglion; TO: tonsil; TY: thyroid

Appendix 6. Microtomy and histological stains

Sections were cut from paraffin-embedded tissue blocks on a microtome (Leica Microystems, Milton Keynes, UK, catalogue RM2255) using Accu-Edge Low-Profile microtome blades (Sakura, Thatcham, UK, catalogue 4689). Sections were floated onto a water bath (Section Floatation Bath, Fisher Scientific, Loughborough, UK, catalogue E65) at 38ºC and picked up on SuperFrost plus microscope slides (Fisher Scientific, Loughborough, UK, catalogue 10149870).

6.1. *Haematoxylin and eosin staining*

Paraffin embedded tissue sections were deparaffinised in Xylene for 5min followed by stepwise re-hydration (5min incubations) in absolute alcohol, 74% industrial methylated spirits (IMS) and 70% IMS (see Appendix 1 for sources of Xylene and IMS). Sections were immersed in saturated picric acid solution (Sigma-Aldrich, Poole, UK, catalogue 197378) for 15min to remove residual formalin pigment and washed well in running water. Following removal of the picric acid solution, sections were immersed in haematoxylin solution (Leica Biosystems, Milton Keynes, UK, catalogue 380154E) for 2min before a thorough wash in water. After a single dip in a 1% acid alcohol solution (999mls 70% alcohol; 1ml concentrated HCl (Fisher Scientific, Loughborough, UK, catalogue 12352301)), sections were dipped three times in lithium carbonate solution (300ml tap water; 5-10ml saturated aqueous lithium carbonate (Fisher Scientific, Loughborough, UK, catalogue L/2100/50)) and stained in eosin solution (Leica Microsystems, Milton Keynes, UK, catalogue 3801600E) for 5min. Following a final rinse in water, sections were dehydrated by immersing (approximately 10sec) in 70% IMS, 74% IMS and absolute alcohol. Sections were cleared in Xylene, cover slipped on a Coverslipper (Leica Microsystems, Milton Keynes, UK, catalogue CV 5030) using VHM coverslips number 1 (CellPath, Newtown, UK, catalogue SAJ-2450-03A) with Pertex mountant (CellPath Ltd, Newtown, UK, catalogue SEA 0100-00A) and left to harden overnight. In order to analyse the slides outside the laboratory, sections were immersed in 96% formic acid (Fisher Scientific, Loughborough, UK catalogue 10478020) for 5min, washed well in water and dried.

6.2. *Luxol Fast Blue/Cresyl Violet staining*

Paraffin embedded sections were deparaffinised in Xylene for 5min followed by stepwise rehydration (5min incubations) in absolute alcohol, 74% industrial methylated spirits (IMS) and 70% IMS (see Appendix 1 for sources of Xylene and IMS). Tissue sections were immersed in saturated picric acid solution (Sigma-Aldrich, Poole, UK, catalogue 197378) for 15min and washed well in running water. Following removal of the picric acid solution, sections were immersed in Luxol Fast Blue solution (95% alcohol, 0.1% of 10% acetic acid, 0.1% Luxol Fast Blue (Fisher Scientific, Loughborough, UK, catalogue 11418356)) and incubated at 60ºC for approximately 3-4h. Tissue sections were differentiated in 0.1% lithium carbonate (Fisher Scientific, Loughborough, UK, catalogue L/2100/50) for a few seconds before continuing the differentiation in 70% alcohol for approximately 20-30sec. Sections were then rinsed well in water, examined under a staining microscope and the differentiation step repeated if required. Following the differentiation, tissue sections were washed in water and counterstained with Cresyl Violet solution (0.1% Cresyl Violet acetate solution (Fisher Scientific, Loughborough, UK, catalogue 10137180) in 1% acetic acid). Tissue sections were rinsed in water and further differentiated in 95% alcohol. Finally, tissue sections were dehydrated by immersing (for approximately 10sec) in 70% IMS, 74% IMS and absolute alcohol. Sections were cleared in Xylene, cover slipped on a Coverslipper (Leica Microsystems, Milton Keynes, UK, catalogue CV 5030) using VHM coverslips number 1 (CellPath, Newtown, UK, catalogue SAJ-2450-03A) with Pertex mountant (CellPath Ltd, Newtown, UK, catalogue SEA 0100-00A) and left to harden overnight. In order to analyse the slides outside the laboratory, sections were immersed in 96% formic acid (Fisher Scientific, Loughborough, UK catalogue 10478020) for 5min, washed well in water and dried.

6.3. *Bielschowsky silver staining*

Blocks were selected for Bielschowsky silver staining according to the National Institute on Aging-Alzheimer's Association guidelines (Hyman *et al*., 2012). Paraffin embedded CNS sections were deparaffinised in Xylene for 5min followed by stepwise rehydration (5min incubations) in absolute alcohol, 74% industrial methylated spirits (IMS) and 70% IMS (see Appendix 1 for sources of Xylene and IMS). Tissue sections

were immersed in saturated picric acid solution (Sigma-Aldrich, Poole, UK, catalogue 197378) for 15min and washed well in running water. Following removal of the picric acid solution, sections were immersed in filtered 20% silver nitrate (Scientific Laboratory Supplies, Nottingham, UK, catalogue CHE3224) solution for 10min before washing in distilled water (dH_2O) produced using an ELIX 5 CT water purification system (Millipore (UK), Watford, UK, catalogue ZLXE0050WW). Sections were immersed in freshly prepared silver impregnating solution (ammonia hydroxide (Fisher Scientific, Loughborough, UK, catalogue 423305000), added dropwise to 20% silver nitrate solution (only adding enough drops to dissolve the dark precipitate that initially forms) for 15min. The silver impregnating solution was decanted from tissue sections before re-immersing in a solution comprising 20mls impregnating solution and 600µl of reducing solution (20ml of 10% formalin, 0.5g citric acid (VWR International, Lutterworth, UK, catalogue 20276.235), 50µl concentrated nitric acid (Fisher Scientific, Loughborough, UK, catalogue 10381313) , 100mls dH_20). Tissue sections were stained in this solution for approximately 4-8min until they developed a dark brown colour. Following a wash in dH_2O, sections were toned in 0.1% gold chloride (Scientific Laboratory Supplies, Nottingham, UK, catalogue G4022) for approximately 5sec, washed in dH_2O and fixed in 5% sodium thiosulphate (Scientific Laboratory Supplies, Nottingham, UK, catalogue 217263) for 5min. Finally, sections were thoroughly washed in dH_2O and counterstained with neutral red solution (Scientific Laboratory Supplies, Nottingham, UK, catalogue CHE2624) for 30sec. Following a final rinse in water, sections were de-hydrated by immersing (approximately 10sec) in 70% IMS, 74% IMS and absolute alcohol. Sections were cleared in Xylene, cover slipped on a Coverslipper (Leica Microsystems, Milton Keynes, UK, catalogue CV 5030) using VHM coverslips number 1 (CellPath, Newtown, UK, catalogue SAJ-2450-03A) with Pertex mountant (CellPath Ltd, Newtown, UK, catalogue SEA 0100-00A) and left to harden overnight. In order to analyse the slides outside the laboratory, sections were immersed in 96% formic acid (Fisher Scientific, Loughborough, UK catalogue 10478020) for 5min, washed well in water and dried.

Appendix 7. Antibodies used in this thesis

Antibody clone	Antigen Specificity	Source	Protocol
5A9	Human apoE-4	BioLegend, UK Product: 811701	IHC
5B5	Human apoE-4	BioLegend, UK Product: 811601	IHC
D6E10	Human apoE	BioLegend, UK Product: 803301	IHC
11A50-B10	Human Aβ (1-40)	BioLegend, UK Product: 805401	IHC
12F4	Human Aβ (1-42)	BioLegend, UK Product: 805501	IHC
6F/3D	Human Aβ (residues 8-17 with an additional C-terminal cysteine)	Dako, UK Product: M 0872	IHC
4G8	Human Aβ (Epitope 17-24)	BioLegend, UK Product: 800709	IHC
5G4	Human α-synuclein	ajROBOSCREEN, Germany Product: 0102004001	IHC
AT8	Human PHF-tau	Thermo Scientific, UK Product:MN1020B	IHC
11-9	Human phospho TDP-43	2BScientific, UK Product: TIP-PTD-M01	IHC
3F4	Human prion protein (Epitope 109-112)	Cambridge Bioscience, UK Product: SIG-39640	IHC, PET blot
3F4	Human prion protein (Epitope 109-112)	Millipore, Watford, UK; Product: MAB1562	WB, NaPTA CDI, PMCA
12F10	Human prion protein (Epitope 142-160)	Bertin pharma, UK Product: A03221	IHC, PET blot
KG9	Human prion protein (Epitope 140-180)	TSE Resource Centre, Roslin Institute, UK	IHC
12B2	Human prion protein (Epitope 89-93)	Central Veterinary Institute of Wageningen UR, Lelystad, Netherlands	WB
PGM1	CD 68	Dako, UK Product: M 0876	IHC
GFAP	Glial fibrillary acidic protein (GFAP)	Dako, UK Product: M 0876	IHC
Ubiquitin	Ubiquitin	Dako, UK Product: Z0458	IHC

Abbreviations: Aβ: amyloid beta; apoE: apolipoprotein E; CD68: cluster of differentiation 68; CDI: conformation-dependent immunoassay; IHC: immunohistochemistry; NaPTA: western blotting following sodium phosphotungstic acid precipitation; PMCA: protein misfolding cyclic amplification; TDP-43: transactive response DNA binding protein 43; WB: western blotting

Appendix 8. Immunohistochemistry protocols

8.1. *Immunohistochemistry*

Paraffin embedded tissue sections were deparaffinised in Xylene for 5 min followed by stepwise re-hydration in absolute alcohol, 74% IMS and 70% IMS (5min incubations) (see Appendix 1 for sources of Xylene and IMS). Endogenous peroxidase activity was blocked by immersing sections in 1% hydrogen peroxidise (Fisher Scientific, Loughborough, UK, catalogue BP2633-500) in methanol (Fisher Scientific, Loughborough, UK, catalogue M/3950/17) for 30min. Following a thorough wash in water, various pre-treatment protocols were performed, specific for each antibody, as detailed in Appendix 4. Following the pre-treatment protocol, tissue sections were washed thoroughly in water and incubated for 5min in Tris-buffered saline (TBS) (50mmol Tris-HCl (VWR, Lutterworth, UK, catalogue 10354M); 150mmol NaCL (VWR International, Lutterworth UK, catalogue 27810295); pH 7.6) before incubating with the primary antibodies at the dilution and time detailed in Table 4.1. After 3 x 5min washes in TBS, immunolabelling was completed using the Novolink^{TM} Polymer Detection System (Leica Microsystems, Milton Keynes, UK, catalogue RE7280-K) with 30min incubations in the post primary and Novolink^{TM} polymer reagents. Washes in TBS were carried out between each reagent. After a final wash, staining was visualised with 3, 3' diaminobenzidine (DAB). The DAB was prepared immediately before use from Novolink^{TM} Polymer Detection Kit (1ml of Novolink^{TM} DAB substrate buffer (Polymer); 50µl DAB chromagen). Sections were washed well in water before lightly counterstained (immerse in haematoxylin solution for 20sec, wash in water, dip once in a 1% acid alcohol solution, rinse in water and dip four times in saturated aqueous lithium carbonate solution). After a wash in water sections were dehydrated by immersing (approximately 10sec) in 70% IMS, 74% IMS and absolute alcohol. After clearing in Xylene, sections were cover slipped on a Coverslipper (Leica Microsystems, Milton Keynes, UK, catalogue CV 5030) using VHM coverslips number 1 (CellPath, Newtown, UK, catalogue SAJ-2450-03A) with Pertex mountant (CellPath Ltd, Newtown, UK, catalogue SEA 0100-00A) and left to harden overnight. In order to analyse the slides outside the laboratory, sections were immersed in 96%

formic acid (Fisher Scientific, Loughborough, UK, catalogue 10478020) for 5min, washed well in water and dried.

8.2. *Double immunohistochemistry*

To investigate the co-localisation of PrP, CD68, phospho-tau and GFAP with Aβ deposits, paraffin embedded tissue sections were deparaffinised in Xylene for 5min followed by stepwise re-hydration in absolute alcohol, 74% IMS and 70% IMS (5min incubations) (see Appendix 1 for sources of Xylene and IMS). Endogenous peroxidase activity was blocked by immersing sections in 1% hydrogen peroxidise (Fisher Scientific, Loughborough, UK, catalogue BP2633-500) in methanol (Fisher Scientific, Loughborough, UK, catalogue M/3950/17) for 30min.

Following a thorough wash in water, the pre-treatment protocol required for the 12F10 anti-PrP/6F3D anti-Aβ antibody (hydrated autoclaving, formic acid treatment and proteinase K digestion); PGM1 anti-CD68/6F3D anti-Aβ antibody (microwaving in citric acid and formic acid); AT8 anti-phospho-tau/6F3D anti-Aβ antibody (microwaving in citric acid and formic acid); or GFAP anti-GFAP/6F3D anti-Aβ antibody (formic acid) was performed as detailed in Appendix 4. Following the pre-treatment protocol, tissue sections were washed thoroughly in water and incubated for 5min in Tris-buffered saline (TBS) (50mmol Tris-HCl (VWR, Lutterworth, UK, catalogue 10354M); 150mmol NaCL (VWR International, Lutterworth UK, catalogue 27810295) ; pH7.6).

Immunohistochemistry for the prion protein, CD68 and phospho-tau was performed first using in combination with the Vectastain Elite ABC HRP (Peroxidase, Mouse IgG) Kit (Vector Laboratories, Peterborough, UK, catalogue PK-6102). All reagents were prepared as per manufacturer's instructions. All sections were blocked in normal horse serum for 20min before incubation in the primary antibody; 12F10 at a dilution of 1/800, PGM1 at a dilution of 1/50 and AT8 at a dilution of 1/100 in TBS for 1h. After 3 x 5min washes in TBS, sections were incubated in the anti-mouse IgG biotinylated antibody for 1h before a further 3 x 5min washes. Sections were then incubated in the Vectastain ABC reagent for 30min before a final 3x5min washes in

TBS. Staining was visualised with 3,3' diaminobenzidine (DAB). The DAB was prepared immediately before use from Novolink™ Polymer Detection Kit (1ml of Novolink™ DAB substrate buffer (Polymer); 50µl DAB chromagen) (Leica Microsystems, Milton Keynes, UK, catalogue RE7280-K). Immunohistochemistry for GFAP was performed in combination with the Vectastain Elite ABC HRP (Peroxidase, Rabbit IgG) Kit (Vector Laboratories, Peterborough, UK, catalogue PK-6101). All reagents were prepared as per manufacturer's instructions. All sections were blocked in normal goat serum for 20min before incubation in the primary antibody; GFAP at a dilution of 1/800 in TBS for 1h. After 3 x 5min washes in TBS, sections were incubated in the anti-rabbit IgG biotinylated antibody for 1h before a further 3 x 5min washes. Sections were then incubated in the Vectastain ABC reagent for 30min before a final 3 x 5min washes in TBS. Staining was visualised with 3, 3' diaminobenzidine (DAB). The DAB was prepared immediately before use from Novolink™ Polymer Detection Kit (1ml of Novolink™ DAB substrate buffer (Polymer); 50µl DAB chromagen) (Leica Microsystems, Milton Keynes, UK, catalogue RE7280-K). Sections were washed well in water before incubating in TBS for 5min.

Staining was continued for Aβ protein. Sections were blocked in normal rabbit serum (Vector Laboratories, Peterborough, UK, catalogue S-5000) diluted 1/5 in TBS for 20min before incubating in the primary antibody 6F/3D at a dilution of 1/250 overnight a room temperature. After 3 x 5min washes in TBS, sections were incubated in a biotin-SP-conjugated affinity pure rabbit anti-mouse IgG antibody (Jackson Immunoresearch Laboratories Inc, Baltimore, USA, catalogue 315-065-003) at a dilution of 1/400 in TBS for 1h. Sections were further washed in TBS before a final incubation in Vectastain ABC alkaline phosphatase standard (Vector Laboratories, Peterborough, UK, catalogue AK-5000) prepared as per instructions (2 drops of reagent A and 2 drops of reagent B in 10 mls of TBS) for 30min. Sections were washed in thoroughly in TBS before staining with Vector red alkaline phosphatase substrate kit (Vector Laboratories, Peterborough, UK, catalogue PK-SK-5100) prepared according to instructions (to 5ml of 200mmol Tris-HCL add 2 drops of reagent 1, 2 drops of reagent 2 and 2 drops of reagent 3). Sections were washed well in water before lightly counterstained (immerse in haematoxylin solution for 20sec, wash in water, dip once

in a 1% acid alcohol solution, rinse in water and dip 4 times in saturated aqueous lithium carbonate solution). After a wash in water sections were dehydrated by immersing (approximately 10sec) in 70% IMS, 74% IMS and absolute alcohol. After clearing in Xylene, sections were cover slipped on a Coverslipper (Leica Microsystems, Milton Keynes, UK, catalogue CV 5030) using VHM coverslips number 1 (CellPath, Newtown, UK, catalogue SAJ-2450-03A) with Pertex mountant (CellPath Ltd, Newtown, UK, catalogue SEA 0100-00A) and left to harden overnight. In order to analyse the slides outside the laboratory, sections were immersed in 96% formic acid (Fisher Scientific, Loughborough, UK, catalogue 10478020) for 5min, washed well in water and dried.

Abbreviations: Aβ: amyloid beta; CD68: cluster of differentiation 68; PrP: prion protein

Appendix 9. PET blot protocol

5µm formalin fixed, paraffin embedded tissue sections were blotted onto a 0.45µm nitrocellulose membrane (Bio-Rad, Hemel Hempstead, UK, catalogue 9004700) and dried at 55ºC overnight. The tissue sections were deparaffinised in Xylene for 10min followed by re-hydration with 5min incubations in 95%, 85% and 70% propan-1-ol (Scientific Laboratory Supplies, Nottingham, UK, catalogue CHE3104). Following re-hydration, the membranes were air-dried before a thorough wash in TBST (10mmol Tris HCl (VWR International, Lutterworth UK, catalogue 10354M) pH 7.8, 100mmol NaCl (VWR International, Lutterworth UK, catalogue 27810295), 0.05% Tween 20 (Sigma-Aldrich, Poole, UK, catalogue P9416)) until membranes were fully saturated. Membranes were incubated at 55ºC overnight in 25µg/ml proteinase K (Roche Diagnostics, West Burgess, UK, catalogue 03115 836 001) in digestion buffer (10mmol Tris HCl (VWR International, Lutterworth UK, catalogue 10354M) pH 7.8, 100mmol NaCl (VWR International, Lutterworth, UK, catalogue 27810295), 0.1% Brij (Sigma-Aldrich, Poole, UK; catalogue B4184)), a step which ensures the complete digestion of PrP^{C} in the tissue sections, leaving only PrP^{res}.

Following protease digestion, membranes were washed in TBST before treating with 3M guanadine isothiocynate (Sigma-Aldrich, Poole, UK, catalogue G6639) for 10min. After a further three washes in TBST, membrane bound tissues were blocked in casein (Vector Laboratories, Peterborough, UK, catalogue SP5020) for 30min before incubated for 1h with the primary antibodies (12F10, 1/22 000; 3F4, 1/500) diluted in casein. After 3 x 5min washes in TBST, immunolabelling was completed using the Vectastain ABC-AmP kit (Vector Laboratories, Peterborough, UK, catalogue AK-6400), with a 1h incubation in reagent A (streptavidin solution) and a 30min incubation in reagent B (biotinylated alkaline phosphatase). Washes in TBST were carried out between each reagent. After a final wash, staining was visualised with 5-bromo-4-chloro-3-indolyl phosphate/nitroblue tetrazolium (NBT/BCIP) (Vector Laboratories, Peterborough, UK, catalogue SK-5400). Membrane bound sections were washed thoroughly in water, air dried and mounted for analysis.

Abbreviations: PrP^{C}: cellular prion protein; PrP^{res}: protease-resistant prion protein.

Appendix 10. DNA Extraction protocols and *PRNP* codon 129 analysis

10.1. *DNA extraction from frozen tissues*

DNA was extracted from unfixed grey matter-enriched frozen brain tissue samples (20-30mg) of the cerebellar cortex or frontal cortex using the Qiagen DNeasy Blood and Tissue kit (Qiagen, Hilden, Germany, catalogue number 69504; www.qiagen.com for Handbook). Unless referenced, all reagents and consumables used in the following DNA extraction protocol are from this Qiagen DNeasy Blood and Tissue kit. To lyse the tissue, each sample was placed into a 1.5ml microcentrifuge tube (Sarstedt, Cat# 72.607.772) in 180µl of ATL buffer and 20µl of Proteinase K, and incubated overnight at 56 °C. 200µl of AL buffer was added to each lysate and briefly vortexed before a further incubation at 70ºC for 10min. 200µl of ethanol was added to the sample and vortexed again. To bind the DNA, each lysate was pipetted into a DNeasy Minispin column (complete with 2ml collection tube) and this spin column was centrifuged at 8,000 rpm for 1min. The flow-through and collection tube were discarded and the DNeasy Minispin column was placed in a new 2ml collection tube. To wash the DNA, 500µl of buffer AW1 was added to the column and was again centrifuged at 8,000 rpm for 1min. The flow-through and collection tube were again discarded, the collection tube replaced and 500µl of buffer AW2 was added. The column was then centrifuged for 3min at 1,4000 rpm to complete the wash and to dry the DNeasy membrane.

10.2. *DNA extraction from paraffin-embedded tissues*

A similar protocol to Appendix 5 was followed after these pre-treatment steps: Up to 25mg of paraffin-embedded tissue were cut as 10µm sections and placed in a 2ml microcentrifuge tube. 1200µl Xylene (Genta Medical, York, UK, catalogue XYL050) was added. The tube was vortexed vigorously, centrifuged for 5min at 1,4000 rpm and without disturbing the pellet, the supernatant was decanted. To remove any residual xylene from the remaining pellet, 1200µl ethanol (96-100%) (Haymankimia, Witham, UK, catalogue DRA 00020001) was added to the tube. The tube was vortexed, centrifuged for 5min at 1,4000 rpm and the ethanol was decanted. The ethanol wash step was repeated and after the third period of centrifuging, the microcentifuge tube was opened, the ethanol decanted and the tube incubated at 37°C for 10-15min, or until

the ethanol had evaporated. The tissue pellet was then ready to be re-suspended in 180µl of ATL buffer and treated to the same protocol as above in Appendix 7.1 'DNA extraction from frozen tissues' using the Qiagen DNeasy Blood and Tissue kit (Qiagen, Hilden, Germany, catalogue 69504).

The method of Nicoll *et al*. (Nicoll *et al*., 1997) was also used in an attempt to extract DNA from paraffin-embedded tissues. Briefly, 1ml Xylene (Genta Medical, York, UK, catalogue XYL050) was added to a reaction tube containing 1-5 10µm tissue sections of cerebellar cortex from each case. The tubes were vortexed for 1min and centrifuged for 3min at 13,000 rpm, and the Xylene was decanted. 1ml ethanol (Haymankimia, Witham, UK, catalogue DRA 00020001) was added to each tube. The tubes were vortexed for 1min, centrifuged for 3min and the ethanol was decanted. The ethanol wash was repeated and residual ethanol was removed by overnight evaporation. 50µl of proteinase K (800µg/ml) (Roche Diagnostic, West Burgess, UK, catalogue 03 115 828 001), 20µl 10x PCR buffer (Qiagen, Hilden, Germany, catalogue 203203) and 130µl Analar water (VWR International, Lutterworth, UK, catalogue 10292) were added to each sample. The solutions were overlaid with 100µl mineral oil and incubated at 37 °C overnight. The samples were then heated to 95°C to inactivate the proteinases; the resulting solution was used for DNA analysis.

10.3. *PCR of the prion protein gene for codon 129 analysis*

Using a PCR cabinet, a PCR reaction mix was prepared in a sterile 1.5ml microcentrifuge tube. The following reagents were used and the volumes were calculated to give the necessary final concentrations, in the required number of reaction tubes:

Reagent	**Final concentration**
10x PCR Buffer (+ 15mmol $MgCl_2$) (Qiagen, Hilden, Germany, catalogue 203203)	1x PCR Buffer
PCR Nucleotide Mix (Promega, Southampton, UK, catalogue C1141).	0.2mmol
Primer Pair (A2/A3) *Primer A2 (forward): TGA TAC CAT TGC TAT GCA CTC ATT C* *Primer A3 (reverse): GAC ACC ACC ACT AAA AGG GCT GCA G*	5pmol
HotStarTaq DNA Polymerase (Qiagen, Hilden, Germany, catalogue 203203)	1 Unit
dH20 (Sigma-Aldrich, Poole, UK, catalogue W3513)	81.8µl per reaction.

The PCR reaction mix was inverted to ensure homogeneity and 97µl was aliquoted into each 0.5ml PCR tube (Axygen, Loughborough, UK, catalogue AX-PCR-05-C). The tubes were transferred to a Class II Cabinet where 3µl of DNA template, acquired from the previous DNA extraction method, was added to each PCR tube bringing the total volume to 100µl. A negative control was included by adding 3µl of dH20 (Sigma-Aldrich, Poole, UK, catalogue W3513) to one of the PCR tubes, and the positive controls were included by adding 3µl of known DNA templates (MM, MV and VV) to a further three PCR tubes. After the addition of the DNA template, the tubes were placed on the T3000 Thermocycler (Biometra, Gottingen, Germany, catalogue 050-723) using the PCR Program PRPA2A3.

PCR Programme (PRPA2A3)

1. 95°C 15min
2. 94°C 1min
3. 65°C 1min (decrease 0.5°C per cycle)
4. 72°C 2min
5. Go to step 2 - 10 times
6. 94°C 45sec
7. 60°C 30sec
8. 72°C 1min
9. Go to step 6 - 30 times
10. 72°C 15min
11. 4°C Held until completion
12. END

10.4. *NspI restriction fragment length polymorphism digest for codon 129 analysis*

The digest reaction mix was prepared in a 0.5ml PCR tube (Axygen, Loughborough, UK, catalogue AX-PCR-05-C) using the following reagents, the total volumes were calculated by multiplying by the number of reactions required.

Reagent	**Volume per reaction tube**
CutSmart® Buffer (New England Biolabs, Hitchin, UK, catalogue B7204S)	1.0µl
dH_20 (Sigma-Aldrich, Poole, UK, catalogue W3513)	5.6µl
NspI (5U/µl) (New England Biolabs, Hitchin, UK, catalogue R0602S)	0.4µl

The digest reaction mix was inverted to ensure homogeneity and 7µl was aliquoted into each 0.2ml PCR tube (Axygen, Loughborough, UK, catalogue AX-PCR-02-C). For each digest, 3µl of the PCR reaction was added to the tube bringing the total volume to 10µl. The tubes were placed on the T3000 Thermocycler, using the Digest Program 37DEGDIG (37°C, 8 h). On completion, the digest products were stored in the fridge at 4°C until required.

10.5. *Agarose gel electrophoresis of amplified PCR products and restriction digest products for codon 129 analysis*

Ultrapure Agarose (Invitrogen, Loughborough, UK, catalogue 16500100) was weighed out and combined with 1 x UltraPure™ TBE Buffer (Invitrogen, Loughborough, UK, catalogue 15581044) to make a 1.5% agarose gel. The solution was heated in the microwave until the agarose had melted completely and was clear of small bubbles. The solution was cooled under running water until hand hot, SYBR® Safe DNA Gel Stain 10000X (Invitrogen, Loughborough, UK, catalogue S33102) was added at a final concentration of 1:10000 and the bottle agitated gently until mixed. Using the Mini-Sub Cell GT Horizontal Electropheresis System (Bio-Rad, Hemel Hempstead, UK, catalogue 1704467), the melted agarose solution was poured into the casting try, the combs were inserted and the gel was left to set for 45min. The gel was transferred to the electrophoresis tank, the wash tank was filled with 1 x UltraPure™ TBE Buffer (Invitrogen, Loughborough, UK, catalogue 15581044) to submerge the gel and the combs were removed. 5µl of Gel Loading Buffer (Sigma-Aldrich, Poole, UK, catalogue G2526) was added to each sample before being loaded onto the gel with 1µl of 100bp Ladder (Life Technologies, Paisley, UK, catalogue 15628019) being loaded at the beginning of each comb. Electrophoresis was performed at 100V for 1h so that the dye front has migrated ~5cm. Once complete, an image of the gel was captured using the UV setting on the ChemiDoc XRS+ system (Bio-Rad, Hemel Hempstead, UK, catalogue 1708256).

Abbreviations: A:adenine; bp: base pair; C:cytosine; G; guanine; PCR: polymerase chain reaction; *PRNP*: prion protein gene; T: thymine; UV ultraviolet light; V: volts

Appendix 11. Western blot analysis for PrP^{res}

11.1. *Preparation of PrP^{res} from frozen brain tissue*

Preparation of tissue for Western blot analysis was carried out in a Class 1 Microbiological Safety Cabinet within the High Risk Laboratory of NCJDRSU. A small piece (approximately 100mg) of frozen grey matter enriched brain tissue was sampled and placed in a sterile 2ml Eppendorf tube (Fisher Scientific, Loughborough, UK, catalogue 10038760) on ice. The precise weight of each brain sample was recorded and sufficient lysis buffer with high buffer capacity (LB100) (100mmol Tris (Sigma-Aldrich, Poole, UK, catalogue TRIS-OR) pH6.9 at 37°C; 100mmol NaCL (VWR International, Lutterworth, UK, catalogue 27810295), 10mmol ethylenediamine tetra-acetic acid (EDTA) (Sigma-Aldrich, Poole, UK, catalogue E-4884), 0.5% Nonident P-40 (Fisher Scientific, Loughborough, UK, catalogue 19628); 0.5% sodium deoxycholate (Sigma-Aldrich, Poole, UK, catalogue 30970) added to give a 10% mass per volume brain homogenate. Tissues were then homogenised in the LB100 using a disposable micropestle. Insoluble material was pelleted by spinning at 2,000 rpm for 5min at 4°C using a microcentrifuge (Eppendorf AG, Stevenage, UK, catalogue 5417R) with a fixed angle motor (Eppendorf AG, Stevenage, UK, catalogue F-45-30-11). The supernatant was aspirated using an aerosol resistant tip into a fresh 1.5ml Eppendorf tube (VWR International, Lutterworth, UK; 2112139) and the remaining pellet frozen at -20°C. A 0.2ml volume of the supernatant was then aspirated into a fresh Eppendorf tube and proteinase K (PK) (Roche Diagnostics, West Burgess, UK, catalogue 03 115 828 001) added to a final specific activity of 10U/ml. PK treated samples were then incubated at 37°C for 1h before stopping the reaction with the addition of Pefabloc™ (Roche Diagnostics, Burgess Hill, UK, catalogue 11429868001) to a final concentration of 1mmol. The PK treated sample along with any residual supernatant were frozen at -20°C until required.

11.2. *SDS-PAGE and Western blot transfer*

PK treated samples were thawed and given a brief vortex before removing a 5µl volume and adding to 2.5µl of 4X NuPAGE LDS sample buffer (Fisher Scientific, Loughborough, UK, catalogue NP0007), supplemented with 2.5µl of LB100 buffer. After a brief vortex, samples were denatured by boiling at 100°C for 10min before a

brief spin at 14,000 rpm. In addition to the human diagnostic reference standards, protein molecular weight markers were included in each run (1µl Magic Marker™ XP (Fisher Scientific, Loughborough, UK, catalogue LC5602); 5µl Benchmark (Fisher Scientific, Loughborough, UK, catalogue 10748-010); 1.5µl of LB100 buffer; 2.5µl of NuPAGE LDS sample buffer). Molecular weight markers were not boiled. Samples were electrophoretically separated on NuPAGE™ Novex™ 10% Bis-Tris Protein Gels (Fisher Scientific, Loughborough, UK catalogue NP0301BOX) by running at 200V (constant current) for 55min in 1X NuPAGE MES running buffer (50mls 20X running buffer (Fisher Scientific, Loughborough, UK, catalogue NP0002-02); 950ml dH_2O) within a Western blot running tank. Proteins separated by sodium dodecyl sulphate polyacrylamide gel electrophoresis (SDS-PAGE) were electrotransferred onto polyvinylidene difluoride (PVDF) membrane (Bio-Rad, Hemel Hempstead, UK, catalogue 1620177) at 30V (constant current) for 1h using the NuPAGE transfer system. Transfers were carried out in 1X NuPAGE transfer buffer (25ml 20X NuPAGE transfer buffer (Fisher Scientific, Loughborough, UK, catalogue NP0006-1); 375ml dH_2O, 100ml methanol).

11.3. *Detection of PrP^{res} bound to PDVF membrane*

Membranes were rinsed in TBS-T (100mls 10X TBS (Sigma-Aldrich, Poole, UK, catalogue T5912); 900ml dH_2O; 0.1% Tween 20 (Sigma-Aldrich, Poole, UK, catalogue P2287)) before incubating in 5% powdered milk (from a supermarket)/TBS-T for 45min at room temperature or overnight at 4°C to block non-specific binding sites. Membranes were then washed (3 x 5min) in TBS-T prior to incubating in the primary anti-PrP antibody 3F4 (Millipore, Watford, UK, catalogue MAB1562) at a final concentration of 75ng/mL, or the monoclonal antibody 12B2 (Central Veterinary Institute of Wageningen UR, Lelystad, The Netherlands) at a final concentration of 200ng/ml for 1h at room temperature. After a further wash, immunolabelling was completed by incubating the membrane in the Amersham ECL Mouse IgG, HRP-linked $F(ab')_2$ fragment (from sheep) (GE Healthcare Life Sciences, Little Chalfont, UK, catalogue NA9310-1ML) diluted 1:25,000 in TBS-T for 1h at room temperature. Immunodetection was carried out by incubating the membrane with the chemiluminescent substrate ECL 2 (50µl of reagent B per 2 ml of reagent A (Fisher

Scientific, Loughborough, UK, catalogue 80196)). After draining off the excess ECL plus, membranes were exposed to Hyperfilm ECL (GE Healthcare, Little Chalfont, UK, catalogue 28-9068-37) for 30sec, 3min and 30min before the films were developed in an automatic film hyperprocessor (Konica Minolta SRX-101A medical film processor).

Appendix 12. Western blotting with NaPTA precipitation

Samples of frozen non-CNS tissues were weighed and placed into Lysing matrix D tubes (Fisher Scientific, Loughborough, UK, catalogue MB116913050). These samples were homogenised in ice-cold 2% sarkosyl/phosphate buffered saline pH 7.4 (PBS) (Sigma Aldrich, Poole, UK, catalogue 11666789001) containing 2% N-Laurosarcosine, (Sigma Aldrich, Poole, UK, catalogue 61745). An appropriate volume of homogenisation buffer was used to give a final tissue concentration of 10% (mass per volume). The tissue was homogenised in a Fastprep-24 homogeniser (MP Biomedicals, Santa Ana, CA, USA, catalogue 116004500) at room temperature using three cycles of 45sec at a speed of $6ms^{-1}$. Cellular debris was cleared from the homogenates by centrifugation at 5200*g* at 4°C for 5min using a microcentrifuge (Eppendorf AG, Stevenage, UK, catalogue 5417R) with a fixed angle motor (Eppendorf AG, Stevenage, UK, catalogue F-45-30-11). The cleared homogenate was transferred to a fresh tube and either stored at -80ºC, or immediately subjected to sodium phosphotungstic acid (NaPTA) precipitation.

12.1. *NaPTA precipitation*

The cleared 10% homogenates of the non-CNS tissues were each diluted to 5% with 2% N-Laurosarcosine/PBS. Cleared spleen tissue homogenate (5%) from a patient proven not to have any form of human prion disease was used as a non-CJD neurological negative control. In addition, iCJD or sCJD brain tissue homogenate (10%, 10µl, corresponding to 100µg brain) was diluted and mixed into 1ml of 5% cleared non-CJD spleen tissue homogenate, for use as positive control. The 5% cleared peripheral tissue homogenates (each 1ml) and the abovementioned positive and negative controls were incubated at 37ºC for 10min. To degrade nucleic acids, the samples were incubated with 50 Units of benzonase™ nuclease (Sigma-Aldrich, Poole, UK, catalogue E1014) and 1mmol $MgCl_2$ (Sigma-Aldrich, Poole, UK, catalogue UKM8266) as a cofactor. To effect the precipitation of any PrP^{Sc}, the samples were mixed with 81µl of a pH7.4 solution of 4% (mass per volume) NaPTA (Sigma-Aldrich, Poole, UK, catalogue 31648) and 170mmol $MgCl_2$ to give final concentrations of 0.3% NaPTA and 13.62mmol $MgCl_2$ (including the $MgCl_2$ added in

the benzonase step). The samples were incubated at 37ºC for 30min. Precipitated protein was pelleted by centrifugation at 21,000 rpm for 30 at 37ºC. The pellets were resuspended in 20µl of 0.1% N-Laurosarcosine/PBS by breaking the pellets into pieces with the pipette tip, and then pipetting up and down repeatedly. Protease sensitive protein was eliated from the resuspensions by incubation with 2µl of 550µg/ml proteinase K (PK) (Roche Diagnostics, West Burgess, UK, catalogue 03 115 828 001) for 30 at 37°C (final PK concentration of 50µg/ml). Protease digestion was terminated by the addition of 1µl of 23mmol PefaBloc SC™ (Sigma-Aldrich, Poole, UK, catalogue 76307, final concentration of 1mmol). The proteins in the sample were then denatured prior to their electrophoretic separation by mixing with 8µl of NuPAGE™ LDS sample buffer (4x) (Fisher Scientific, Loughborough, UK, catalogue NP0007) and incubating at 100°C for 10.

12.2. *SDS-PAGE and Western blot transfer following NaPTA precipitation*

Samples were electrophoretically separated on NuPAGE™ Novex™ 10% Bis-Tris Protein Gels (Fisher Scientific, Loughborough, UK catalogue NP0301BOX) in 1X NuPAGE MES running buffer (50mls 20X running buffer (Fisher Scientific, Loughborough, UK, catalogue NP0002-02) using the method described above in Appendix 8. A sample of brain homogenate prepared in 2% N-Laurosarcosine/PBS and digested with 50µg/ml PK at 37ºC for 1h, was separated alongside the NaPTA precipitated peripheral tissue samples and the NaPTA precipitated positive and negative controls. After electrophoresis, the separated proteins were electrotransferred onto Immun-Blot PVDF™ membrane, (Bio-Rad, Hemel Hempstead, UK 1620177) using the method described above in Appendix 8.

12.3. *Immunoblotting for PrP^{res} following NaPTA precipitation*

To block non-specific binding sites the PVDF membrane was incubated overnight at 4°C in 5% non-fat dried milk powder (from a supermarket) made up in Tris Buffered Saline (Sigma-Aldrich, Poole, UK, catalogue T5912) containing 0.1% (volume/volume) Tween 20 (Sigma-Aldrich, Poole, UK, catalogue P2287). The latter is referred to here as TBS-T. Since non-CNS tissues from CJD patients contain only low levels of PrP^{Sc}, the immunoblotting technique was designed to maximise

sensitivity. All wash steps were 5min using TBS-T. All washing and antibody incubation steps were performed on a shaking platform set at 100 rpm. After blocking, the membranes were washed three times and probed for 1h with a 1:10,000 dilution of anti-PrP antibody 3F4 (Millipore, Watford, UK, catalogue MAB1562, final concentration: 200ng/ml). After a further three washes the membrane was probed with a 1:25,000 dilution of Amersham ECL Mouse IgG, HRP-linked $F(ab')_2$ fragment (from sheep) (GE Healthcare Life Sciences, Little Chalfont, UK, catalogue NA9310-1ML) for 1h at room temperature. The membrane was then washed five times and treated with SuperSignal™ West Femto Maximum Sensitivity Substrate (Fisher Scientific, Loughborough, UK, catalogue 34095) according to the manufacturer's instructions. The membrane was then developed by exposure to Amersham Hyperfilm ECL (GE Healthcare, Little Chalfont, UK, catalogue 28906835), for periods of time up to 3min. Alternatively, the images from the membrane were recorded using the ChemiDoc™ XRS+ System with Image Lab™ Software (Bio-Rad, Hemel Hempstead, UK, catalogue 170-8265), for periods of time up to 30min.

Appendix 13. RT-QuIC protocols

13.1. *Preparation of brain homogenates for use as seeds in RT-QuIC*

Samples of frozen grey matter enriched cerebral cortex samples were weighed and placed into Lysing matrix D tubes (Fisher Scientific, Loughborough, UK, catalogue MB116913050). These samples were homogenised in phosphate buffered saline (PBS) (Sigma-Aldrich, Poole, UK, catalogue 11666789001) containing 1mmol EDTA (Sigma Aldrich, Poole, UK, catalogue 03690-100ML), 150mmol NaCl (SAFC Biosciences, Irvine, U, catalogue 59222C) 0.5 % Triton X-100 (Sigma-Aldrich, Poole, UK, catalogue X100) and cOmplete^{TM} Mini EDTA-free protease inhibitor cocktail (Roche Diagnostics, West Burgess, UK, catalogue 05892791001). An appropriate volume of homogenisation buffer was used to give a final tissue concentration of 10% (mass per volume). The tissue was homogenised in a Fastprep-24 homogeniser (MP Biomedicals, Santa Ana, CA, USA, catalogue 116005500) at room temperature using one cycle of 45sec at a speed of 6ms^{-1}. Cellular debris was cleared from the homogenates by centrifugation at 5200*g* at 4°C using a microcentrifuge (Eppendorf AG, Stevenage, UK, catalogue 5417R) with a fixed angle motor (Eppendorf AG, Stevenage, UK, catalogue F-45-30-11). Prior to the use of these samples as seeds in RT-QuIC, further serial ten-fold dilutions of the cleared homogenates were made using PBS. The equivalent masses of brain contained within these ten-fold dilutions are shown in the Table below.

Dilution factor of 10% brain homogenate	Dilution factor of brain	Equivalent wet mass of brain (g) per microlitre (µl)
1	10^{-1}	10^{-4}
10^{-1}	10^{-2}	10^{-5}
10^{-2}	10^{-3}	10^{-6}
10^{-3}	10^{-4}	10^{-7}
10^{-4}	10^{-5}	10^{-8}
10^{-5}	10^{-6}	10^{-7}
10^{-6}	10^{-7}	10^{-8}

13.2. *RT-QuIC reaction setup*

The method used for the RT-QuIC was the one described previously by Peden *et al.* (Peden *et al*., 2012, 2014) with minor modifications. Full length hamster (*Meocricetus auratus*) recombinant PrP (recPrP, amino acids 23–231; GenBank accession no. K02234) was used as a substrate for seeded conversion. Hamster recPrP was used as this substrate has been shown to detect brain PrP^{Sc} from CJD patients with greater sensitivity and specificity compared with human recPrP substrate (Peden *et al*., 2012). This recPrP was obtained from the Bristol Institute of Transfusion Sciences, Bristol, UK. The method used by Bristol for the expression and purification of recPrP in *Escherichia coli* was as described previous by Wilham *et al.* (Wilham *et al*., 2010). Aliquots of frozen recPrP were thawed at room temperature and then 500µl batches were filtered through a 100kDa Nanosep centrifugal concentrator (VWR International, Lutterworth, UK) at 3000*g* for 20min. The concentration of recPrP was determined by diluting samples 1:10 in PBS containing 0.1% sodium dodecyl sulphate (SDS). The absorbance was measured at 280nm in an Ultraspec 3000 (GE Healthcare, Little Chalfont, UK, catalogue 80-2116-30). After multiplying by the dilution factor, the concentration of recPrP was calculated using an extinction coefficient of 2.6 l/g cm^{-1}.

The 100µl RT-QuIC reactions were set up in quadruplicate in the wells of a clear-bottomed black 96-well microplate (Fisher Scientific, Loughborough, UK, catalogue 15142799). Stock solutions containing the reaction components were filtered through 0.22µM Millex^{TM} PES filters (Millipore, Watford, UK, catalogue SLGP033NB). A master mix containing all reaction components except the brain seed was prepared, with recPrP being added last. The recPrP was the final addition to the master mix, which was mixed by gently inversion of the container tube. This master mix was then dispensed into the wells of the 96-well plate as 98µl volumes. The RT-QuIC reactions were initiated by the addition of 2µl of a dilution of 10% (w/v) homogenate. For the determination of lag times as a measure of seeding potential 2µl of a 10^{-3} fold dilution of the 10% (mass per volume) homogenate was added to the wells (see *Lag time as a measure of seeding* below). This amount is equivalent to $2x10^{-7}$g brain (wet mass) per 100µl reaction (Table 4.5). After adding this volume of diluted brain homogenate, the final reactions contained PBS, 324mmol NaCl (including the NaCl present in PBS),

1mmol EDTA, 10mmol ThT, $1x10^{-7}$% Triton^{TM} X-100 and 0.1 mg/ml recPrP. In contrast to the method given in Peden *et al.* (Peden *et al*., 2012), no SDS or N-2 Supplement was added, as improved specificity can be achieved when these components are omitted.

13.3. *Quaking conditions and real-time fluorescence readings*

The plates were sealed with film. The sealed 96-well plates were incubated at 42◦C and shaken intermittently (87sec of shaking at 900 rpm in a double orbital configuration followed by 33sec of rest) using a FLUOstar Omega microplate reader (BMG Labtech Ltd, Bucks, UK, catalogue 1524782). Fluorescence readings were taken at 480 nm every 15min from the clear bottoms of the wells after excitation of each well with 20 flashes at 450nm.

13.4. *Lag time as a measure of seeding*

In order to quantify prion seeding efficiency we used a method based on the one described by Shi *et al* (Shi *et al*, 2013). In this method, the lag time to conversion is used as an inverse measure of seeding potential, (i.e. a shorter lag time to conversion corresponds to greater seeding efficiency). The lag period to the start of conversion was defined as the time (in hours (h)) from the start of the assay to when the RT-QuIC fluorescence reading was three times the baseline. The baseline for each RT-QuIC reaction was taken to be the mean reading (for at least four replicate reactions) at 0.5h. A lag period was thus obtained for each replicate reaction and a mean lag period for each patient sample was calculated.

A preliminary analysis was conducted to determine the relationship between seed dilution and lag period. Brain homogenates (10%) from sCJD and iCJD patients were serially diluted in PBS by factors of 10^{-2}, 10^{-3}, 10^{-4}, 10^{-5} and 10^{-6} (see below). Samples (2µl) of these serial dilutions were introduced into the RT-QuIC reactions. Analysis of these RT-QuIC reactions concluded that differences in seeding efficiency between iCJD and sCJD subgroups could best be discriminated by seeding RT-QuIC reactions with 2µl of a 10^{-3} dilution of 10% brain homogenate.

Appendix 14. PMCA protocol

14.1. *Sample preparation*

Normal brain homogenates from humanised transgenic mice (HuTg) of the *PRNP* codon 129 methionine homozygous (129MM), valine homozygous (129VV) and methionine/valine heterozygous (129MV) genotypes (Bishop *et al*., 2006) were prepared using a manual homogeniser (KONTES Potter-Elvehjem Tissue Grinder 17ml, VWR International, Lutterworth, UK, catalogue 885500-0023) and conversion buffer composed of phosphate-buffered saline 1X (Sigma-Aldrich, Poole, UK, catalogue D8537), 150mmol NaCl (Sigma-Aldrich, Poole, UK, catalogue S3014-500G), 1% Triton X-100 (Sigma-Aldrich, Poole, UK, catalogue T9284-100ml) and 1X protease inhibitors ((Roche Diagnostics, West Burgess, UK, catalogue 11697498001), to obtain a final 10% mass per volume solution (termed a PMCA "substrate"). The homogenised tissue was cleared by centrifugation at 2000 rpm for 40sec in a refrigerated centrifuge (4°C), and the supernatant was aliquoted and stored at −80°C. The sCJD and iCJD brain homogenates (termed PMCA "seeds") were prepared following the same method used for substrate preparation

14.2. *PMCA method*

Aliquots of 10% brain homogenate substrate were mixed with 10% CJD brain homogenate seeds in PCR tubes. Low molecular weight heparin (Heparin Sodium, Cambridge Bioscience, Cambridge, UK, catalogue H1658) was added at 100µg/ml for all PMCA reactions. Prior to the amplification procedure, 19µl of the PMCA reaction mixture was taken (from the final volume of 120µl) for each reaction (referred to as the "frozen" sample) for comparison with the sonicated samples (referred to as the "sonicated" sample). Amplification employed cycles of sonication and incubation in a programmable sonicator (Qsonica, Newtown, USA, model Q-700) at 37°C. A total of 96 PMCA cycles were performed comprising 20sec of sonication (at an amplitude of 38%, wattage: 275-300) followed by 29min 40sec of incubation for each cycle. Frozen and sonicated samples were digested with proteinase K (Roche Diagnostics, West Burgess, UK, catalogue 03115828001), in a final concentration of 50µg/ml at 37˚C for 1h and analysed by Western blotting using the anti-PrP monoclonal antibody 3F4

(Millipore, Watford, UK; Product: MAB1562). Amplification efficiency was expressed as the increase in PrP^{res} signal in the sonicated compared to the frozen sample.

14.3. *Western blotting analysis – PMCA products*

Samples were boiled at 100°C for 10min and centrifuged at 2000 rpm for 10sec (Eppendorf AG, Stevenage, UK, catalogue 5417R). The samples were loaded into the wells of a NuPAGE Novex 10% Bis-Tris Gel 1.0mm, 10 well (Fisher Scientific, Loughborough, UK, catalogue NP0301BOX) and electrophoresed at 200V for 55min in NuPAGE MES SDS Running Buffer (Fisher Scientific, Loughborough, UK, catalogue NP000202).

Proteins were transferred to a polyvinylidene difluoride membrane (PVDF) (Bio-Rad, Hemel Hempstead, UK, catalogue 1620177) using 800 mA (constant) for 1h. The PVDF membranes were blocked with 2% milk for 1h followed by incubation with the anti-PrP monoclonal antibody 3F4 (Millipore, Watford, UK, catalogue MAB1562) diluted in 1X Tris-buffered saline with 0.05% Tween 20 (Sigma-Aldrich, Poole, UK, catalogue P9416) (TBS-T) in a dilution 1:10,000. Blots were rinsed 3 times (10min each time) with 1X PBST (washing buffer). Amersham ECL Anti-mouse IgG, peroxidase-linked species specific F(ab')2 fragment (from sheep) (GE Healthcare Life Sciences, Little Chalfont UK, catalogue NA9310-1ML) was used as a secondary antibody diluted 1:25,000 in washing buffer and incubated for 1h. Finally, blots were rinsed 3 times for 10min each with washing buffer to eliminate any excess of secondary antibody. Membranes were developed using the Amersham ECL-Prime luminescent peroxidase detection reagent (GE, Little Chalfont, UK, catalogue RPN2232). Image of the WB were acquired using the XRS digital CCD camera system (Bio-Rad, Hemel Hempstead, UK, catalogue 1708265SP).

14.4. *PMCA normalisation and quantification*

To estimate the PMCA amplification efficiency, PrP^{res} densitometric signals (after PK treatment and Western blotting) were calculated using the Image Lab software 2.0.1 (Bio-Rad, Hemel Hemptsead, UK, catalogue 1709692). The densitometric value of the

intensity of PrP immunoreactive bands was calculated for the samples before and after PMCA measuring an equal designated area (number of pixels). To obtain a better comparison between samples, background subtraction was performed. The densitometric values of "sonicated" samples were divided by the "frozen" measures. The increase in signal (the ratio between the detectable levels of PrP^{res} before and after PMCA) was designated as the amplification efficiency of the in vitro PMCA conversion.

14.5. *Densitometric Analysis*

Densitometric analyses were performed using Image Lab software version 2.01 (Bio-Rad, Hemel Hempstead, UK, catalogue 1709692). All images were captured using a charge-coupled device (CCD camera HQ2, Bio-Rad, Hemel Hempstead, UK, catalogue 1708255) and saved in TIFF format for further analysis. Densitometric analysis of relative band intensity was performed assuming a linear range for the PrP immunodetection signal by Western blotting.

Appendix 15. Publication of work included in this thesis

Ritchie DL, Barria MA, Peden AH, Yull HM, Kirkpatrick J, Adlard P, Ironside JW, Head MW.
UK iatrogenic Creutzfeldt-Jakob disease: investigating prion transmission across genotypic barriers using human tissue-based and molecular approaches.
Acta Neuropathologica 2016; November 3rd. Epub ahead of print.